Adriana Arrulo Pereira

SILENCING OF CYPX GENE IN THE HYPOTHALAMUS AND ITS IMPACT ON WHOLE-BODY METABOLISM

UAlg
UNIVERSIDADE DO ALGARVE
DEPARTAMENTO DE CIÊNCIAS BIOMÉDICAS E MEDICINA

2019

Adriana Arrulo Pereira
Nº52795

SILENCING OF CYPX GENE IN THE HYPOTHALAMUS AND ITS IMPACT ON WHOLE-BODY METABOLISM

Master's degree in Oncobiology – Molecular Mechanisms in Cancer

Supervisors: Prof. Clévio Nóbrega, PhD
Célia Aveleira, PhD

UNIVERSITY OF ALGARVE
Department of Biomedical Sciences and Medicine

Faro, 2019

Authorship Statement

I hereby declare to be the author of this work, which is original and unpublished. Authors and papers consulted are duly cited in the text and are listed in the included references.

Acknowledgments/Agradecimentos

Inicialmente, gostaria de agradecer ao meu orientador, o Professor Doutor Clévio Nóbrega, por me ter acolhido no seu laboratório e por toda a transmissão de conhecimentos. Um simples obrigado não é suficiente para lhe agradecer todo o apoio, toda a paciência, orientação e disponibilidade, a animação e lanchinhos nas reuniões, e sobretudo, a dedicação que sempre demonstrou ao longo do ano. Não seria possível sem si. Muito obrigada, por tudo.

Gostaria de agradecer à minha coorientadora, a Doutora Célia Aveleira, por toda a disponibilidade, transmissão de conhecimentos, apoio e carinho demonstrado. Muito obrigada por toda a animação, por me ter recebido em Coimbra e por toda a ajuda ao longo do ano. Um obrigada gigante à Marisa Marques e à Sara Silva, por me terem recebido de braços abertos em Coimbra e por todo o carinho e apoio. Marisa, obrigada por teres sido incansável comigo.

Agradeço à Adriana Marcelo por ter imensa paciência comigo e por todos os conhecimentos que partilhou. Adriana, obrigada pelos bons conselhos, por disponibilizares o teu tempo, por estares sempre presente e por todos os bons momentos que partilhámos juntas. Agradeço também à Rebekah Koppenol, por me ter ajudado constantemente no laboratório, por disponibilizar o seu tempo, pela paciência, e por todos os conhecimentos que partilhou.

Gostaria de agradecer também à Joana Rolo pelos bons momentos passados fora e dentro do laboratório, ao Rafael Costa pela companhia e boa disposição durante os fins de semanas no laboratório e aos restantes membros do laboratório.

Um obrigada à Inês Santos e ao Leonardo Silva por toda a disponibilidade demonstrada.

Quero agradecer a todos os meus amigos que contribuíram para a concretização deste projeto. À Joana Delbone e à Sara Martins, um gigantesco obrigada por estarem sempre presentes para me ouvir, por todo o apoio quando mais precisei e pela maravilhosa companhia. À Filipa Medinas e ao Miguel Militão, obrigada por todo o apoio moral, companhia e por todas as idas até à praia. À Sheila Pereira por ser incansável comigo no primeiro ano de mestrado, por me ter apoiado e nunca me ter deixado desistir.

Gostaria ainda de agradecer à minha família, por todo o apoio, a múltiplos níveis. À minha mãe, Anabela Arrulo, um obrigada do tamanho do mundo por apoiares todas as minhas decisões e porque sem ti nada seria possível. Aos restantes membros da família, em especial

ao Daniel Arrulo, Raquel Costa, Manuel Dias e Lucília Rato, um obrigada por me acompanharem desde sempre.

Obrigada a todos, por tudo!

Adriana Arrulo

Faro, Outubro 2019

Contents

Abstract

Cholesterol metabolism is tightly controlled in the brain, through an equilibrium of cholesterol *de novo* synthesis and cholesterol efflux. Most of the cholesterol in the brain is in myelin sheaths to insulate axons and to maintain their morphology and synaptic transmission. The importance of cholesterol in the brain is highlighted by the fact that dysfunctions in its metabolism homeostasis are correlated with different neurodegenerative disorders. The hypothalamus, specially the ARC, is the principal brain region in the control of whole-body energy homeostasis, having a crucial role in metabolic organ regulation.

This project goal was to silence the expression of the *Cyp46a1* mouse gene in the hypothalamus of C57BL/6J wild-type mice fed with Chow and HFD, and to investigate its impact in the whole-body metabolism homeostasis. As the ARC is implicated in the control of whole-body energy metabolism, and oxysterols levels are altered in obesity, we hypothesize that the silencing of *Cyp46a1* gene could lead to an obesity and TIIDM phenotypes.

In this study, C57BL/6J wild-type mice (*n=45*) were divided into two groups corresponding to two different diets. One group (*n=24*) had access to a Chow containing 10% of fat and the other group (*n=21*) had access to an HFD containing 60% of fat. This study was conducted during 12 weeks. In the 4th week, the two groups of mice (Chow and HFD) were divided into four subgroups, from which two were submitted to the stereotaxic injection delivering the AAV of the serotype 5, with the shRNA targeting the mouse *Cyp46a1* gene in each side of the ARC and two remained non-injected, as control.

The silencing of *Cyp46a1* mouse gene in the ARC of mice fed with Chow and HFD leads to an increase of BW, changes in food and water intake, to a reduction of glucose tolerance, of insulin sensitivity and leads also to modifications in several metabolic organs, comparatively to the non-injected animals. In fact, in the Chow AAV5-sh*Cyp46a1* animals, the impact of the silencing *Cyp46a1* gene appears to mimic an HFD effect, whereas in HFD AAV5-sh*Cyp46a1* mice this silencing exacerbates the phenotype of obesity. These results could suggest an important role of the cholesterol metabolism in the brain, specially of the Cyp46a1 enzyme in the control of whole-body homeostasis. Finally, additional studies are needed to continue this project and it would be interesting to perform the overexpression of *Cyp46a1* in the ARC to investigate if this gene could be a potential target to further genetic therapies.

Keywords: hypothalamus • cholesterol metabolism • *Cyp46a1* • oxysterols • obesity • whole-body energy homeostasis

Resumo

No cérebro, o metabolismo do colesterol é extremamente controlado através do equilíbrio entre a síntese *de novo*, conversão e efluxo do colesterol. Quando a síntese do colesterol excede a sua necessidade no cérebro, ocorre o processo hidroxilação do colesterol em 24-hidroxicolesterol (24-OHC) através da ação da enzima CYP46A1, uma enzima codificada pelo gene *CYP46A1*. O oxisterol 24-OHC, ao contrário do colesterol, possui a capacidade de atravessar a barreira hematoencefálica contribuindo desta forma para a homeostasia do colesterol no cérebro. Este está maioritariamente localizado nas bainhas de mielina, de modo a isolar os axónios e manter a sua morfologia e transmissão sináptica. Diversas doenças neurodegenerativas, como a doença de Alzheimer e a doença de Huntington, foram correlacionados com disfunções na homeostasia do colesterol no cérebro, destacando desta forma a sua importância no organismo.

O hipotálamo, especialmente o núcleo arqueado, é a região do cérebro responsável pela regulação da homeostasia energética corporal, apresentando um papel crucial no equilíbrio entre o consumo e o gasto energético.

O objetivo deste projeto foi silenciar a expressão do gene *Cyp46a1* no hipotálamo de ratinhos C57BL/6J *wild-type* alimentados com uma dieta de controlo com baixo teor em gordura (Chow – *low fat control diet*) e com uma dieta com alto teor em gordura (HFD - *high fat diet*) e investigar o seu impacto na homeostasia energética corporal. Uma vez que o núcleo arqueado está implicado regulação da homeostasia energética corporal e que os níveis de oxisteróis encontram-se alterados na obesidade, criou-se a hipótese de que o silenciamento do gene *Cyp46a1* poderia resultar em um fenótipo de obesidade e de diabetes mellitus do tipo 2. Desta forma, os ratinhos C57BL/6J (*n=45*) foram divididos em dois grupos correspondentes a dietas distintas. Um dos grupos (*n=24*) teve acesso a uma dieta Chow, contendo 10% de gordura, e o outro grupo (*n=21*) teve acesso a uma dieta HFD, contendo 60% de gordura.

Este estudo foi conduzido durante o período de 12 semanas, no qual, na quarta semana os dois grupos (Chow e HFD) foram divididos em quatro subgrupos. Dois grupos foram submetidos à injeção estereotáxica bilateral no ARC, constituindo os grupos tratados, (Chow AAV5-sh*Cyp46a1* e HFD AAV5-sh*Cyp46a1*) e os restantes grupos não foram submetidos à injeção estereotáxica, constituindo os grupos de controlo.

O silenciamento do gene *Cyp46a1* no núcleo arqueado dos ratinhos C57BL/6J alimentados com uma dieta Chow resultou em um aumento no peso corporal, na ingestão de alimentos e de água, na redução da tolerância à glucose, na sensibilidade à insulina e ainda, em modificações em vários órgãos metabólicos. Da mesma forma, o silenciamento do gene *Cyp46a1* dos ratinhos C57BL/6J alimentados com uma dieta HFD resultou em um aumento do peso corporal, em uma diminuição da ingestão de alimentos, da sensibilidade à insulina e em modificações nos órgãos metabólicos.

O silenciamento do gene *Cyp46a1* no núcleo arqueado dos ratinhos C57BL/6J parece modificar a morfologia do tecido adiposo branco, do tecido adiposo castanho e do fígado, nos animais submetidos à injeção estereotáxica. Os grupos tratados apresentaram importantes modificações na acumulação lipídica nestes órgãos, bem como modificações nos níveis de proteína.

Além disso, o silenciamento do gene *Cyp46a1* resulta em modificações no comportamento nos ratinhos C57BL/6J alimentados com dietas Chow e uma HFD.

Nos animais Chow AAV5-sh*Cyp46a1*, o impacto do silenciamento parece mimetizar o efeito de uma HFD, enquanto nos ratinhos HFD AAV5-sh*Cyp46a1* esse silenciamento parece exacerbar o fenótipo da obesidade, uma vez que estes animais já se encontravam metabolicamente desregulados.

Os resultados podem desta forma sugerir um papel importante do metabolismo do colesterol no cérebro, especialmente da enzima CYP46A1 no controlo da homeostasia energética corporal.

Finalmente, estudos adicionais ainda são necessários e seria interessante realizar a sobre expressão do gene *Cyp46a1,* no núcleo arqueado, para investigar se este gene poderá ser um potencial alvo terapêutico.

Palavras chave: hipotálamo • metabolismo do colesterol • *Cyp46a1* • oxisteróis • obesidade • homeostasia energética corporal

List of figures

List of tables

List of annexes

List of abbreviations

24-OHC – 24-hydroxycholesterol

4β-OHC – 4β-hydroxycholesterol

AAE – American Association of Endocrinology

AAV – adeno-associated virus

AAV5 – adeno-associated viral vector serotype 5

ABC – ATP binding cassette

ABCA1 – ABC transporters A1

AC – anterior commissure

ACAT1 – acyl-coenzyme A cholesterol acyltransferase 1

ACVD – atherosclerotic cardiovascular disease

AD – Alzheimer's disease

AgRP – agouti-related peptide

AHA – anterior hypothalamic area

AHA/NHLBI – American Heart Association/ National Heart, Lung and Blood Institute

Akt – protein kinase B

ANS – autonomic nervous system

Apo – apolipoprotein

ApoER2 – apolipoprotein E receptor 2

APP – amyloid precursor protein

ARC – arcuate nucleus

ATGL – adipose triglyceride lipase

AUC – area under the curve

Aβ – amyloid β-peptide

BAT – brown adipose tissue

BBB – blood-brain barrier

BCA – bicinchoninic acidic

BMI – body mass index

BW – body weight

C-peptide – connecting peptide

C/EBP-α – CCAAT/enhancer-binding protein α

CART – cocaine and amphetamine-regulated transcript

Chow – low-fat control diet

CKK – cholecystokinin

cm – centimeter

CNS – central nervous system

CRP – C-reactive protein

CSF – cerebrospinal fluid

CVD – cardiovascular diseases

CYP46A1 – cytochrome P450 family 46 subfamily A member 1

DHA – dorsal hypothalamic area

DHCR7 – 7-dehydrocholesterol reductase

dL – deciliter

DM – diabetes mellitus

DMN – dorsomedial nucleus

DRPLA – dentatorubral-pallidoluysian atrophy

EGIR – European Group for the study of Insulin Resistance

ER – endoplasmic reticulum

FA – fatty acid

FFA – free fatty acids

g – gram

GABA – gamma-aminobutyric acid

GLP-1 – Glucagon-like peptide 1

GLUT – glucose transporters

GLUT4 – glucose transporter 4

GTT – glucose tolerance test

HD – Huntington's disease

HDL-Chol – high-density lipoprotein cholesterol

HEK – human embryonic kidney

HFD – high-fat diet

HMG-CoA – 3-hidroxi-3-methyl-glutaril-CoA

HSL – hormone sensitive lipase

HTT – huntingtin gene

IDF – International Diabetes Federation

IGT – impaired glucose tolerance

IL-6 – interleukin 6

INR – insulin receptor

INRS – insulin receptor substrate

IR – insulin resistance

IRS – insulin resistance syndrome

ITT – insulin tolerance test

kg – kilogram

kITT – constant for glucose clearance

LDL – low density lipoprotein

LDL-R – low density lipoprotein receptor

Lep – leptin

LepR – leptin receptor

LHA – lateral hypothalamic area

LL – lipoprotein lipase

Ln – natural logarithm

LPOA – medial preoptic area

LXR – liver X receptors

m^2 – square meter

MB – mammillary body

MC3/4R – melanocortin receptor 3/4

MCH – melanin-concentrating hormone

MCP-1 – monocyte chemoattract protein-1

ME – median eminence

MetS – metabolic syndrome

mg – milligram

min – minutes

MJD – Machado-Joseph disease

mm Hg – millimeter of mercury

mmol – millimol

MPN – median preoptic nucleus

MPOA – lateral preoptic area

MSH – melanocyte stimulating hormone

NAFLD – non-alcoholic fatty liver disease

NASH – non-alcoholic steatohepatitis

NCEP/ATPIII – National Cholesterol Education Program Adult Treatment Panel III

NEFA – non-esterified acids

nm – nanometer

NPC1/2 – Niemann-Pick type C1/2

NPY – neuropeptide Y

OC – optic chiasm

OSA – obstructive sleep apnea

PAI-1 – angiotensinogen and plasminogen activator inhibitor-1

PBS – phosphate-buffered saline solution

PC1/3 – prohormone convertase 1/3

PC2 – prohormone convertase 2

PCOS – polycystic ovary syndrome

PD – Parkinson's disease

PGK1 – phosphoglycerate kinase 1

PHN – posterior hypothalamic nucleus

PI3K – phosphatidylinositol-3-kinase

POA – preoptic area

POMC – pro-opiomelanocortin

PPAR-γ – proliferator-activated receptors-γ

PVN – paraventricular nucleus

RAS – renin-angiotensin system

RCF – relative centrifugal force

RER – rough endoplasmic reticulum

rpm – revolutions per minute

RT-qPCR – quantitative real-time polymerase chain reaction

s – seconds

SBMA – spinal and bulbar muscular atrophy

SCA – spinocerebellar ataxia

SCAP – SREBP cleavage-activating protein

SCN – suprachiasmatic nucleus

SEM – standard error of mean

shRNA – short hairpin RNA

SLOS – Smith-Lemli-Optizy

SMN – supramammillary nucleus

SNS – sympathetic nervous system

SON – supraoptic nucleus

SREBP – sterol regulatory element-binding proteins

TG – triglyceride

TIIDM – type II diabetes mellitus

TMN – tuberomammillary nucleus

TNF-α – tumor necrosis factor-α

UCP-1 – uncoupling protein-1

USA – United States of America

v.g. – viral genomes

VEGF – vascular endothelial growth factor

VLDL – very-low-density lipoprotein

VLDLR – very-low-density lipoprotein receptor

VMN – ventromedial nucleus

VPN – ventrolateral preoptic nucleus

WAT – white adipose tissue

WC – waist circumference

WHO – World Health Organization

α – alpha

β – beta

γ – gamma

µg – microgram

µL – microliter

µm – micromete

Introduction

1. Metabolic syndrome

1.1. Definition of metabolic syndrome

The concept of metabolic syndrome (MetS) exists for decades and consists in a clustering of several metabolic abnormalities, which are correlated with an increased risk for developing cardiovascular diseases (CVD) and type II diabetes mellitus (TIIDM)(Eckel, Grundy, and Zimmet 2005). This concept is also known as Syndrome X, the deadly quartet and as the insulin resistance syndrome (IRS) (Reaven 1988; Kaplan 1989; DeFronzo and Ferrannini 1991).

Already in 1921, it was documented the coexistence of hypertension and diabetes; and now is established that hypertension is correlated with hyperglycemia and gout (Cornier et al. 2008).

Later, in 1947, it was noted that abdominal obesity was commonly correlated with other metabolic abnormalities, such hypertension and gout, and with an increased risk for CVD and diabetes mellitus (Eckel et al. 2005). The correlation of different abnormalities continued to be documented, and in 1981, it was reported the existence of an increased risk for CVD and for TIIDM in individuals presenting several metabolic abnormalities (Sarafidis and Nilsson 2006). At the time it was originally nominated this concept as MetS, which included metabolic abnormalities such TIIDM, hyperinsulinemia, obesity, hypertension and gout (Sarafidis and Nilsson 2006). Reaven, in 1988, observed that insulin resistance (IR) was present in the majority of individuals with TIIDM or with impaired glucose tolerance (IGT)(Reaven 1988). The author introduced the concept of IR as an etiological factor for metabolic abnormalities as hypertension, IGT, hyperinsulinemia, high levels of very-low-density lipoprotein (VLDL), and low levels of high-density lipoprotein cholesterol (HDL-Chol)(Reaven 1988). The author designated the clustering of these metabolic abnormalities as Syndrome X and pointed it as an increased risk for developing atherosclerotic cardiovascular disease (ACVD) in individuals with this syndrome (Reaven 1988).

Posteriorly, the abdominal obesity was also introduced as a clinical feature of MetS by Norman Kaplan, which named the clustering of metabolic abnormalities as the deadly quartet, thus including abdominal obesity, IGT, hyperglyceridemia and hypertension (Kaplan 1989). DeFronzo, Ferrannini and Haffner, in 1990s, attributed to IR the underlying pathogenic role

for the increased risk for CVD and TIIDM and nominated the IRS (DeFronzo and Ferrannini 1991). Later, it was documented the role of mutations in peroxisome proliferator-activated receptors-γ (PPAR-γ) in predisposition to the MetS (**Table 1**) (Sarafidis and Nilsson 2006).

The different clustering of metabolic abnormalities and names to designate the MetS, led to an effort from several health organizations to create a clinical definition of MetS, which could be important to identify individuals at high risk for developing both CVD and TIIDM (**Table 2**) (Alberti, Zimmet, and Shaw 2005; Grundy 2016).

In 1998, the first propose to define the MetS was from the World Health Organization (WHO) which attributed a pathological role of IR in the progression of other metabolic abnormalities (Sarafidis and Nilsson 2006). In this clinical definition, IR, identified by the presence of TIIDM or IGT, was required for establish a clinical diagnosis, as well as the presence of at least two other more metabolic abnormalities, including obesity (BMI >30kg/m^2), hypertension (blood pressure >140/90 mm Hg), high triglyceride (TG) levels (150 mg/dL or >1,7 mmol/L), low HDL-Chol (35 mg/dL in male and 40 mg/dL in female or <0,9 mmol/L in male and <1,0 mmol/L in female) or microalbuminuria (albumin excretion >20 µg/min)(Eckel et al. 2005; Alberti et al. 2009).

A year later, the European Group for the study of Insulin Resistance (EGIR) proposed an alternative to the WHO definition, in which the presence of IR with two more metabolic abnormalities, including abdominal obesity (waist circumference (WC) >94 cm in male and >80 cm in female), hypertension (blood pressure >140/90 mm Hg), dyslipidemia (high TG levels (TG >2,0 mmol/L) or low HDL-Chol (<1,0 mmol/L)), or hyperglycemia (fasting plasma glucose >6,1 mmol/L), were required for a clinical diagnosis (Eckel et al. 2005; Sarafidis and Nilsson 2006).

Another proposal to define MetS came in 2001, from the National Cholesterol Education Program Adult Treatment Panel III (NCEP/ATPIII) in the USA and was completed in 2002 (Eckel et al. 2005; Sarafidis and Nilsson 2006). This health organization integrated as metabolic abnormalities: abdominal obesity (WC >102 cm in male or >88 cm in female), hypertension (blood pressure >130/85 mm Hg), high TG levels (>150 mg/dL or >1,7 mmol/L), low HDL-Chol ((<40 mg/dL in male and <50 mg/dL in female or <1,0 mmol/L in male and <1,3 mmol/L in female) or hyperglycemia (fasting plasma glucose >110 mg/dL or >6,1 mmol/L)). According to this, for the establishment of the clinical diagnosis is required the presence of three metabolic

Table 1 | Timeline of the metabolic syndrome concept and its main metabolic abnormalities

	Kylin (1923)	**Vague** (1947)	**Hanefeld and Leonhardt** (1981)	**Reaven (**1988)	**Kaplan** (1989)	**DeFronzo Ferranini and Haffner** (1991)
Hypertension	✓	✓	✓	✓	✓	
Hyperglycemia	✓					
Gout	✓	✓	✓			
Obesity		✓	✓		✓	✓
IR				✓		✓
DM or IGT			✓	✓	✓	✓
Dyslipidemia				✓	✓	✓
ACVD						✓
Term	Hypertension, hyperglycemia and hyperuricemia syndrome	Clustering of metabolic abnormalities	Metabolic syndrome	Syndrome X	Deadly quartet	Insulin resistance syndrome

Table 1: Shows the timeline of the metabolic syndrome concept; the authors, the year of publication, the main metabolic abnormalities that composed the concept and the term used. **Abbreviations: ACVD:** atherosclerotic cardiovascular disease; **DM:** diabetes mellitus; **IGT**: impaired glucose tolerance; **IR:** insulin resistance.

abnormalities although IR is not included in this definition (Eckel et al. 2005; Sarafidis and Nilsson 2006; Cornier et al. 2008).

Another definition was proposed by the American Association of Endocrinology (AAE), in 2002, which nominated the MetS as IRS (Eckel et al. 2005). This health organization suggests that the main metabolic abnormalities of IRS are hypertension (blood pressure > 130/85 mm Hg), high TG levels (>150 mg/dL), low HDL-Chol (<40 mg/dL in male or <50 mg/dL in female), hyperglycemia (fasting plasma glucose (110-126 mg/dL) or post load plasma glucose (140-200 mg/dL)) and that obesity was not included (Eckel et al. 2005; Sarafidis and Nilsson 2006; Cornier et al. 2008).

In 2005, the International Diabetes Federation (IDF) proposed a distinct clinical definition considering different ethnic groups (Sarafidis and Nilsson 2006). In this IDF definition, the IR is not a metabolic abnormality required for establishing a clinical diagnosis. On the contrary, the abdominal obesity is one of the five metabolic abnormalities required (WC >94 cm in male or >80 cm in female, in Europe, or ethnicity-specific values four other groups) (Alberti et al. 2009). The remaining metabolic abnormalities included hypertension (blood pressure >130/85 mm Hg), high TG levels (>150 mg/dL or >1,7 mmol/L), low HDL-Chol (<40 mg/dL in males and <50 mg/dL in females or <1,03 mmol/L in males and <1,29 mmol/l in females), and hyperglycemia (fasting plasma glucose (>100 mg/dl or >5,6 mmol/L)) (Sarafidis and Nilsson 2006).

The American Heart Association/National Heart, Lung and Blood Institute (AHA/NHLBI), in 2005, slightly modified the NCEP/ATPIII definition, considering that abdominal obesity is not required for establishing a clinical diagnosis. Later, the IDF and the AHA/NHLBI agreed that abdominal obesity is a main metabolic abnormality, however not a requirement for the diagnosis (Sarafidis and Nilsson 2006).

Recently, the most commonly and consensus clinical definition for MetS includes abdominal obesity (WC >102 cm in male or >88 cm in female), IR, hypertension (blood pressure >130/85 mm Hg), dyslipidemia (high TG levels (>150 mg/dL or >1,7 nmol/L), low HDL-Chol (<40 mg/dL or 1 mmol/L in males and <50 mg/dL or 1,3 mmol/L in female) and

Table 2 | Comparisons of metabolic syndrome clinical definitions

Metabolic abnormalities	Measure	Cut points			
		WHO (1998)	**EGIR** (1999)	**NCEP/ATPIII** (2001)	**IDF** (2005)
Obesity		BMI >30k g/m^2	>94 cm in male or >80 cm in female	>102 cm in male or >88 cm in female	>94 cm in male or >80 cm in female
Dyslipidemia	**TG levels**	150 mg/dL or >1,7 mmol/L	>2,0 mmol/L	>150 mg/dL or >1,7 mmol/L	>150 mg/dL or >1,7 mmol/L
	HDL-Chol	<35 mg/dL in male and <40 mg/dL in female or <0,9 mmol/L and <1,0 mmol/L	<1,0 mmol/L	<40mg/dL in male and <50 mg/dL in female or <1,0 mmol/L and <1,3 mmol/L	<40 mg/dL in males and <50 mg/dL in females or <1,03 mmol/L and <1,29 mmol/l
Hypertension	**Blood pressure**	>140/90 mm Hg	>140/90 mm Hg	>130/85 mm Hg	>130/85 mm Hg
Hyperglycemia	**Fasting plasma glucose**		>6,1 mmol/L	>110 mg/dL or >6.1 mmol/L	>100 mg/dl or >5,6 mmol/L
Required for clinical diagnosis		IR or IGT + 2 MA	IR + 2 MA	Abdominal obesity + 2 MA	Abdominal obesity + 2 MA
Others		Albumin excretion >20 µg/min			

Table 2: Shows the metabolic syndrome clinical definition from several health organizations, the year of publication, the metabolic abnormalities required for the clinical diagnosis and their cut points. **Abbreviations: BMI:** body mass index; **EGIR:** European Group for the study of Insulin Resistance; **HDL-Chol:** high-density lipoprotein cholesterol; **IDF:** International Diabetes Federation; **IGT**: impaired glucose tolerance; **IR:** insulin resistance; **MA:** metabolic abnormalities; **mm Hg:** millimeter of mercury; **NCEP/ATPIII:** National Cholesterol Education Program Adult Treatment Panel III; **TG:** triglyceride; **WHO:** World Health Organization.

hyperglycemia (fasting plasma glucose (>100 mg/dl or >5,6 mmol/L)) as the common metabolic abnormalities. Individuals presenting three or more of these metabolic abnormalities are clinical diagnosed with MetS and for consequence high risk for CVD and TIIDM (**Table 3**) (Alberti et al. 2009; Grundy 2016).

Table 3| Metabolic abnormalities of consensus clinical definition of metabolic syndrome

Metabolic abnormalities	**Measure**	**Cut points**	
		Male	Female
Waist circumference		>102 cm	>88 cm
Dyslipidemia	TG levels	>150 mg/dL or >1.7 nmol/L	
	HDL-Chol	<40 mg/dL or 1 mmol/L	<50 mg/dL or 1.3 mmol/L
Hypertension	Blood pressure	>130/85 mm Hg	
Hyperglycemia	Fasting plasma glucose	>100 mg/dl or >5,6 mmol/L	

Table 3: Shows the metabolic abnormalities of the consensus clinical definition of metabolic syndrome and the cut points in males and females. **Abbreviations: HDL-Chol:** high-density lipoprotein cholesterol; **mm Hg:** millimeter of mercury; **TG:** triglyceride**.**

1.2. Epidemiology and susceptibility factors

The incidence of MetS is variable, as it depends on genetic and environmental factors, as well as, on the geographic location (urban or rural), features of the population (sex, age, race, BMI and ethnicity), and of course, on the clinical definition of MetS that was used. Susceptibility factors as socioeconomic status and tobacco exposure can also contribute to the MetS (Eckel et al. 2005; Sun, Liu, and Ning 2012; Kaur 2014). Worldwide, the MetS

incidence is increasing, which is being related to an increase of age, obesity and sedentary lifestyle and currently one-fourth of world population is clinically diagnosed with MetS (Cornier et al. 2008; Saklayen 2018).

1.3. Pathophysiology

As mentioned, the most common clinical definition of MetS includes IR, abdominal obesity, hypertension, dyslipidemia and hyperglycemia, as the common metabolic abnormalities found. However, from these, IR and obesity stand out for presenting a potential pathological role in the progression of the MetS (Alberti, Zimmet, and Shaw 2006).

1.3.1. Insulin resistance

1.3.1.1. Insulin synthesis and secretion

Insulin is an anabolic polypeptide hormone synthesized and secreted in the pancreatic islets of Langerhans by the β-cells. Insulin is a crucial regulator of carbohydrates, lipids and proteins metabolism, to maintain the whole-body glucose homeostasis and to promote cell division and growth (Pessin and Saltiel 2000; Wilcox 2005).

Initially, in β-cells of the pancreatic islets of Langerhans the ribosomes of the rough endoplasmic reticulum (RER) synthetize preproinsulin, a precursor of insulin. The preproinsulin is processed to proinsulin and transported from the RER to the trans-Golgi network into immature secretory granules. In these granules, the proinsulin is processed via prohormone convertases (PC1/3 and PC2), which are endopeptidases that convert proinsulin in mature insulin and connecting peptide (C-peptide) (Najjar 2003; Wilcox 2005). Posteriorly, mature insulin, in mature secretory granules, wait for metabolic signals, as high blood glucose levels and other stimuli, to be released from β-cells by exocytosis into the circulation (Najjar 2003). Insulin is secreted into the portal venous circulation for clearance on liver, whereas the remaining insulin exits to the systemic circulation to exert its action in the central and sympathetic nervous system (CNS and SNS), as well as in peripheral organs and tissues as the skeletal muscle, adipose tissue and liver (Tokarz, MacDonald, and Klip 2018).

1.3.1.2. Insulin action in the central nervous system

Insulin can cross the blood-brain barrier (BBB) through brain-specific receptors and act in the regulation of energy homeostasis, through the regulation of food consumption and energy expenditure, in the arcuate nucleus (ARC) of hypothalamus (Tokarz et al. 2018). Insulin can cause a decrease of the expression of orexigenic neuropeptides, as neuropeptide Y (NPY) and Agouti-related peptide (AgRP) and an increase of the expression of anorexigenic neuropeptides, as pro-opiomelanocortin (POMC) and the cocaine and amphetamine-regulated transcript (CART) (Tokarz et al. 2018). The modifications in orexigenic and anorexigenic neuropeptides expression results in a diminution of appetite and an increase in energy expenditure.

1.3.1.3. Insulin action in sympathetic nervous system

Insulin also stimulates the SNS activity on brown adipose tissue (BAT) to promote heat production from mitochondrial fatty acid (FA) oxidation. This process is known as thermogenesis (Porte, Baskin, and Schwartz 2005).

1.3.1.4. Insulin action in peripheral organs and tissues

The action of insulin in peripheral organs and tissues is related with regulation of whole-body glucose homeostasis. Organs and tissues, as the skeletal muscle and the adipose tissue, need tissue-specific insulin signal transduction pathways to execute their physiological functions (Petersen and Shulman 2018). Insulin and glucagon, the principal counter-regulatory hormone of insulin, regulate the blood glucose levels (Tokarz et al. 2018). Posteriorly to food consumption and the subsequent high blood glucose levels, insulin binds to the extracellular subunit-α of the insulin receptor (INR), a heterotetrametric receptor tyrosine kinase in the plasmatic membrane of target cells (Schmeltz and Metzger 2007; Peterson, 2018). This leads to the activation of the intrinsic tyrosine kinase activity, which acts in regulation of tyrosine phosphorylation of the insulin receptor substrate (INRS) proteins. These INRS proteins act as docking platforms for phosphoinositide 3-kinases (PI3K) and the activation of the PI3K/Akt pathway promotes the stimulation of glycogen synthesis, inhibition of gluconeogenesis and stimulation of cellular glucose uptake (Könner and Brüning 2012).

Insulin acts in inhibiting glucose production in the liver (gluconeogenesis and glycogenolysis), through the direct action on hepatic insulin receptors and stimulation of

genetic transcription of enzymes that are involved in glycolytic pathways, when a glucose stimulus occurs (McCracken, Monaghan, and Sreenivasan 2017). In the skeletal muscle and adipose tissue, insulin induces the cellular glucose uptake through the simulation of glucose transporter 4 (GLUT4) translocation to the plasmatic membrane of myocytes and adipocytes and the intra-cellular captation of glucose (Wilcox 2005; Schmeltz and Metzger 2007; Petersen and Shulman 2018). Posteriorly to the glucose entry in myocytes and adipocytes, the glucose is stored as glycogen and TG, which is used for glycolysis and for physical functions. Insulin also presents an important role on lipolysis inhibition and consequently in regulation of blood free fatty acids (FFA) levels (Petersen and Shulman 2018). In conditions of low blood glucose levels, the levels of glucagon and catecholamines levels increase, the insulin levels decrease, occurring a stimulation of translocation and transport of FFA from adipocytes to the skeletal muscle, liver and to other organs and tissues, for oxidation or re-esterification, to form TG, and for physiological functions (Vázquez-Vela, Torres, and Tovar 2008).

In low blood glucose conditions, when energy expenditure is superior to energy consumption, lipolysis increases in adipose tissue, occurring synthesis of FAs from TGs stored in lipid droplets (Vázquez-Vela et al. 2008). This TG are initially hydrolyzed by the enzyme adipose TG lipase (ATGL) releasing a diacylglycerol and FA. Subsequently, diacylglycerols are hydrolyzed by action of cyclic AMP-dependent enzyme hormone sensitive lipase (HSL) and monoglyceride lipase producing FFA, that are non-esterified fatty acids (NEFA), and glycerol, which is posteriorly used to produce energy (Vázquez-Vela et al. 2008).

1.3.1.5. Insulin resistance

In many definitions of MetS, the IR stand out for its pathological role in the progression of MetS. IR is commonly described as an inability in insulin action, which results in fasting hyperinsulinemia, which is characterized by a high insulin secretion to maintain euglycemia, in pancreatic β-cells dysfunction and impaired intra-cellular captation of glucose (Reaven 1988; Eckel et al. 2005; Brown and Walker 2016). Upon an excess of food consumption, the β-cells of the pancreatic islets of Langerhans increase the insulin secretion as a compensatory mechanism to maintain euglycemia (McCracken et al. 2017). However, with a continuous excess of food consumption, the β-cells become incapable of secreted sufficient insulin in response to glucose stimulus (**Figure 1**). Subsequently it occurs an incorrectly intra-cellular

captation of glucose by GLUT4 and an incorrectly antilipolytic effect of insulin, which result in hyperglycemia (Kahn, Hull, and Utzschneider 2006).

Moreover, in IR, the peripheral organs and tissues are incapable of maintaining a normal glucose response, involving the suppression of lipolysis and glucose production in liver, intra-cellular captation of glucose by GLUT4 and glycogen synthesis in the presence of normal blood insulin levels (Petersen and Shulman 2018). When an inappropriate and excessive lipolysis of stored TG occurs, FFA are secreted an abundance into circulation and ectopic lipid accumulation occurs, which create insulin resistance by adding substrate availability and modifying the downstream signaling in the liver and skeletal muscle. The overabundance of FFA leads to the inhibition of insulin antilipolytic effect on lipolysis in the liver and skeletal muscle, contributing in IR (Eckel et al. 2005; Arora 2010; McCracken et al. 2017).

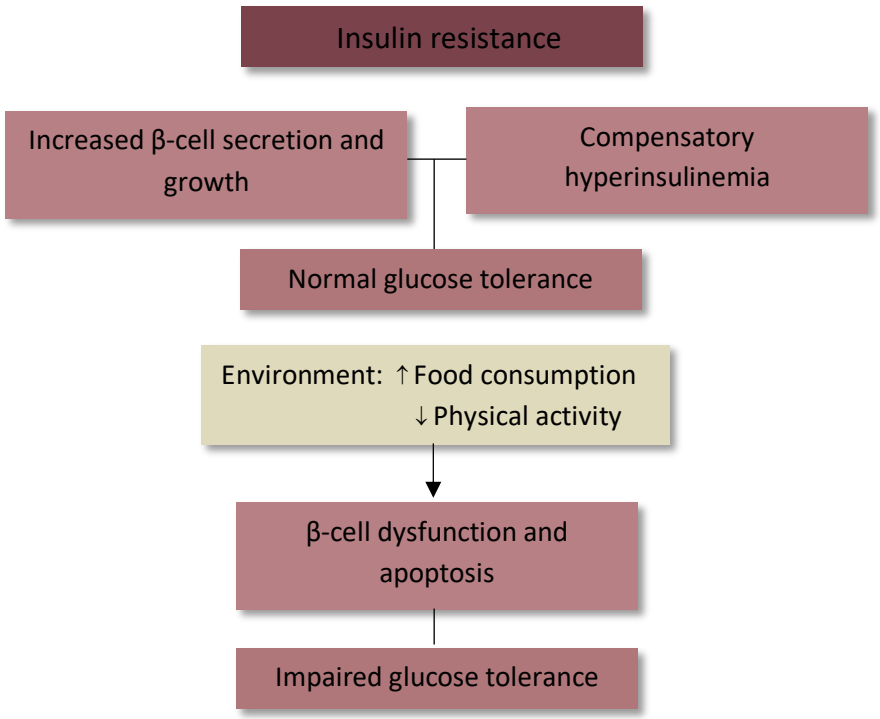

Figure 1 | Mechanism of insulin resistance

Insulin resistance is commonly characterized by an increase of the pancreatic β-cells insulin secretion and growth, as a compensatory mechanism to maintain euglycemia. Upon a continuous excess of food consumption and other risk factors, the pancreatic β-cells became dysfunctional occurring an impaired glucose tolerance.

Defects in insulin receptors and in insulin signaling pathway are strongly correlated with IR (Hunter and Garvey 1998). In fact, several mutations in *INR* gene have been identified in patients with IR (Hunter and Garvey 1998). The main mutations in the INR included: non-sense or frame-shift mutations, which promote a premature stop codon and as consequence termination of translation and decrease of receptor synthesis; mutations that impair intra-cellular transport and post-translational processing of receptors; mutations in the insulin binding domain, which affect the ligand affinity; and mutations that promote endocytosis and degradation of insulin receptors (Hunter and Garvey 1998). Decreases in the tyrosine kinase activity, accompanied by impaired phosphorylation of INR and activation of PI3K, and decreases in GLUT expression were also identified in patients with obesity and TIIDM (Hunter and Garvey 1998).

The autophagy is a process involved in the degradation of cytoplasmatic components, such as damaged organelles and proteins, producing energy for cells in low nutrient conditions (Yorimitsu and Klionsky 2005). Significant defects in autophagy, accompanied with ER stress and IR, were observed in *ob/ob* mice (Yang et al. 2010).

In addition, in obesity occurs a lipid accumulation in the adipose tissue that result in an abundant secretion of FFA, adipokines, pro-inflammatory cytokines, which acts in the liver and skeletal muscle modifying the inflammatory response and inducing insulin resistance through multiple mechanisms (Olefsky and Glass 2010).

The PPAR-γ is a member of the nuclear receptor superfamily of ligand-inducible transcription factors 1. PPAR-γ is more expressed in white adipose tissue (WAT) and BAT, where is a regulator of adipogenesis and a potent modulator of whole-body lipid metabolism and of insulin sensitivity (Maruam et al. 2013). In fact, thiazolidinediones (TZD), which are antidiabetic agents that act directly reducing the systemic insulin resistance of peripheral organs and tissues through promotion of the insulin stimulated glucose uptake, are high-affinity PPAR-γ ligands (He et al. 2003; Lehrke and Lazar 2005). Previous observations documented that mutations in PPAR-γ are correlated with severe insulin resistance (Barroso et al. 1999). However, other mechanisms act in IR and are also involved in many pathologies (Petersen and Shulman 2018).

1.3.2. Obesity

1.3.2.1. Definition of obesity

Obesity is a condition resulting from an abnormal or excessive accumulation of adipose tissue and posterior changes in physiological functions, as consequence of an abundant food consumption, genetic factors and sedentary lifestyle, which results in an imbalance between calories intake and calories consumption (Kopelman 2000). Three types of obesity forms were documented based on genetic and phenotypic characteristics. 1) The monogenic syndromic obesity, resulting from mutations in *Wilm's tumor 1*, *paired box 6* and other genes; 2) the monogenic non-syndrome obesity form, characterized by mutations in leptin *(Lep)*, Lep receptor (*LepR)*, *POMC*, melanocortin receptor 4 (*MC4R)* genes which result in extreme obesity with an early-onset obesity and endocrine dysfunctions, and 3) the polygenic obesity form, which is the most common form of obesity and result from alterations in several genes (Albuquerque et al. 2015).

In obesity, the accumulation of the adipose tissue can be distributed in different parts of the organism. In generalized obesity, more common in women, the adipose tissue is distributed around the body, whereas in abdominal obesity, more common in men, the distribution of adipose tissue can be visceral or subcutaneous (Grundy 2016). The visceral adipose tissue has an important role in the secretion of FFA into circulation (Grundy 2004). The subcutaneous adipose tissue is divided into gluteofemoral and upper-body adipose tissue and is a major contributor to metabolic abnormalities and further progression to MetS (Grundy 2004; Grundy 2016).

1.3.2.2. Adipocytokines secretion from adipose tissue in obesity

The adipose tissue exhibits important functions related with the secretion of adipocytokines, which integrates the endocrine, autocrine and paracrine signals that regulates several processes, such as insulin sensitivity, energy homeostasis and inflammation (Kaur 2014).

Adipocytes can respond rapidly and dynamically to overabundant food consumption through adipocytes hypertrophy and hyperplasia (Kaur 2014). In obesity, the existence of adipocytes hypertrophy leads to a dysfunction in the production of adipocytokines such FFA, adiponectin, Lep, resistin, inflammatory cytokines, angiotensinogen and plasminogen activator inhibitor-1 (PAI-1) (**Figure 2**) (Grundy 2016; Furukawa et al. 2017).

In obesity, it also occurs an increase in secretion of FFA into circulation, resulting from the lipolysis of TG in WAT. The amount of FFA secreted are directly proportional to the amount of TG stored in adipose tissue and inversely proportional to the antilipolytic effect of insulin that contributes to IR and other metabolic abnormalities (Grundy 2004; Grundy 2016). Moreover, overabundance of FFA results in an increase of TG content in liver, known as fatty liver, which can progress to non-alcoholic fatty liver disease (NAFLD) (Grundy 2004).

Adiponectin is an important adipocytokine secreted by the WAT for the regulation of glucose homeostasis, insulin sensitivity, food consumption, body weight (BW) and for protection against inflammation. Adiponectin also suppresses gluconeogenic enzymes in liver, increases glucose captation in skeletal muscle and enhances FA oxidation (Kaur 2014). The adiponectin levels are inversely correlated with metabolic abnormalities as dyslipidemia and hypertension (Kaur 2014). Lep, whose levels are increased in obesity, is involved in the regulation of satiety, food consumption and energy expenditure through the LepR in the hypothalamus and in the brain stem. Lep also acts in the hypothalamus through the activation of SNS to increase the blood pressure, thus contributing to hypertension (Kaur 2014).

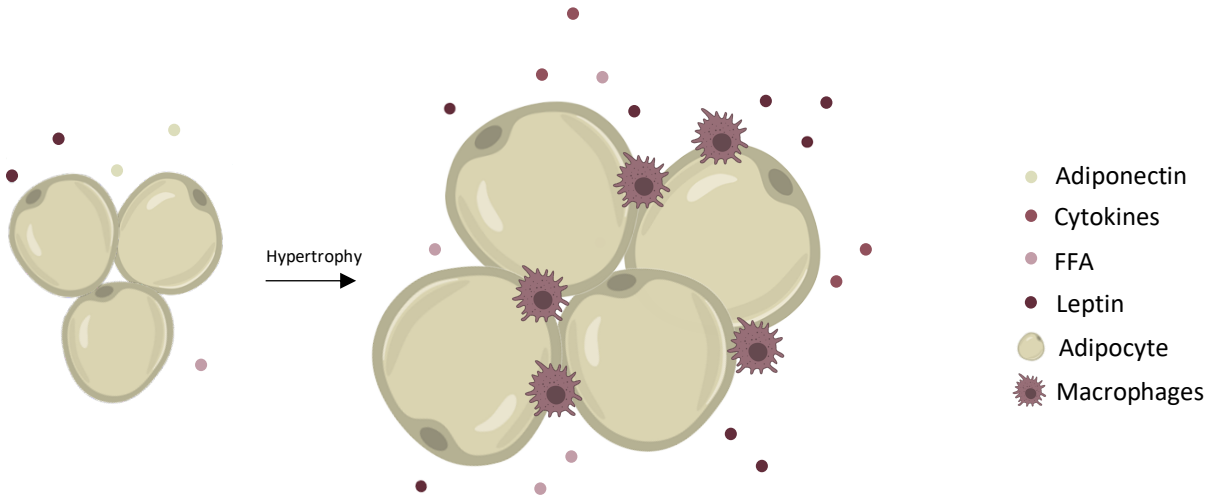

Figure 2 | Adipocytokines dysfunctional secretion from white adipose tissue in obesity

The adipose tissue exhibits important functions related with the secretion of adipocytokines, which regulates several processes, such as insulin sensitivity, energy homeostasis and inflammation. The adipocytes can respond rapidly and dynamically to overabundant food consumption through adipocytes hypertrophy and hyperplasia. In hypertrophic adipocytes occur an increase in the production of adipocytokines such as FFA and Lep, a decrease in the production of adiponectin and infiltration of macrophages. This dysregulated production of adipocytokines and cytokines, such as

TNF-α and IL-6, promotes a pro-inflammatory state and ectopic accumulation in the liver and in the skeletal muscle contributing to the IR in these metabolic organs. **Abbreviations: FFA:** free fatty acids.

1.3.2.3. Obesity and inflammation

In obesity and with the progressive adipocyte hypertrophy, hypoxia (low blood oxygen) can occur, which leads to macrophages infiltration into the adipose tissue. The monocyte chemoattract protein-1 (MCP-1), is a potent signal for the recruitment of macrophages into adipose tissue. It exists in high levels in blood in obesity, leading to an increase on macrophages infiltration in obesity, and posteriorly to a pro-inflammatory state and an additional overproduction of adipocytokines, such as, tumor necrosis factor-α (TNF-α) and interleukin 6 (IL-6). This overabundance of adipocytokines results in a localized inflammation that propagates to a systemic inflammation into other peripheral organs and tissues contributing to the IR observed in obesity (Kaur 2014). TNF-α and IL-6 are increased in individuals with obesity (Grundy 2004). TNF-α is a pro-inflammatory cytokine that act in adipose tissue to decrease the insulin sensitivity of adipocytes (Kaur 2014).TNF-α promotes adipocyte apoptosis and acts in the regulation of other pro-inflammatory cytokines, whereas IL-6 can act as anti-inflammatory and pro-inflammatory cytokine, and controls the appetite and food consumption, acting in the hypothalamus (Kaur 2014). IL-6 is secreted by the adipose tissue and skeletal muscle and their receptor is expressed in several regions of the brain. In obesity, it exists an increase of this inflammatory cytokine, being involved in IR and in the production of C-reactive protein (CRP) in the liver (Grundy 2004). IR and other metabolic abnormalities are correlated with high levels of CRP, which are correlated with a pro-inflammatory state (Alberti et al. 2006; Kaur 2014). This inflammatory state, that occur in obesity and results in IR and other metabolic abnormities found in MetS, accounts for an increased risk of CVD and DM (Wisse 2004).

1.3.2.4. Obesity and the metabolic syndrome

Obesity is strongly correlated with metabolic abnormalities, such as dyslipidemia, hypertension, inflammation and CVD, through the hypertrophy of adipocytes and consequent dysfunction in the secretion of adipocytokines. Given the strong correlation between obesity and metabolic abnormalities, in many clinical definitions of MetS the obesity was required to

stablish a clinical diagnosis and individuals with abdominal obesity, that can be measured by WC, have an increased risk for CVD, specially ACVD, and TIIDM.

1.3.3. Hypertension

Hypertension is commonly correlated with several metabolic abnormalities such obesity, dyslipidemia and CVD (Kaur 2014). The IR results in an increase of renal reabsorption sodium, expansion of intravascular volume, activation of renin-angiotensin system (RAS) and SNS, which acts in the regulation of blood pressure (Grundy 2016). An increase of angiotensinogen secretion from adipose tissue in obesity also contributes to hypertension through arteries response with vasoconstriction (Kaur 2014).

1.3.4. Dyslipidemia

This metabolic abnormality is characterized by abnormalities in lipids, perturbing the structure, metabolism and biological activities of lipoproteins and antiatherogenic HDL-Chol and its commonly present in individuals with established clinical diagnosis for MetS (Kaur, 2014).

Insulin suppresses the production and secretion of apolipoprotein B (ApoB), an important lipoprotein of VLDL particle (Cornier et al. 2008). In IR, occurs an overabundance of FFA levels in liver, which are used for TG synthesis, stabilizing the ApoB production, and as result an increase in the TG and VLDL production (Eckel et al. 2005). This increase in TGs levels is also known as hypertriglyceridemia and is strongly correlated with an increased risk for CVD (Ginsberg 2000). Other lipoprotein abnormality in MetS is a reduction in HDL-Chol and small dense LDL particles, which are also correlated with higher risk for developing ACVD (Grundy 2016).

1.4. Risks associated with the metabolic syndrome

The clustering of metabolic abnormalities, which constitute the MetS is strongly correlated with an increase of risk for CVD and TIIDM (Cornier et al. 2008). Individuals with MetS have at least a 2-fold increase of risk for ASCVD in comparison with healthy individuals (Grundy 2004).

TIIDM is characterized by IR in the adipose tissue, liver and skeletal muscle, and by an incorrect insulin secretion due to dysfunctions in β-cells (Schmeltz and Metzger 2007). Individuals with MetS, both men and female, have a 5-fold increase of risk for TIIDM (Grundy 2004).

1.5. Correlated conditions

1.5.1. Non-alcoholic fatty liver disease

Liver is an organ that is vulnerable to ectopic fat accumulation as consequence of an increased influx of FFA to the liver (Cornier et al. 2008). This accumulation can lead to different disease conditions, including NAFLD. This disease ranges from simple fatty liver, known as steatosis, to more severe steatosis coupled with marked inflammation, known as non-alcoholic steatohepatitis (NASH), which can progress to fibrosis, liver cirrhosis and liver failure (Bruce and Byrne 2009). The NAFLD is commonly correlated with MetS and severe NAFLD is also correlated with CVD pathogenesis (Bruce and Byrne 2009). NAFLD, as consequence of ectopic fat accumulation, can lead to hepatocellular carcinoma (Bruce and Byrne 2009).

1.5.2. Polycystic ovary syndrome

Polycystic ovary syndrome (PCOS) is a syndrome correlated with high androgen levels and IR. Women with obesity have a higher incidence of PCOS and have fertility problems as consequence of high androgen levels. The presence of IR in this condition seems to have a pathological role, and when is correlated with obesity is implicated in a clustering of metabolic abnormalities and an increase of the risk for CVD (Cornier et al. 2008).

1.5.3. Cancer

The MetS is composed of many pathologies that can contribute to cancer development and progression (Cowey and Hardy 2006). However, this correlation between the MetS and cancer is complex, involving many metabolic abnormalities that can increase the incidence for several types of cancer (Micucci et al. 2016). Cancer is group of numerous distinct neoplasia diseases characterized by a multistep process involving genetic modifications in normal cells, which progressively become tumorigenic and malignant (Hanahan and Weinberg 2011). The hallmarks of cancer comprise ten biological capabilities acquired during the multistep

development and progression of tumors, including: sustentation of proliferative signaling, evasion of growth suppressor, resistance to cell death, enabling replicative immortality, inducing angiogenesis, activating invasion and metastasis, genome instability, promoting inflammation, reprogramming of energy metabolism and evading immune destruction (Hanahan and Weinberg 2011).

Obesity, a common metabolic abnormality of MetS, is strongly correlated to a high risk of cancer incidence due to dysfunctions in secretion of adipokines, cytokines and various growth factors, such as adiponectin, Lep, TNF-α, IL-6 and vascular endothelial growth factor (VEGF) by WAT. As the adiponectin is characterized by anti-inflammatory properties, the low level of adiponectin in obesity can increase the incidence of breast, endometrial and gastric cancers (Micucci et al. 2016). Moreover, dysregulations in Lep secretion, which results in an increase of Lep levels in obesity, act in cancer progression through neoplasia transformation promotion, cancer cells proliferation and tumor angiogenesis, increasing this way the incidence of prostate, colon, breast and endometrial cancers. Additionally, the increase of proangiogenic factors secretion, such as VEGF, which is involved in tumor formation and metastasis, intensifying the incidence for several types of cancers (Micucci et al. 2016).

Cytokines dysregulated secretion, such TNF-α and IL-6, play a crucial role in pathogenesis of cancer, promoting the angiogenic process, cancer cells proliferation and ROS formation (Micucci et al. 2016). Chronic hyperinsulinemia is also correlated to colorectal, pancreatic, endometrial and breast cancer through dysfunction in insulin signaling pathway involved in cancer cell proliferation (Micucci et al. 2016).

1.5.4. Obstructive sleep apnea

Obstructive sleep apnea (OSA) is characterized by recurrent upper airway obstruction resulting in hypoxia and other dysfunctions (Tasali and Ip 2008). OSA correlated dysfunctions, such as the hypoxia, the high levels of pro-inflammatory cytokines and the dysregulation of adipokines are involved in the development and progression of obesity and of MetS. In fact, OSA severity is correlated with the incidence of the MetS (Calvin et al. 2009).

1.6. Therapeutic strategies

Individuals presenting clinical diagnosis for MetS mostly are obese and mostly have a sedentary lifestyle. This way, current therapeutic strategies focus mainly in BW loss through

caloric restriction and an increase of physical activity. Through caloric restriction, a reduction in carbohydrate, protein and fat consumption can lead to BW loss, improving all the metabolic abnormalities correlated with the MetS (Cornier et al. 2008). A reduction in sodium consumption through diet also had a strong impact improving the regulation of blood pressure (Cornier et al. 2008).

The metformin treatment combined with changes in lifestyle resulted in a decrease of the incidence for TIIDM in individuals with high risk (Knowler et al. 2002). The metformin act in the reduction of fasting plasma glucose concentration through reduction of hepatic glucose production rate (Hundal et al. 2000). The metformin treatment act in the reduction of plasma FFA concentration in patients with DM (Hundal et al. 2000).

Complete cessation of smoking and antihypertensive drugs to control hypertension is also a therapeutic strategy (Eckel et al. 2005).

2. Hypothalamus

2.1. Localization and structure of hypothalamus

The hypothalamus is an important part of diencephalon located at medio-basal region of the brain, ventrally to thalamus and dorsally to the pituitary gland (Machluf, Gutnick, and Levkowitz 2011). It is bordered anteriorly by the rostral limit of optic chiasm (OC), laterally by the optic tracts and posteriorly by the caudal limit of mammillary body (MB) (Saper and Lowell 2014). From rostral limit of OC to the caudal limit of MB the hypothalamic nuclei that composed the hypothalamus are distributed in three zones: the preoptic area (POA), the tuberal hypothalamus and the posterior hypothalamus (**Figure 3**) (Saper and Lowell 2014).

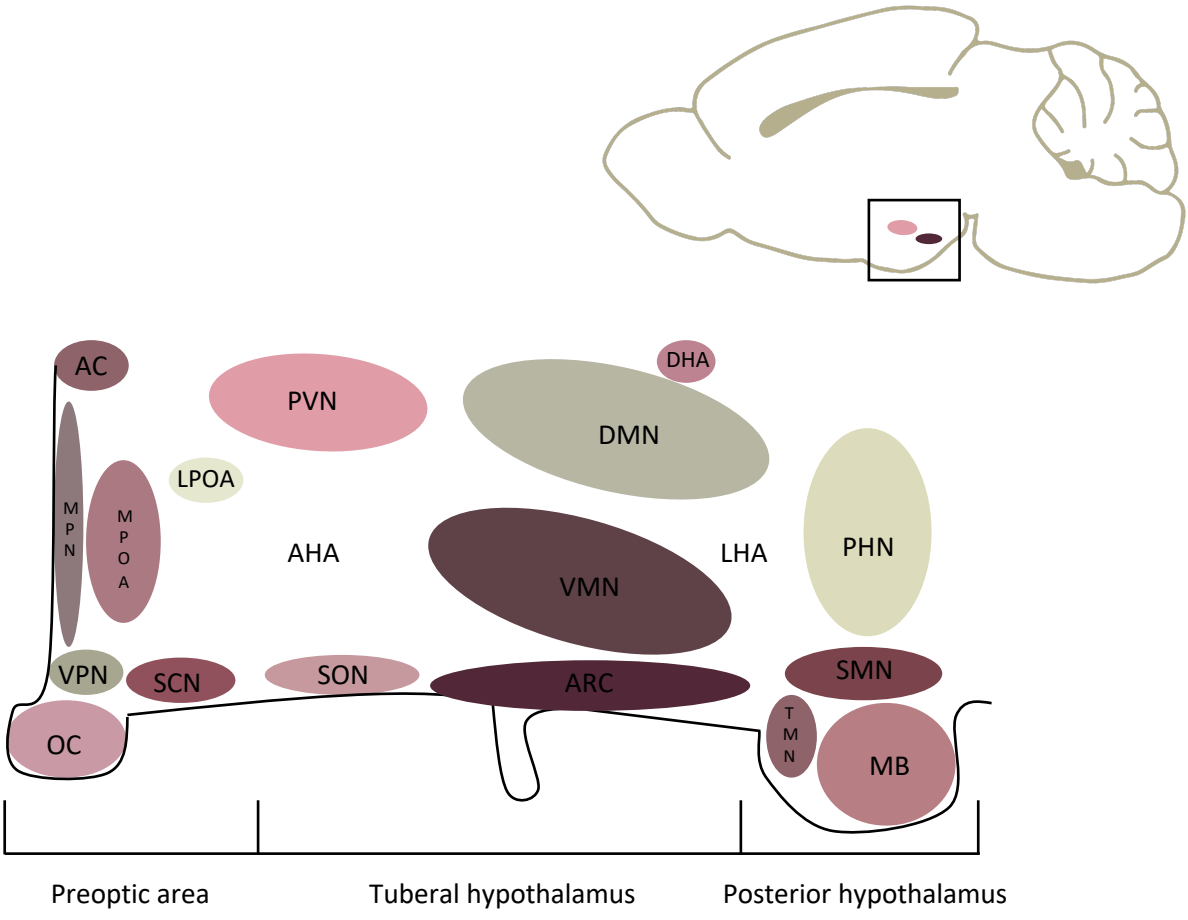

Figure 3| Hypothalamic nuclei

The midsagittal section of a brain and hypothalamic nuclei. The hypothalamic nuclei that composed the hypothalamus are distributed in three zones, from the rostral limit of optic chiasm to the caudal limit of mammillary bodies: the preoptic area, the tuberal hypothalamus and the posterior

hypothalamus. The preoptic area is localized above the OC and is composed by the median and ventrolateral preoptic nuclei, the medial and lateral preoptic areas and the suprachiasmatic nucleus. The tuberal hypothalamus is composed by: the anterior and lateral hypothalamic areas, the dorsomedial, ventromedial, paraventricular, arcuate and supraoptic nuclei, the dorsal hypothalamic area. The posterior hypothalamus is composed by the mammillary body, the tuberomammillary, supramammillary and posterior hypothalamic nuclei. Adaptation from: (Saper and Lowell 2014). **Abbreviations: AC:** anterior commissure; **AHA:** anterior hypothalamic area; **ARC:** arcuate nucleus; **DHA:** dorsal hypothalamic area; **DMN:** dorsomedial nucleus; **LHA:** lateral hypothalamic area; **LPOA:** lateral preoptic area; **MB:** mammillary body; **MPN:** median preoptic nucleus; **MPOA:** medial preoptic area; **OC:** optic chiasm; **PHN:** posterior hypothalamic nucleus; **PVN:** paraventricular hypothalamic nucleus; **SCN:** suprachiasmatic nucleus; **SMN:** supramammillary nucleus; **SON:** supraoptic nucleus; **TMN:** tuberomammillary nucleus; **VMN:** ventromedial nucleus; **VPN:** ventrolateral preoptic nucleus.

The hypothalamic nuclei that compose the hypothalamus include the arcuate nucleus (ARC), the paraventricular nucleus (PVN), supraoptic nucleus (SON), suprachiasmatic nucleus (SCN), dorsomedial nucleus (DMN), ventromedial nucleus (VMN), anterior and lateral hypothalamus area (AHA and LHA) (Qin, Li, and Tang 2018). The POA is localized above the OC and is composed by the median (MPN) and ventrolateral preoptic (VPN) nuclei, the medial and lateral POAs (MPOA and LPOA) and the SCN. The tuberal hypothalamus is composed by: AHA, LHA, DMN, VMN, PVN, SON, DHA and ARC. The posterior hypothalamus is composed by the MB, the tuberomammillary (TMN), supramammillary (SMN) and posterior hypothalamic nuclei (PHN) (**Figure 3**) (Saper and Lowell 2014).

The hypothalamic nuclei contain distinct populations of neuronal cells that communicate each other, with other hypothalamic nuclei and with other parts of the brain (Biran et al. 2015). These populations of neuronal cells integrate internal and external sensory signals, process the signals and through the production of neurotransmitters and neuropeptides provides autonomous, endocrine and behavior responses acting in the regulation of physiological functions (Carmo-silva and Cavadas 2017).

2.2. Hypothalamic nuclei

The ARC is located close to the third ventricle, to the pituitary gland and to the median eminence (ME), which present a BBB with fenestrated capillaries providing to the populations of neuronal cells access to circulating peripheral nutrient signals and hormones, from metabolic organs and tissues such the stomach, gut, pancreas and adipose tissues (Roh and Kim 2016; Carmo-silva and Cavadas 2017). These peripheral nutrient signals and hormones,

such as ghrelin, insulin and Lep, are integrated in ARC by first-order orexigenic and anorexigenic neurons, which project their axons into second-order neurons of PVN, LHA and autonomic preganglionic neurons in the brain stem and spinal cord orchestrating the regulation of whole-body energy homeostasis (Roh and Kim 2016).

The PVN is also located close to the third ventricle and is composed by distinct populations of neural cells (Swanson and Sawchenko 1980). The PVN integrate signals from distinct hypothalamic nuclei, as the ARC, and their populations of neurons projects the axons to the ME, to the posterior pituitary gland, to the brainstem and to the spinal cord (Swanson and Sawchenko 1980). This nucleus is also densely innervated by NPY/AgRP and POMC/CART neurons and operate as second-order neurons, acting in the regulation of energy homeostasis (Roh and Kim 2016).

The DMN is involved in several physiological processes, including energy homeostasis, the thermogenesis, stress responses and circadian rhythms. This nucleus receive projections from most of the hypothalamic nuclei, specially from the ARC, and project their axons into the PVN and LHA nuclei (Chao et al. 2011; Guan et al. 1998).

The LHA contains two distinct population of neurons that produce melanin-concentrating hormone (MCH) and orexin (Berthoud, 2011). The orexin act in activation of AgRP/NPY orexigenic neurons and in inhibition of POMC anorexigenic neurons in the ARC (Berthoud and Munzberg 2011).

2.3. Hypothalamus functions

The hypothalamus has a crucial role in the control of whole-body homeostasis, regulation of the endocrine system and of the autonomic nervous system (Mayer et al. 2009). In the control of whole-body homeostasis, the hypothalamus acts in the regulation of water balance, thermogenesis, energy and glucose homeostasis and circadian rhythm. Concerning the control of endocrine system, the hypothalamus via pituitary gland, acts in the regulation of reproduction, growth, stress and energy homeostasis. The hypothalamic autonomic nervous system (ANS) regulation includes the control of blood pressure, gut mobility and respiration (Mayer et al. 2009; Saper and Lowell 2014).

2.3.1. Hypothalamic regulation of whole-body energy homeostasis

Several hypothalamic nuclei such the ARC, VMN, DMN, PVN and LHA, are involved in the

control of whole-body energy homeostasis, providing an equilibrium between food intake and energy expenditure (Carmo-silva and Cavadas 2017).

2.3.2. Regulation of food consumption

In ARC exits two populations of first-order neurons with opposing functions, the orexigenic neurons and the anorexigenic neurons. The first-order orexigenic neurons, the NPY and AgRP neurons integrate the peripheral signals, producing and releasing the neurotransmitter NPY and the neuropeptide AgRP providing orexigenic and anti-thermogenic signals (**Figure 4**) (Cavadas et al. 2016). On the other hand, the first-order anorexigenic neurons, POMC and CART neurons integrate the peripheral signals and release the neurotransmitters POMC and CART providing anorexigenic signals and pro-thermogenic signals (Cavadas et al. 2016). POMC anorexigenic neurons release melanocortin neuropeptides (α-, β-, and γ-melanocyte stimulating hormone (MSH) by post-translational processing of POMC) (Zagmutt et al. 2018).

NPY and AgRP neurons act in the stimulation of hunger through the release of NPY, which acts as a neurotransmitter in Y1 and Y2 receptors in the second-order neurons, and through the release of the AgRP neuropeptide, which is a melanocortin antagonist that inhibits the binding of α-MSH into MC3R and MC4R, thus increasing the hunger. NPY and AgRP neurons also release GABA which is an inhibitory neurotransmitter that have orexigenic action through GABAergic mediated inhibition of POMC/CART anorexigenic neurons (Zagmutt et al. 2018). CART anorexigenic neurons are colocalized with the POMC anorexigenic neurons, acting in the inhibition of appetite and food intake through of production of the peptides CART I and CART II (Elias et al. 1998; Lau and Herzog 2014).

2.3.3. Regulation of energy expenditure

Physical activity, metabolism and thermogenesis are processes of energy expenditure controlled by the brain (Roh and Kim 2016). Thermogenesis refers to the process of heat production in order to maintained body temperature or in order to dissipate excess energy after food consumption, and occurs in BAT (Roh and Kim 2016). The high mitochondrial density, oxidation capacity and expression of the uncoupling protein-1 (UCP-1) in the inner mitochondrial membrane, allows that thermogenesis occur in BAT. The UCP-1 is a proton transporter that disrupts the mitochondrial electrochemical gradient through the leak of

protons across the inner mitochondrial membrane. UCP-1 uncouples mitochondrial oxidative phosphorylation leading to energy loss in form of heat (Kozak and Anunciado-Koza 2008).

In addition to food consumption regulation, the ARC also regulates the energy expenditure through NPY/AgRP neurons, which reduce BAT thermogenesis (Waterson and Horvath 2015; Contreras et al. 2017;). Conversely, POMC anorexigenic neurons through a α-MSH-modulation of PVN and DMN population of neurons increase BAT thermogenesis (Waterson and Horvath 2015).

2.3.4. Hypothalamic regulation of peripheral energy metabolism

2.3.4.1. Hypothalamic regulation of autonomic nervous system

The CNS integrates signals of energetic availability, from the peripheral metabolic organs and tissues, and response through regulation of food consumption and energy expenditure (Carmo-silva and Cavadas 2017). The ANS is responsible for the innervation of peripheral metabolic organs such the liver, WAT, BAT, pancreas, and skeletal muscle (Carmo-silva and Cavadas 2017). It is important in the regulation of BAT thermogenesis and also plays a role in the regulation of lipid metabolism in WAT, in hepatic glucose production, in pancreatic insulin secretion and in muscle glucose uptake (Seoane-Collazo et al. 2015).

2.4. Hormones, peptides and other signaling molecules

POMC/CART and AgRP/NPY neurons express receptor for peripheral metabolic hormones such as insulin, Lep and ghrelin. Upon food consumption, the high blood glucose and FFA levels, along with the high levels of insulin and Lep act in ARC activating POMC/CART anorexigenic neurons and inhibiting NPY and AgRP orexigenic neurons (Roh and Kim 2016). The activation of POMC/CART anorexigenic neurons and the inhibition of NPY/AgRP orexigenic neurons results in a decrease of food consumption, promoting satiety, and an increase of energy expenditure (Carmo-silva and Cavadas 2017). Previously, was reported that deletions in insulin and Lep receptors from POMC neurons results in systemic insulin resistance (Hill et al. 2010).

Ghrelin is a gut hormone of 28 amino acids secreted from stomach in fasting conditions. In fasting conditions, the gastric epithelium produce and secrete ghrelin, which binds with the ghrelin receptor in the ARC, activating NYP/AgRP orexigenic neurons, leading to a posterior

inhibition of POMC neurons through releasing of NPY and GABA, thus promoting food consumption (Carmo-silva and Cavadas 2017). Upon food consumption its levels are decreased, resulting in an activation of POMC anorexigenic neurons and inhibition of NPY/AgRP orexigenic neurons (**Figure 4**) (Waterson and Horvath 2015; Roh and Kim 2016). This inhibition of orexigenic neurons results in a decrease of food consumption (Roh and Kim 2016). Ghrelin also play a role in promotion of body weight gain and adiposity through direct effects on PVN neurons (Andrews 2011). Additional nutrient signals, hormones and peptides are also implicated in the control of food consumption (**Table 4**).

Table 4| Anorexigenic and orexigenic molecules in the control of energy homeostasis

	Site of production	**Type**	**Function**
POMC/CART	Hypothalamus	Neuropeptide	Anorexigenic
AgRP/NPY	Hypothalamus	Neuropeptide	Orexigenic
GABA	Hypothalamus	Neurotransmitter	Anorexigenic
Glucose and FFA		Nutrient	Anorexigenic
Insulin	Pancreas	Hormone	Anorexigenic
Leptin	WAT	Hormone	Anorexigenic
Ghrelin	Stomach	Hormone	Orexigenic
GLP-1	Gut	Peptide	Anorexigenic
CKK	Gut	Peptide	Anorexigenic
Peptide YY3-36	Gut	Peptide	Anorexigenic
Orexin	Hypothalamus	Neuropeptide	Orexigenic
MCH	Hypothalamus	Hormone	Orexigenic

Table 4: Shows the anorexigenic and orexigenic molecules involved in the control of energy homeostasis, its site of production, molecule type and function. **Abbreviations: AgRP:** agouti-related peptide; **CART:** cocaine and amphetamine-regulated transcript; **CKK:** cholecystokinin; **FFA:** free fatty acids; **GABA:** gamma-aminobutyric acid; **GLP-1:** Glucagon-like peptide 1; **MCH:** melanin-concentrating hormone; **NPY:** neuropeptide Y; **POMC:** pro-opiomelanocortin.

2.5. Hypothalamic dysfunction

2.5.1. Hypothalamus correlation with obesity and the metabolic syndrome

Obesity is correlated with inflammation and resistance to Lep and insulin action, in periphery and in the CNS (Timper and Brüning 2017). Food overconsumption is known to lead

to hypothalamic inflammation through the activation of inflammatory pathways, which occur previously to inflammation in peripheral metabolic organs and tissues (Valdearcos, Xu, and Koliwad 2015). This inflammation results in cellular damage and as consequence the progression of obesity (Cavadas et al. 2016). The consumption of fat dietary content results in an increase of FA from the peripheral organs and tissues. This FA have the ability to cross the BBB and induce an inflammatory response in hypothalamic neurons through activation of macrophages in the CNS.

Hypothalamic inflammation is correlated with reduced responsiveness of POMC and AgRP neurons to insulin and Lep, in the ARC and with a dysfunctional insulin secretion β-cells in pancreas (Valdearcos, Xu, and Koliwad 2015; Cavadas et al. 2016). The ARC and PVN inflammation promote endoplasmic reticulum stress in hypothalamic neurons and as consequence an insulin and Lep resistance (Timper and Brüning 2017). Posteriorly, Lep resistance leads to hyperphagia and to an increase of weight gain. The consumption of fat dietary content is associated with Lep and insulin resistance in CNS, and with an impaired ability of ghrelin to induce food consumption, through AgRP and NPY orexigenic neurons. On the other hand, the activation of ghrelin in PVN neurons can be maintain in obesity and could increase adiposity, independently of food consumption (Timper and Brüning 2017).

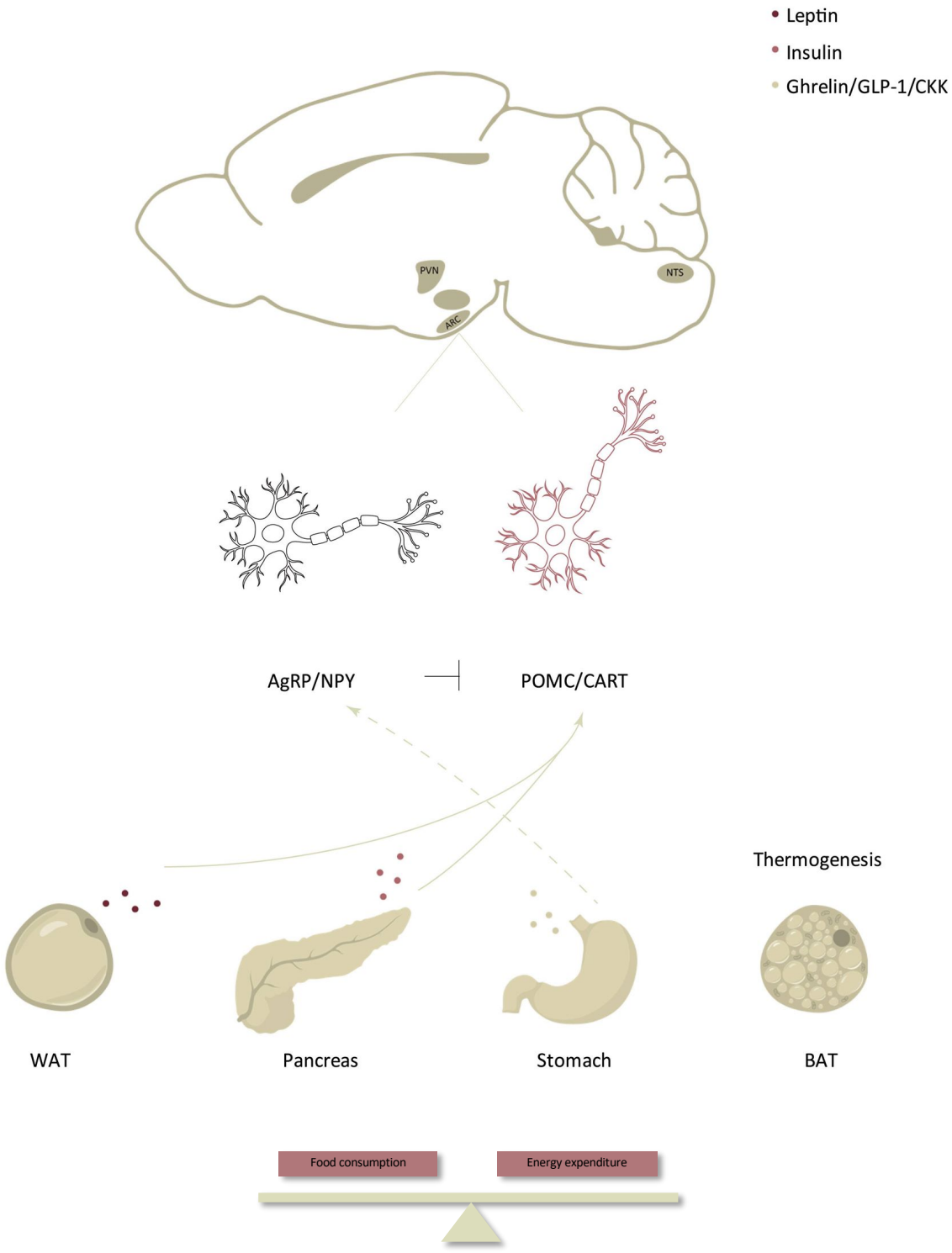

Figure 4 |Hypothalamic regulation of whole-body energy homeostasis

The hypothalamic nuclei act in the control of the whole-body homeostasis, providing an equilibrium between food intake and energy expenditure. The ARC is located close to the third ventricle and to the

median eminence, which present a BBB with fenestrated capillaries providing to the populations of neuronal cells access to circulating peripheral nutrient signals and hormones, from metabolic organs and tissues such the adipose tissues, pancreas and stomach. These peripheral nutrient signals and hormones, such Lep, insulin and ghrelin, are integrated in ARC by first-order orexigenic (AgRP and NPY) and anorexigenic (POMC and CART) neurons, which project their axons into second-order neurons of other hypothalamic nuclei, such as PVN and autonomic preganglionic neurons in the brain stem, orchestrating the regulation of whole-body energy homeostasis. Upon food consumption, the WAT produces and secrete Lep, and the pancreas secrete insulin, which act in activation of POMC/CART anorexigenic neurons and inhibiting NPY and AgRP orexigenic neurons, promoting satiety and an increase of energy expenditure. However, in fasting conditions, the stomach produces and secrete ghrelin, which binds with the ghrelin receptor in the ARC, activating NYP/AgRP orexigenic neurons, leading to a posterior inhibition of POMC neurons through releasing of NPY and GABA, thus promoting food consumption. **Abbreviations: AgRP:** agouti-related peptide; **ARC:** arcuate nucleus; **BAT:** brown adipose tissue; **CART:** cocaine and amphetamine-regulated transcript; **CKK:** cholecystokinin; **GLP-1:** glucagon-like peptide 1; **NPY:** neuropeptide Y; **NTS:** nucleus tractus solitarius; **POMC:** pro-opiomelanocortin**; PVN:** paraventricular nucleus; **WAT:** white adipose tissue.

3. **Cholesterol metabolism in brain**

Cholesterol is an essential lipid for neural physiology, and its concentration in the brain accounts for 20%-25% of whole-body cholesterol (Petrov, Kasimov, and Zefirov 2016). The cholesterol in the adult CNS is in myelin sheaths, formed by oligodendrocytes to insulate axons, and the remaining is concentrated in the plasmatic membranes, in the lipid rafts of neurons and astrocytes, allowing them to maintain their morphology (Bjorkhem and Meaney 2004; Benarroch 2008). Cholesterol has also crucial role in the brain development, maintenance of synaptic transmission, through the regulation of cell signaling pathways, gene transcription and bioactive steroids availability (Benarroch 2008).

3.1. Cholesterol synthesis

In the brain, the cholesterol is primarily produced by *de novo* synthesis and its metabolism vary from the rest of body, as the BBB prevents entry and exit of lipoproteins cholesterol from systemic circulation (Zhang and Liu 2015).

The cholesterol synthesis in the brain occurs with high intensity during the development of the CNS and also in the injured CNS This synthesis occurs primarily in the ER and starts with the conversion of acetyl-CoA to 3-hydroxy-3-methylglutary-CoA by 3-hidroxi-3-methyl-glutaril-CoA (HMG-CoA) and to mevalonate by HMG-CoA reductase (Bjorkhem and Meaney 2004). Posteriorly, through a series of enzymatic reactions the mevalonate is converted into lanosterol (Pfrieger and Ungerer 2011; Zhang and Liu 2015). In this phase, cholesterol synthesis is splits in two pathways, the Kandutsch-Russel pathway and the Bloch pathway. The Kandutsch-Russel pathway uses lanosterol precursors such 7-dehydrocholesterol and lathosterol for cholesterol synthesis and occurs mainly in neurons. The Bloch pathway use 7-dehydrodesmosterol and is mainly observed in astrocytes and oligodendrocytes (Bjorkhem and Meaney 2004; Zhang and Liu 2015).

3.2. Cholesterol transport

The cholesterol circulates in the brain bound with lipoproteins (Björkhem 2006). Astrocytes secrete apolipoprotein (Apo) such as ApoE, ApoJ and ApoD, to transport cholesterol and other lipids into neurons, as neurons have a low cholesterol synthesis rate

(Björkhem 2006). The ApoE binds to cholesterol to form the HDL-Chol lipoproteins, which binds to the low density lipoprotein receptor (LDL-R), the low density lipoprotein receptor-related protein (LRP) and the apolipoprotein E receptor 2 (ApoER2) in neurons (**Figure 6**) (Wood et al. 1999; Zhang and Liu 2015).The brain also expresses other receptors such as very-low-density lipoprotein receptor (VLDLR) and the ApoE receptor 2. The lipoproteins can exit the brain through the cerebrospinal fluid, thus representing an important route for cholesterol excretion (Chen et al. 2012).

Niemann-Pick type C1/2 (NPC1 and NPC2) are other important proteins involved in cholesterol transport within the cell and in cholesterol entry in endosomes and lysosomes (**Figure 5**) (Wood et al. 1999; Zhang and Liu 2015).

When the unesterified cholesterol synthesis rate exceeds the neurons and astrocytes necessities, a cholesterol turnover occurs. This unesterified cholesterol can be stored, converted or excreted into systemic circulation (Zhang and Liu 2015).

3.3. Cholesterol storage

In response to high levels of unesterified cholesterol in the ER, the acyl-coenzyme A cholesterol acyltransferase 1 (ACAT1) expression increases and the cholesterol in excess is esterified and stored in cytoplasmic lipid droplets for posterior formation of myelin sheaths and maintenance of synaptic transmission (Zhang and Liu 2015; Petrov et al. 2016).

3.4. Conversion to oxysterol

The conversion of unesterified cholesterol to oxysterol is the main way of cholesterol excretion from the brain (Zhang and Liu 2015). When cholesterol levels exceed the neuronal cell needs, the unesterified cholesterol is hydroxylated by the CYP46A1 enzyme into 24-hydroxycholesterol (24-OHC) (**Figure 5**) (Zhang and Liu 2015). *CYP46A1,* cytochrome P450 family 46 subfamily A member 1, gene is mainly and almost exclusively expressed in neurons of the brain and retina (Ramirez, Andersson, and Russell 2008; Bretillon et al. 2007). The *CYP46A1* gene is located on chromosome 14q32.1, contain 15 exons and encodes the CYP46A1 enzyme, a protein of approximately 500 amino acids (Lund, Guileyardo, and Russell 1999). The mRNA sequence of *CYP46A1* is highly conserved in the vertebrates highlighting the crucial role of this enzyme in cholesterol metabolism homeostasis.

24-OHC has the ability to cross the BBB into systemic circulation (Zhang and Liu 2015). These oxysterols are posteriorly metabolized in the liver to bile acids (Benarroch 2008). 24-OHC not only acts in brain cholesterol excretion, but also as a signaling molecule in the regulation of cholesterol homeostasis (Pfrieger and Ungerer 2011).

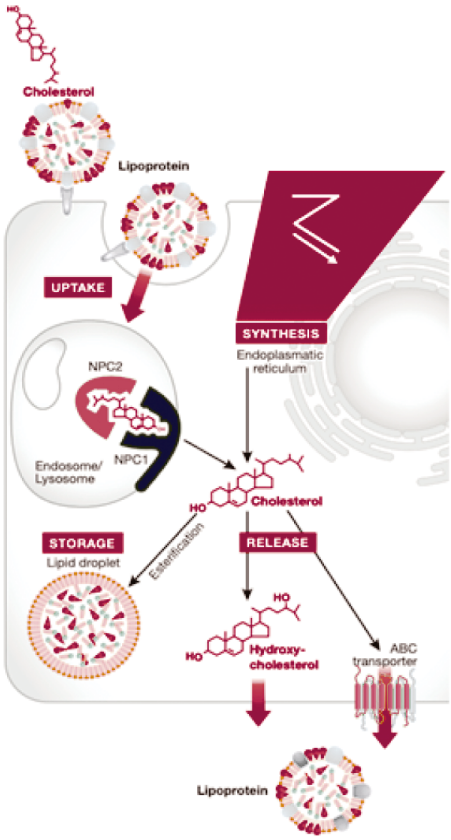

Figure 5| Cholesterol synthesis and excretion in the brain

The cholesterol synthesis occurs primarily in the endoplasmic reticulum (ER) through a series of enzymatic steps (pathway symbol). Posteriorly to cholesterol synthesis, the cholesterol in excess can be esterified and stored in cytoplasmic lipid droplets, hydroxylated into oxysterols, which has the has the ability to cross the BBB or can be eliminated by ABC transporter. The NPC1 and NPC2 are other important proteins involved in cholesterol transport within the cell and in cholesterol entry in endosomes and lysosomes. Adapted from: (Martín, Pfrieger, and Dotti 2014). **Abbreviations: NPC1 and NPC2**: Niemann-Pick type C1/2.

3.5. Cholesterol excretion

Some neurons express ATP binding cassette (ABC) transporters, such as ABCA1, ABCG1 and ABCG4 (Zhang and Liu 2015). ABC transporters A1 (ABCA1) act in the mediation of

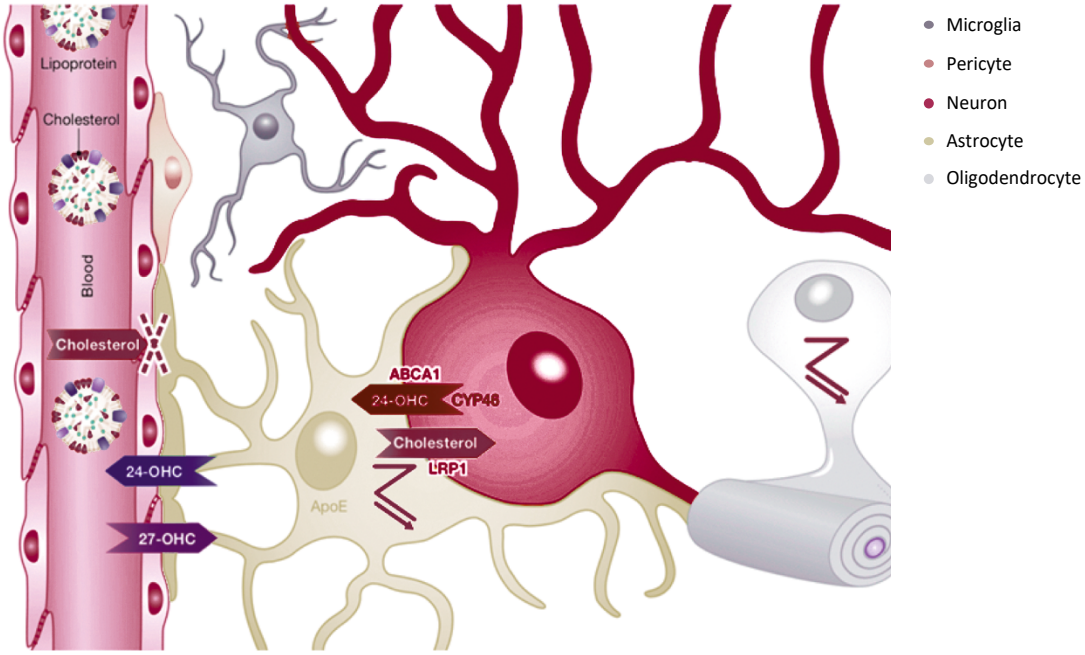

Figure 6| Cholesterol metabolism in the brain

In the brain, the cholesterol is primarily produced by *de novo* synthesis as the BBB prevents entry and exit of lipoproteins cholesterol from systemic circulation. Cholesterol is synthetized by several cells, as neurons and glia cells, such as astrocytes and oligodendrocytes (pathway symbol). Astrocytes secrete Apo, such as ApoE, to transport cholesterol and other lipids into neurons, as neurons have a low cholesterol synthesis rate. The ApoE binds to cholesterol to form the HDL-Chol lipoproteins, which binds to the LDL-R1 in neurons. In neurons, the cholesterol is hydroxylated by the CYP46A1 enzyme into 24-OHC, which can be secreted via ABCA1. The 24-OHC also has the ability to cross the BBB into systemic circulation. Adapted from: (Martín et al. 2014). **Abbreviations: ABCA1:** ATP-binding cassette transporter A1; **Apo:** apolipoproteins; **BBB:** blood brain barrier; **LDL-R1:** low-density lipoprotein receptor 1;

intracellular ApoE-bound cholesterol complex transport, for cholesterol excretion (Schmitz and Langmann 2001). This process of cholesterol excretion is independent of the CYP46A1 enzyme, however, the ABCA1 can also eliminate the 24-OHC, protecting the neuronal cells from the toxic effects of 24-OHC accumulation (**Figure 6**) (Martín et al. 2014).

3.6. Regulation of brain cholesterol metabolism homeostasis

Neuronal cells balance the cholesterol biosynthesis, storage, conversion and excretion maintaining the cholesterol metabolism homeostasis in which sterol regulatory element-binding proteins (SREBPs) and the liver X receptors (LXR) have an important regulation role (Zhang and Liu 2015).

Neuronal cells detect the cholesterol levels through the binding of ER-membrane-anchored transcription factors, known as SREBPs, to SREBP cleavage-activating protein (SCAP) that function as a detector of cholesterol levels. Upon detection of cholesterol levels, the SREBPs/SCAP complex acts in the regulation of the transcription of genes encoding enzymes of cholesterol and FA synthesis, as well as, lipoprotein receptors (Zhang and Liu 2015; Petrov et al. 2016). Previous studies documented that the knockdown of SREBP-2 in the brain leads to a decrease in cholesterol synthesis and in markers of synapse formation (Suzuki et al. 2010).

Oxysterols, namely the 24-OHC, are endogenous ligands of nuclear transcription factors such the LXR α and β, which regulates the expression of genes involved in lipid metabolism, acting in the control of ABCA1 expression in neuronal cells and cholesterol efflux (Pfrieger and Ungerer 2011; Ulven et al. 2005). The oxysterol binding with LXR can also inhibit *de novo* cholesterol synthesis through the repression of HMG-CoA reductase (Benarroch 2008).

3.7. Cholesterol dysfunctions

Dysfunctions in the brain cholesterol metabolism homeostasis contribute to neurodegenerative disorders in CNS, such as Alzheimer's disease (AD), Huntington's disease (HD), Parkinson's disease (PD), Niemann-Pick disease type C and SLOS (Nóbrega et al. 2019).

3.7.1. Alzheimer and Parkinson diseases

Alzheimer disease (AD) is a common progressive neurodegenerative disorder that affect neurons involved with memory and cognition (Vance 2012). This disorder involves the progressive deposition of amyloid β-peptide (Aβ). In neurons, oxidative stress and the neurotoxic form of Aβ results in dysfunctions and degeneration (Cutler et al. 2004).

Previous studies showed that genetic and environmental factors are involved in the pathogenesis of AD and that cholesterol metabolism homeostasis has a crucial role in AD pathogenesis (Garcia et al. 2009). For example, CYP46A1 in the brain of individuals with AD has an abnormal activity (Bogdanovic et al. 2001). Importantly, it was shown that 24-OHC has the ability to reduce the production of Aβ through the inhibition amyloid precursor protein (APP) trafficking (Moutinho, Nunes, and Rodrigues 2016).

Moreover, previous studies documented that the injection of AAV5-sh*Cyp46a1* in the mouse hippocampus results in a decrease of *Cyp46a1* expression and as outcome a significant decrease of 24-OHC and an increase of cholesterol in hippocampus (Djelti et al. 2015).

Hippocampal neurons, upon *Cyp46a1* expression inhibition, showed signals of apoptosis, including shrinkage of the cell soma, presence of pyknotic nuclei and caspase activation (Djelti et al. 2015). Around 80% of neurons in C57BL/6J wild-type mice presented cleaved caspase 3 and cleaved caspase 9, the main players in apoptosis (Djelti et al. 2015). Beyond progressive apoptotic neuronal loss in C57BL/6J mice, the *Cyp46a1* inhibition was also correlated with impaired cognitive abilities and hippocampal atrophy (Djelti et al. 2015). The *Cyp46a1* expression inhibition in APP3 mice result also in neuronal loss, and exacerbated amyloid accumulation and tau phosphorylation (Djelti et al. 2015).

Impairments in brain cholesterol metabolism is also correlated with PD. PD is also a progressive neurodegenerative disorder affecting dopaminergic neurons of the *substantia nigra*. 24-OHC levels are increased in the cerebrospinal fluid (CSF) of PD and show a strong correlation to Tau (Björkhem et al. 2018). This modification may result as consequence of the loss of neurons and posterior release of 24-OHC, increasing their levels in CSF (Björkhem et al. 2018).

3.7.2. Polyglutamine diseases

Polyglutamine diseases are a group of rare neurodegenerative disorders caused by an abnormal expansion of CAG trinucleotide sequences (Nóbrega and Almeida 2018). This group of disorders include nine disorders such as HD, dentatorubral-pallidoluysian atrophy (DRPLA), spinal and bulbar muscular atrophy (SBMA), and six different types of spinocerebellar ataxia (SCA).

HD is an autosomal dominant disorder caused by an abnormal repeat of CAG trinucleotide near the start of exon 1 of the Huntingtin gene (HTT) in the short arm of chromosome 4 (Nóbrega and Almeida 2018). Wild-type *HHT* gene carries 10 to 35 CAG trinucleotide repeats (Nóbrega and Almeida 2018). Previous studies documented that in HD, the dysfunction in cholesterol metabolism homeostasis occurs through *CYP46A1* dysfunctions and is a consequence of dysregulation of cholesterol clearance (Boussicault et al. 2016). Motor deficits and spontaneous striatal neurons death were founded in wild-type *Cyp46a1* knock-down mice (Boussicault et al. 2016). In vivo the restoring of *Cyp46a1* in the striatum of HD mouse model improved the motor deficits and restored cholesterol metabolism homeostasis suggesting a neuroprotective role in HD (Boussicault et al. 2016).

Dysfunctions in brain cholesterol metabolism were also correlated with Machado-Joseph disease (MJD)/SCA3. In cerebellar samples from MJD/SCA2 patients and mouse models presented a decrease in *CYP46A1* expression accompanied by a decrease in 24-OHC levels (Nóbrega et al. 2019).

3.7.3. Smith-Lemli-Optizy syndrome and Niemann-Pick disease type C

Smith-Lemli-Optizy (SLOS) are rare autosomal recessive disorder caused by mutations in the gene encoding 7-dehydrocholesterol reductase (DHCR7) (Martín et al. 2014). The SLOS patients present low cholesterol levels in the brain, organ defects, such liver diseases and cardiac defects, affective disorders and sleeping problems (Martín et al. 2014). The symptoms can be result of an accumulation of 7,8-dehydrodesmosterol, a substrate of DHCR7 (Martín et al. 2014).

Niemann-Pick disease type C is a rare autosomal recessive lysosomal storage disorder caused by a mutation in *NCP1* and *NCP2* genes in 95% of the cases (Benarroch 2008; Martín et al. 2014). This lysosomal storage disorder is characterized by cholesterol accumulation which develops neurodegeneration and neural abnormalities (Vance 2012).

3.8. Oxysterols correlation with obesity and the metabolic syndrome

Changes in oxysterol metabolism were correlated with obesity (Guillemot-Legris et al. 2016). In an HFD induced obesity mouse model the quantification of oxysterols levels in hypothalamus did not showed significant modifications in 24-OHC levels and either in *Cyp46a1* mRNA expression (Guillemot-Legris et al. 2016). Nonetheless, it was observed variations in the levels of other oxysterols, specially the decrease of 4β-hydroxycholesterol (4β-OHC) levels in the hypothalamus, liver and adipose tissue (Guillemot-Legris et al. 2016). In genetic models of obesity, the *db/db* mice also did not present alterations in the 24-OHC levels (Guillemot-Legris et al. 2016). Additionally, the C57BL/6J animals in a diet-induced obesity presented alterations of the oxysterols levels in plasma and in the adipose tissue (Wooten et al. 2014).

In the hypothalamus changes in the cholesterol metabolism modify the feeding behavior (Suzuki et al. 2010).

Objective

The investigation of the cholesterol metabolism in the brain is a hot research topic, as cholesterol is been implicated in several neurodegenerative diseases, such as AD and HD (Zhang and Liu 2015). In fact, the decrease in *Cyp46a1* expression, which is an essential enzyme in cholesterol metabolism and the consequent reduction in 24-OHC and increase of cholesterol levels, results in a progressive apoptotic death of neurons in the hippocampus (Djelti et al. 2015). In the hypothalamus, previous studies showed that mice with obesity induced by HFD and *ob/ob* mice models show a decrease in oxysterols levels (Guillemot-Legris et al. 2016). These results could suggest a possible correlation in cholesterol homeostasis in the brain and whole-body metabolic abnormalities.

In this study, our main goal was to silence the expression of the *Cyp46a1* mouse gene in the hypothalamus of C57BL/6J wild-type mice fed with Chow and HFD, and to investigate its impact in the whole-body metabolism homeostasis. More specifically, the project aims to investigate the impact of the silencing of *Cyp46a1* gene in BW, in food and water intake, in glucose tolerance, insulin sensibility, locomotor and anxiety-like behavior, and in the integrity of several metabolic organs. We hypothesized that the silencing of *Cyp46a1* gene in the hypothalamus, namely in the ARC, leads to a reduction in the Cyp46a1 enzymatic activity, as consequence of the reduction of 24-OHC levels and accumulation of cholesterol in ARC neurons. The ARC is implicated in the control of whole-body metabolism homeostasis, so the silencing of *Cyp46a1* gene, could induce metabolic abnormalities, such as, obesity and TIIDM.

This study and its results could be an important basis for future investigation of cholesterol metabolism and its impact on whole-body metabolism homeostasis.

Materials and Methods

In vivo experiments

1. Animals and diets

In several strains of mice (*Mus musculus*), an increase in dietary fat content results in features associated with obesity (West et al. 1992). For example, the C57BL/6J mouse strain has a genetic susceptibility for diet-induced obesity and diet-induced diabetes mellitus type II (Surwit et al. 1988).

C57BL/6J wild-type mice were obtained from in-house breeding (founders were bought from Charles River, Barcelona, Spain), and maintained in the animal pathogen-free facility of Centre for Biomedical Research (CBMR) of the University of Algarve. Both male and female mice were used for all experiments throughout the study. Twelve weeks-old mice, with an average body weight of 20-25g, were housed (two or three per cage) in a controlled environment under a 12 hours light / 12 hours dark cycle in a temperature and humidity-controlled room (22±2ºC).

Initially, the entire cohort of animals (*n=45*) were randomly divided into two groups, corresponding to two different diets. One group (*n=24*) had access to a low-fat control diet (Chow, D12450J, 10% fat, Research Diets, USA) and the other group (*n=21*) had access to a high-fat diet (HFD, D12492, 60% fat, Research Diets, USA). Both diets, Chow and HFD, and autoclaved water were provided *ad libitum*. The percentage of kcal derived from protein, fat and carbohydrate of both diets are detailed in **Table 5**.

This study was performed for 12 weeks, in which the animals had access to the described food and were maintained in the described conditions.

The mice were accommodated to the diets, for four weeks, until the stereotaxic injection (**Figure 7**).

Table 5| Caloric information of diets

	Low-fat control diet (Chow) – D12450J	**High-fat diet (HFD) – D12492**
Protein	20% kcal	20 % kcal
Fat	10% kcal	60% kcal
Carbohydrate	70% kcal	20% kcal
Energy Density	3,82 kcal/g	5,21 kcal/g

Table 5: Shows the caloric information (kcal) of each diet, Chow and HFD. **Abbreviations: Chow:** low fat control diet; **HFD:** high fat diet.

Before the stereotaxic injection the two groups of mice (Chow and HFD) were then divided into four groups. Two groups of mice were not submitted to the stereotaxic injection, constituting the control groups (Chow-Non-injected and HFD-Non-injected), whereas the two others groups were submitted to the stereotaxic injection to deliver the adeno-associated vectors (AAV) with the shRNA targeting the *Cyp46a1* gene, thus constituting the treated groups (Chow-AAV-sh*Cyp46a1* and HFD-AAV-sh*Cyp46a1*).

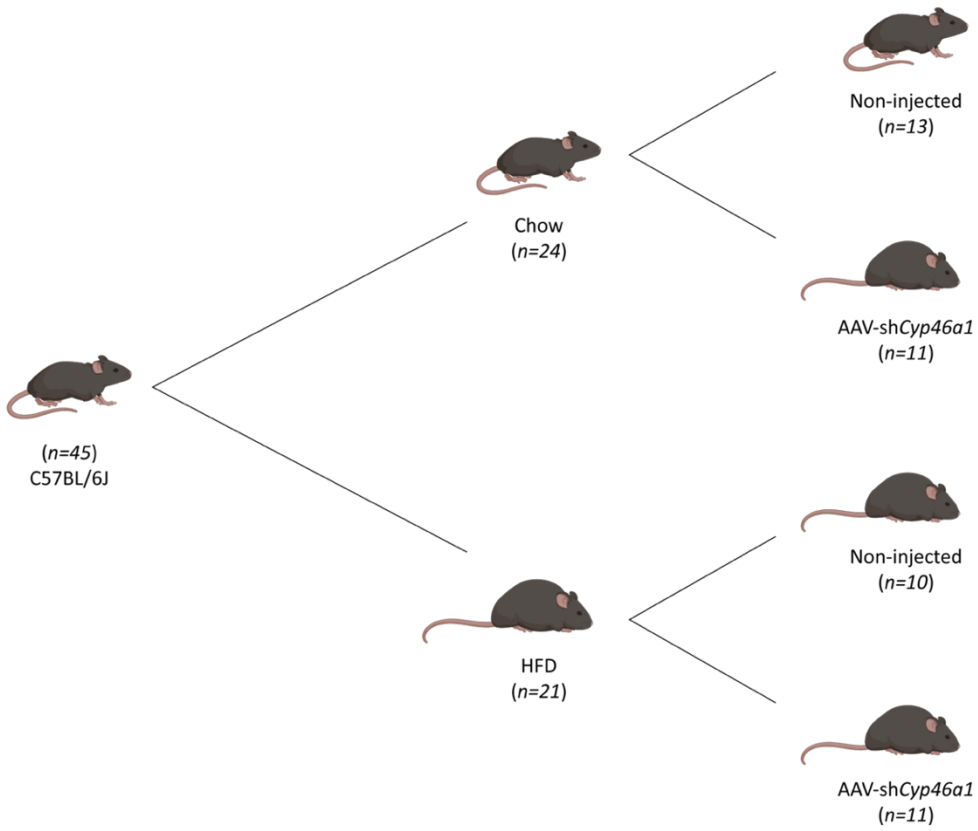

Figure 7| Representation of the experimental conditions

Initially, 12 weeks-old C57BL/6J mice (*n=45*) were divided into two groups of animals corresponding to the two different diets, a low-fat control diet (Chow, 10% fat) (*n=24*) and a high-fat diet (HFD, 60% fat) (*n=21*). Before the stereotaxic injection in 4 week, the two groups of mice (Chow and HFD) were divided into four groups (Chow Non-injected: *n=13*, female: *n=4* and male: *n=9*; Chow AAV-sh*Cyp46a1:* *n=11*, female: *n=4* and male: *n=7*; HFD Non-injected: *n=10*, female: *n=6* and male: *n=4*; HFD AAV-sh*Cyp46a1*: *n=11*, female: *n=7* and male: *n=4*). The two groups of animals, not submitted to the stereotaxic injection (Chow Non-injected and HFD Non-injected) constituted the control groups, and the other two groups of mice, submitted to the stereotaxic injection (Chow AAV-sh*Cyp46a1* and HFD AAV-sh*Cyp46a1*) constituted the treated groups. **Abbreviations: AAV5:** adeno-associated viral vector serotype 5; **Chow:** low fat control diet; **HFD:** high fat diet; **sh:** short hairpin.

The experiments were performed in accordance with the European Union Directive (86/609/EEC) for the care and use of laboratory animals. The researchers received appropriate training and certification (Federation of Laboratory Animal Science Associations [FELASA] certified course) to perform the experiments from the Portuguese authorities (*Direcção Geral de Alimentação e Veterinária*).

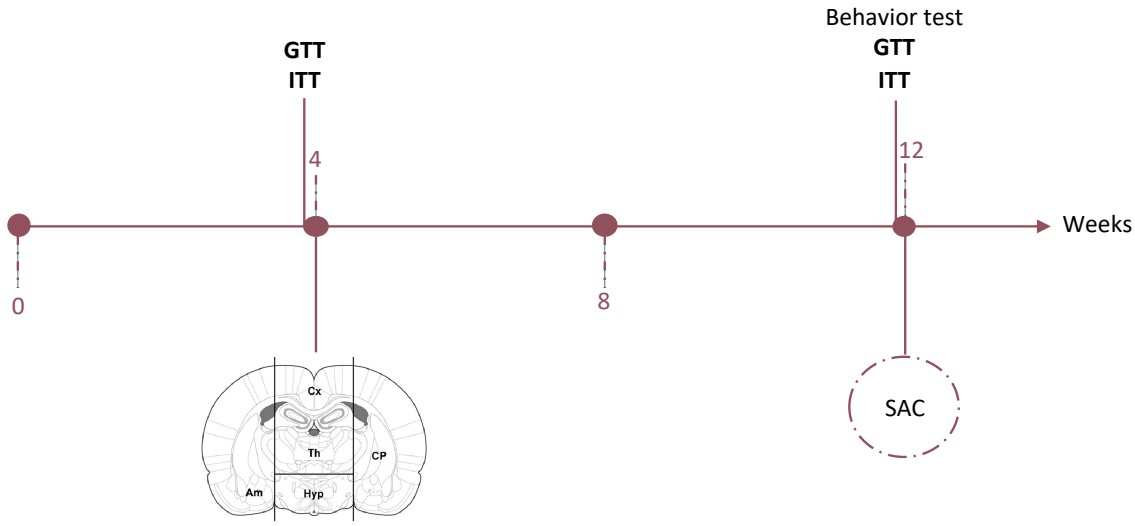

AP: 1,65 mm**; DL:** -0,5 mm; **MV:** -5,8 mm

Figure 8| Representation of experimental timeline

This study was performed for 12 weeks. Initially, the C57BL/6J mice were accommodated to the diets (Chow and HFD). The stereotaxic surgery was performed in the 4th week of study, aiming to deliver the AAV5-sh*Cyp46a1* into hypothalamus of the mice. Mice for the different experimental groups were subject to a GTT, an ITT and to a behavior test, at the 4th and 12th weeks. The animals were sacrificed by decapitation at 12 weeks. **Abbreviations: Am:** amygdala; **Chow:** low fat control diet; **HFD:** high fat diet; **ITT:** insulin tolerance test; **GTT:** glucose tolerance test; **SAC:** sacrifice; **sh:** short hairpin; **AP:**

anteroposterior; **DL:** dorsoventral; **MV:** mediolateral; **Hyp:** hypothalamus; **Th:** thalamus; **Cx:** cerebral cortex; **CP:** caudate nucleus and putamen.

2. Production of viral vectors

The AAV vectors were produced and purified by Atlantic Gene therapies (Inserm U1089, Nantes, France). The viral constructs (AAV5-sh*Cyp46a1*-GFP) contained the expression cassette of a short hairpin RNA (shRNA) targeting the mouse *Cyp46a1* gene, driven by a human U6 promoter and a GFP reporter gene driven by the phosphoglycerate kinase 1 (PGK1) promoter in the adeno-associated viral vector serotype 5 (AAV5)(Boussicault et al. 2016). The AAV5 vectors encoding sh*Cyp46a1* sequences were generated by transient transfection of human embryonic kidney (HEK) 293T cells and purified on caesium chloride ultracentrifugation gradients, as previously described (Sevin et al. 2006).

3. Stereotaxic injections of the adeno-associated virus

The stereotaxic injections were performed in the 4th week of study (**Figure 8**), aiming to deliver the AAV5-sh*Cyp46a1* into hypothalamus of the mice. Briefly, mice were anesthetized with an intraperitoneal injection of ketamine (100 mg/ml, Dechra) and medetomidine (1 mg/ml, Esteve) (50-75 mg/kg + 1-10 mg/kg IP), and placed on a stereotaxic frame (Stoelting Company, USA) (**Figure 9**) with the upper incisors teeth's and ears in the support bars to immobilize the skull.

Figure 9| Representation of the stereotaxic frame and immobilization of the mice skull

The stereotaxic injections were performed in the 4th week of the study, aiming to deliver the AAV5-sh*Cyp46a1* into hypothalamus of the mice. The mice were anesthetized and placed on a stereotaxic frame with the upper incisors teeth's and ears in the support bars to immobilize the skull.

After the immobilization of the mice skull, the bregma point was identified and used as a reference point for the origin of the coordinates. The hypothalamus coordinates were defined using The Paxinos and Franklin's Mouse Brain Atlas and the stereotaxic injection was performed bilaterally, targeting both side of the arcuate nucleus of hypothalamus: 0.5 mm lateral to the middle line (in each side of the brain), 1.65 mm posterior to the bregma and −5.8 mm ventral to the brain surface: (AP= -1,65; DL= -0,5; MV= -5,8) (Franklin and Paxinos 2019).

The skull was drilled using a surgical drill and the two treated groups (Chow AAV5-sh*Cyp46a1* and HFD-AAV-sh*Cyp46a1*) received $1x10^9$ v.g. (viral genomes) of AAV5-sh*Cyp46a1*-GFP in each side of the arcuate nucleus of hypothalamus. The injection was performed at a rate of 0.5 µL/min using a 10 mL-Hamilton syringe attached to a Quintessential Stereotaxic Injector (QSI™) (Stoelting Company). After the end of the administration, the needle was kept in place for 5 min to minimize backflow (Aveleira et al. 2015).

After the animal was sutured, a reverser of anesthesia was administered; Atipamezole (5 mg/ml, Esteve) (1-2,5 mg/kg IM or SC) and post injection care were performed. The health status of the animal was carefully monitored in the following days of the stereotaxic surgery.

At the end of the experiment (12 weeks after the food treatment and 8 weeks after the stereotaxic injection), the mice were sacrificed. Mice were anesthetized using volatile anesthesia with 100% isoflurane (Zoetis) and were sacrificed by decapitation.

4. Animal behavior tests

Animals from all the experimental groups were subjected to an open field behavior test at the 12 weeks for the assessment of locomotor and anxiety-like behavior. Briefly, the mice were placed in a square transparent box, without a roof, measuring 40x40cm and 40 cm high walls, in a sound-attenuating controlled room, illuminated with a white light during the tests.

The floor of the transparent box was divided by lines, into nine equally sized squares, and was defined one square as the center zone and the eight squares along the walls as the periphery zones (**Figure 10**). The animals were gently placed in the center zone of the floor of the transparent box and their movement activity was recorded by video for 10 min in day-time period (*n=45*) and 5 min in the night time period (*n=24*) using a GoPro Hero camera

(GoPro Inc., USA). After, the following parameters were measured using the ANY-maze behavioral tracking software (Stoelting Company, Europe): total distance, mean speed, time spend immobile, immobile episodes, number of line crossings, number and time of rearing, number and time of grooming, number of entries and time in the middle. These parameters were scored from the video recordings. The number of crossing lines were counted as horizontal activity. The number of rearing and grooming were counted as vertical activity and rearing was only scored when mice raised both of front paws from the floor and leaned against a wall.

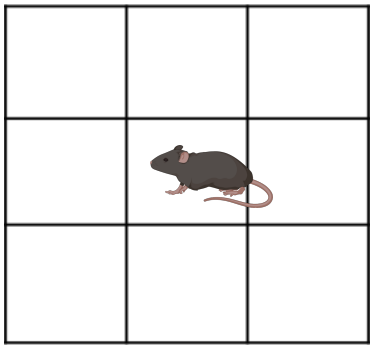

Figure 10| Representation of the floor of the square transparent box used in the open field tests

The C57BL/6J mice were subjected to an open field behavior test. The floor of the transparent box used was divided by lines into nine equally sized squares. A central square was defined as the center zone of the box, surrounded by eight squares along the walls, which were defined as the periphery zone of the box.

5. Glucose tolerance test

Several animals from the different experimental groups were subject to a glucose tolerance test (GTT) at the 4th and 12th week (*n=14*). Briefly, animals were subjected to starvation for about 12-16 hours (overnight period). After this period, for each animal the tip of the tail was cut, and the resulting blood used to measure the fasting blood glucose levels (time 0). The blood glucose levels measurements were performed using the FreeStyle Precision Neo glucometer and FreeStyle Precision strips (Abbot). After the measurement of the fasting blood glucose level, mice were injected intraperitoneally with a 20% glucose solution (Fisher Chemical - G/0500/60), dissolved in saline solution, 0,9 % NaCl. The injection volume was calculated according to the formula: Body weight (BW) (g) X 10 µl of 20% glucose

solution (Andrikopoulos et al. 2008). The blood glucose levels were measured at 5, 10, 15, 30, 60, 90 and 120 min after the intraperitoneal injection of glucose solution.

The measured levels were used to perform the calculation of the area under the curve (AUC). For this, the blood glucose measurements were converted into natural logarithm (Ln) and the total peak area was calculated using xy analysis, namely the AUC. Two values were calculated: the total AUC, from 0 until 120 min, and the AUC between 5 and 60 min.

6. Insulin tolerance test

Similarly, to the GTT, the animals were also subjected to an insulin tolerance test (ITT), at the 12th week (*n=11*), after a starvation period of 4 hours. After this period, for each animal the end of the tail was cut, and the resulting blood was used to measure the fasting blood glucose levels (time 0). The blood glucose levels measurements were performed using the FreeStyle Precision Neo glucometer and FreeStyle Precision strips (Abbot). After the measurement of the fasting blood glucose level, mice were injected intraperitoneally with a 4 mg/ml human insulin solution (Gibco^{TM}) in a phosphate-buffered saline solution (PBS X1). The injection volume was calculated using the formula: BW (g) X 7,5 µL of 4 mg/mL insulin solution. The blood glucose levels were measured at 5, 10, 15, 30, 60, 90 and 120 min after the insulin intraperitoneal injection. At the end of the ITT test, the animals were injected with a 20% glucose solution to revert insulin effect and prevent animal death.

The blood glucose measurements were then converted into natural logarithm (Ln) and the slope was calculated using linear regression and multiplied by 100 to obtain the constant for glucose clearance (kITT), per minute (%/min) obtained during the insulin tolerance test (Bonora et al. 1989).

7. Tissues and blood collection

The blood was collected upon decapitation of the animals, and the serum was separated by centrifugation at 2000 rpm for 20 min at 4ºC. The serum samples were stored at -80ºC for posterior analysis.

After, the important metabolic organs and tissues were collected: hypothalamus, rest of the brain, liver, white and brown adipose tissue (WAT and BAT, respectively), spleen, pancreas, muscle, gut, colon, stomach, heart and kidneys.

The liver, WAT and spleen were weighed after organ collection with an analytical balance (AA-200 by Denver Instrument Company). The brain was individually collected, and the hypothalamus dissected for molecular analysis.

The liver, WAT, BAT and muscle of each animal were divided in three different portions for posterior molecular analysis and histological processing. The pancreas and the heart of half of the animals were collected for posterior molecular analysis and the other half were collected for histological processing. Also, the gut, colon, stomach and spleen were collected for histological processing and one kidney was stored for molecular analysis and the other for histological processing.

For the histological processing the organs and tissues were fixed in 3,7%-4% formaldehyde (w/v) buffered (pH=7) and stabilized with methanol fixative solution and stored at room temperature until the processing.

For the molecular analysis, small portions of the collected organs and tissues were stored at -80ºC for posterior analysis.

8. Body weight, food and water intake analyses

During the 12 weeks of the experiment, mice were weighted twice a week for BW analysis, namely calculation of total BW gain (g) and cumulative BW gain (g). Additionally, the food was weighted, twice a week, and water measured, once a week, to calculate food and water intake per g/ml of BW. The ratio of food ingested (g) per total BW for cage (g) was calculated and then multiplied for the body weight of each mouse to obtain the food intake [(food ingested/total BW for cage) X BW of each mouse)]. The ratio of water ingested (ml) per total body weight for cage (g) was calculated and then multiplied for the body weight of each mouse to obtain the water intake.

Analysis

9. Histology

9.1. Tissue processing and paraffin inclusion

For tissue processing and paraffin inclusion, the organs and tissues previously fixed in a formaldehyde solution were divided into smaller pieces and placed in tissue

processing/embedding cassettes. After, the dehydration of tissues was performed with 70% ethanol (v/v) (dilution from Fisher Chemical) for 1 hour; 95% ethanol (v/v) for 45 min; 95% ethanol (v/v) for 40 min and two series of 100% ethanol (v/v) for 1 hour each, follow by the clearing with two series of xylene (Fisher Chemical) for 1 hour each and by the infiltration with two series of paraffin (Luso Palex) in the incubator, at 56ºC for 1 hour each. After, the tissue processing/embedding cassettes (Labor Spirit) were removed from the incubator. The organs and tissues samples were mounted in embedding molds (Tebu-bio) at the desired orientation and filled with liquid paraffin at 56ºC. The cassettes, with the tissues, were placed on top and the block was allowed to cool down and hardened. Afterwards, the block was removed from the mold and stored at room temperature in a dry place until use.

9.2. Sectioning

Paraffin blocks were sectioned in paraffin sections on a HM 325 Rotary Microtome (Thermo Fisher Scientific) at room temperature.

The paraffin blocks containing white or brown adipose tissue were sectioned in paraffin sections with 4 or 5 µm of thickness. Other organs, such the liver and pancreas, were sectioned in paraffin sections with 3 to 4 µm of thickness. The paraffin sections were placed into microscopy slides and stored at room temperature until use.

9.3. Hematoxylin-eosin staining

Hematoxylin-eosin staining was performed according to the, manufacturer's guidelines (Merck Milipore). Briefly, the paraffin sections were placed in microscopy slide holders, deparaffinized with two series of xylene for 3 and 2 min and rehydrate with 100% ethanol (v/v), 95% ethanol (v/v) for 4 and 2 min, respectively, and with two series of distilled water for 30 seconds each. Posteriorly, the sections were stained with a hematoxylin solution modified, according to Gill III (Merck Milipore), for 30 seconds, washed two series of in distilled water for 2 and 1 minute, counterstained with a 0,5% aqueous eosin Y solution for 1 minute and washed again in two series of distilled water for 1 minute each. For the dehydration and clearing, the sections were submitted to 95% ethanol (v/v), two series of 100% ethanol (v/v) for 1 minute each and two series of xylene for 2 min. The sections were allowed to dry and next mounted with Richard-Allan Scientific Mounting Medium (HM325, Thermo Fisher Scientific) and microscopy slide cover slips. Upon hematoxylin-eosin staining, the cells nuclei

will stain dark purple and the cells cytoplasm will stain pink (acidophilic cytoplasm) or will stain light purple (basophilic cytoplasm).

9.4. Histological analysis of white adipose tissue and liver

Images of hematoxylin-eosin staining were acquired in the Axio Imager Z2 microscope (Carl Zeiss), using the Plan-Neo FLUAR 20X/0.5 Ph2 objective, the AXIOCAM-ICC3 camera and the AxioVision software (Carl Zeiss). The images obtained were analyzed using Image J – Fiji software. Images of WAT were analyzed to calculate the adipocytes area, respective mean and the relative frequency in percentage.

10. Protein expression analysis

10.1. Protein extraction

The organs and tissues previously maintained at -80ºC were used for analysis of protein expression.

The WAT of Chow AAV5-sh*Cyp46a1*, HFD-Non-Injected and HFD AAV5-sh*Cyp46a1* groups was weighed (100 mg) with an analytical balance (AA-200 by Denver Instrument Company), lysed in RIPA (radio-immunoprecipitation assay) buffer (Lysis Buffer, 20-188 Merck Millipore), supplemented with a protease inhibitor cocktail (Complete ULTRA Tablets, Mini, EASY PACK – Roche).

The following steps were performed 4 to 5 times: The samples were mechanical disrupted and sonicated (Vibra-Cell™ - 75186) (Amplitude: 60; 2 pulses of 30 seconds) in RIPA buffer always on ice. Posteriorly, the sample was centrifuged at 10ºC, at 1000 RCF for 5 min and the soluble fraction was collected using a syringe (BD Micro-fine, Insulin U100 [0,5ml]) to a new Eppendorf tube, without disturbing the other layers, and was centrifuged again at 8ºC, at 3300 RCF for 5 min.

The WAT of Chow-Non-injected group was weighed (100-150 mg) and using the QIAzol Lysis Reagent (QIAGEN) and a 2,5 ml syringe (Terumo) with a 23G needle (BD Microlance^{TM}), according to the manufacturer's instructions, the WAT was lysed and homogenized. The samples were maintained at room temperature for 5 min, were homogenized with chloroform (VWR Chemicals) and were maintained again at room temperature for 3 min before a centrifugation at 4ºC, at 12,000 rpm for 15 min. After, the top layer was discarded and the

QIAzol layer was collected. To the QIAzol layer was added 0,3 mL of 100% ethanol, maintained at room temperature for 3 min and centrifuged, to sediment the DNA, at 4ºC, at 2000 RCF for 2 min. To the supernatant was added isopropanol (Fisher Chemical), to precipitate the protein. The volume was separated and maintained at room temperature for 10 min. The following steps were performed 3 times: The samples were centrifuged at 4ºC, at 12 000 rpm for 10 min, the supernatant was discarded, was added 1 mL of guanidine-ethanol solution (SIGMA), maintained to room temperature for 20 min, centrifuged at 7500 RCF for 5 min and the supernatant removed.

To the pellets were added 1 mL of 100% ethanol and maintained at room temperature for 20 min. Posteriorly were centrifugated at 7500 RCF for 5 min and the supernatant removed. The pellets were maintained at room temperature for 10 min, were added 100 µL of a urea (SIGMA) / dithiothreitol (DTT) (Fisher Scientific) solution with a protease inhibitor cocktail, were maintained at room temperature for 1 hour and incubated at 95ºC for 3 min. Finally, the samples were then sonicated.

The BAT, similarly to the WAT, was weighed (20 mg) with an analytical balance (AA-200 by Denver Instrument Company), lysed in RIPA (radio-immunoprecipitation assay) buffer (Lysis Buffer, 20-188 Merck Millipore), supplemented with a protease inhibitor cocktail (Complete ULTRA Tablets, Mini, EASY PACK – Roche). The following steps were performed 2 times: The sample was mechanical disrupted and sonicated (Vibra-Cell™ - 75186) (Amplitude: 60; 2 pulses of 30 seconds) in RIPA buffer always on ice. Posteriorly was centrifuged at 10ºC, at 1000 RCF for 5 min and the soluble fraction was collected using a syringe (BD Micro-fine, Insulin U100 [0,5ml]) to a new Eppendorf tube, without disturbing the other layers, and was centrifuged at 8ºC, at 3300 RCF for 5 min.

The liver was weighed (10 - 15 mg) with an analytical balance (AA-200 by Denver Instrument Company), lysed in RIPA (radio-immunoprecipitation assay) buffer (Lysis Buffer, 20-188 Merck Millipore), supplemented with a protease inhibitor cocktail (Complete ULTRA Tablets, Mini, EASY PACK – Roche). The sample was mechanical disrupted and sonicated (Vibra-Cell™ - 75186) (Amplitude: 60; 3 pulses of 30 seconds) in RIPA buffer always on ice. Posteriorly was centrifuged at 10ºC, at 20 000 RCF for 20 min and the soluble fraction was collected using a syringe (BD Micro-fine, Insulin U100 [0,5ml]) to a new Eppendorf tube, without disturbing the other layers.

10.2. Quantification of protein

The total protein concentration was quantified using the bicinchoninic acidic (BCA) protein assay (Pierce™ BCA Protein Assay Kit – Thermo Scientific) or the Bradford assay (NZY Tech) according with the manufacture's instruction.

The total protein concentration of WAT, (Chow AAV5-sh*Cyp46a1*, HFD-Non-Injected and HFD AAV5-sh*Cyp46a1* groups), BAT and liver samples were quantified using the BCA protein assay in a Falcon® 96 Well Clear Microplate. This microplate contained a 50 µl of standard concentrations, prepared from a 25 µl serial dilution of Bovine Serum Albumin (BSA) solution [Albumin Bovine Fraction (NZY Tech)] in H_2O MilliQ with an initial concentration of 2 mg/mL and with 25 µl RIPA (Merck Millipore) diluted in H_2O MilliQ (1:20), contained 50 µl of a calibration blank solution with 25 µl RIPA (1:20) plus 25 µl of H_2O MilliQ, contained 50 µl of sample, diluted in H_2O MilliQ (1:20) plus 25 µl of H_2O MilliQ, and finally 200 µl of BCA in all the wells. Posteriorly, the microplate was incubated at 37ºC for 30 min and the absorbance of each sample was calculated by a spectrophotometer (TECAN – Infinite M200) in a wavelength of 562 nm.

The total protein concentration of the WAT, Chow-Non injected group, were quantified using the Bradford assay in a Falcon® 96 Well Clear Microplate. This microplate contained 5 µL of standard concentrations, prepared from a serial dilution of BSA solution in H_2O MilliQ with an initial concentration of 2 mg/mL, 5 µL of H_2O MilliQ as calibration blank solution, contained 5 µL of sample diluted in H_2O MilliQ (1:10) and 250 µL of Bradford reagent in all the wells. This microplate was maintained at room temperature for 10 min and the absorbance of each sample was calculated in the Glomax Multi Detection System (Promega) luminometer in a wavelength of 600 nm.

The WAT, BAT and liver samples, in a total concentration of 80-60 µg, were denaturized by adding Laemmli SDS sample buffer (4X) (Alfa Aesar by Thermo Fisher Scientific) and heated at 95ºC for 5 min (CH-100 BIOSAN). RIPA was used to minimize variations in protein extracts.

The samples were stored at -20ºC until the Western Blot (WB) analysis.

11. Western Blotting

WB is a technique used for analysis of specific proteins fractionated on the basis of molecular weight in an electrophoresis gel coupled with an electrophoretic transfer and an immunodetection with specific antibodies (Burnette 1981).

11.1. Electrophoresis

Sodium dodecyl sulfate-polyacrylamide gels (SDS-PAGE) were used in electrophoresis. The resolving gel, at 12%, was prepared using 3,65 ml of H_2O milliQ, 2,8 ml of resolving buffer [Tris HCl 1,5M, pH=8,3 and Sodium Docecyl Sulfate (SDS) (Fisher Chemical) at 4%], 4,59 ml of 30% acrylamide-Bis (BIO-RAD), 40 µl of 10% ammonium persulfate (APS) (Fisher Chemical) and 9,2 µl of tetramethyl-ethylene-diamine (TEMED) (Fisher Chemical). Isopropanol (Propan-2-ol (Fisher Chemical) was used for oxygen removal after the resolving gel and removed before the stacking gel. The stacking gel, at 4%, was prepared using 175 ml of H_2O milliQ, 1,25 ml of stacking buffer [Tris HCL 0,5M, pH=6,8 and SDS at 0,4%], 500 µl of 30% acrylamide, 50 µl of 10% APS and 5 µl of TEMED.

The same amount of total protein (80 µg/20-30 µl) and a protein marker ((8 µl) NZY Tech) were loaded per lane and fractionated by electrophoresis (BIO-RAD) in the 12 % resolving gel and the 4% stacking gel on an electrophoresis buffer [Tris-base (Fisher Chemical), Bicine (PanReac AppliChem) and a 20% SDS solution at 80 V for 30 min and 120 V for 1 hour, until proper fractionation of proteins, according with their molecular weight.

11.2. Membrane activation

For the activation of polyvinylidene fluoride membranes (PVDF) (Merck Millipore), they were placed in Methanol 99,9% (Fisher Chemical) for 20 s, washed with distilled H_2O for 5 min, followed by electrophoretic buffer (CAPS (Fisher Chemical) with 10% Methanol) for 15 min.

11.3. Electrophoretic transfer

Posteriorly to the PVDF membrane activation, the electrophoretic transfer was performed in a Wet Tank Blotting System (BIO-RAD), with two sponges, 8 filter papers, the PVDF membrane, the electrophoresis gel and with electrophoretic buffer (CAPS with 10% Methanol) at a constant current of 500 mA for 4 hours at 4ºC.

11.4. Membrane blocking

After the transfer, the membranes were blocked with 30 ml of a 5% BSA (NZY Tech) blocking solution in TBS (Tris-base, NaCl and H_2O) and Tween™ 20 (Fisher BioReafents™) (TBS-T: Tris-Buffered Saline-Tween) for 1 hour at room temperature.

11.5. Antibodies

The primary and secondary antibodies used in WB technique are described in **Table 6**.

Table 6| List of antibodies used in western blots

Type	Antibody	Dilution	Weight	Source
Primary	Mouse Anti-PPAR-γ (81B8)	1:1000	57 kDa	Cell Signaling Technology ®
	Rabbit Anti-UCP1 (D9D6X)	1:1000	30 kDa	Cell Signaling Technology ®
	Mouse Anti- β-Actin	1:5000	42 kDa	SIGMA
Secondary	Anti-Mouse	1:10000		GE Healthcare
	Anti-Rabbit	1:10000		GE Healthcare

Table 6: Shows the type of antibody, the animal species, the protein target, the dilution used, the molecular weight of the protein target and the supplier. **Abbreviations: PPAR-γ:** peroxisome proliferator activated receptor γ; **UCP-1**: uncoupling protein 1.

11.5.1. Primary antibody

The PVDF membranes were incubated with the respective primary antibody (**Table 6**), diluted in a 5% BSA and sodium azide (Alfa Aesar - 99%) solution, at 4ºC overnight with shaking.

11.5.2. Secondary antibody

The PVDF membranes were washed with three series of TBS-T 1X for 10 min each and incubated with a rabbit or mouse IgG-specific secondary antibody, diluted in 5% BSA, for one/two hours, with shaking.

11.6. Membrane detection

Posteriorly, the PVDF membranes were washed with three series of TBS 1X for 10 min each. Using 600 µl of the Amersham™ ECL™, Prime or Select, Western Blotting Detection Reagent (GE Healthcare- Life Sciences) for 5 min in light protected conditions; the proteins were detected by chemiluminescence on a ChemiDoc™ XRS+ Imaging System (BIO-RAD) couple to Image Lab software (BIO-RAD).

For membranes re-probing, the PVDF membranes were washed with three series of TBS-T 1X, one series for 10 min and two series of 1 hour. Next, the PVDF membranes were incubated with the respective antibodies.

11.7. Stripping

Stripping was used to remove the primary and secondary antibodies from PVDF membranes.

The PVDF membranes were washed, under agitation and at room temperature, with 40% methanol for 30 min, distillated H_2O for 5 min, 0.2M NaOH for 5 min and again with distillated H_2O for 5 min. Posteriorly, the PVFD membranes were placed in BSA 5% blocking solution for one hour under agitation at room temperature and were incubated with the respective primary antibody, at 4ºC overnight with shaking.

11.8. Quantification

The optical density of the bands was quantified with Image J – Fiji software.

Membranes were re-probed with a monoclonal anti- β-actin for protein load control.

The specific optical density was then normalized with respect to the amount of β-actin loaded in the corresponding lane of the gel.

12. Statistical analysis

Statistical analyses and graphing were performed using GraphPad Prism 6 (GraphPad Prism Software). All results are expressed as mean ± SEM. Values identified as outliers by Grubbs' test (α=0.05) were excluded from analysis. The comparison of two independent groups the unpaired two-tailed Student's t-test was used. For the comparison of more than

two groups was performed by two-way analysis of variance (ANOVA), with Bonferroni's multiple comparisons test. Statistical significance defined as $p<0,05$. [*P*-value < 0,05 (*), *P*-value < 0,01 (**), *P*-value < 0,001 (***), *P*-value < 0,0001 (****)].

Results

1. HFD increases body weight of C57BL/6J wild-type mice

The consumption of a high-fat dietary content often results in obesity, which is strongly correlated with an increase of body weight (Miller et al. 1990).

In this study, C57BL/6J wild-type mice (*n=45*), which is a strain genetically susceptible for diet-induced obesity, were divided into two groups corresponding to two different diets. One group (*n=24*) had access to a low-fat control diet (Chow) containing 10% of fat and the other group (*n=21*) had access to a high-fat diet (HFD) containing 60% of fat. The animals were weighted twice a week for posterior BW analysis. In the 4th week of food access, and before the stereotaxic injection to silence Cyp46a1 levels in the hypothalamus, the total and cumulative BW gain was analyzed **(Figure 11 – A/B**) in order to observe the impact of HFD feeding in the body weight of the C57BL/6J wild-type mice.

In the 4th week, the C57BL/6J mice group fed with HFD (HFD animals) presented a significant increase on total BW gain comparatively to the mice group fed with Chow (Chow animals) [Chow (0,3600 ± 0,1835); *n=24* versus HFD (5,574 ± 0,7989); *n=21* – *P*-value <0,0001] (**Figure 11 – A**). In the cumulative BW gain (**Figure 11 – B**), both groups, Chow and HFD animals, started the study with an average BW of 20-25g and over time, in 1st, 2nd, 3rd and 4th week, the HFD animals exhibited a significant increase on the body weight gain comparatively to Chow animals [Chow; *n=24* versus HFD; *n=21* – 0: *P*-value >0,9999; 1: *P*-value =0,0007; 2: *P*-value <0,0001; 3: *P*-value <0,0001; 4: P-value <0,0001].

Additionally, the food was also weighted, twice a week, and the water measured, once a week, to analyze the total food and water intake (**Figure 11 – C/E**) and the cumulative food and water intake (**Figure 11 – D/F**). In the total food intake analysis, the HFD animals showed a significant increase on total food intake comparatively to the Chow animals [Chow (87,23 ± 2,266); *n=24* versus HFD (171,8 ± 8,903); *n=21* – *P*-value <0,0001] in the 4th week (**Figure 11 – C)**. The HFD animals, in the cumulative food intake analysis, presented a significant increase of food intake, in the 2nd, 3rd and 4th week, comparatively to the Chow animals [Chow; *n=24* versus HFD; *n=21* – 0: *P*-value >0,9999; 1: *P*-value =0,0010; 2: *P*-value <0,0001; 3: *P*-value <0,0001; 4: P-value <0,0001] (**Figure 11 – D**). Curiously, the HFD animals, in total water intake analysis presented a significant decrease relatively to the Chow animals [Chow (94,19 ± 2,947); *n=24* versus HFD (121,3 ± 9,116); *n=21* – *P*-value =0,0107] (**Figure 11 – E)**. In the cumulative

water intake analysis, the HFD animals showed an increase in water intake, in 3rd and 4th week, relatively to the Chow animals [Chow; *n=24* versus HFD; *n=21* – 0: *P*-value >0,9999; 1: *P*-value > 0,9999; 2: *P*-value =0,0509; 3: *P*-value =0,0090; 4: P-value =0,0013] (**Figure 11 – F**).

Overall, these results show suggest that an HFD leads to an increase on total and cumulative BW gain and an increase in the food intake of C57BL/6J wild-type mice.

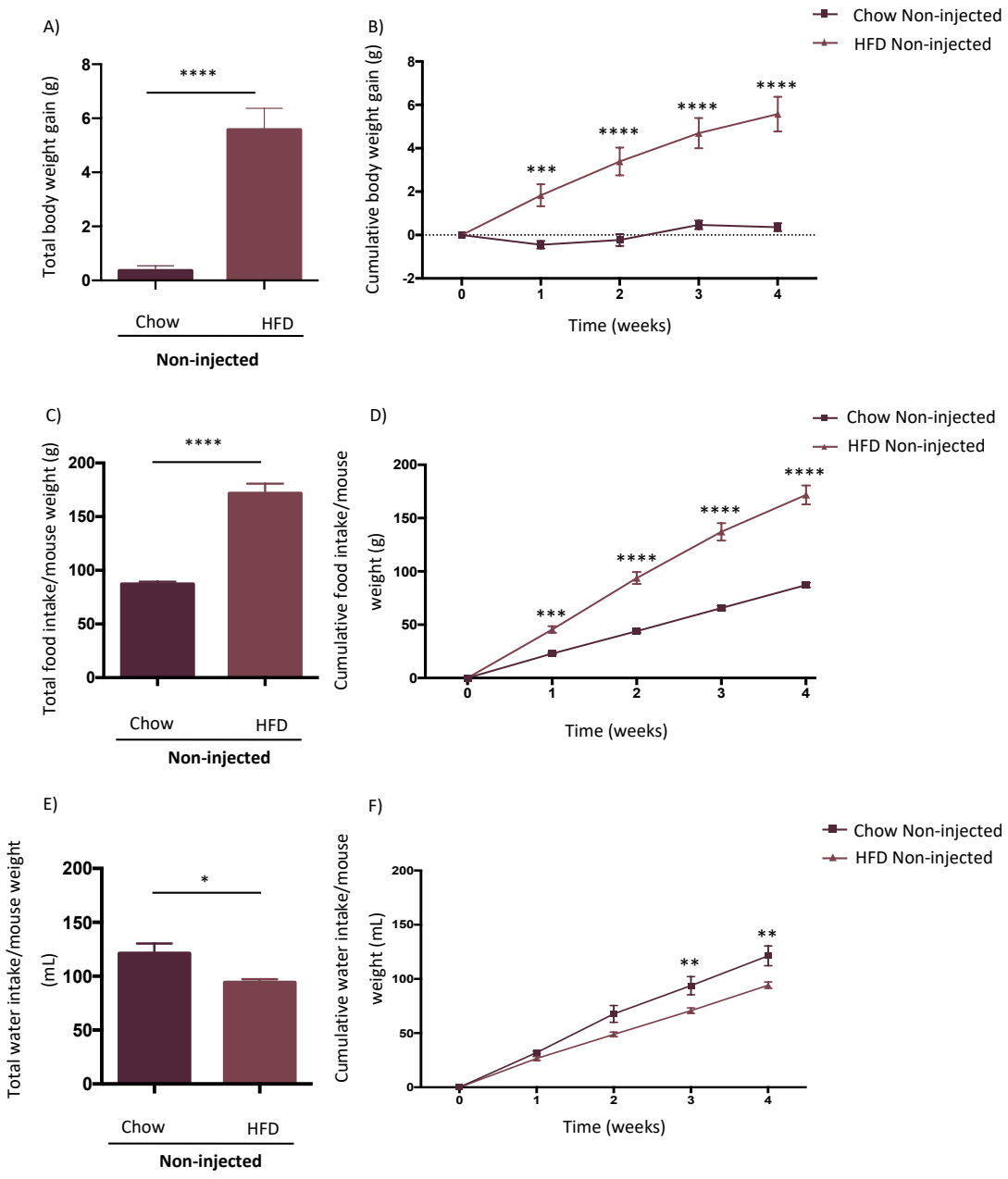

Figure 11| HFD increases in body weight, and increases the food intake of C57BL/6J wild-type mice

The C57BL/6J wild-type mice (*n=45*) were primarily into two groups corresponding to two different diets. One group (*n=24*) had access to a low-fat control diet (Chow) containing 10% of fat and the other group (*n=21*) had access to a high-fat diet (HFD) containing 60% of fat. In the 4th week, the total and

cumulative BW gain was analyzed. **A)** The C57BL/6J mice fed with HFD, HFD animals, presented a statistically significant increase on total BW gain comparatively to the mice fed with Chow, Chow animals [Chow (0,3600 ± 0,1835); *n=24* versus HFD (5,574 ± 0,7989); *n=21* – *P*-value <0,0001]. **B)** The HFD animals presented a statistically significant increase on cumulative BW gain comparatively to the Chow animals [Chow; *n=24* versus HFD; *n=21* – 0: *P*-value >0,9999; 1: *P*-value =0,0007; 2: *P*-value <0,0001; 3: *P*-value <0,0001; 4: P-value <0,0001]. **C)** The HFD animals presented a statistically significant increase of the total food intake comparatively to the Chow animals [Chow (87,23 ± 2,266); *n=24* versus HFD (171,8 ± 8,903); *n=21* – *P*-value <0,0001]. **D)** The HFD animals presented a statistically significant increase of the cumulative food intake, in the 1st, 2nd, 3rd and 4th week, comparatively to the Chow animals [Chow; *n=24* versus HFD; *n=21* – 0: *P*-value >0,9999; 1: *P*-value =0,0010; 2: *P*-value <0,0001; 3: *P*-value <0,0001; 4: P-value <0,0001]. **E)** The HFD animals presented a statistically significant reduction of the total water intake comparatively to the Chow animals in the 4th week [Chow (94,19 ± 2,947); *n=24* versus HFD (121,3 ± 9,116); *n=21* – *P*-value =0,0107]. **F)** The HFD animals presented a statistically significant increase of the cumulative water intake, in the 3rd and 4th week, comparatively to the Chow animals [Chow; *n=24* versus HFD; *n=21* – 0: *P*-value >0,9999; 1: *P*-value > 0,9999; 2: *P*-value =0,0509; 3: *P*-value =0,0090; 4: P-value =0,0013]. Data were represented as mean ± SEM. [*P*-value < 0,05 (*), *P*-value < 0,01 (**), *P*-value < 0,001 (***), *P*-value < 0,0001 (****) - unpaired Student's t-test: A-C-E; Two-way ANOVA with Bonferroni's multiple comparisons test: B-D-F. **Abbreviations: AAV5:** adeno-associated vectors of the serotype 5; **BW:** body weight; **Chow:** low fat control diet; **HFD:** high fat diet; **sh:** short hairpin.

2. Silencing *Cyp46a1* gene in the hypothalamus increases body weight of C57BL/6J mice fed with Chow and HFD

Cholesterol is crucial in neuronal physiology and therefore its metabolism is tightly controlled through an equilibrium between cholesterol synthesis, storage, conversion to oxysterol and cholesterol excretion (Zhang and Liu 2015). The conversion of cholesterol into oxysterols is catalyzed by CYP46A1 enzyme, a member of the cytochrome P450 family, which is encoded by *CYP46A1* gene. The CYP46A1 converts cholesterol into 24-OHC in the neurons of CNS. Contrarily to cholesterol, 24-OHC is a molecule with capacity to cross BBB and reach systematic circulation to posterior elimination in biliary acids (Björkhem 2006).

Previous studies documented that a stereotaxic injection delivering a shRNA targeting the *Cyp46a1* gene, in the hippocampus of C57BL/6J wild-type mice, decreases the expression of *Cyp46a1* resulting in a decrease of 24-OHC oxysterols levels in hippocampus and as consequence an accumulation of cholesterol (Djelti et al. 2015; Boussicault et al. 2016). The cholesterol content increased 2 to 2.5-fold, which induced the apoptotic death of hippocampal neurons in C57BL/6J wild-type mice (Djelti et al. 2015). Hippocampal neurons, upon *Cyp46a1* expression inhibition, showed signals of apoptosis, including shrinkage of the cell soma, presence of pyknotic nuclei and caspase activation (Djelti et al. 2015). Moreover,

alterations in oxysterol metabolism were correlated with obesity (Guillemot-Legris et al. 2016). In fact, previous studies showed decreases in the oxysterols levels of obese mice models (Guillemot-Legris et al. 2016).

Therefore, we hypothesized that the silencing of *Cyp46a1* gene in the hypothalamus, namely in the ARC, leads to a reduction in the Cyp46a1 enzymatic activity, as consequence to a reduction of 24-OHC levels and a cholesterol accumulation in ARC neurons. As the ARC is implicated in the control of whole-body energy metabolism, this silencing of *Cyp46a1* gene, could lead to an obesity and TIIDM phenotypes.

This study was conducted during a period of 12 weeks. In the 4th week, the two groups of mice (Chow and HFD) were divided into four subgroups, two that were submitted to the stereotaxic injection delivering the AAV of the serotype 5, with the shRNA targeting the mouse *Cyp46a1* gene (Chow AAV5-sh*Cyp46a1* and HFD AAV5-sh*Cyp46a1*), and the remaining two subgroups were not submitted to the stereotaxic injection (Chow-Non-injected and HFD-Non-injected), which constituted the control groups. The stereotaxic injection was performed in each side of the ARC. The four subgroups were composed by both females and males (Chow Non-injected: *n=13*, female: *n=4* and male: *n=9*; Chow AAV5-sh*Cyp46a1: n=11*, female: *n=4* and male: *n=7*; HFD Non-injected: *n=10*, female: *n=6* and male: *n=4*; HFD AAV5-sh*Cyp46a1*: *n=11*, female: *n=7* and male: *n=4*). The analysis of the total and cumulative BW gain was performed from the 4th until the 12th week of the study in order to understand the impact of silencing *Cyp46a1* gene in ARC in the body weight (**Figure 12 – A/B and 3 – A/B**).

In the group of Chow animals, the mice submitted to the stereotaxic injection (Chow AAV5-sh*Cyp46a1* animals) presented a significant increase in the total BW gain comparatively to the group of mice not submitted to the stereotaxic injection (Chow Non-injected animals) [Chow Non-injected (2,466 ± 0,3101); *n=13* versus Chow AAV5-sh*Cyp46a1* (8,593 ± 2,088); *n=11* – *P*-value =0,0046] (**Figure 12 – A**). This analysis was also performed comparing the total BW gain between the females and between the males (**Annexes 1 – A/B and 2 – A/B**). Between females the Chow AAV5-sh*Cyp46a1* animals presented an increase in the total BW gain comparatively to Chow Non-injected animals, however, this increase is not significant [Chow Non-injected (1,650 ± 0,4245); *n=4* versus Chow AAV5-sh*Cyp46a1* (7,610 ± 2,965); *n=4* – *P*-value =0,0937] (**Annex 1 – A**). Among males, the Chow AAV5-sh*Cyp46a1* animals presented a significant increase in the total BW gain comparatively to Chow Non-injected

animals [Chow Non-injected (2,829 ± 0,3534); *n=9* versus Chow AAV5-sh*Cyp46a1* (9,154 ± 2,614); *n=7* – *P*-value =0,0297] (**Annex 2 – A**).

In the cumulative BW gain analysis (**Figure 12 – B**), the Chow AAV5-sh*Cyp46a1* animals exhibited a significant increase of body weight gain relatively to Chow Non-injected animals in the 6th and 8th week, after the stereotaxic injection [Chow Non-injected: *n=13* versus Chow AAV5-sh*Cyp46a1*: *n=11* – 0: *P*-value > 0,9999; 3: *P*-value > 0,9999; 6: *P*-value <0,0001; 8: *P*-value =0,0002]. This analysis was additionally performed among the females and the males (**Annex 1 – B and 2 – B**). The analysis of the cumulative BW gain between females and between males show that Chow AAV5-sh*Cyp46a1* animals presented a significant increase in the body weight gain relatively to Chow Non-injected animals, in the 6th and 8th week, after the stereotaxic injection (**Annex 1 – B and 2 – B**) [Females: Chow Non-injected: *n=4* versus Chow AAV5-sh*Cyp46a1*: *n=4* – 0: *P*-value > 0,9999; 3: *P*-value > 0,9999; 6: *P*-value =0,0315; 8: *P*-value =0,0368; Males: Chow Non-injected: *n=9* versus Chow AAV5-sh*Cyp46a1*: *n=7* – 0: *P*-value > 0,9999; 3: *P*-value =0,8459; 6: *P*-value <0,0001; 8: *P*-value =0,0064].

In the HFD animals groups, the mice submitted to the stereotaxic injection (HFD AAV5-sh*Cyp46a1* animals) did not showed a significant increase in the total BW gain, comparatively to the group of mice not submitted to the stereotaxic injection (HFD Non-injected animals) [HFD Non-injected (7,034 ± 0,8942); *n=10* versus HFD AAV5-sh*Cyp46a1* (11,59 ± 2,192); *n=11* – *P*-value =0,0790] (**Figure 13 – A/C/D**). The analysis of the total BW gain was also performed between the females and between the males (**Annexes 3 – A/B and 4 – A/B**). Between females, the HFD AAV5-sh*Cyp46a1* animals comparatively to the HFD Non-injected animals did not presented significant alterations on total body weight gain [HFD Non-injected (6,440 ± 1,413); *n=6* versus HFD AAV5-sh*Cyp46a1* (9,561 ± 2,865); *n=7* – *P*-value =0,3748] (**Annex 3 – A**). Between males, the HFD AAV5-sh*Cyp46a1* animals presented a higher total BW gain comparatively to HFD Non-injected animals, although it was not significant [HFD Non-injected (7,925 ± 0,7522); *n=4* versus HFD AAV5-sh*Cyp46a1* (15,15 ± 2,950); *n=4* – *P*-value =0,0503] (**Annex 4 – A**). The HFD AAV5-sh*Cyp46a1* animals, in the cumulative BW gain analysis, (**Figure 13 – B**) presented a significant increase in the cumulative body weight gain relatively to HFD Non-injected animals in the 8th week after the stereotaxic injection [HFD Non-injected: *n=10* versus HFD AAV5-sh*Cyp46a1*: *n=11* – 0: *P*-value > 0,9999; 3: *P*-value >0,9999; 6: *P*-value =0,5882; 8: *P*-value =0,0452].

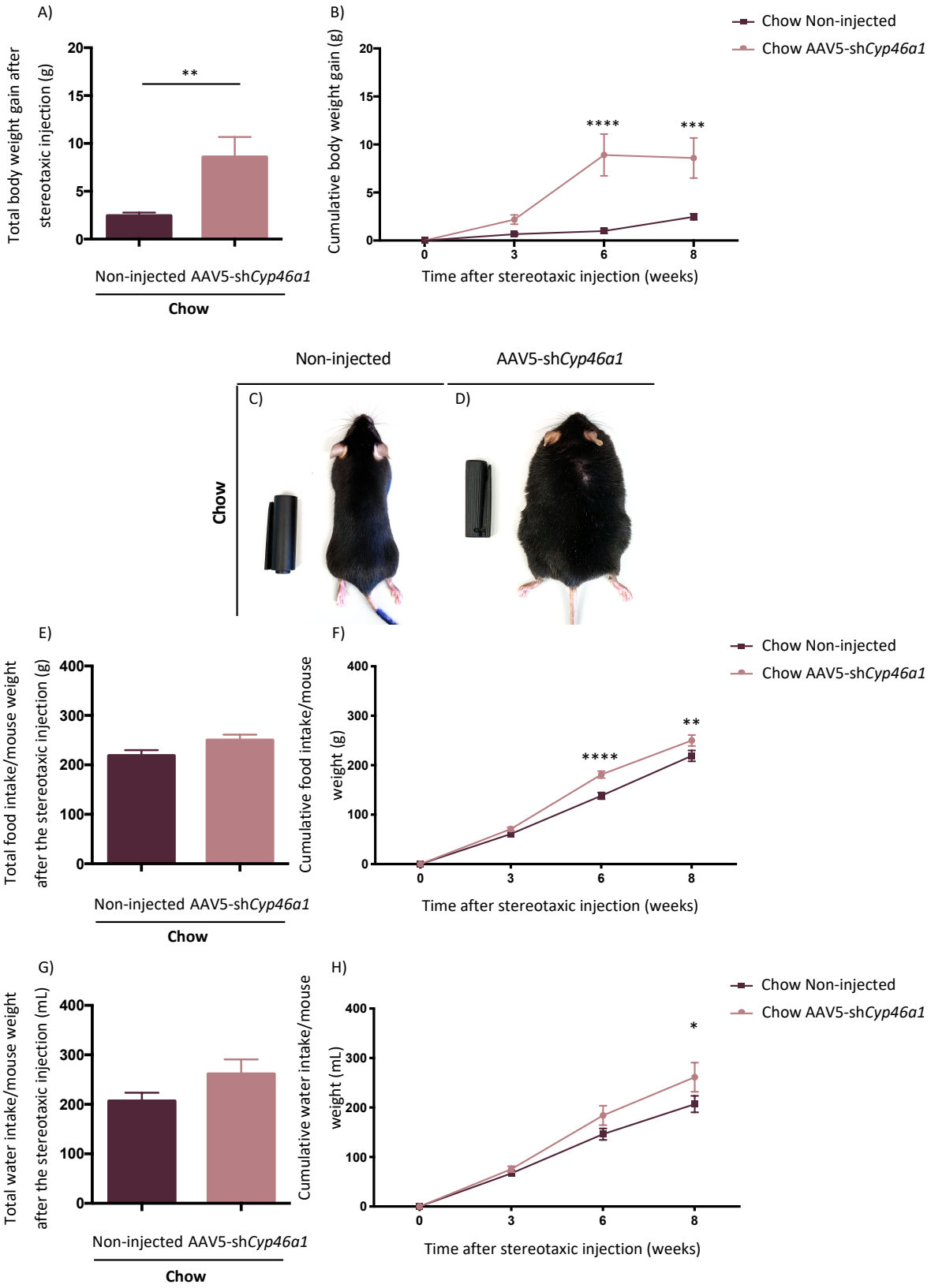

Figure 12| Silencing *Cyp46a1* gene in the hypothalamus induces an increase in body weight of C57BL/6J mice fed with a Chow

In the 4th week of the study the stereotaxic injections were performed in C57BL/6J wild-type mice fed with Chow [Chow AAV5-sh*Cyp46a1* animals – (*n=11)*]. The stereotaxic injection was performed in each

side of the ARC to deliver the AAV5-sh*Cyp46a1*. An analysis of the total and cumulative BW gain from the 4th until the 12th week of the study was performed. **A)** Chow animals submitted to the stereotaxic injection (Chow AAV5-sh*Cyp46a1* animals) showed a statistically significant increase in the total BW gain comparatively to the group of mice not injected (Chow Non-injected animals) [Chow Non-injected (2,466 ± 0,3101); *n=13* versus Chow AAV5-sh*Cyp46a1* (8,593 ± 2,088); *n=11* – *P*-value =0,0046] **B)** Chow AAV5-sh*Cyp46a1* animals presented a statistically significant increase of body weight gain comparatively to Chow Non-injected animals in the 6th and 8th week after the stereotaxic injection [Chow Non-injected: *n=13* versus Chow AAV5-sh*Cyp46a1*: *n=11* – 0: *P*-value > 0,9999; 3: *P*-value > 0,9999; 6: *P*-value <0,0001; 8: *P*-value =0,0002]. **C)** Image of C57BL/6J wild-type mice fed with Chow and non-submitted to stereotaxic injection, at the 12th week of the study. **D)** Image of C57BL/6J wild-type mice fed with Chow and submitted to stereotaxic injection delivering AVV5-sh*Cyp46a1* in the hypothalamus, at the 12th week of the study. **E)** Chow AAV5-sh*Cyp46a1* animals presented an increase in the total food intake comparatively to the Chow Non-injected animals [Chow Non-injected (218,9 ± 11,03); *n=13* versus Chow AAV5-sh*Cyp46a1* (250,1 ± 11,11); *n=11* – *P*-value =0,0609]. **F)** Chow AAV5-sh*Cyp46a1* animals showed an increase of food intake comparatively to Chow Non-injected animals in the 6th and 8th week [Chow Non-injected: *n=13* versus Chow AAV5-sh*Cyp46a1*: *n=11* – 0: *P*-value > 0,9999; 3: *P*-value > 0,9999; 6: *P*-value <0,0001; 8: *P*-value =0,0061]. **G)** Chow AAV5-sh*Cyp46a1* animals presented an increase in the total water intake relatively to the Chow Non-injected animals [Chow Non-injected (206,9 ± 16,60); n=13 versus Chow AAV5-sh*Cyp46a1* (261,4 ± 29,45); n=11 – P-value =0,1080]. **H)** Chow AAV5-sh*Cyp46a1* animals presented an increased in water intake comparatively to the Chow Non-injected animals, in the 8th week [Chow Non-injected: *n=13* versus Chow AAV5-sh*Cyp46a1*: *n=11* – 0: *P*-value >0,9999; 3: *P*-value >0,9999; 6: *P*-value =0,2408; 8: *P*-value =0,0304]. Data were represented as mean ± SEM. [*P*-value < 0,05 (*), *P*-value < 0,01 (**), *P*-value < 0,001 (***), *P*-value < 0,0001 (****) - unpaired Student's t-test: A-E-G; Two-way ANOVA with Bonferroni's multiple comparisons test: B-F-H. **Abbreviations: AAV5:** adeno-associated vectors of the serotype 5; **BW:** body weight; **Chow:** low fat control diet; **HFD:** high fat diet; **sh:** short hairpin.

Between females no alterations were observed in the body weight gain of HFD AAV5-sh*Cyp46a1* animals comparatively to the HFD Non-injected animals (**Annex 3 – B**) [Females: HFD Non-injected: *n=6* versus HFD AAV5-sh*Cyp46a1*: *n=7* – 0: *P*-value > 0,9999; 3: *P*-value =0,9998; 6: *P*-value =0,9110; 8: *P*-value =0,5489]. Between males, the HFD AAV5-sh*Cyp46a1* animals presented a significant increase of BW gain relatively to the HFD Non-injected animals in the 8th week after the stereotaxic injection (**Annex 4 – B**) [Males: HFD Non-injected: *n=4* versus HFD AAV5-sh*Cyp46a1*: *n=4* – 0: *P*-value > 0,9999; 3: *P*-value >0,9999; 6: *P*-value =0,3988; 8: *P*-value =0,0276]. The analysis of the total BW gain was also performed comparing females and males of the same study group (**Annex 5**), however the differences between groups were not significant.

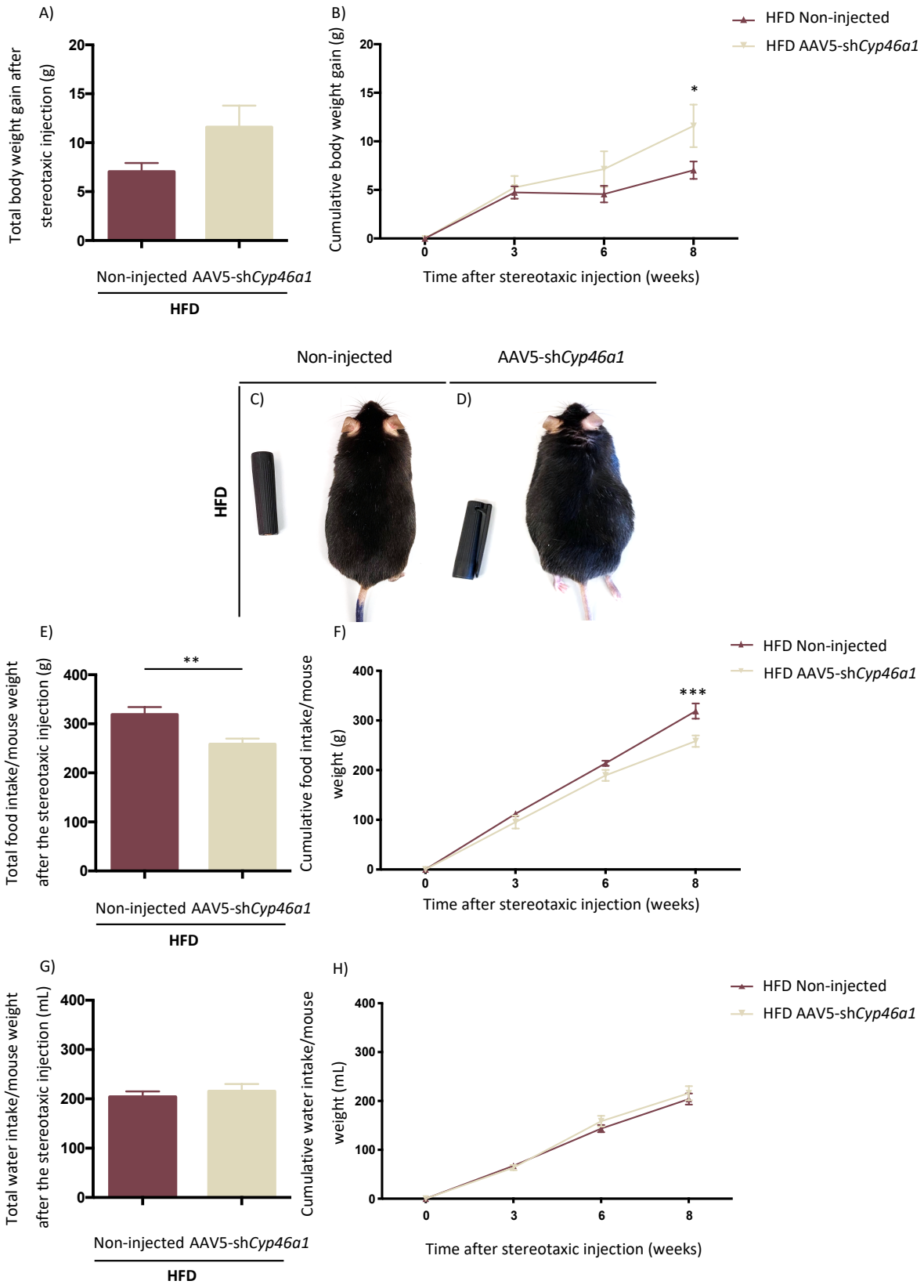

Figure 13| Silencing *Cyp46a1* gene in the hypothalamus induces an increase in body weight and decreases the food intake of C57BL/6J mice fed with an HFD

In the 4th week of the study the stereotaxic injections were performed in C57BL/6J wild-type mice fed

with HFD [HFD AAV5-sh*Cyp46a1* animals – (*n=11)*]. The stereotaxic injection was performed in each side of the ARC, aiming the deliver the AAV5-sh*Cyp46a1* thus inhibiting the *Cyp46a1* expression. An analysis of the total and cumulative BW gain from the 4th until the twelfth week of the study was performed. **A)** HFD animals submitted to the stereotaxic injection (HFD AAV5-sh*Cyp46a1* animals) showed an increase in the total BW gain comparatively to the group of mice not injected (HFD Non-injected animals) [HFD Non-injected (7,034 ± 0,8942); *n=10* versus HFD AAV5-sh*Cyp46a1* (11,59 ± 2,192); *n=11* – *P*-value =0,0790]. **B)** HFD AAV5-sh*Cyp46a1* animals presented a statistically significant increase of body weight gain comparatively to HFD Non-injected animals in the 8th week after the stereotaxic injection [HFD Non-injected: *n=10* versus HFD AAV5-sh*Cyp46a1*: *n=11* – 0: *P*-value > 0,9999; 3: *P*-value >0,9999; 6: *P*-value =0,5882; 8: *P*-value =0,0452]. **C)** Image of C57BL/6J wild-type mice fed with HFD and non-submitted to stereotaxic injection, at the 12th week of the study. **D)** Image of C57BL/6J wild-type mice fed with HFD and submitted to stereotaxic injection delivering AVV5-sh*Cyp46a1* in the hypothalamus, at the 12th week of the study. **E)** HFD AAV5-sh*Cyp46a1* animals presented a statistically significance decrease in the total food intake comparatively to the HFD Non-injected animals [HFD Non-injected (318,9 ± 15,35); *n=10* versus HFD AAV5-sh*Cyp46a1* (258,5 ± 11,49); *n=11* – *P*-value =0,0055]. **F)** HFD AAV5-sh*Cyp46a1* animals showed an increase of food intake comparatively to HFD Non-injected animals in the 8th week [HFD Non-injected: *n=10* versus HFD AAV5-sh*Cyp46a1*: *n=11* – 0: *P*-value > 0,9999; 3: *P*-value =8203; 6: *P*-value =0,2973; 8: *P*-value =0,0001]. **G)** HFD AAV5-sh*Cyp46a1* animals did not presented alterations in the total water intake relatively to the HFD Non-injected animals [HFD Non-injected (204,0 ± 11,26); *n=10* versus HFD AAV5-sh*Cyp46a1* (215,5 ± 14,70); *n=11* – *P*-value =0,5497]. **H)** HFD AAV5-sh*Cyp46a1* animals did not showed alterations in water intake comparatively to the HFD Non-injected animals [HFD Non-injected: *n=4* versus HFD AAV5-sh*Cyp46a1*: *n=4* – 0: *P*-value >0,9999; 3: *P*-value >0,9999; 6: *P*-value =0,8285; 8: *P*-value >0,9999]. Data were represented as mean ± SEM. [*P*-value < 0,05 (*), *P*-value < 0,01 (**), *P*-value < 0,001 (***), *P*-value < 0,0001 (****) - unpaired Student's t-test: A-E-G; Two-way ANOVA with Bonferroni's multiple comparisons test: B-F-H. **Abbreviations: AAV5:** adeno-associated vectors of the serotype 5; **BW:** body weight; **Chow:** low fat control diet; **HFD:** high fat diet; **sh:** short hairpin.

Altogether, these results suggest that the silencing of the *Cyp46a1* gene in the hypothalamus leads to increase on total and cumulative BW gain in C57BL/6J wild-type mice fed either with a Chow or with HFD.

3. Silencing *Cyp46a1* gene in the hypothalamus alters food and water intake of C57BL/6J mice fed with a Chow and HFD

The food was weighted, twice a week, and water measured, once a week, to perform the analysis of the total food and water intake (**Figure 12 – E/G and 13 – E/G**) and the cumulative food and water intake from the 4th until the 12th week of the study (**Figure 12 – F/H and 13 – F/H**) in order to investigate the impact of silencing *Cyp46a1* gene in food and water intake.

In the Chow groups, the Chow AAV5-sh*Cyp46a1* animals presented an increase in the total food intake comparatively to the Chow Non-injected animals in the twelfth week [Chow Non-injected (218,9 ± 11,03); *n=13* versus Chow AAV5-sh*Cyp46a1* (250,1 ± 11,11); *n=11* – *P*-value =0,0609], although, it was not significant (**Figure 12 – E**). Between females, the Chow AAV5-sh*Cyp46a1* animals did not showed alterations in the total food intake comparatively to Chow Non-injected animals, [Chow Non-injected (246,8 ± 12,96); *n=4* versus Chow AAV5-sh*Cyp46a1* (233,1 ± 17,37); *n=4* – *P*-value =0,5505] (**Annex 1 – C**). Between males, the Chow AAV5-sh*Cyp46a1* animals presented a significant increase in the total food intake comparatively to Chow Non-injected animals [Chow Non-injected (206,5 ± 13,16); *n=9* versus Chow AAV5-sh*Cyp46a1* (259,7 ± 13,94); *n=7* – *P*-value =0,0156] (**Annex 2 – C**).

In the cumulative food intake analysis, the Chow AAV5-sh*Cyp46a1* animals exhibited an increase of food intake comparatively to Chow Non-injected animals, in the 6th and 8th week, after the stereotaxic injection [Chow Non-injected: *n=13* versus Chow AAV5-sh*Cyp46a1*: *n=11* – 0: *P*-value > 0,9999; 3: *P*-value > 0,9999; 6: *P*-value <0,0001; 8: *P*-value =0,0061] (**Figure 12 – F**). Females of the Chow AAV5-sh*Cyp46a1* group did not presented alterations in food intake comparatively to females of the Chow Non-injected animals group [Chow Non-injected: *n=4* versus Chow AAV5-sh*Cyp46a1*: *n=4* – 0: *P*-value >0,9999; 3: *P*-value >0,9999; 6: *P*-value >0,9999; 8: *P*-value >0,9999] (**Annex 1 – D**). On the other hand, between males, the Chow AAV5-sh*Cyp46a1* animals showed a significant increase of food intake, in the 6th and 8th week, relatively to Chow Non-injected animals [Chow Non-injected: *n=9* versus Chow AAV5-sh*Cyp46a1*: *n=7* – 0: *P*-value >0,9999; 3: *P*-value =0,5206; 6: *P*-value <0,0001; 8: *P*-value <0,0001] (**Annex 2 – D**).

In the HFD groups, the HFD AAV5-sh*Cyp46a1* animals presented a significant decrease in the total food intake comparatively to the HFD Non-injected animals in the twelfth week [HFD Non-injected (318,9 ± 15,35); *n=10* versus HFD AAV5-sh*Cyp46a1* (258,5 ± 11,49); *n=11* – *P*-value =0,0055] (**Figure 13 – E**). Among females, no differences were observed in the food intake pf the HFD AAV5-sh*Cyp46a1* animals comparatively to HFD Non-injected animals, [HFD Non-injected (300,9 ± 22,72); *n=6* versus HFD AAV5-sh*Cyp46a1* (261,7 ± 19,50); *n=6* – *P*-value =0,2198] (**Annex 3 – C**). Between males, the HFD AAV5-sh*Cyp46a1* animals showed a significant reduction in the total food intake comparatively to HFD Non-injected animals [HFD Non-injected (253,6 ± 5,169); *n=4* versus HFD AAV5-sh*Cyp46a1* (346,0 ± 8,349); *n=4* – *P*-value <0,0001] (**Annex 4 – C**).

The HFD AAV5-sh*Cyp46a1* animals presented a decrease of the cumulative food intake comparatively to HFD Non-injected animals, in the 8th week after the stereotaxic injection [HFD Non-injected: *n=10* versus HFD AAV5-sh*Cyp46a1*: *n=11* – 0: *P*-value > 0,9999; 3: *P*-value =8203; 6: *P*-value =0,2973; 8: *P*-value =0,0001] (**Figure 13 – F**). Between females, the HFD AAV5-sh*Cyp46a1* animals did not presented alterations in the food intake comparatively to the HFD Non-injected animals [HFD Non-injected: *n=6* versus HFD AAV5-sh*Cyp46a1*: *n=7* – 0: *P*-value >0,9999; 3: *P*-value >0,9999; 6: *P*-value >0,9999; 8: *P*-value =0,2771] (**Annex 3 – D**). Among males, the HFD AAV5-sh*Cyp46a1* animals showed a significant reduction of food intake in the 6th and 8th week comparatively to the HFD Non-injected animals[HFD Non-injected: *n=4* versus HFD AAV5-sh*Cyp46a1*: *n=4* – 0: *P*-value > 0,9999; 3: *P*-value =0,0525; 6: *P*-value =0,0006; 8: *P*-value <0,0001] (**Annex 4 – D**).

Regarding the total and cumulative water intake analysis, in the Chow groups, the Chow AAV5-sh*Cyp46a1* animals showed an increase in the total water intake relatively to the Chow Non-injected animals [Chow Non-injected (206,9 ± 16,60); n=13 versus Chow AAV5-sh*Cyp46a1* (261,4 ± 29,45); n=11 – P-value =0,1080], however, this increase was not significant (**Figure 12 – G**). The HFD AAV5-sh*Cyp46a1* animals did not showed significant alterations in this analysis comparatively to the HFD Non-injected group [HFD Non-injected (204,0 ± 11,26); *n=10* versus HFD AAV5-sh*Cyp46a1* (215,5 ± 14,70); *n=11* – *P*-value =0,5497] (**Figure 13 – G**). Between females, in both groups (Chow and HFD animals), the Chow AAV5-sh*Cyp46a1* and the HFD AAV5-sh*Cyp46a1* animals did not showed alterations in the total water intake comparatively to the control groups (Non-injected) [Chow Non-injected (237,5 ± 14,81); *n=4* versus Chow AAV5-sh*Cyp46a1* (255,0 ± 57,32); *n=4* – *P*-value =0,7775] (**Annex 1 – E**) [HFD Non-injected (228,3 ± 8,653); *n=6* versus HFD AAV5-sh*Cyp46a1* (224,3 ± 21,84); *n=6* – *P*-value =0,8745] (**Annex 3 – E**). Between males, the Chow AAV5-sh*Cyp46a1* animals exhibited an increase in total water intake, comparatively to the Chow Non-injected animals, although it was not significant [Chow Non-injected (193,3 ± 22,03); *n=9* versus Chow AAV5-sh*Cyp46a1* (265,0 ± 36,43); *n=7* – *P*-value =0,0991] (**Annex 2 – E**). Concerning the HFD males, the HFD AAV5-sh*Cyp46a1* animals did not showed a significant increase in total water intake relatively to the HFD Non-injected animals [HFD Non-injected (167,5 ± 4,922); *n=4* versus HFD AAV5-sh*Cyp46a1* (200,0 ± 13,71); *n=4* – *P*-value =0,0671] (**Annex 4 – E**).

In the cumulative water intake analysis, in the Chow animals groups, the Chow AAV5-sh*Cyp46a1* animals presented an increased in water intake, in the 8th week, comparatively to

the Chow Non-injected animals [Chow Non-injected: *n=13* versus Chow AAV5-sh*Cyp46a1*: *n=11* – 0: *P*-value >0,9999; 3: *P*-value >0,9999; 6: *P*-value =0,2408; 8: *P*-value =0,0304] (**Figure 12 – H**). The HFD AAV5-sh*Cyp46a1* animals did not showed significant modifications of water intake comparatively to the HFD Non-injected animals [HFD Non-injected: *n=4* versus HFD AAV5-sh*Cyp46a1*: *n=4* – 0: *P*-value >0,9999; 3: *P*-value >0,9999; 6: *P*-value =0,8285; 8: *P*-value >0,9999] (**Figure 13 – H**). Among females, in both groups (Chow and HFD animals), the Chow AAV5-sh*Cyp46a1* and the HFD AAV5-sh*Cyp46a1* animals did not exhibited alterations in water intake comparatively to control mice (Non-injected animals) [Chow Non-injected: *n=4* versus Chow AAV5-sh*Cyp46a1*: *n=4* – 0: *P*-value >0,9999; 3: *P*-value >0,9999; 6: *P*-value >0,9999; 8: *P*-value >0,9999] (**Annex 1 – F**) [HFD Non-injected: *n=6* versus HFD AAV5-sh*Cyp46a1*: *n=7* – 0: *P*-value >0,9999; 3: *P*-value >0,9999; 6: *P*-value >0,9999; 8: *P*-value >0,9999] (**Annex 3 – F**). Between males, in the Chow groups, the Chow AAV5-sh*Cyp46a1* animals presented a significant increase in water intake, in the 8th week, comparatively to the Chow Non-injected animals [Chow Non-injected: *n=9* versus Chow AAV5-sh*Cyp46a1*: *n=7* – 0: *P*-value >0,9999; 3: *P*-value >0,9999; 6: *P*-value =0,1617; 8: *P*-value =0,0209] (**Annex 2 – F**). Between males, the HFD AAV5-sh*Cyp46a1* animals showed a significant increase in water intake, in the 6th and 8th week, comparatively to the HFD Non-injected animals [HFD Non-injected: *n=4* versus HFD AAV5-sh*Cyp46a1*: *n=4* – 0: *P*-value >0,9999; 3: *P*-value >0,9999; 6: *P*-value =0,0127; 8: *P*-value =0,0092] (**Annex 4 – F**).

Overall, these results indicate that the silencing of the *Cyp46a1* gene in the hypothalamus leads to different profiles of food and water intake. In the Chow groups there was an increase on total and cumulative food and water intake, whereas in the HFD animals showed a reduction on total and cumulative food intake.

4. Silencing *Cyp46a1* gene in the hypothalamus induces hyperglycemia and a diminution of insulin sensitivity in C57BL/6J wild-type mice fed with a Chow and HFD

It is known that hyperglycemia and insulin resistance are tightly correlated with obesity and other metabolic abnormalities. Therefore, to study the impact of HFD feeding in glucose levels, a GTT was performed in the 4th week (**Figure 14 – A**). Briefly, the Chow and HFD animals were subjected to a starvation overnight period for about 12-16 hours and then to fasting blood glucose measurement (t=0 min). After the measurement of fasting blood glucose levels, C57BL/6J mice were injected intraperitoneally with a glucose solution (20%) and the blood

glucose levels were measured at 5, 15, 30, 60, 90 and 120 min after the injection. The HFD animals presented higher fasting blood glucose levels relatively to the Chow animals, and also showed higher blood glucose levels at 5, 15, 30, 60, 90 and 120 min after the intraperitoneal injection comparatively to the Chow animals. Nevertheless, the differences were only significant at 0 and 60 min after intraperitoneal injection of glucose solution [Chow *n=3* versus HFD *n=3* – 0: *P*-value =0,0189; 5: *P*-value =0,3343; 15: *P*-value >0,9999; 30: *P*-value =0,0996; 60: *P*-value =0,0090; 90: *P*-value =0,2844; 120: *P*-value =0,8713] (**Figure 14 – A**). It was also possible to observe that the levels of blood glucose in Chow animals started to decrease at 15 min after intraperitoneal injection, whereas in HFD animals they only decrease at 30 min after the intraperitoneal injection. Beyond GTT analysis, the measured blood glucose levels were used to perform the analysis of the total area under the curve (AUC) where, the higher, the lower the glucose tolerance. The HFD animals showed a significant increase of total AUC comparatively to the Chow animals [Chow (667,9 ± 0,8327); *n=3* versus HFD (702,4 ± 7,026); *n=3* – *P*-value =0,0082] (**Figure 14 – B**), suggesting reduced glucose tolerance.

In order to study the impact of HFD feeding in the insulin sensibility, an ITT was performed in the 4th week (**Figure 14 – C**). Briefly, the Chow and HFD animals were subjected to a starvation period for 4 hours and posterior fasting blood glucose measurement (t=0 min). After the measurement of fasting blood glucose levels, the animals were injected intraperitoneally with a 4 mg/ml insulin solution and the blood glucose levels were measured at 5, 15, 30, 60, and 90 min after the injection. The HFD animals presented an increased in blood glucose levels, which were significant 15 min after the insulin injection comparatively to the Chow animals [Chow *n=3* versus HFD *n=3* – 0: *P*-value >0,9999; 5: *P*-value =0,0669; 15: *P*-value =0,0002; 30: *P*-value =0,3156; 60: *P*-value >0,9999; 90: *P*-value >0,9999] (**Figure 14 – C**). The blood glucose levels in Chow animals started to decrease at 5 min after intraperitoneal injection, whereas in the HFD animals only started to decrease at 15 min after the injection. Posteriorly to ITT, the constant for glucose clearance (kITT), per minute (%/min) was analyzed. The HFD animals did not exhibited alterations of kITT comparatively to the Chow animals [Chow (2,027 ± 0,4060); *n=3* versus HFD (2,052 ± 0,7857); *n=3* – *P*-value =0,9793] (**Figure 14 – D**).

Overall, these data suggest that HFD feeding induces hyperglycemia, reduction of glucose tolerance and of insulin sensitivity in C57BL/6J wild-type mice.

In order to investigate the impact of silencing *Cyp46a1* gene in hypothalamus in glucose tolerance and in insulin sensibility, the GTT and ITT were also performed at the end of the study.

In the Chow groups, the Chow AAV5-sh*Cyp46a1* animals presented higher fasting blood glucose levels and higher blood glucose levels at 30, 60, 90 and 120 min after the glucose injection, comparatively to the Chow Non-injected animals in GTT analysis. However, the differences were only significant at 30 min after intraperitoneal injection of glucose solution [Chow Non-injected *n=3* versus Chow AAV5-sh*Cyp46a1 n=3*; 0: *P*-value >0,9999; 5: *P*-value >0,9999; 15: *P*-value =0,8214; 30: *P*-value =0,0025; 60: *P*-value >0,9999; 90: *P*-value >0,9999; 120: *P*-value >0,9999] (**Figure 15 – A**). The levels of blood glucose in the Chow Non-injected animals started to decrease at 15 min after the injection, whereas they only started to decrease at 30 min after the intraperitoneal in the Chow AAV5-sh*Cyp46a1* animals. In total AUC analysis, Chow AAV5-sh*Cyp46a1* animals did not exhibit alterations of total AUC comparatively to the Chow Non-injected [Chow Non-injected (634,8 ± 8,889); *n=3* versus Chow AAV5-sh*Cyp46a1* (642,0 ± 23,57); *n=3* – *P*-value =0,7883] (**Figure 15 – B**).

Concerning the analysis of ITT in the Chow groups, the Chow AAV5-sh*Cyp46a1* animals showed higher blood glucose levels at 15, 30 and 60 min after the insulin injection, comparatively to the Chow control animals. However, the differences were not significant [Chow Non-injected *n=1* versus Chow AAV5-sh*Cyp46a1 n=2*; 0: *P*-value >0,9999; 5: *P*-value >0,9999; 15: *P*-value >0,9999; 30: *P*-value >0,9999; 60: *P*-value =0,2981; 90: *P*-value >0,9999; 120: *P*-value >0,9999] (**Figure 15 – C**). The blood glucose levels of the Chow AAV5-sh*Cyp46a1* animals started to increase at 30 min after the insulin injection. Comparatively, the blood glucose levels of Chow Non-injected animals only started to increase at 60 min after the injection. The constant for glucose clearance (kITT), per minute (%/min) was analyzed and the Chow AAV5-sh*Cyp46a1* animals presented a reduction of kITT comparatively to the Chow Non-injected animals (**Figure 15 – D**), suggesting reduced insulin sensitivity.

In the HFD animals groups, the HFD AAV5-sh*Cyp46a1* animals did not showed significant alterations in the fasting blood glucose levels and in the blood glucose, relative to the HFD Non-injected [HFD Non-injected *n=4* versus HFD AAV5-sh*Cyp46a1 n=4* – 0: *P*-value >0,9999; 5: *P*-value >0,9999; 15: *P*-value >0,9999; 30: *P*-value >0,9999; 60: *P*-value =0,2785; 90: *P*-value >0,9999; 120: *P*-value >0,9999] (**Figure 15 – E**). The blood glucose levels in the HFD Non-injected animals started to decrease at 30 min after the injection, whereas they only

started to decrease at 60 min after the insulin injection, in the HFD AAV5-sh*Cyp46a1* animals. Moreover, HFD AAV5-sh*Cyp46a1* animals did not exhibited alterations of total AUC comparatively to the HFD Non-injected [HFD Non-injected (699,7 ± 5,607); *n=4* versus HFD AAV5-sh*Cyp46a*1 (706,0 ± 11,99); *n=4* – *P*-value =0,6522] (**Figure 15 – B**).

In the ITT analysis, the HFD AAV5-sh*Cyp46a1* animals presented higher blood glucose levels at 5, 15, 30, 60 and 90 min after the insulin injection relatively to the HFD animals, being significant at 5, 15, 60 and 90 min [HFD Non-injected *n=4* versus HFD AAV5-sh*Cyp46a1 n=4*; 0: *P*-value >0,9999; 5: *P*-value =0,0144; 15: *P*-value =0,0030; 30: *P*-value =0,2270; 60: *P*-value =0,0383; 90: *P*-value =0,0290; 120: *P*-value >0,9999] (**Figure 15 – G**). The HFD AAV5-sh*Cyp46a1* animals presented a reduction of kITT comparatively to the HFD Non-injected animals [HFD Non-injected (1,916 ± 0,1041); *n=4* versus HFD AAV5-sh*Cyp46a1* (1,398 ± 0,09075); *n=4* – *P*-value =0,0095] (**Figure 15 – H**), suggesting reduced insulin sensitivity.

Altogether, the results suggest that the silencing *Cyp46a1* gene leads to hyperglycemia and to a reduction of insulin sensitivity in mice fed with Chow and HFD.

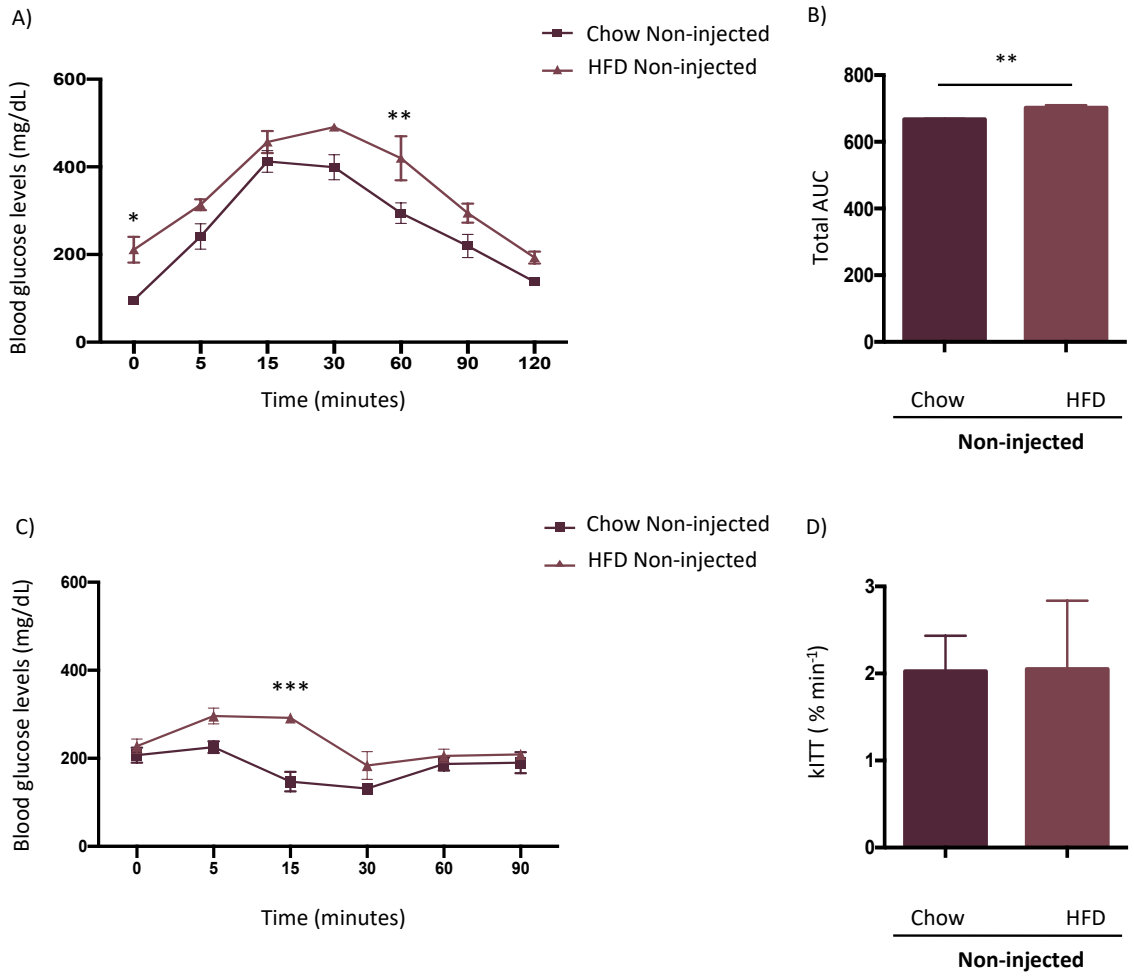

Figure 14| HFD induces hyperglycemia and a diminution of insulin sensitivity of C57BL/6J wild-type mice

In the 4th week of the study, were performed the GTT and the ITT. Briefly, the Chow and HFD animals were subjected to a starvation overnight period for about 12-16 hours in the GTT and a starvation period for 4 hours in ITT, and posterior fasting blood glucose measurement (0). After the measurement of fasting blood glucose levels, in the GTT, the C57BL/6J mice were injected intraperitoneally with a glucose solution (20%) and the blood glucose levels were measured at 5, 15, 30, 60, 90 and 120 min after the injection. In the ITT, the C57BL/6J mice were injected intraperitoneally with an insulin solution and the blood glucose levels were measured at 5, 15, 30, 60, and 90 min after the injection. **A)** The HFD animals presented higher fasting blood glucose levels and higher blood glucose levels at 5, 15, 30, 60, 90 and 120 min after the intraperitoneal injection of glucose solution, comparatively to the Chow animals [Chow *n=3* versus HFD *n=3* – 0: *P*-value =0,0189; 5: *P*-value =0,3343; 15: *P*-value >0,9999; 30: *P*-value =0,0996; 60: *P*-value =0,0090; 90: *P*-value =0,2844; 120: *P*-value =0,8713]. **B)** The HFD animals showed a statistically significant increase of total AUC comparatively to the Chow animals [Chow (667,9 ± 0,8327); *n=3* versus HFD (702,4 ± 7,026); *n=3* – *P*-value =0,0082]. **C)** The HFD animals presented an increased in blood glucose levels, which were statistically significant 15 min after the insulin injection comparatively to the Chow animals [Chow *n=3* versus HFD *n=3* – 0: *P*-value >0,9999; 5: *P*-value =0,0669; 15: *P*-value =0,0002; 30: *P*-value =0,3156; 60: *P*-value >0,9999; 90: *P*-value >0,9999]. **D)** The HFD animals did not exhibited alterations of kITT comparatively to the Chow animals

[Chow (2,027 ± 0,4060); *n=3* versus HFD (2,052 ± 0,7857); *n=3* – *P*-value =0,9793]. Data were represented as mean ± SEM. [*P*-value < 0,05 (*), *P*-value < 0,01 (**), *P*-value < 0,001 (***), *P*-value < 0,0001 (****) - unpaired Student's t-test: B-D; Two-way ANOVA with Bonferroni's multiple comparisons test: A-C. **Abbreviations: AUC**: area under the curve; **Chow:** low fat control diet; **GTT:** glucose tolerance test; **ITT:** insulin tolerance test; **kITT:** constant for glucose clearance; **HFD:** high fat diet.

5. Silencing *Cyp46a1* gene in the hypothalamus modify behavior activity of C57BL/6J mice fed with a Chow and HFD

The animals were subjected to an open field behavior test in the twelfth week in order to study the impact of silencing the *Cyp46a1* gene in the locomotor and anxiety-like behavior. The open field behavior test consisted in placing the mouse in a wall-closed box sufficient high to prevent escaping, and the mouse motor activity was recorded (Seibenhener and Wooten 2015) for 10 min in day-time period (*n=45*) and 5 min in the night-time period (*n*=24). The following parameters were scored: total distance, mean speed, time spend immobile, immobile episodes, number of line crossings, number and time of rearing, number and time of grooming, number of entries and time spend in the middle.

In day-time period, the injected animals (AAV5-sh*Cyp46a1*) in both diets, Chow and HFD, did not showed significant alteration in the total distance traveled comparatively to the Non-injected animals (**Figure 16 – A/B**) (**Table 7**). In the night-time period, the Chow AAV5-sh*Cyp46a1* animals showed a significant decrease of total distance traveled relatively to Chow Non-injected animals [Chow Non-injected (18,68 ± 1,084); *n=8* versus Chow AAV5-sh*Cyp46a1* (9,538 ± 3,489); *n=5* – *P*-value =0,0116] (**Figure 17 – A**) (**Table 8**). The HFD AAV5-sh*Cyp46a1* animals in comparison to the HFD Non-injected animals did not show any differences in total distance traveled (**Figure 17 – B**) (**Table 8**). The Chow AAV5-sh*Cyp46a1* and HFD AAV5-sh*Cyp46a1* animals, in the day-time period, did not showed significant alterations in the mean speed comparatively to the Non-injected animals (**Figure 16 – C/D**) (**Table 7**). Between males, the HFD AAV5-sh*Cyp46a1* animals presented a significant decrease in the mean speed relatively to the HFD Non-injected animals [HFD Non-injected (0,0480 ± 0,00465); *n=4* versus HFD AAV5-sh*Cyp46a1* (0,015 ± 0,0039); *n=4* – *P*-value =0,0017] (**Annex 6 – H**) (**Annex 20**).

In the night-time period, the Chow AAV5-sh*Cyp46a1* animals exhibited a significant decrease in the mean speed comparatively to Chow Non-injected animals [Chow Non-injected (0,06238 ± 0,0036); *n=8* versus Chow AAV5-sh*Cyp46a1* (0,0318 ± 0,0118); *n=5* – *P*-value =0,0120] (**Figure 17 – C**) (**Table 8**).

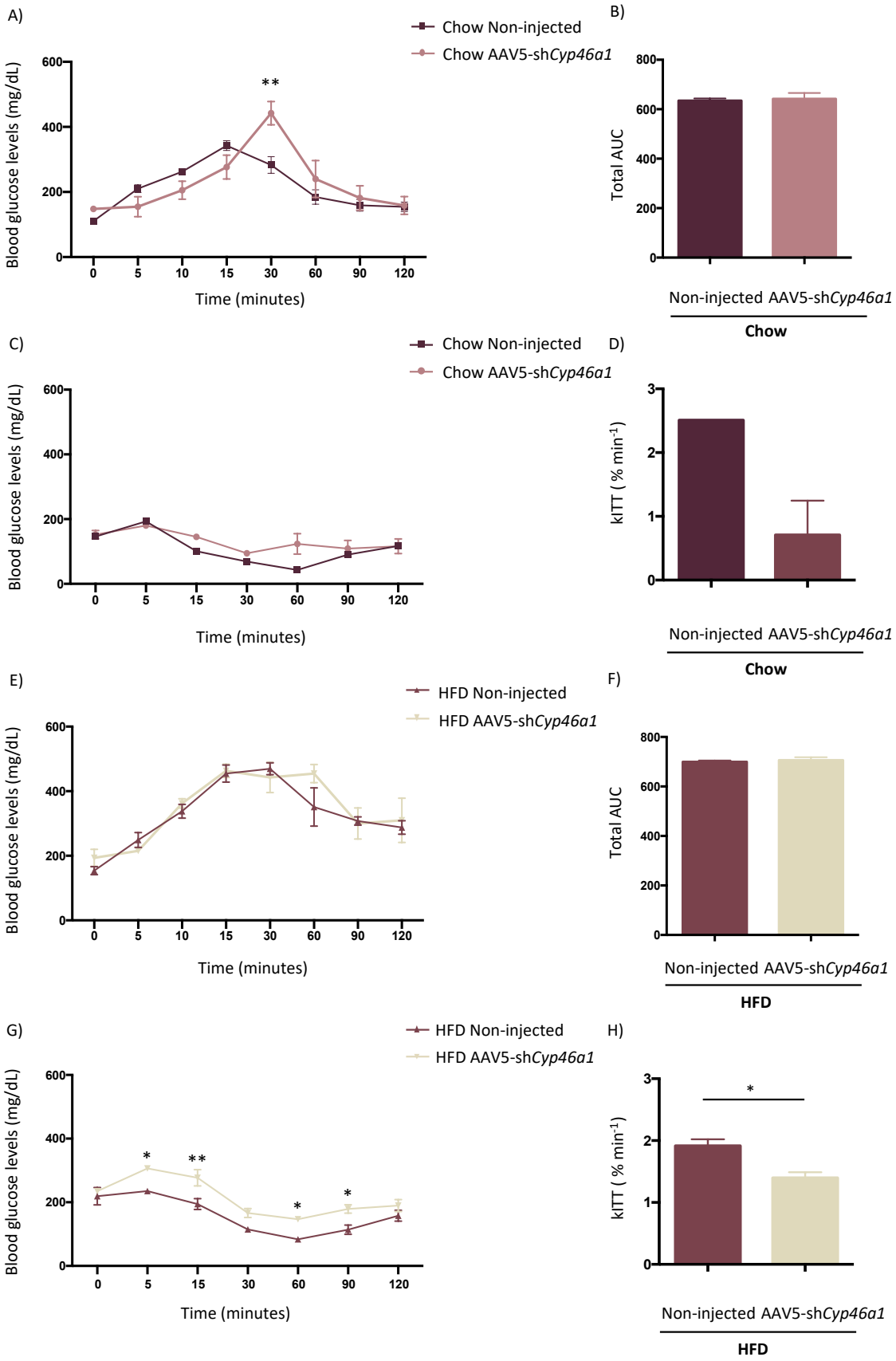

Figure 15| Silencing *Cyp46a1* gene in the hypothalamus induces hyperglycemia and a diminution of insulin sensitivity of C57BL/6J wild-type mice fed with a Chow and an HFD

In the 12th week of the study, were performed the GTT and the ITT. **A)** The Chow AAV5-sh*Cyp46a1*

animals showed higher fasting blood glucose levels and higher blood glucose levels at 30, 60, 90 and 120 min after the glucose injection, comparatively to the Chow Non-injected animals [Chow Non-injected *n=3* versus Chow AAV5-sh*Cyp46a1 n=3*; 0: *P*-value >0,9999; 5: *P*-value >0,9999; 15: *P*-value =0,8214; 30: *P*-value =0,0025; 60: *P*-value >0,9999; 90: *P*-value >0,9999; 120: *P*-value >0,9999]. **B)** The Chow AAV5-sh*Cyp46a1* animals did not exhibit alterations of total AUC comparatively to the Chow Non-injected animals [Chow Non-injected (634,8 ± 8,889); *n=3* versus Chow AAV5-sh*Cyp46a1* (642,0 ± 23,57); *n=3* – *P*-value =0,7883]. **C)** The Chow AAV5-sh*Cyp46a1* animals showed higher blood glucose levels at 15, 30 and 60 min after the insulin injection, comparatively to the Chow Non-injected animals [Chow Non-injected *n=1* versus Chow AAV5-sh*Cyp46a1 n=2*; 0: *P*-value >0,9999; 5: *P*-value >0,9999; 15: *P*-value >0,9999; 30: *P*-value >0,9999; 60: *P*-value =0,2981; 90: *P*-value >0,9999; 120: *P*-value >0,9999]. **D)** The Chow AAV5-sh*Cyp46a1* animals presented a reduction of kITT comparatively to the Chow Non-injected animals [Chow Non-injected *n=1* versus Chow AAV5-sh*Cyp46a1 n=2*]. **E)** The HFD AAV5-sh*Cyp46a1* animals did not showed significant alterations in the blood glucose levels comparatively to the HFD Non-injected [HFD Non-injected *n=4* versus HFD AAV5-sh*Cyp46a1 n=4* – 0: *P*-value >0,9999; 5: *P*-value >0,9999; 15: *P*-value >0,9999; 30: *P*-value >0,9999; 60: *P*-value =0,2785; 90: *P*-value >0,9999; 120: *P*-value >0,9999]. **F)** The HFD AAV5-sh*Cyp46a1* animals did not exhibited alterations of total AUC comparatively to the HFD Non-injected [HFD Non-injected (699,7 ± 5,607); *n=4* versus HFD AAV5-sh*Cyp46a*1 (706,0 ± 11,99); *n=4* – *P*-value =0,6522]. **G)** The HFD AAV5-sh*Cyp46a1* animals presented higher blood glucose levels at 5, 15, 30, 60 and 90 min after the insulin injection relatively to the HFD Non-injected animals [HFD Non-injected *n=4* versus HFD AAV5-sh*Cyp46a1 n=4*; 0: *P*-value >0,9999; 5: *P*-value =0,0144; 15: *P*-value =0,0030; 30: *P*-value =0,2270; 60: *P*-value =0,0383; 90: *P*-value =0,0290; 120: *P*-value >0,9999]. **H)** The HFD AAV5-sh*Cyp46a1* animals presented a reduction of kITT comparatively to the HFD Non-injected animals [HFD Non-injected (1,916 ± 0,1041); *n=4* versus HFD AAV5-sh*Cyp46a1* (1,398 ± 0,09075); *n=4* – *P*-value =0,0095]. Data were represented as mean ± SEM. [*P*-value < 0,05 (*), *P*-value < 0,01 (**), *P*-value < 0,001 (***), *P*-value < 0,0001 (****) - unpaired Student's t-test: B-D-F-H; Two-way ANOVA with Bonferroni's multiple comparisons test: A-C-E-G. **Abbreviations: AAV5:** adeno-associated vectors of the serotype 5; **AUC**: area under the curve; **Chow:** low fat control diet; **GTT:** glucose tolerance test; **ITT:** insulin tolerance test; **kITT:** constant for glucose clearance; **HFD:** high fat diet.

The HFD AAV5-sh*Cyp46a1* animals in comparison to the HFD Non-injected animals did not showed modifications in the mean speed (**Figure 17 – D**) (**Table 8**). Between males (**Annex 7 – G/H**), the Chow AAV5-sh*Cyp46a1* animals showed a decreased in mean speed comparatively to Chow Non-injected animals (**Annex 21**) [Chow Non-injected (0,06517 ± 0,0043); *n=6* versus Chow AAV5-sh*Cyp46a1* (0,0153 ± 0,0101); *n=3* – *P*-value =0,0010].

The number of immobile episodes in day-time period, in both groups, the Chow AAV5-sh*Cyp46a1* and HFD AAV5-sh*Cyp46a1* animals did not presented significant alterations comparatively to the Non-injected animals (**Figure 16 – E/F**) (**Table 7**). Among females, the HFD AAV5-sh*Cyp46a1* animals exhibited a significant decrease of the number of immobile episodes relatively to the HFD Non-injected animals [HFD Non-injected (47,00 ± 2,887); *n=6* versus HFD AAV5-sh*Cyp46a1* (32,29 ± 4,839); *n=7* – *P*-value =0,0296] (**Annex 8 – B**) (**Annex**

18). In the night-time period, in both groups, Chow and HFD animals, the AAV5-sh*Cyp46a1* animals did not show significant alterations in the number of immobile episodes compared to Non-injected animals (**Figure 17 – E/F**) (**Table 8**).

The analysis of the time immobile in day-time period demonstrated that the Chow AAV5-sh*Cyp46a1* and HFD AAV5-sh*Cyp46a1* animals did not presented significant alterations in the time immobile comparatively to the Non-injected animals (**Figure 16 – G/H**) (**Table 7**). Between males, the HFD AAV5-sh*Cyp46a1* animals presented a significant increase in the time immobile in comparison to the HFD Non-injected animals [HFD Non-injected (190,1 ± 34,95); *n=4* versus HFD AAV5-sh*Cyp46a1* (430,8 ± 42,52); *n=4* – *P*-value =0,0047] (**Annex 8 – H**) (**Annex 20**). In the night-time period, the Chow AAV5-sh*Cyp46a1* animals exhibited a significant increase in the time immobile comparatively to Chow Non-injected animals [Chow Non-injected (54,24 ± 8,265); *n=8* versus Chow AAV5-sh*Cyp46a1* (149,5 ± 45,60); *n=5* – *P*-value =0,0247] (**Figure 17 – G**) (**Table 8**). The HFD AAV5-sh*Cyp46a1* animals did not exhibited alterations in the time immobile comparatively to the HFD Non-injected animals (**Figure 17 – H**) (**Table 8**). Between males (**Annex 9 – G/H**), the Chow AAV5-sh*Cyp46a1* animals showed a significant increase in the time immobile relatively to Chow Non-injected animals [Chow Non-injected (51,17 ± 10,60); *n=6* versus Chow AAV5-sh*Cyp46a1* (205 ± 54,92); *n=3* – *P*-value =0,0056] (**Annex 21**).

The Chow AAV5-sh*Cyp46a1* and HFD AAV5-sh*Cyp46a1* animals did not presented significant alterations in the number of crossing lines comparatively to the Non-injected animals (**Figure 18 – A/B**) (**Table 7**). Between males the HFD AAV5-sh*Cyp46a1* animals presented a significant decrease in the number of crossing lines relatively to the HFD Non-injected animals [HFD Non-injected (242,3 ± 29,55); *n=2* versus HFD AAV5-sh*Cyp46a1* (64,25 ± 12,93); *n=2* – *P*-value =0,0015] (**Annex 10 – D**) (**Annex 20**). In the night-time period, the Chow AAV5-sh*Cyp46a1* animals exhibited a significant decrease in the number of crossing lines comparatively to Chow Non-injected animals [Chow Non-injected (135,0 ± 8,726); *n=8* versus Chow AAV5-sh*Cyp46a1* (63,00 ± 22,13); *n=5* – *P*-value =0,0047] (**Figure 19 – A**) (**Table 8**). The HFD AAV5-sh*Cyp46a1* animals relatively to the HFD Non-injected animals did not displayed modifications in the number of crossing lines (**Figure 19 – B**) (**Table 8**). Between males (**Annex 11 – G/H**), the Chow AAV5-sh*Cyp46a1* animals showed a decrease in the number of crossing lines comparatively to Chow Non-injected animals [Chow Non-injected (138,3 ± 11,40); *n=6* versus Chow AAV5-sh*Cyp46a1* (33,00 ± 21,78); *n=3* – *P*-value =0,0020] (**Annex 21**).

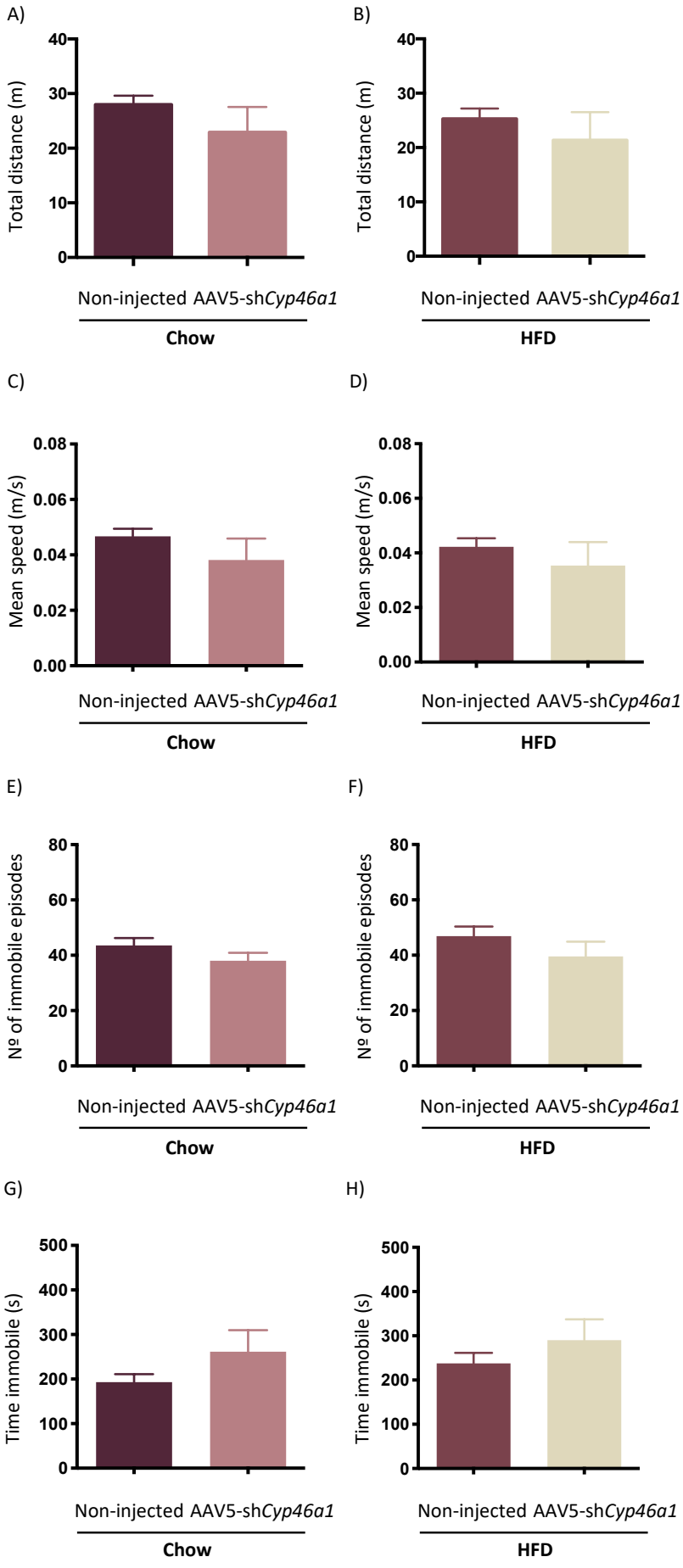
A)
B)
Total distance (m)
40
30
20
10
0
Non-injected
AAV5-sh*Cyp46a1*
Chow
HFD
C)
D)
Mean speed (m/s)
0.08
0.06
0.04
0.02
0.00
E)
F)
Nº of immobile episodes
80
60
40
20
0
G)
H)
Time immobile (s)
500
400
300
200
100
0

Figure 16|Silencing *Cyp46a1* gene in the hypothalamus of C57BL/6J wild-type mice fed with Chow and HFD, did not modified the total distance traveled, mean speed, number of immobile episodes and the time immobile, in the day-time period

The animals were subjected to an open field behavior test in the twelfth week which consisted in placing the mouse in a wall-closed box and the motor activity was recorded for 10 min in day-time period. **A)** The Chow AAV5-sh*Cyp46a1* did not showed significant alteration in the total distance traveled comparatively to the Chow Non-injected animals [Chow Non-injected (27,99 ± 1,622); *n=13* versus Chow AAV5-sh*Cyp46a1* (22,93 ±4,626); *n=11* – *P*-value =0,2823]. **B)** The HFD AAV5-sh*Cyp46a1* did not showed significant alteration in the total distance traveled comparatively to the HFD Non-injected animals [HFD Non-injected (25,29 ± 1,874); *n=10* versus HFD AAV5-sh*Cyp46a1* (21,34 ± 5,179); *n=11* – *P*-value =0,4988]. **C)** The Chow AAV5-sh*Cyp46a1* did not showed significant alterations in the mean speed comparatively to the Chow Non-injected animals [Chow Non-injected (0,047 ± 0,003); *n=13* versus Chow AAV5-sh*Cyp46a1* (0,035 ± 0,008); *n=11* – *P*-value =0,2799]. **D)** The HFD AAV5-sh*Cyp46a1* animals did not presented significant alterations in the mean speed comparatively to the HFD Non-injected animals [HFD Non-injected (0,042 ± 0,003); *n=10* versus HFD AAV5-sh*Cyp46a1* (0,035 ± 0,009); *n=11* – *P*-value =0,4828]. **E)** The Chow AAV5-sh*Cyp46a1* animals did not showed statistically significant alterations in the number of immobile episodes comparatively to the Chow Non-injected animals [Chow Non-injected (43,54 ± 2,707); *n=13* versus Chow AAV5-sh*Cyp46a1* (38,00 ± 2,908); *n=11* – *P*-value =0,1776]. **F)** The HFD AAV5-sh*Cyp46a1* animals did not presented statistically significant alterations in the number of immobile episodes comparatively to the HFD Non-injected animals [HFD Non-injected (46,80 ±3,495); *n=10* versus HFD AAV5-sh*Cyp46a1* (39,55 ± 5,362); *n=11* – *P*-value =0,2815]. **G)** The Chow AAV5-sh*Cyp46a1* animals did not presented significant alterations in the time immobile comparatively to the Chow Non-injected animals [Chow Non-injected (193,1 ± 18,01); *n=13* versus Chow AAV5-sh*Cyp46a1* (261,7 ± 48,24); *n=11* – *P*-value =0,1703]. **H)** The HFD AAV5-sh*Cyp46a1* animals did not presented significant alterations in the time immobile comparatively to the HFD Non-injected animals [HFD Non-injected (237,3 ± 23,91); *n=10* versus HFD AAV5-sh*Cyp46a1* (290,4 ± 46,78); *n=11* – *P*-value =0,3399]. Data were represented as mean ± SEM. [*P*-value < 0,05 (*), *P*-value < 0,01 (**), *P*-value < 0,001 (***), *P*-value < 0,0001 (****) – unpaired Student's t-test: A-B-C-D-E-F-G-H; **Abbreviations: Chow:** low fat control diet; **HFD:** high fat diet; **AAV5:** adeno-associated vectors of the serotype 5; **sh:** short hairpin**.**

In day-time period, the Chow AAV5-sh*Cyp46a1* and HFD AAV5-sh*Cyp46a1* animals showed a significant decrease in the number of entries in the middle zone comparatively to the Non-injected animals [Chow Non-injected (23,15 ±2,643); *n=13* versus Chow AAV5-sh*Cyp46a1* (11,82 ± 2,486); *n=11* – *P*-value =0,0054] (**Figure 18 – C**) [HFD Non-injected (18,90 ± 2,523); *n=10* versus HFD AAV5-sh*Cyp46a1* (8,545 ± 1,956); *n=11* – *P*-value =0,0040] (**Figure 18 – D**) (**Table 7**). Between males, the HFD AAV5-sh*Cyp46a1* animals presented a significant decrease in the number of entries in the middle zone in comparison to the HFD Non-injected animals (**Annex 10 – G**) [HFD Non-injected (24,25 ± 4,526); *n=4* versus HFD AAV5-sh*Cyp46a1*

(4,00 ± 0,7071); *n=4* – *P*-value =0,0044] (**Annex 20**). In night-time period, the Chow AAV5-sh*Cyp46a1* animals showed a significant decrease in the number of entries in the middle zone comparatively to Chow Non-injected animals [Chow Non-injected (11,00 ± 1,512); *n=8* versus Chow AAV5-sh*Cyp46a1* (5,400 ± 1,568); *n=5* – *P*-value =0,0324] (**Figure 19 – C**) (**Table 8**). The HFD AAV5-sh*Cyp46a1* animals did not showed a significant decrease relatively to HFD Non-injected animals (**Figure 19 – D**) (**Table 8**). Between males (**Annex 11 – G/ H**), the Chow AAV5-sh*Cyp46a1* animals showed a significant decrease in the number of crossing lines comparatively to Chow Non-injected animals (**Annex 21**) [Chow Non-injected (11,83 ± 1,887); *n=6* versus Chow AAV5-sh*Cyp46a1* (3,333 ± 1,8453); *n=3* – *P*-value =0,0227].

In day-time period, the Chow AAV5-sh*Cyp46a1* animals showed a decrease in the time spend in the middle zone comparatively to the Chow Non-injected animals, although it was not significant (**Figure 18 – E**). The HFD AAV5-sh*Cyp46a1* presented a significant decrease in the time spend in the middle comparatively to the HFD Non-injected animals [HFD Non-injected (16,94 ± 2,436); *n=10* versus HFD AAV5-sh*Cyp46a1* (9,255 ± 1,699); *n=11* – *P*-value =0,0160] (**Figure 18 – F**) (**Table 7**). Between males, the AAV5-sh*Cyp46a1* animals presented a significant increase in the time spend in the middle zone relatively to the Non-injected animals [Chow Non-injected (29,79 ± 4,922); *n=6* versus Chow AAV5-sh*Cyp46a1* (10,60 ± 2,600); *n=3* – *P*-value =0,0107] (**Annex 12 – C**) [HFD Non-injected (29,50 ± 7,098); *n=2* versus HFD AAV5-sh*Cyp46a1* (8,750 ± 4,422); *n=2* – *P*-value =0,0477] (**Annex 12 – D**) (**Annex 20**). In the night-time period, the Chow AAV5-sh*Cyp46a1* animals presented an increase of time spend in the middle comparatively to Chow Non-injected animals, however, was not significant (**Figure 19 – E**) (**Table 8**). The HFD AAV5-sh*Cyp46a1* animals exhibited a significant increase comparatively to HFD Non-injected animals [HFD Non-injected (7,550 ± 1,414); *n=10* versus HFD AAV5-sh*Cyp46a1* (106,8 ± 36,97); *n=11* – *P*-value =0,0230] (**Figure 19 – F**) (**Table 2**). Amongst females (**Annex 13 – A/B**) the HFD AAV5-sh*Cyp46a1* animals presented a significant increase in the time spend in the middle comparatively to the Non-injected animals [HFD Non-injected (9,075 ± 1,499); *n=4* versus HFD AAV5-sh*Cyp46a1* (133,3 ± 19,65); *n=3* – *P*-value =0,0007] (**Annex 19**).

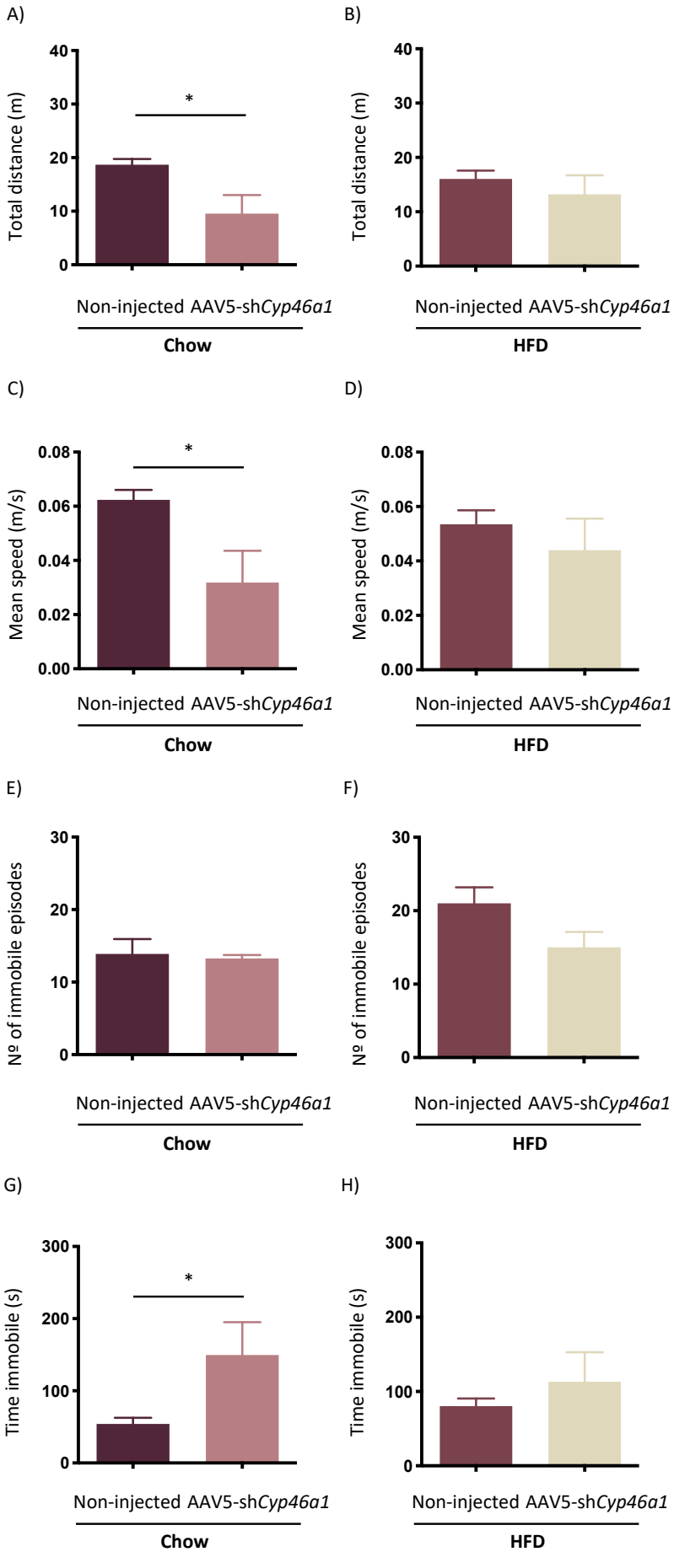
A)
B)
Total distance (m)
40
30
20
10
0
*
Non-injected
AAV5-sh*Cyp46a1*
Chow
HFD
C)
D)
Mean speed (m/s)
0.08
0.06
0.04
0.02
0.00
E)
F)
Nº of immobile episodes
G)
H)
Time immobile (s)
300
200
100

Figure 17| Silencing *Cyp46a1* gene in the hypothalamus of C57BL/6J wild-type mice fed with Chow, modify the total distance traveled, mean speed and the time immobile, in the night-time period

The animals were subjected to an open field behavior test in the twelfth week which consisted in placing the mouse in a wall-closed box and the motor activity was recorded for 5 min in night-time period. **A)** The Chow AAV5-sh*Cyp46a1* animals showed a statistically significant decrease of total distance traveled relatively to Chow Non-injected animals [Chow Non-injected (18,68 ± 1,084); *n=8* versus Chow AAV5-sh*Cyp46a1* (9,538 ± 3,489); *n=5* – *P*-value =0,0116]. **B)** The HFD AAV5-sh*Cyp46a1* did not showed significant alteration in the total distance traveled comparatively to the HFD Non-injected animals [HFD Non-injected (16,04 ± 1,538); *n=6* versus HFD AAV5-sh*Cyp46a1* (13,21 ±3,514); *n=5* – *P*-value =0,4516]. **C)** The Chow AAV5-sh*Cyp46a1* animals showed a statistically significant decrease in the mean speed comparatively to the Chow Non-injected animals [Chow Non-injected (0,06238 ± 0,0036); *n=8* versus Chow AAV5-sh*Cyp46a1* (0,0318 ± 0,0118); *n=5* – *P*-value =0,0120]. **D)** The HFD AAV5-sh*Cyp46a1* animals did not presented significant alterations in the mean speed comparatively to the HFD Non-injected animals [HFD Non-injected (0,0535 ± 0,0051); *n=6* versus HFD AAV5-sh*Cyp46a1* (0,0440 ± 0,0012); *n=5*– *P*-value =0,4460]. **E)** The Chow AAV5-sh*Cyp46a1* animals did not showed statistically significant alterations in the number of immobile episodes comparatively to the Chow Non-injected animals [Chow Non-injected (13,88 ± 2,074); *n=8* versus Chow AAV5-sh*Cyp46a1* (13,25 ± 0,4787); *n=5* – *P*-value =0,8403]. **F)** The HFD AAV5-sh*Cyp46a1* animals did not presented statistically significant alterations in the number of immobile episodes comparatively to the HFD Non-injected animals [HFD Non-injected (21,00 ± 2,176); *n=6* versus HFD AAV5-sh*Cyp46a1* (15,00 ± 2,121); *n=5*– *P*-value =0,0828]. **G)** The Chow AAV5-sh*Cyp46a1* animals exhibited a statistically significant increase in the time immobile comparatively to Chow Non-injected animals [Chow Non-injected (54,24 ± 8,265); *n=8* versus Chow AAV5-sh*Cyp46a1* (149,5 ± 45,60); *n=5* – *P*-value =0,0247]. **H)** The HFD AAV5-sh*Cyp46a1* animals did not presented significant changes in the time immobile comparatively to the HFD Non-injected animals [HFD Non-injected (80,33 ± 10,36); *n=6* versus HFD AAV5-sh*Cyp46a1* (113,1 ± 39,75); *n=5*– *P*-value =0,4067]. Data were represented as mean ± SEM. [*P*-value < 0,05 (*), *P*-value < 0,01 (**), *P*-value < 0,001 (***), *P*-value < 0,0001 (****) – unpaired Student's t-test: A-B-C-D-E-F-G-H; **Abbreviations: Chow:** low fat control diet; **HFD:** high fat diet; **AAV5:** adeno-associated vectors of the serotype 5; **sh:** short hairpin.

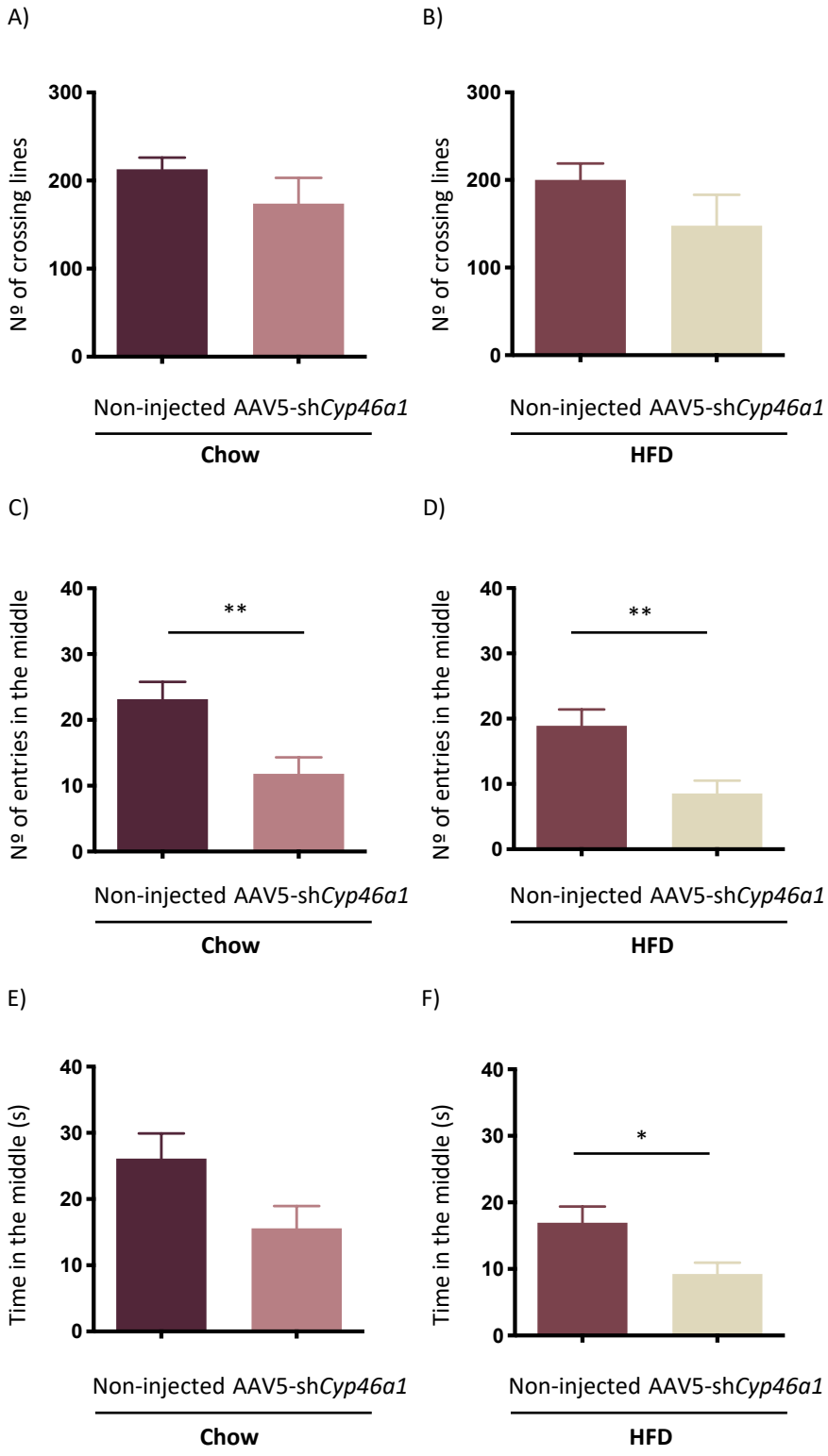

Figure 18| Silencing *Cyp46a1* gene in the hypothalamus of C57BL/6J wild-type mice fed with Chow and HFD, modify the number of entries in the middle and the time in the middle in the day-time period

A) The Chow AAV5-sh*Cyp46a1* did not showed significant alteration in the number of crossing lines comparatively to the Chow Non-injected animals [Chow Non-injected (212,9 ± 13,15); *n=13* versus

Chow AAV5-sh*Cyp46a1* (173 ± 29,41); *n=11* – *P*-value =0,2135]. **B)** The HFD AAV5-sh*Cyp46a1* did not showed significant alteration in the number of crossing lines comparatively to the HFD Non-injected animals [HFD Non-injected (200 ± 18,87); *n=10* versus HFD AAV5-sh*Cyp46a1* (147 ± 35,27); *n=11* – *P*-value =0,2214]. **C)** The Chow AAV5-sh*Cyp46a1* animals showed a statistically significant decrease in the number of entries in the middle zone comparatively to the Chow Non-injected animals [Chow Non-injected (23,15 ±2,643); *n=13* versus Chow AAV5-sh*Cyp46a1* (11,82 ± 2,486); *n=11* – *P*-value =0,0054]. **D)** The HFD AAV5-sh*Cyp46a1* animals showed a statistically significant decrease in the number of entries in the middle zone comparatively to the HFD Non-injected animals [HFD Non-injected (18,90 ± 2,523); *n=10* versus HFD AAV5-sh*Cyp46a1* (8,545 ± 1,956); *n=11* – *P*-value =0,0040]. **E)** The Chow AAV5-sh*Cyp46a1* animals showed a decrease in the time spend in the middle zone comparatively to the Chow Non-injected animals, however it was not statistically significant [Chow Non-injected (26,12 ± 3,810); *n=13* versus Chow AAV5-sh*Cyp46a1* (15,57 ± 3,364); *n=11* – *P*-value =0,0536]. **F)** The HFD AAV5-sh*Cyp46a1* presented a statistically significant decrease in the time spend in the middle comparatively to the HFD Non-injected animals [HFD Non-injected (16,94 ± 2,436); *n=10* versus HFD AAV5-sh*Cyp46a1* (9,255 ± 1,699); *n=11* – *P*-value =0,0160]. Data were represented as mean ± SEM. [*P*-value < 0,05 (*), *P*-value < 0,01 (**), *P*-value < 0,001 (***), *P*-value < 0,0001 (****) – unpaired Student's t-test: A-B-C-D-E-F; **Abbreviations: Chow:** low fat control diet; **HFD:** high fat diet; **AAV5:** adeno-associated vectors of the serotype 5; **sh:** short hairpin.

In the analysis of the number of grooming's, in day-time period, the Chow AAV5-sh*Cyp46a1* animals did not showed modifications comparatively to the Chow Non-injected animals (**Figure 20 – A**). The HFD AAV5-sh*Cyp46a1* animals presented a decrease in the number of grooming's comparatively to the HFD-Non-injected animals, however, it was not significative (**Figure 20 – B**) (**Table 7**). In night-time period, the Chow AAV5-sh*Cyp46a1* animals did not exhibited alterations in the number of grooming's comparatively to Chow Non-injected animals (**Figure 21 – A**) (**Table 8**). The HFD AAV5-sh*Cyp46a1* animals relatively to the HFD Non-injected animals demonstrated a significative decrease in the number of grooming's [HFD Non-injected (1,667 ± 0,2108); *n=10* versus HFD AAV5-sh*Cyp46a1* (1,00 ± 0,0); *n=11* – *P*-value =0,0353] (**Figure 21 – B**) (**Table 8**).

In day-time period, the Chow AAV5-sh*Cyp46a1* exhibited an increase, which was not significant comparatively to the Chow Non-injected animals (**Figure 20 – C**). The HFD AAV5-sh*Cyp46a1* animals did not presented changes in the time of grooming's relatively to the HFD Non-injected animals (**Figure 20 – D**) (**Table 7**). In night-time period, the Chow AAV5-sh*Cyp46a1* animals showed a significant increase in the time of grooming's comparatively to Chow Non-injected animals [Chow Non-injected (4,925 ± 0,7952); *n=8* versus Chow AAV5-sh*Cyp46a1* (111,50 ± 3,452); *n=5* – *P*-value =0,0412] (**Figure 21 – C**) (**Table 8**). The HFD AAV5-

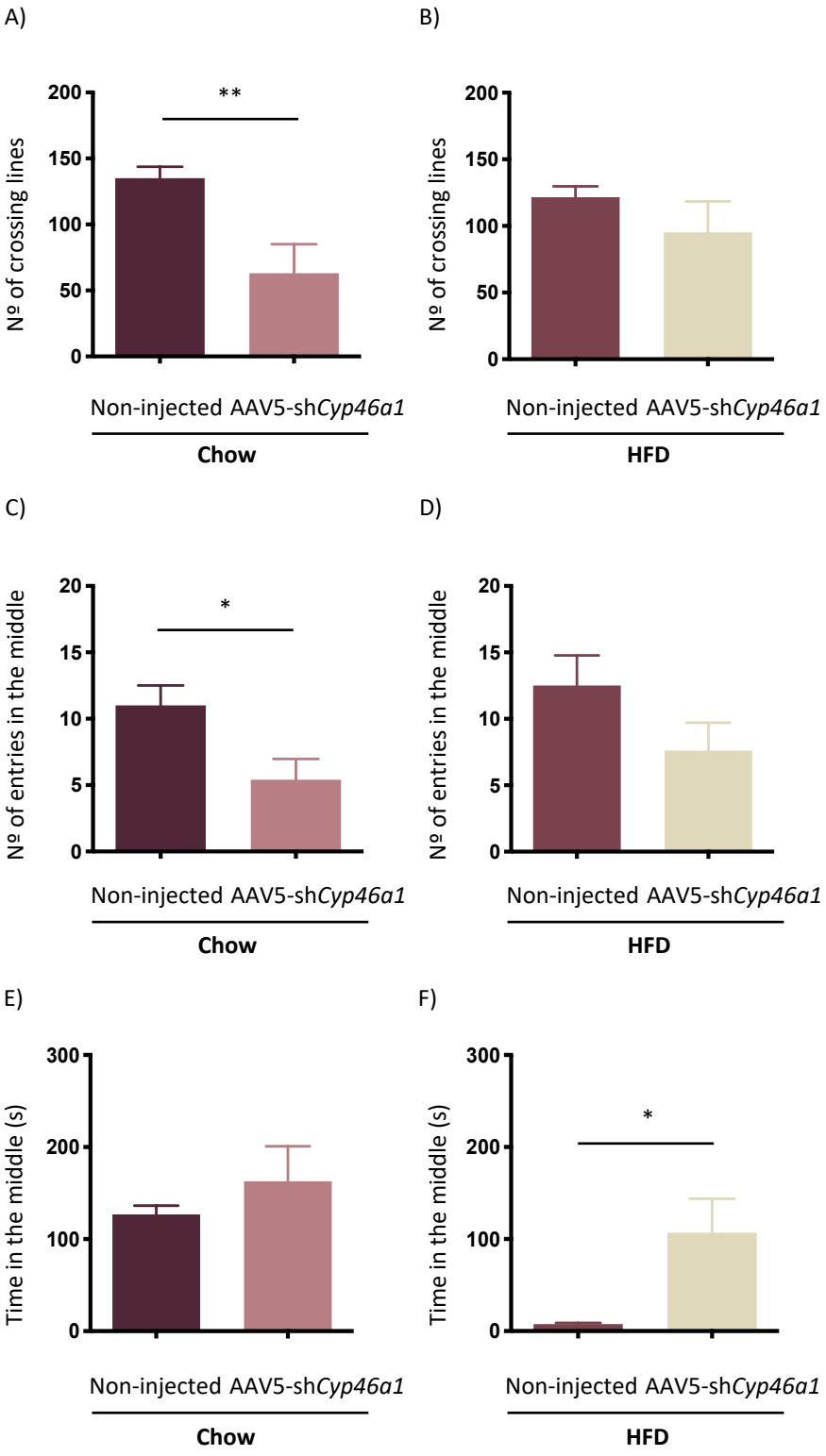

Figure 19| Silencing *Cyp46a1* gene in the hypothalamus of C57BL/6J wild-type mice fed with Chow and HFD, modify the number of crossing lines, of entries in the middle and the time in the middle in the night-time period

A) The Chow AAV5-sh*Cyp46a1* animals exhibited a statistically significant decrease in the number of crossing lines comparatively to Chow Non-injected animals [Chow Non-injected (135,0 ± 8,726); *n=8* versus Chow AAV5-sh*Cyp46a1* (63,00 ± 22,13); *n=5* – *P*-value =0,0047]. **B)** The HFD AAV5-sh*Cyp46a1*

did not showed significant alteration in the number of crossing lines comparatively to the HFD Non-injected animals [HFD Non-injected (121,5 ± 8,168); *n=6* versus HFD AAV5-sh*Cyp46a1* (95,20 ± 23,17); *n=5* – *P*-value =0,2780]. **C)** The Chow AAV5-sh*Cyp46a1* animals showed a statistically significant decrease in the number of entries in the middle zone comparatively to the Chow Non-injected animals Chow Non-injected (11,00 ± 1,512); *n=8* versus Chow AAV5-sh*Cyp46a1* (5,400 ± 1,568); *n=5* – *P*-value =0,0324]. **D)** The HFD AAV5-sh*Cyp46a1* animals did not showed alterations in the number of entries in the middle zone comparatively to the HFD Non-injected animals [HFD Non-injected (12,50 ± 2,277); *n=6* versus HFD AAV5-sh*Cyp46a1* (7,600 ± 2,112); *n=5* – *P*-value =0,1551]. **E)** The Chow AAV5-sh*Cyp46a1* animals presented an increase of time spend in the middle comparatively to Chow Non-injected animals, however, was not statistically significant [Chow Non-injected (127,0 ± 9,326); *n=8* versus Chow AAV5-sh*Cyp46a1* (162,9 ± 37,94); *n=5* – *P*-value =0,3137]. **F)** The HFD AAV5-sh*Cyp46a1* animals presented a statistically significant increase comparatively to HFD Non-injected animals [HFD Non-injected (7,550 ± 1,414); *n=6* versus HFD AAV5-sh*Cyp46a1* (106,8 ± 36,97); *n=5* – *P*-value =0,0230]. Data were represented as mean ± SEM. [*P*-value < 0,05 (*), *P*-value < 0,01 (**), *P*-value < 0,001 (***), *P*-value < 0,0001 (****) – unpaired Student's t-test: A-B-C-D-E-F; **Abbreviations: Chow:** low fat control diet; **HFD:** high fat diet; **AAV5:** adeno-associated vectors of the serotype 5; **sh:** short hairpin.

sh*Cyp46a1* animals relatively to the HFD Non-injected animals demonstrated an increase in the time of grooming's, however, it was not significant (**Figure 21 – D**) (**Table 8**).

In the analysis of the number of rearing's, in day-time period, the Chow AAV5-sh*Cyp46a1* presented a significant decrease comparatively to the Chow Non-injected animals [Chow Non-injected (47,15 ± 4,652); *n=13* versus Chow AAV5-sh*Cyp46a1* (30,36 ± 5,031); *n=11* – *P*-value =0,0227] (**Figure 19 – E**). The HFD AAV5-sh*Cyp46a1* animals did not presented alterations in the number of rearing's comparatively to the HFD-Non-injected animals (**Figure 19 – F**) (**Table 7**). Among males, the AAV5-sh*Cyp46a1* animals presented a significant decrease in the number of rearing's comparatively to the Non-injected animals (Chow Non-injected (47,00 ± 4,813); *n=6* versus Chow AAV5-sh*Cyp46a1* (26,29 ± 5,567); *n=3* – *P*-value =0,0136] (**Annex 14 – G**) [HFD Non-injected (37,25 ± 9,437); *n=2* versus HFD AAV5-sh*Cyp46a1* (11,25 ± 1,931); *n=2* – *P*-value =0,0356] (**Annex 14 – H**) (**Annex 20**). In night-time period, the Chow AAV5-sh*Cyp46a1* animals presented a significant decrease in the number of rearing´s comparatively to Chow Non-injected animals [Chow Non-injected (28,38 ± 1,209); *n=8* versus Chow AAV5-sh*Cyp46a1* (13,80 ± 5,398); *n=5* – *P*-value =0,0072] (**Figure 21 – E**) (**Table 8**). The HFD AAV5-sh*Cyp46a1* animals demonstrated a decrease in the number of rearing´s, however, it was not significative (**Figure 21 – F**) (**Table 8**). Among males in the Chow AAV5-sh*Cyp46a1* animals it was observed a decrease in the number of rearing's comparatively to the Non-

injected animals (**Annex 21**) [Chow Non-injected (28,33 ± 1,520); *n=6* versus Chow AAV5-sh*Cyp46a1* (7,00 ± 3,512); *n=3* – *P*-value =0,0003] (**Annex 15 – G**).

In day-time period, the Chow AAV5-sh*Cyp46a1* and HFD AAV5-sh*Cyp46a1* animals showed a significant decrease in the time of rearing's comparatively to the Non-injected animals [Chow Non-injected (45,87 ± 4,937); *n=13* versus Chow AAV5-sh*Cyp46a1* (23,97 ± 3,759); *n=11* – *P*-value =0,0024] (**Figure 19 – G**) [HFD Non-injected (36,13 ± 4,163); *n=10* versus HFD AAV5-sh*Cyp46a1* (18,85 ± 5,022); *n=11* – *P*-value =0,0169] (**Figure 19 – H**) (**Table 7**). Among males, the AAV5-sh*Cyp46a1* animals showed a significant decrease in the time of rearing comparatively to the Non-injected animals (Chow Non-injected (43,78 ± 4,397); *n=6* versus Chow AAV5-sh*Cyp46a1* (20,50 ± 3,808); *n=3* – *P*-value =0,0017] (**Annex 16 – C**) [HFD Non-injected (39,00 ± 8,103); *n=2* versus HFD AAV5-sh*Cyp46a1* (4,833 ± 0,6173); *n=2* – *P*-value =0,0162] (**Annex 16 – D**) (**Annex 20**). In the night-time period, the AAV5-sh*Cyp46a1* animals, in both diet groups, showed a significant decrease in the time of rearing's comparatively to Non-injected animals [Chow Non-injected (20,53 ± 1,081); *n=8* versus Chow AAV5-sh*Cyp46a1* (18,00 ± 2,522); *n=5* – *P*-value =0,0003] (**Figure 21 – G**) [HFD Non-injected (21,77 ± 2,673); *n=10* versus HFD AAV5-sh*Cyp46a1* (7,860 ± 3,722); *n=11* – *P*-value =0,0126] (**Figure 21 – H**) (**Table 8**). Between males (**Annex 17 – A/B/C/D**) it was observed a decrease in the time of rearing's in the AAV5-sh*Cyp46a1* animals comparatively to the Non-injected animals (**Annex 21**) [Chow Non-injected (19,75 ± 1,168); *n=6* versus Chow AAV5-sh*Cyp46a1* (5,033 ± 2,234); *n=3* – *P*-value =0,0003] (**Annex 17 – C**) [HFD Non-injected (18,75 ± 2,150); *n=2* versus HFD AAV5-sh*Cyp46a1* (1,150 ± 1,50); *n=2* – *P*-value =0,0187] (**Annex 17 – D**).

Briefly, in day-time period, the Chow AAV5-sh*Cyp46a1* and HFD AAV5-sh*Cyp46a1* animals, showed a significant decrease in the number of entries and time in the middle zone and in the time of rearing's comparatively to the Non-injected animals. The HFD AAV5-sh*Cyp46a1* animals presented a decrease in the number of grooming's a comparatively to the Non-injected groups.

In the night-time period, in both diet groups, the AAV5-sh*Cyp46a1* animals showed a significant decrease in the time of rearing's comparatively to the Non-injected animals. The Chow AAV5-sh*Cyp46a1* animals showed a significant decrease of total distance traveled, in the mean speed, in the number of crossing lines, in the number of entries in the middle zone, in the number of rearing and a significant increase in the time immobile and in the time of grooming's, comparatively to the Chow Non-injected animals. The HFD AAV5-sh*Cyp46a1*

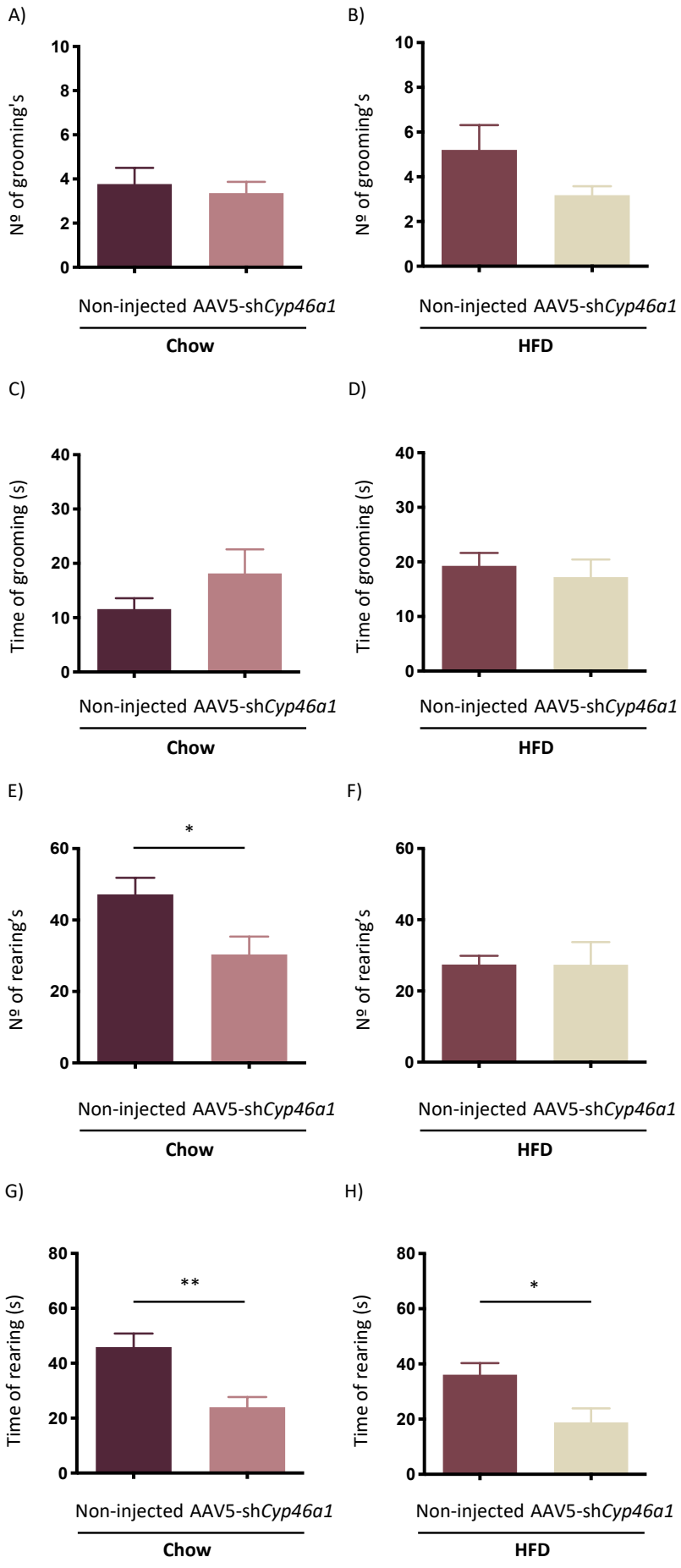
A)
Nº of grooming's
10
8
6
4
2
0
Non-injected
AAV5-shCyp46a1
Chow
B)
Nº of grooming's
10
8
6
4
2
0
Non-injected
AAV5-shCyp46a1
HFD
C)
Time of grooming (s)
40
30
20
10
0
Non-injected
AAV5-shCyp46a1
Chow
D)
Time of grooming (s)
40
30
20
10
0
Non-injected
AAV5-shCyp46a1
HFD
E)
*
Nº of rearing's
60
40
20
0
Non-injected
AAV5-shCyp46a1
Chow
F)
Nº of rearing's
60
40
20
0
Non-injected
AAV5-shCyp46a1
HFD
G)
**
Time of rearing (s)
80
60
40
20
0
Non-injected
AAV5-shCyp46a1
Chow
H)
*
Time of rearing (s)
80
60
40
20
0
Non-injected
AAV5-shCyp46a1
HFD

Figure 20| Silencing *Cyp46a1* gene in the hypothalamus of C57BL/6J wild-type mice fed with Chow and HFD, modify the number and time of rearing in the day-time period

A) The Chow AAV5-sh*Cyp46a1* animals did not showed modifications comparatively to the Chow Non-injected animals [Chow Non-injected (3,769 ± 0,7351); *n=13* versus Chow AAV5-sh*Cyp46a1* (3,364 ± 0,5094); *n=11* – *P*-value =0,6663]. **B)** The HFD AAV5-sh*Cyp46a1* animals presented a decrease in the number of grooming's comparatively to the HFD-Non-injected animals, although, it was not statistically significative [HFD Non-injected (5,200 ± 1,114); *n=10* versus HFD AAV5-sh*Cyp46a1* (3,182 ± 0,4004); *n=11* – *P*-value =0,0926]. **C)** The Chow AAV5-sh*Cyp46a1* showed an increase, comparatively to the Chow Non-injected animals, however, was not statistically significant [Chow Non-injected (11,59 ± 1,982*n=13* versus Chow AAV5-sh*Cyp46a1* (18,16 ± 4,430); *n=11* – *P*-value =0,1572]. **D)** The HFD AAV5-sh*Cyp46a1* animals did not presented alterations in the time of grooming relatively to the HFD Non-injected animals [HFD Non-injected (19,29 ± 2,353); *n=10* versus HFD AAV5-sh*Cyp46a1* (17,23 ± 3,234); *n=11* – *P*-value =0,6270]. **E)** The Chow AAV5-sh*Cyp46a1* presented a statistically significant decrease comparatively to the Chow Non-injected animals [Chow Non-injected (47,15 ± 4,652); *n=13* versus Chow AAV5-sh*Cyp46a1* (30,36 ± 5,031); *n=11* – *P*-value =0,0227]. **F)** The HFD AAV5-sh*Cyp46a1* animals did not presented alterations in the number of rearing comparatively to the HFD-Non-injected animals [HFD Non-injected (27,44 ± 2,433); *n=10* versus HFD AAV5-sh*Cyp46a1* (27,36 ± 6,344); *n=11* – *P*-value =0,9914]. **G)** The Chow AAV5-sh*Cyp46a1* animals showed a statistically significant decrease in the time of rearing comparatively to the Non-injected animals [Chow Non-injected (45,87 ± 4,937); *n=13* versus Chow AAV5-sh*Cyp46a1* (23,97 ± 3,759); *n=11* – *P*-value =0,0024]. **H)** The HFD AAV5-sh*Cyp46a1* animals showed a statistically significant decrease in the time of rearing comparatively to the Non-injected animals [HFD Non-injected (36,13 ± 4,163); *n=10* versus HFD AAV5-sh*Cyp46a1* (18,85 ± 5,022); *n=11* – *P*-value =0,0169]. Data were represented as mean ± SEM. [*P*-value < 0,05 (*), *P*-value < 0,01 (**), *P*-value < 0,001 (***), *P*-value < 0,0001 (****) – unpaired Student's t-test: A-B-C-D-E-F; **Abbreviations: Chow:** low fat control diet; **HFD:** high fat diet; **AAV5:** adeno-associated vectors of the serotype 5; **sh:** short hairpin**.**

animals exhibited a significant decrease in the number of grooming's and an increase in time spend in the middle zone.

Overall, these results suggest that the silencing of *Cyp46a1* mouse gene modify the behavior of C57BL/6J.

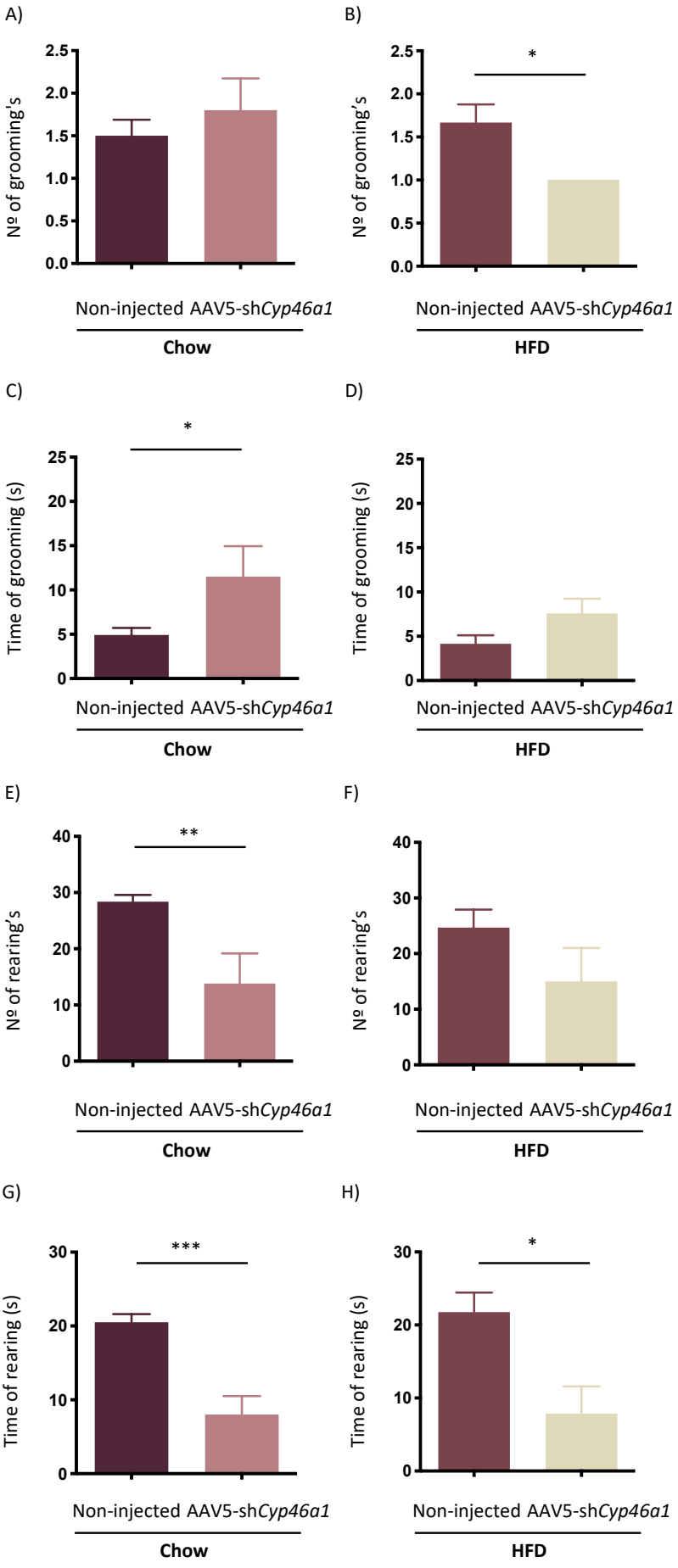
A)
Nº of grooming's
2.5
2.0
1.5
1.0
0.5
0.0
Non-injected
AAV5-shCyp46a1
Chow
B)
Nº of grooming's
*
2.5
2.0
1.5
1.0
0.5
0.0
Non-injected
AAV5-shCyp46a1
HFD
C)
Time of grooming (s)
*
25
20
15
10
5
0
Non-injected
AAV5-shCyp46a1
Chow
D)
Time of grooming (s)
25
20
15
10
5
0
Non-injected
AAV5-shCyp46a1
HFD
E)
Nº of rearing's
**
40
30
20
10
0
Non-injected
AAV5-shCyp46a1
Chow
F)
Nº of rearing's
40
30
20
10
0
Non-injected
AAV5-shCyp46a1
HFD
G)
Time of rearing (s)
***
30
20
10
0
Non-injected
AAV5-shCyp46a1
Chow
H)
Time of rearing (s)
*
30
20
10
0
Non-injected
AAV5-shCyp46a1
HFD

Figure 21 | Silencing *Cyp46a1* gene in the hypothalamus of C57BL/6J wild-type mice fed with Chow and HFD, modify the number and time of grooming and rearing, in the night-time period

A) The Chow AAV5-sh*Cyp46a1* animals did not exhibited alterations in the number of grooming's comparatively to Chow Non-injected animals [Chow Non-injected (1,500 ± 0,1890); *n=8* versus Chow AAV5-sh*Cyp46a1* (1,800 ± 0,3742); *n=5* – *P*-value =0,4425]. **B)** The HFD AAV5-sh*Cyp46a1* animals showed a statistically significative decrease in the number of grooming's relatively to the HFD Non-injected animals [HFD Non-injected (1,667 ± 0,2108); *n=6* versus HFD AAV5-sh*Cyp46a1* (1,00 ± 0,0); *n=5* – *P*-value =0,0353]. **C)** The Chow AAV5-sh*Cyp46a1* animals showed a statistically significant increase in the time of grooming's comparatively to Chow Non-injected animals [Chow Non-injected (4,925 ± 0,7952); *n=8* versus Chow AAV5-sh*Cyp46a1* (11,50 ± 3,452); *n=5* – *P*-value =0,0412]. **D)** The HFD AAV5-sh*Cyp46a1* animals exhibited an increase in the time of grooming's, comparatively to the HFD Non-injected animals, however, it was not statistically significant [HFD Non-injected (4,150 ± 0,9584); *n=6* versus HFD AAV5-sh*Cyp46a1* (7,600 ± 1,634); *n=5* – *P*-value =0,0899]. **E)** The Chow AAV5-sh*Cyp46a1* animals presented a statistically significant decrease in the number of rearing´s comparatively to Chow Non-injected animals [Chow Non-injected (28,38 ± 1,209); *n=8* versus Chow AAV5-sh*Cyp46a1* (13,80 ± 5,398); *n=5* – *P*-value =0,0072]. **F)** The HFD AAV5-sh*Cyp46a1* animals showed a decrease in the number of rearing´s, however, it was not statistically significative [HFD Non-injected (24,67 ± 3,252); *n=6* versus HFD AAV5-sh*Cyp46a1* (15,00 ± 6,033); *n=5* – *P*-value =0,1727]. **G)** The Chow AAV5-sh*Cyp46a1* animals showed a statistically significant decrease in the time of rearing comparatively to the Non-injected animals [Chow Non-injected (20,53 ± 1,081); *n=8* versus Chow AAV5-sh*Cyp46a1* (8,00 ± 2,522); *n=5* – *P*-value =0,0003]. **H)** The HFD AAV5-sh*Cyp46a1* animals showed a significant decrease in the time of rearing comparatively to the Non-injected animals [HFD Non-injected (21,77 ± 2,673); *n=6* versus HFD AAV5-sh*Cyp46a1* (7,860 ± 3,722); *n=5* – *P*-value =0,0126]. Data were represented as mean ± SEM. [*P*-value < 0,05 (*), *P*-value < 0,01 (**), *P*-value < 0,001 (***), *P*-value < 0,0001 (****) – unpaired Student's t-test: A-B-C-D-E-F-G-H; **Abbreviations: Chow:** low fat control diet; **HFD:** high fat diet; **AAV5:** adeno-associated vectors of the serotype 5; **sh:** short hairpin.

Table 7| Silencing *Cyp46a1* gene in the hypothalamus modifies behavior activity of C57BL/6J mice fed with a Chow and HFD in the day-time period

Day						
	Chow (*n=24*)			**HFD** (*n=21*)		
	Non-injected	AAV5-sh*Cyp46a1*	*P*-value	Non-injected	AAV5-sh*Cyp46a1*	*P*-value
Total distance (m)	27,99 ± 1,622	22,93 ±4,626	0,2823	25,29 ± 1,874	21,34 ± 5,179	0,4988
Mean speed (m/s)	0,047 ± 0,003	0,035 ± 0,008	0,2799	0,042 ± 0,003	0,035 ± 0,009	0,4828
Nº of immobile episodes	43,54 ± 2,707	38,00 ± 2,908	0,1776 (↓)	46,80 ±3,495	39,55 ± 5,362	0,2815
Time immobile (s)	193,1 ± 18,01	261,7 ± 48,24	0,1703 (↑)	237,3 ± 23,91	290,4 ± 46,78	0,3399
Nº of crossing lines	212,9 ± 13,15	173 ± 29,41	0,2135	200 ± 18,87	147 ± 35,27	0,2214
Nº of entries in the middle	23,15 ±2,643	11,82 ± 2,486	0,0054 (↓)	18,90 ± 2,523	8,545 ± 1,956	0,0040 (↓)
Time in the middle (s)	26,12 ± 3,810	15,57 ± 3,364	0,0536 (↓)	16,94 ± 2,436	9,255 ± 1,699	0,0160 (↓)
Nº of grooming' s	3,769 ± 0,7351	3,364 ± 0,5094	0,6663	5,200 ± 1,114	3,182 ± 0,4004	0,0926 (↓)
Time of grooming (s)	11,59 ± 1,982	18,16 ± 4,430	0,1572 (↑)	19,29 ± 2,353	17,23 ± 3,234	0,6270
Nº of rearing' s	47,15 ± 4,652	30,36 ± 5,031	0,0227 (↓)	27,44 ± 2,433	27,36 ± 6,344	0,9914
Time of rearing (s)	45,87 ± 4,937	23,97 ± 3,759	0,0024 (↓)	36,13 ± 4,163	18,85 ± 5,022	0,0169 (↓)

Table 7: Shows the parameters analyzed in the day-time period for each group of the study with respective mean ± SEM and *P*-value [Chow Non-injected: *n=13*, female: *n=4* and male: *n=9*; Chow AAV5-sh*Cyp46a1: n=11*, female: *n=4* and male: *n=7*; HFD Non-injected: *n=10*, female: *n=6* and male:

n=4; HFD AAV5-sh*Cyp46a1*: *n=11*, female: *n=7* and male: *n=4*]. [*P*-value < 0,05 (*), *P*-value < 0,01 (**), *P*-value < 0,001 (***), *P*-value < 0,0001 (****)] – unpaired Student's t-test; **Abbreviations: Chow:** low fat control diet; **HFD:** high fat diet; **AAV5:** adeno-associated vectors of the serotype 5; **sh:** short hairpin**;** **SEM:** standard error of mean; ↓ **:** statistically significant decrease; ↓ **:** non-significant decrease; ↑ : statistically significant increase; ↑ : non-significant decrease.

Table 8| Silencing *Cyp46a1* gene in the hypothalamus modify behavior activity of C57BL/6J mice fed with a Chow and HFD in the night-time period

Night						
	Chow (*n=13*)			**HFD** (*n=11*)		
	Non-injected	AAV5-sh*Cyp46a1*	*P*-value	Non-injected	AAV5-sh*Cyp46a1*	*P*-value
Total distance (m)	18,68 ± 1,084	9,538 ± 3,489	0,0116 (↓)	16,04 ± 1,538	13,21 ±3,514	0,4516
Mean speed (m/s)	0,06238 ± 0,0036	0,0318 ± 0,0118	0,0120 (↓)	0,0535 ± 0,0051	0,0440 ± 0,0012	0,4460
Nº of immobile episodes	13,88 ± 2,074	13,25 ± 0,4787	0,8403	21,00 ± 2,176	15,00 ± 2,121	0,0828 (↓)
Time immobile (s)	54,24 ± 8,265	149,5 ± 45,60	0,0247 (↑)	80,33 ± 10,36	113,1 ± 39,75	0,4067
Nº of crossing lines	135,0 ± 8,726	63,00 ± 22,13	0,0047 (↓)	121,5 ± 8,168	95,20 ± 23,17	0,2780
Nº of entries in the middle	11,00 ± 1,512	5,400 ± 1,568	0,0324 (↓)	12,50 ± 2,277	7,600 ± 2,112	0,1551 (↓)
Time in the middle (s)	127,0 ± 9,326	162,9 ± 37,94	0,3137	7,550 ± 1,414	106,8 ± 36,97	0,0230 (↑)
Nº of grooming' s	1,500 ± 0,1890	1,800 ± 0,3742	0,4425	1,667 ± 0,2108	1,00 ± 0,0	0,0353 (↓)
Time of grooming (s)	4,925 ± 0,7952	11,50 ± 3,452	0,0412 (↑)	4,150 ± 0,9584	7,600 ± 1,634	0,0899 (↑)
Nº of rearing' s	28,38 ± 1,209	13,80 ± 5,398	0,0072 (↓)	24,67 ± 3,252	15,00 ± 6,033	0,1727 (↓)
Time of rearing (s)	20,53 ± 1,081	8,00 ± 2,522	0,0003 (↓)	21,77 ± 2,673	7,860 ± 3,722	0,0126 (↓)

Table 8: Shows the parameters analyzed in the night-time period for each group of the study with respective mean ± SEM and *P*-value [Chow Non-injected: *n=8*, female: *n=2* and male: *n=6*; Chow AAV5-

sh*Cyp46a1: n=5*, female: *n=2* and male: *n=3*; HFD Non-injected: *n=6*, female: *n=4* and male: *n=2*; HFD AAV5-sh*Cyp46a1*: *n=5*, female: *n=3* and male: *n=2*]. [*P*-value < 0,05 (*), *P*-value < 0,01 (**), *P*-value < 0,001 (***), *P*-value < 0,0001 (****)] – unpaired Student's t-test; **Abbreviations: Chow:** low fat control diet; **HFD:** high fat diet; **AAV5:** adeno-associated vectors of the serotype 5; **sh:** short hairpin**; SEM:** standard error of mean; ↓ **:** statistically significant decrease; ↓ **:** non-significant decrease; ↑ : statistically significant increase; ↑ : non-significant decrease.

6. Silencing *Cyp46a1* gene in the hypothalamus induces an increase in WAT weight and hypertrophy of adipocytes of C57BL/6J mice fed with Chow and HFD

Adipocytes respond rapidly and dynamically to overabundant food consumption through adipocytes hypertrophy and hyperplasia (Kaur 2014).

The silencing of *Cyp46a1* gene leads to an increase in BW, therefore, next we wanted to evaluate its impact in WAT. At the end of the experiment, the animals were sacrificed, and the main metabolic organs and tissues were collected and weighted.

The Chow AAV5-sh*Cyp46a1* animals presented a significant increase on WAT weight comparatively to the Chow Non-injected animals [Chow Non-injected (0,6256 ± 0,0604); *n=13* versus Chow AAV5-sh*Cyp46a1* (1,6892 ± 0,3178); *n=11* – *P*-value =0,0017] (**Figure 22 – A**). This increase was also observed in the HFD AAV5-sh*Cyp46a1* animals comparatively to HFD Non-injected animals, however, it was not significant [HFD Non-injected (1,705 ± 0,2792); *n=10* versus HFD AAV5-sh*Cyp46a1* (2,455 ± 0,3916); *n=11* – *P*-value =0,1386](**Figure 22 – B**).

Between females (**Annex 22 – A/B**)and between males (**Annex 22 – C/D**), in both Chow and HFD groups, the AAV5-sh*Cyp46a1* animals presented an increase in WAT weight, however it was only significant in the males [Males: Chow Non-injected (0,7183 ± 0,657); *n=9* versus Chow AAV5-sh*Cyp46a1* (1,907 ± 0,422); *n=7* – *P*-value =0,0070] (**Annex 22 – C**) [HFD Non-injected (2,342 ± 0,1250); *n=4* versus HFD AAV5-sh*Cyp46a1* (2,962 ± 0,1147); *n=4* – *P*-value =0,0106] (**Annex 22 – D**).

Next, to assess whether this increase in WAT weight was concomitant with alterations in the architecture of WAT, hematoxylin-eosin staining was performed in WAT paraffin sections and the area of adipocytes was determined.

The WAT is composed by spherical adipocytes which have a large lipid droplet in the cytoplasm and vary their size in relation to the lipid content (Wronska and Kmiec 2012). In

mature adipocytes, the large lipid droplet fills practically the entire volume of the cell, being known as unilocular adipocytes (Wronska and Kmiec 2012).

The Chow AAV5-sh*Cyp46a1* animals showed a strong increase of adipocytes size comparatively to the Chow Non-injected animals (**Figure 23 – A1/A2**). Consistently, the Chow AAV5-sh*Cyp46a1* animals presented a significant increase of adipocytes area comparatively to the Chow Non-injected animals [Chow Non-injected (1759 ± 209,5); *n=6* versus Chow AAV5-sh*Cyp46a1* (5901 ± 710,9); *n=6* – *P*-value =0,0002] (**Figure 23 – B**).

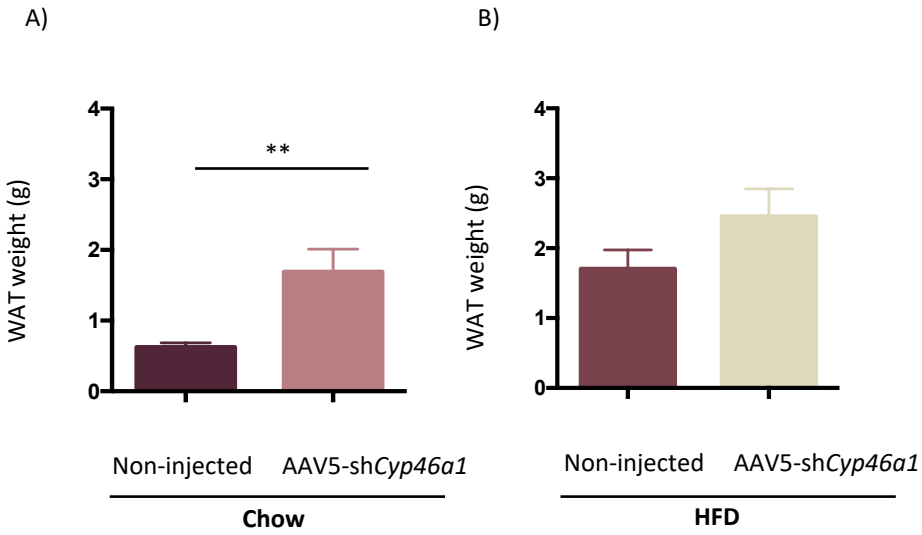

Figure 22|Silencing *Cyp46a1* gene in the hypothalamus induces an increased in WAT weight of C57BL/6J mice fed with a Chow and HFD

In the 12th week of the study, the C57BL/6J mice were sacrificed and the WAT were collected and weighted. **A)** The Chow AAV5-sh*Cyp46a1* animals presented a statistically significant increase on WAT weight comparatively to the Chow Non-injected animals [Chow Non-injected (0,6256 ± 0,0604); *n=13* versus Chow AAV5-sh*Cyp46a1* (1,6892 ± 0,3178); *n=11* – *P*-value =0,0017]**. B)** The HFD AAV5-sh*Cyp46a1* animals presented an increase on WAT weight comparatively to the HFD Non-injected animals, however, was not statistically significant [HFD Non-injected (1,705 ± 0,2792); *n=10* versus HFD AAV5-sh*Cyp46a1* (2,455 ± 0,3916); *n=11* – *P*-value =0,1386]. Data were represented as mean ± SEM. [*P*-value < 0,05 (*), *P*-value < 0,01 (**), *P*-value < 0,001 (***), *P*-value < 0,0001 (****)] – unpaired Student's t-test: A-B; **Abbreviations: WAT:** white adipose tissue; **Chow:** low fat control diet; **HFD:** high fat diet; **AAV5:** adeno-associated vectors of the serotype 5; **sh:** short hairpin**; SEM:** standard error of mean.

In the analysis of relative frequency of adipocytes area, the Chow AAV5-sh*Cyp46a1* animals presented a high frequency of adipocytes with areas between 4000 and 6000 µm^2 and a low frequency of adipocytes with areas below 2000 µm^2, comparatively to the Chow

Non-injected animals, which presented a high frequency of adipocytes with areas below 2000 µm^2 and a low frequency of adipocytes with areas above 4000 µm^2 [Chow Non-injected: *n=6* versus Chow AAV5-sh*Cyp46a1*: *n=6*; <2000: *P*-value <0,0001; 2000-4000: *P*-value =0,0656; 4000-6000: *P*-value <0,0001; 6000-8000: *P*-value <0,0001; 8000-10 000: *P*-value =0,02412; 10 000-12000: *P*-value >0,9999] (**Figure 23 – C**).

On other hand, the HFD AAV5-sh*Cyp46a1* animals showed a lightly increase of the size and signs of necrosis in some adipocytes comparatively to the HFD Non-injected animals (**Figure 23– A3/A4**). In fact, the HFD AAV5-sh*Cyp46a1* animals presented a significant increase of adipocytes area comparatively to the HFD Non-injected animals [HFD Non-injected (5275 ± 453,8); *n=8* versus HFD AAV5-sh*Cyp46a1* (7888 ± 909,4); *n=8* – *P*-value =0,0222] (**Figure 23 – D**). The analysis of relative frequency of adipocytes area between the HFD animals groups did not showed significant differences [HFD Non-injected: *n=8* versus HFD AAV5-sh*Cyp46a1*: *n=8*; <2000: *P*-value >0,9999; 2000-4000: *P*-value =0,2081; 4000-6000: *P*-value >0,9999; 6000-8000: *P*-value =0,6922; 8000-10 000: *P*-value >0,9999; 10 000-12000: *P*-value >0,9999] (**Figure 23 – E**).

Overall, the results suggest that the silencing of the *Cyp46a1* gene in the hypothalamus leads to an increase in the WAT weight and hypertrophy of adipocytes of C57BL/6J wild-type mice fed with Chow and HFD.

7. Silencing *Cyp46a1* gene in the hypothalamus induces modifications in the protein levels in WAT of C57BL/6J mice fed with Chow and HFD

Next, the impact of silencing the *Cyp46a1* gene was evaluated in the PPAR-γ and the UCP-1 protein levels in WAT (**Figure 24 – A /B**).

PPAR-γ exists in two isoforms, PPAR-γ1 and PPAR-γ2. PPARγ1 is expressed in several tissues and the expression of PPARγ2 is restricted to adipose tissue (WAT and BAT), having a crucial role in adipogenesis and insulin sensitivity (Maruam et al. 2013). UCP-1 is a transport protein of the inner mitochondrial membrane of adipocytes and is mainly found in BAT, once had a crucial role in thermogenesis and energy expenditure (Richard and Picard 2011). However, in WAT, some adipocytes under specific conditions can express UCP-1 (Poher et al. 2015). In WAT, adipocytes that express UCP-1 are known as beige adipocytes (Shabalina et al. 2013). This increase in UCP-1 expression of white adipocytes can increase the energy expenditure and therefore protect against obesity (Wu, Cohen, and Spiegelman 2013).

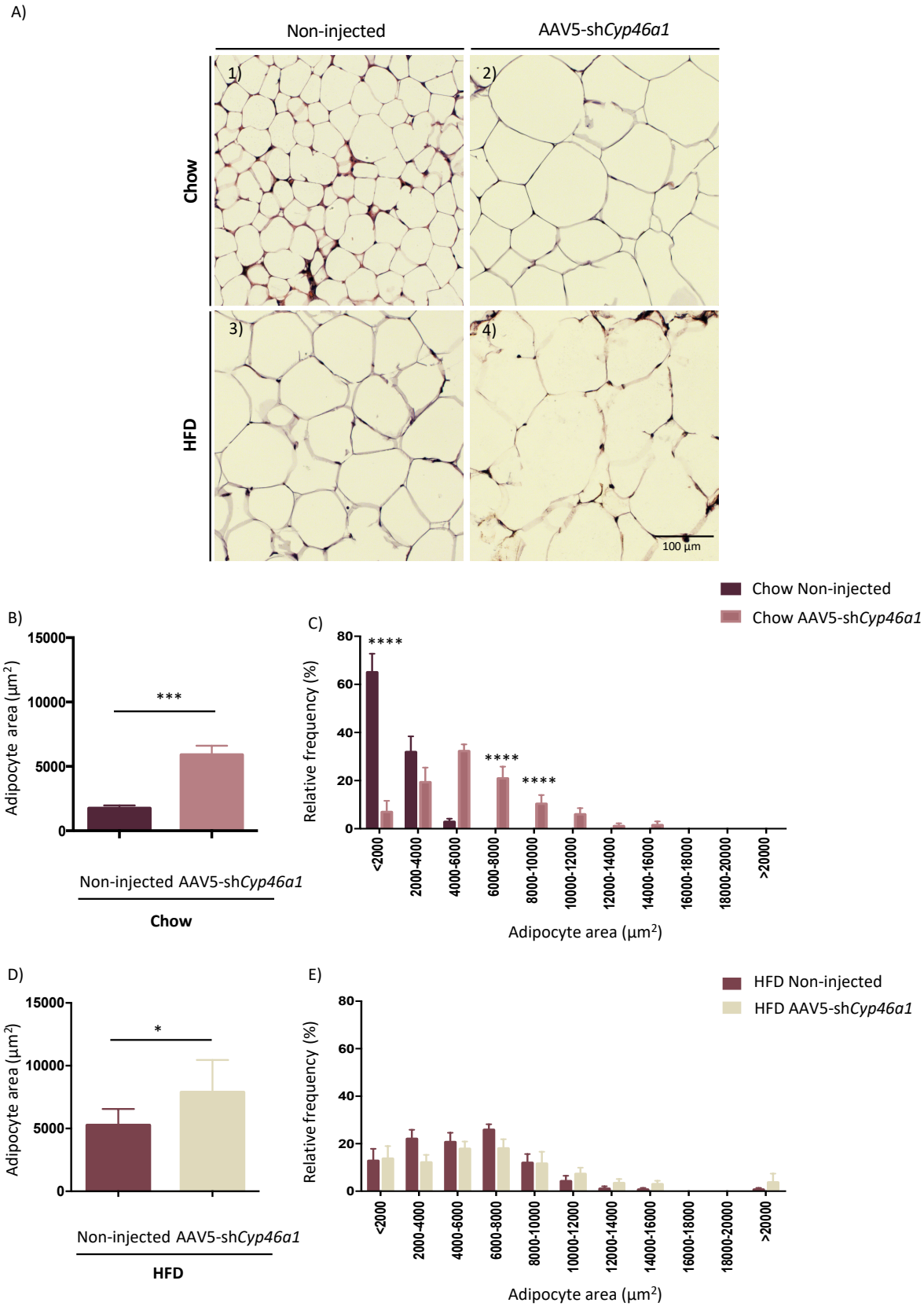
A)
Non-injected
AAV5-shCyp46a1
Chow
HFD
1)
2)
3)
4)
100 µm
B)
Adipocyte area (µm²)
15000
10000
5000
0
***
Non-injected AAV5-shCyp46a1
Chow
C)
Chow Non-injected
Chow AAV5-shCyp46a1
Relative frequency (%)
80
60
40
20
0
****
****
****
<2000
2000-4000
4000-6000
6000-8000
8000-10000
10000-12000
12000-14000
14000-16000
16000-18000
18000-20000
>20000
Adipocyte area (µm²)
D)
Adipocyte area (µm²)
15000
10000
5000
0
*
Non-injected AAV5-shCyp46a1
HFD
E)
HFD Non-injected
HFD AAV5-shCyp46a1
Relative frequency (%)
80
60
40
20
0
<2000
2000-4000
4000-6000
6000-8000
8000-10000
10000-12000
12000-14000
14000-16000
16000-18000
18000-20000
>20000
Adipocyte area (µm²)

Figure 23| Silencing *Cyp46a1* gene in the hypothalamus induces hypertrophy of adipocytes of WAT in C57BL/6J mice fed with a Chow and HFD

The WAT samples were histologically processed and the hematoxylin-eosin (H&E) staining was performed. **A1 and A2)** The Chow AAV5-sh*Cyp46a1* animals showed a strong increase of the adipocytes size, comparatively to the Chow Non-injected animals. **A3 and A4)** The HFD AAV5-sh*Cyp46a1* animals showed a lightly increase of the size and signs of necrosis in some adipocytes, comparatively to the HFD Non-injected animals. **B)** The Chow AAV5-sh*Cyp46a1* animals presented a statistically significant increase of adipocytes area comparatively to the Chow Non-injected animals [Chow Non-injected (1759 ± 209,5); *n=6* versus Chow AAV5-sh*Cyp46a1* (5901 ± 710,9); *n=6* – *P*-value =0,0002]. **C)** Analysis of relative frequency of adipocytes area. The Chow AAV5-sh*Cyp46a1* animals presented a frequency of adipocytes with areas superiors comparatively to the Chow Non-injected animals [Chow Non-injected: *n=6* versus Chow AAV5-sh*Cyp46a1*: *n=6*; <2000: *P*-value <0,0001; 2000-4000: *P*-value =0,0656; 4000-6000: *P*-value <0,0001; 6000-8000: *P*-value <0,0001; 8000-10 000: *P*-value =0,02412; 10 000-12000: *P*-value >0,9999]. **D)** The HFD AAV5-sh*Cyp46a1* animals, presented a statistically significant increase of adipocytes area comparatively to the HFD Non-injected animals [HFD Non-injected (5275 ± 453,8); *n=8* versus HFD AAV5-sh*Cyp46a1* (7888 ± 909,4); *n=8* – *P*-value =0,0222]. **E)** Analysis of relative frequency of adipocytes area. The HFD AAV5-sh*Cyp46a1* animals did not presented significant differences in the frequency of adipocytes area, comparatively to the HFD Non-injected animals [HFD Non-injected: *n=8* versus HFD AAV5-sh*Cyp46a1*: *n=8*; <2000: *P*-value >0,9999; 2000-4000: *P*-value =0,2081; 4000-6000: *P*-value >0,9999; 6000-8000: *P*-value =0,6922; 8000-10 000: *P*-value >0,9999; 10 000-12000: *P*-value >0,9999]. Data were represented as mean ± SEM. [*P*-value < 0,05 (*), *P*-value < 0,01 (**), *P*-value < 0,001 (***), *P*-value < 0,0001 (****) – unpaired Student's t-test: B-C-D-E; **Abbreviations: WAT:** white adipose tissue; **Chow:** low fat control diet; **HFD:** high fat diet; **AAV5:** adeno-associated vectors of the serotype 5; **sh:** short hairpin**; SEM:** standard error of mean.

The PPAR-γ and the UCP-1 levels in WAT were analyzed by WB (**Figure 24 – A**). The optical density of the bands was quantified and then normalized with the optical density of β-actin bands. The AAV5-sh*Cyp46a1* animals, both in Chow and HFD groups showed a significant decrease of PPAR-γ protein levels comparatively to the Non-injected animals [Chow Non-injected (0,7095 ± 0,06330); *n=7* versus Chow AAV5-sh*Cyp46a1* (0,4267 ± 0,1140); *n=6* – *P*-value =0,0454] (**Figure 24 – C**) [HFD Non-injected (0,0090 ± 0,0028); *n=5* versus HFD AAV5-sh*Cyp46a1* (0,0020 ± 0,0011); *n=6* – *P*-value =0,0325] (**Figure 24 – E**).

In the WB analysis of UCP-1 the Chow AAV5-sh*Cyp46a1* animals was showed a significant decrease of UCP-1 protein levels relatively to the Chow Non-injected animals [Chow Non-injected (0,5706 ± 0,1154); *n=7* versus Chow AAV5-sh*Cyp46a1* (0,1425 ± 0,01050); *n=5* – *P*-value =0,00116] (**Figure 24 – D**). The HFD AAV5-sh*Cyp46a1* animals also showed a decrease in UCP-1 protein levels, however, it was not significant [HFD Non-injected (0,008507 ±

0,002524); *n=5* versus HFD AAV5-sh*Cyp46a1* (0,003113 ± 0,0006852); *n=6* – *P*-value =0,0513] (**Figure 24 – F**).

Altogether, the results suggest that the silencing of the *Cyp46a1* gene in the hypothalamus leads to a decrease in the PPAR-γ and UCP-1 protein levels in the WAT of C57BL/6J wild-type mice fed with Chow and HFD.

8. Silencing *Cyp46a1* gene in the hypothalamus induces hypertrophy of adipocytes and modifications in the protein levels in BAT of C57BL/6J mice fed with a Chow and HFD

The BAT samples were histologically processed, and the H&E staining was performed for posterior acquisition of BAT sections images.

The BAT is composed by brown adipocytes that have several lipid droplets in the cytoplasm and are enriched with mitochondria, being known to multilocular adipocytes.

The Chow Non-injected animals showed multilocular adipocytes with several small lipid droplets (**Figure 25 – A1**). The Chow AAV5-sh*Cyp46a1* animals showed an increase of lipid droplets in adipocytes, approaching the morphology of unilocular white adipocytes, comparatively to the Chow Non-injected animals (**Figure 25 – A2**). The HFD Non-injected showed multilocular adipocytes with several big lipid droplets (**Figure 25 – A3**). The HFD AAV5-sh*Cyp46a1* animals showed an increase in lipid droplets and of immune system infiltration (brown arrows) in adipocytes relatively to the HFD Non-injected animals (**Figure 25 – A4**).

The silencing *Cyp46a1* gene in BAT adipocytes appears to mimic an HFD effect, whereas in HFD-AAV5-sh*Cyp46a1* animals this silencing appears exacerbate the phenotype of obesity.

Next, the PPAR-γ and the UCP-1 levels in BAT were analyzed by WB (**Figure 26 – A/B**). The optical density of the bands was quantified and then normalized with the optical density of β-actin bands. The Chow AAV5-sh*Cyp46a1* animals did not showed modifications in the PPAR-γ protein levels comparatively to the Chow Non-injected animals [Chow Non-injected (10,8369 ± 0,1614); *n=5* versus Chow AAV5-sh*Cyp46a1* (0,8477 ± 0,1073); *n=5* – *P*-value =0,9569] (**Figure 26 – C**). Regarding UCP-1, the Chow AAV5-sh*Cyp46a1* animals did not presented alterations in the UCP-1 protein levels comparatively to the Chow Non-injected animals [Chow Non-injected (1,128 ± 0,2478); *n=6* versus Chow AAV5-sh*Cyp46a1* (1,391 ± 0,3175); *n=6* – *P*-value =0,5276] (**Figure 26 – D**).

In the HFD-AAVsh*Cyp46a1* animals it was observed a decrease of PPAR-γ protein levels relatively to the HFD Non-injected animals, although, it was not significant [HFD Non-injected

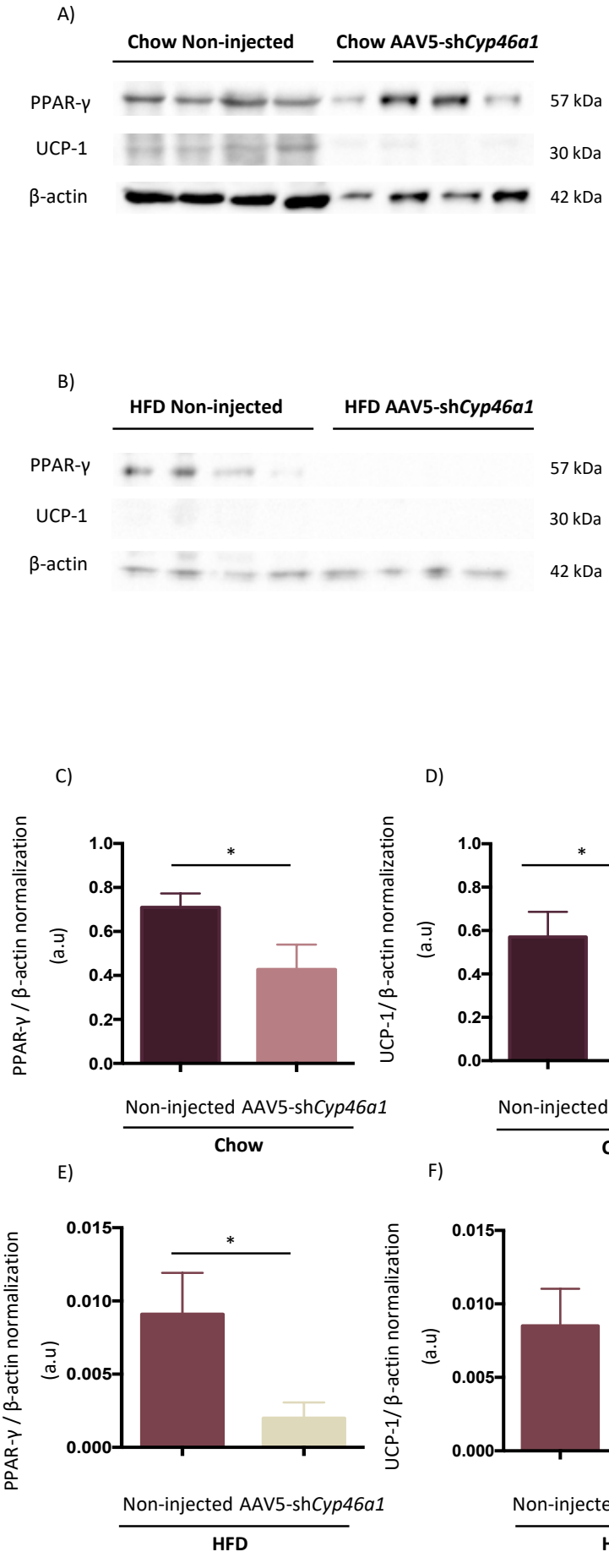
A)
Chow Non-injected
Chow AAV5-shCyp46a1
PPAR-γ
UCP-1
β-actin
57 kDa
30 kDa
42 kDa
B)
HFD Non-injected
HFD AAV5-shCyp46a1
PPAR-γ
UCP-1
β-actin
57 kDa
30 kDa
42 kDa
C)
PPAR-γ / β-actin normalization (a.u)
1.0
0.8
0.6
0.4
0.2
0.0
*
Non-injected
AAV5-shCyp46a1
Chow
D)
UCP-1/ β-actin normalization (a.u)
1.0
0.8
0.6
0.4
0.2
0.0
*
Non-injected
AAV5-shCyp46a1
Chow
E)
PPAR-γ / β-actin normalization (a.u)
0.015
0.010
0.005
0.000
*
Non-injected
AAV5-shCyp46a1
HFD
F)
UCP-1/ β-actin normalization (a.u)
0.015
0.010
0.005
0.000
Non-injected
AAV5-shCyp46a1
HFD

Figure 24| Silencing *Cyp46a1* gene in the hypothalamus induces modifications in the protein levels in WAT C57BL/6J mice fed with a Chow and HFD

The impact of silencing the *Cyp46a1* gene was evaluated in the PPAR-γ and the UCP-1 protein levels in the WAT, through WB analysis. **A)** In both Chow groups, the analysis of PPAR-γ revelated the presence of PPAR-γ bands. The analysis of UCP-1 revelated the presence of UCP-1 bands in the Chow Non-injected animals and in the Chow AAV5-sh*Cyp46a1* animals, however with low density of bands in the Chow AAV5-sh*Cyp46a1* animals. Membranes were probed with anti-β-actin for protein load control [Chow Non-injected; *n=4* versus Chow AAV5-sh*Cyp46a1*; *n=4*]. **B)** The WB analysis of PPAR-γ revelated the presence of PPAR-γ bands in the HFD Non-injected animals and in the HFD AAV5-sh*Cyp46a1* animals, however with very low density of bands in the HFD AAV5-sh*Cyp46a1* animals. The analysis of UCP-1 revelated the presence of UCP-1 bands in the HFD Non-injected animals and in the HFD AAV5-sh*Cyp46a1* animals, however with very low density of bands. Membranes were probed with anti-β-actin for protein load control [HFD Non-injected; *n=4* versus HFD AAV5-sh*Cyp46a1*; *n=4*]. **C)** The optical density of PPAR-γ bands was quantified and then normalized with the optical density of β-actin bands. The Chow AAV5-sh*Cyp46a1* animals showed a significant decrease of PPAR-γ levels comparatively to the Chow Non-injected animals. **D)** The optical density of UCP-1 bands was quantified and then normalized with the optical density of β-actin bands. The Chow AAV5-sh*Cyp46a1* animals was showed a significant decrease of UCP-1 levels relatively to the Chow Non-injected animals [Chow Non-injected (0,5706 ± 0,1154); *n=7* versus Chow AAV5-sh*Cyp46a1* (0,1425 ± 0,01050); *n=5* – *P*-value =0,00116]. **E)** The optical density of PPAR-γ bands was quantified and then normalized with the optical density of β-actin bands. The HFD AAV5-sh*Cyp46a1* animals showed a significant decrease of PPAR-γ levels comparatively to the HFD Non-injected animals [HFD Non-injected (0,0090 ± 0,0028); *n=5* versus HFD AAV5-sh*Cyp46a1* (0,0020 ± 0,0011); *n=6* – *P*-value =0,0325]. **F)** The optical density of UCP-1 bands was quantified and then normalized with the optical density of β-actin bands. The HFD AAV5-sh*Cyp46a1* animals showed a decrease in UCP-1 levels [HFD Non-injected (0,008507 ± 0,002524); *n=5* versus HFD AAV5-sh*Cyp46a1* (0,003113 ± 0,0006852); *n=6* – *P*-value =0,0513]. Data were represented as mean ± SEM. [*P*-value < 0,05 (*), *P*-value < 0,01 (**), *P*-value < 0,001 (***), *P*-value < 0,0001 (****)] – unpaired Student's t-test: C-D-E-F; **Abbreviations: a.u:** arbitrary units; **PPAR-γ:** peroxisome proliferator activated receptor γ; **UCP-1**: uncoupling protein 1; **AAV5:** adeno-associated vectors of the serotype 5; **Chow:** low fat control diet; **HFD:** high fat diet; **sh:** short hairpin.

(2,111 ± 0,5794); *n=6* versus HFD AAV5-sh*Cyp46a1* (1,9030 ± 0,08483); *n=6* – *P*-value =0,0513] (**Figure 26 – E**). The HFD AAV5-sh*Cyp46a1* animals showed a decrease, however, it was not significant [HFD Non-injected (1,004 ± 0,2899); *n=6* versus HFD AAV5-sh*Cyp46a1* (0,4435 ± 0,09882); *n=6* – *P*-value =0,0969] (**Figure 26 – F**).

Overall, these results suggest that the silencing of the *Cyp46a1* gene in the hypothalamus leads to hypertrophy of adipocytes and modifications in the PPAR-γ and UCP-1 protein levels in the BAT of C57BL/6J wild-type mice fed with Chow and HFD.

A)

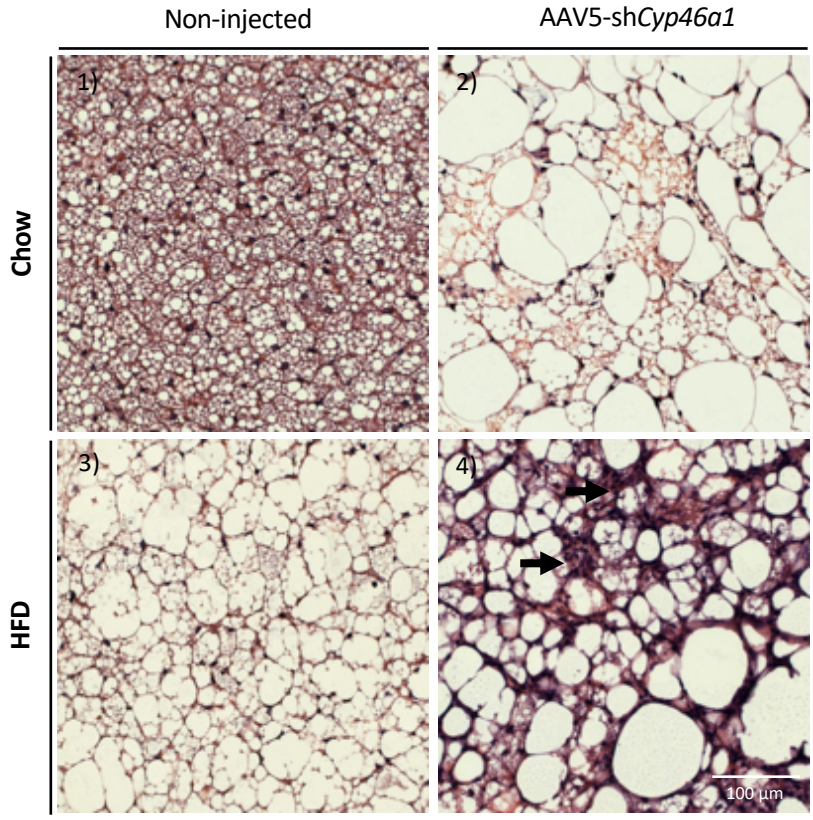

Figure 25| Silencing *Cyp46a1* gene in the hypothalamus induces hypertrophy of adipocytes of BAT in C57BL/6J mice fed with a Chow and HFD

The BAT samples were histologically processed and the H&E staining was performed. **A1 and A2)** The Chow AAV5-sh*Cyp46a1* animals showed a strong increase of lipid droplets size in adipocytes, approaching the morphology of unilocular white adipocytes, comparatively to the Chow Non-injected animals, which showed multilocular brown adipocytes with several small lipid droplets. **A3 and A4)** The HFD AAV5-sh*Cyp46a1* animals showed an increase of lipid droplets size and of immune system infiltration (black arrows) in adipocytes relatively to the HFD Non-injected animals. **Abbreviations: Chow:** low fat control diet; **HFD:** high fat diet; **AAV5:** adeno-associated vectors of the serotype 5; **sh:** short hairpin.

9. Silencing *Cyp46a1* gene in the hypothalamus induces an increased in liver weight and hepatic steatosis in C57BL/6J mice fed with a Chow and HFD

In the liver, fat accumulation and as consequence fatty liver diseases are strongly correlated with IR, dyslipidemia and other metabolic abnormalities that composed the MetS (Marchesini et al. 2005; Kotronen et al. 2007).

The Chow AAV5-sh*Cyp46a1* animals presented an increase on liver weight comparatively to the Chow Non-injected animals, however it was not significant [Chow Non-

injected (1,099 ± 0,03700); *n=13* versus Chow AAV5-sh*Cyp46a1* (1,525 ± 0,2673); *n=11* – *P*-value =0,0997] (**Figure 27 – A**). The HFD AAV5-sh*Cyp46a1* animals presented a significant increase in the liver weight comparatively to HFD Non-injected animals [HFD Non-injected (1,131 ± 0,1244); *n=10* versus HFD AAV5-sh*Cyp46a1* (1,808 ± 0,2810); *n=11* – *P*-value =0,0466] (**Figure 27 – B**). Between females and between males, in Chow and HFD animals, the AAV5-sh*Cyp46a1* animals showed an increase in liver weight, however it was not significant (**Annex 23**).

The liver samples were histologically processed, and the H&E staining was performed for acquisition and analysis of the liver sections images. The Chow Non-injected animals showed hepatocytes with a single nucleus and binucleate (**Figure 27 – C1**). The Chow AAV5-sh*Cyp46a1* animals showed an increase in lipid droplets in the hepatocytes, designated as hepatic steatosis: microvesicular steatosis (white arrows), that is characterized by small lipid droplets in the hepatocytes and macrovesicular steatosis (black arrows), which is characterized by big lipid droplets, comparatively to the Chow Non-injected animals (**Figure 27 – C2**). The HFD Non-injected animals In the HFD AAV5-sh*Cyp46a1* animals it was possible observed microvesicular steatosis (white arrows), macrovesicular steatosis (black arrows) and hepatocytes hypertrophy relatively to the HFD Non-injected animals which only showed microvesicular steatosis (white arrows) (**Figure 27 – C1/C2**).

Overall, the results suggest that the silencing of *Cyp46a1* gene in the hypothalamus induces an increase in liver weight and hepatic steatosis in C57BL/6J mice fed with Chow and HFD.

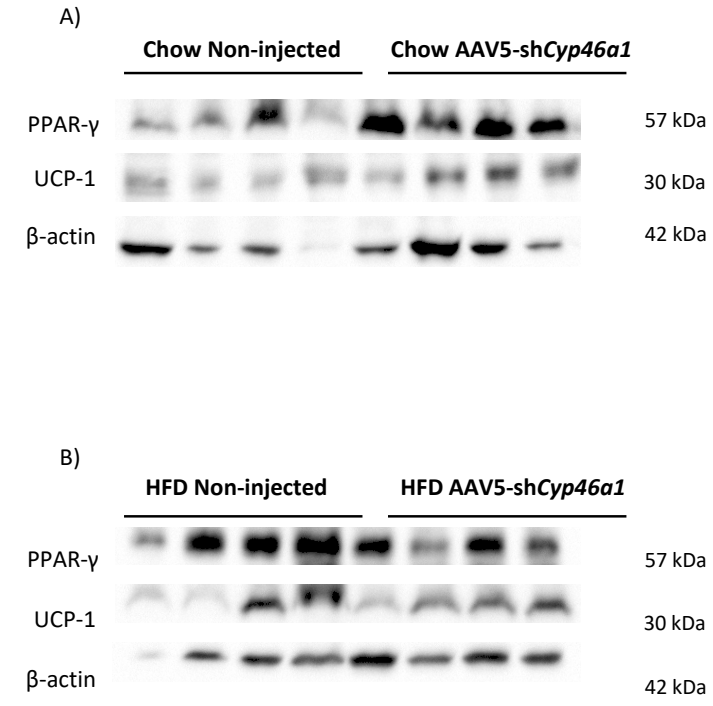
A)
Chow Non-injected
Chow AAV5-shCyp46a1
PPAR-γ
UCP-1
β-actin
57 kDa
30 kDa
42 kDa
B)
HFD Non-injected
HFD AAV5-shCyp46a1
PPAR-γ
UCP-1
β-actin
57 kDa
30 kDa
42 kDa

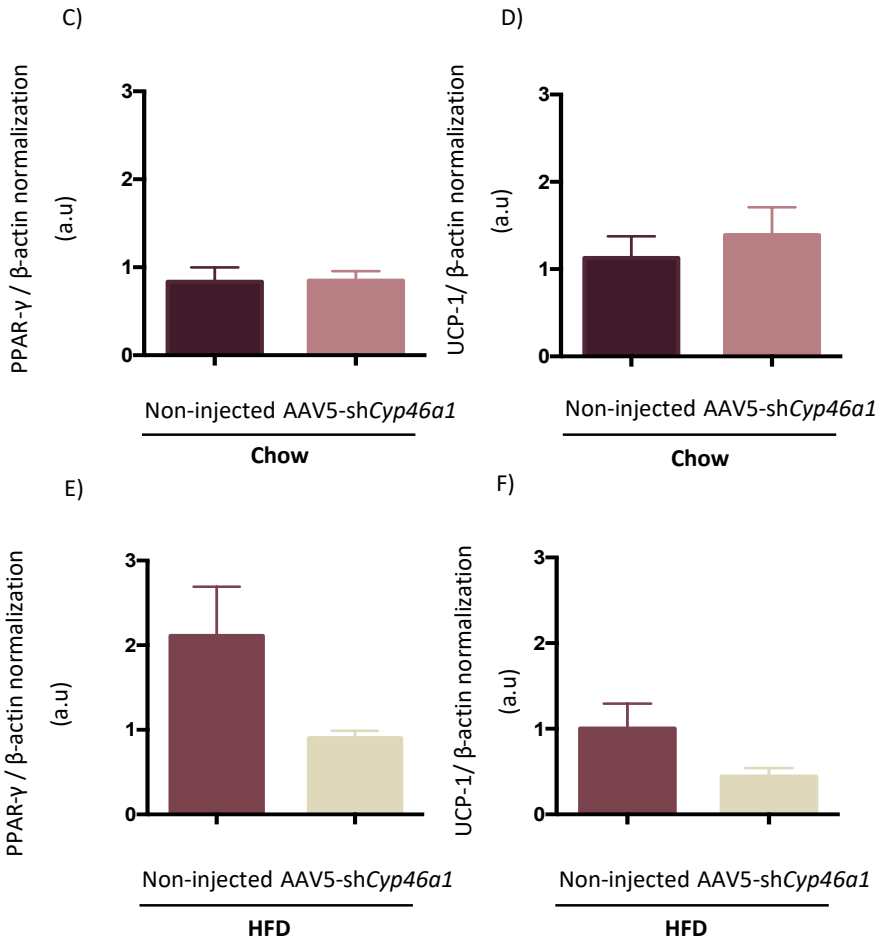
C)
PPAR-γ / β-actin normalization (a.u)
0
1
2
3
Non-injected AAV5-shCyp46a1
Chow
D)
UCP-1/ β-actin normalization (a.u)
0
1
2
3
Non-injected AAV5-shCyp46a1
Chow
E)
PPAR-γ / β-actin normalization (a.u)
0
1
2
3
Non-injected AAV5-shCyp46a1
HFD
F)
UCP-1/ β-actin normalization (a.u)
0
1
2
3
Non-injected AAV5-shCyp46a1
HFD

Figure 26| Silencing *Cyp46a1* gene in the hypothalamus induces modifications in the protein levels in BAT C57BL/6J mice fed with a Chow and HFD

The impact of silencing the *Cyp46a1* gene was evaluated in the PPAR-γ and the UCP-1 protein levels in the BAT, through WB analysis. **A)** The analysis of PPAR-γ revelated a high density of the PPAR-γ bands in the Chow AAV5-sh*Cyp46a1* animals comparatively to the Chow Non-injected. The analysis of UCP-1 revelated the presence of UCP-1 bands in both of the Chow groups. Membranes were probed with anti-β-actin for protein load control [Chow Non-injected; *n=4* versus Chow AAV5-sh*Cyp46a1*; *n=4*]. **B)** The WB analysis of PPAR-γ revelated a low density of the PPAR-γ bands in the HFD AAV5-sh*Cyp46a1* animals, comparatively to the HFD Non-injected animals. The analysis of UCP-1 revelated the presence of UCP-1 bands in both of the HFD groups. Membranes were probed with anti-β-actin for protein load control [HFD Non-injected; *n=4* versus HFD AAV5-sh*Cyp46a1*; *n=4*]. **C)** The optical density of PPAR-γ bands was quantified and then normalized with the optical density of β-actin bands. The Chow AAV5-sh*Cyp46a1* animals did not showed changes in the PPAR-γ levels comparatively to the Chow Non-injected animals [Chow Non-injected (10,8369 ± 0,1614); *n=5* versus Chow AAV5-sh*Cyp46a1* (0,8477 ± 0,1073); *n=5* – *P*-value =0,9569]. **D)** The optical density of UCP-1 bands was quantified and then normalized with the optical density of β-actin bands. The Chow AAV5-sh*Cyp46a1* animals did not presented changes in UCP-1 levels relatively to the Chow Non-injected animals [Chow Non-injected (1,128 ± 0,2478); *n=6* versus Chow AAV5-sh*Cyp46a1* (1,391 ± 0,3175); *n=6* – *P*-value =0,5276]. **E)** The optical density of PPAR-γ bands was quantified and then normalized with the optical density of β-actin bands. The HFD-AAVsh*Cyp46a1* animals presented a decrease of PPAR-γ levels relatively to the HFD Non-injected animals [HFD Non-injected (2,111 ± 0,5794); *n=6* versus HFD AAV5-sh*Cyp46a1* (1,9030 ± 0,08483); *n=6* – *P*-value =0,0513]. **F)** The optical density of UCP-1 bands was quantified and then normalized with the optical density of β-actin bands. The HFD AAV5-sh*Cyp46a1* animals showed a decrease in UCP-1 levels [HFD Non-injected (1,004 ± 0,2899); *n=6* versus HFD AAV5-sh*Cyp46a1* (0,4435 ± 0,09882); *n=6* – *P*-value =0,0969]. Data were represented as mean ± SEM. [*P*-value < 0,05 (*), *P*-value < 0,01 (**), *P*-value < 0,001 (***), *P*-value < 0,0001 (****)] – unpaired Student's t-test: C-D-E-F; **Abbreviations: a.u:** arbitrary units; **PPAR-γ:** peroxisome proliferator activated receptor γ; **UCP-1**: uncoupling protein 1; **AAV5:** adeno-associated vectors of the serotype 5; **Chow:** low fat control diet; **HFD:** high fat diet; **sh:** short hairpin.

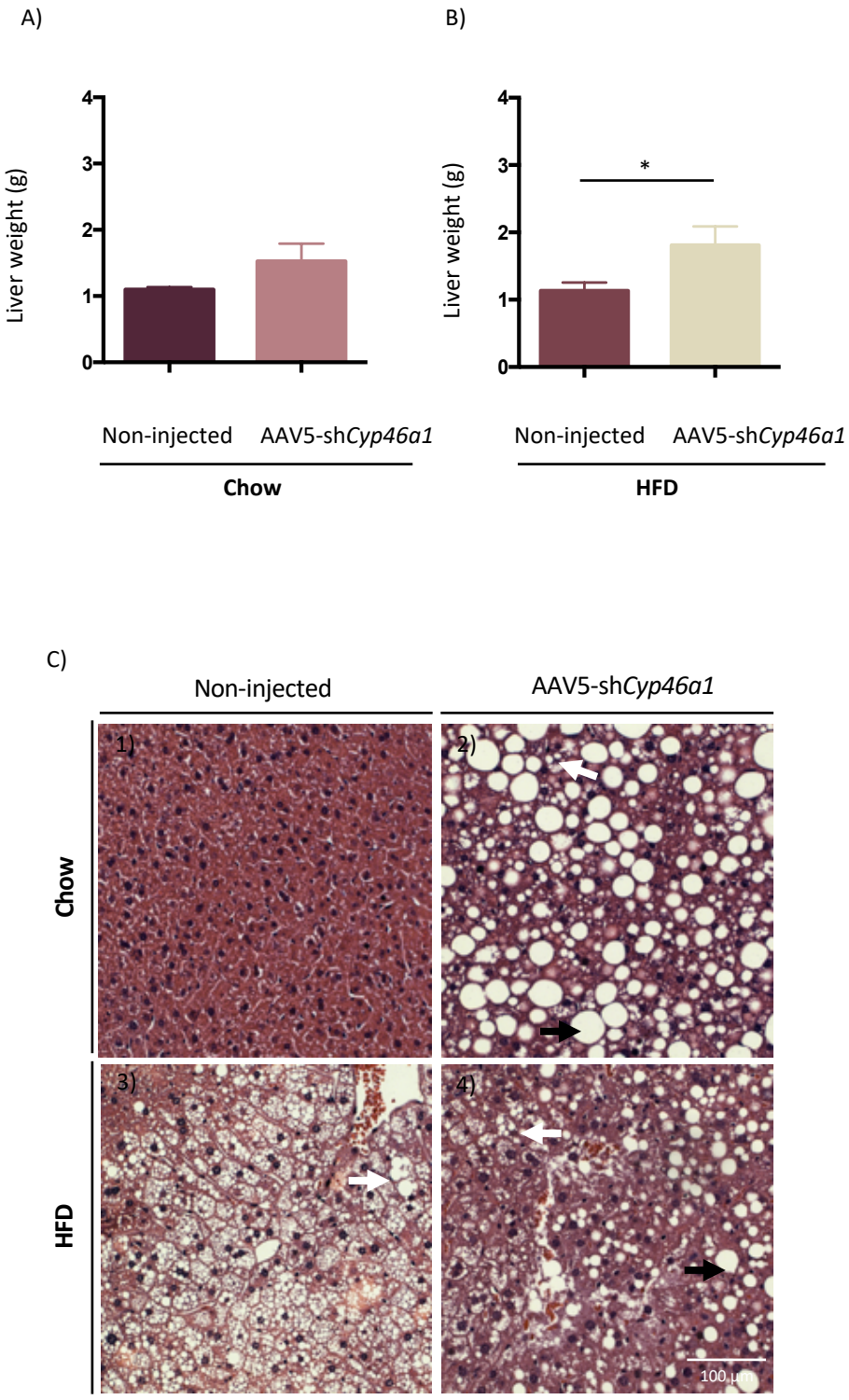

Figure 27| Silencing *Cyp46a1* gene in the hypothalamus induces increases on liver weight and hepatic steatosis in C57BL/6J mice fed with a Chow and HFD

In the 12th week of the study, the C57BL/6J mice were sacrificed and the liver were collected and weighted. **A)** The Chow AAV5-sh*Cyp46a1* animals presented an increase in the liver weight comparatively to the Chow Non-injected animals [Chow Non-injected (1,099 ± 0,03700); *n=13* versus Chow AAV5-sh*Cyp46a1* (1,525 ± 0,2673); *n=11* – *P*- value =0,0997]**. B)** The HFD AAV5-sh*Cyp46a1*

animals presented an increase in the liver weight comparatively to the HFD Non-injected animals [HFD Non-injected (1,131 ± 0,1244); *n=10* versus HFD AAV5-sh*Cyp46a1* (1,808 ± 0,2810); *n=11* – *P*-value =0,0466]. **C1)** Hepatocytes of the Chow Non-injected animals. **C2)** The Chow AAV5-sh*Cyp46a1* animals showed macrovesicular steatosis (black arrows), which is characterized by big lipid droplets in hepatocytes. **C3)** The HFD Non-injected animals which showed microvesicular steatosis (white arrows). **C4)** The HFD AAV5-sh*Cyp46a1* animals showed microvesicular steatosis (white arrows), that is characterized by small lipid droplets, macrovesicular steatosis (black arrows) hepatocytes hypertrophy and immune system infiltration in hepatocytes. Data were represented as mean ± SEM. [*P*-value < 0,05 (*), *P*-value < 0,01 (**), *P*-value < 0,001 (***), *P*-value < 0,0001 (****)] – unpaired Student's t-test: A-B; **Abbreviations: Chow:** low fat control diet; **HFD:** high fat diet; **AAV5:** adeno-associated vectors of the serotype 5; **sh:** short hairpin.

Discussion

Silencing *Cyp46a1* gene in the hypothalamus modifies whole-body energy homeostasis

Cholesterol metabolism is tightly controlled in the brain, through an equilibrium between cholesterol *de novo* synthesis and cholesterol efflux (Björkhem 2006). In this balance, cholesterol hydroxylation into 24-OHC through CYP46A1 enzyme action is essential for its brain excretion. This oxysterol, contrary to cholesterol, has the ability to cross the BBB, thus contributing to the cholesterol balance (Russell et al. 2009). Most of the cholesterol in the brain (70%-80%) is in myelin sheaths to insulate axons and to the maintenance of their morphology and synaptic transmission (Zhang and Liu 2015).

The importance of cholesterol in the brain is highlighted by the fact that dysfunctions in its metabolism homeostasis are correlated with different neurodegenerative disorders including AD, PD, HD and SLOS (Vance 2012). In line with this relation, previous studies documented that the injection of AAV5-sh*Cyp46a1* in the hippocampus of C57BL/6J wild-type mice results in a decrease of *Cyp46a1* expression, of the Cyp46a1 enzyme, a consequent decrease of 24-OHC levels and an increase of cholesterol, which lead to a progressive apoptotic death (Djelti et al. 2015; Boussicault et al. 2016; Ayciriex et al. 2017). In the context of metabolic syndrome, it was shown that changes in oxysterol levels were correlated with obesity (Guillemot-Legris et al. 2016). In the hypothalamus, a study reported a reduction in oxysterol levels in HFD induced mice and in *ob/ob* animals (Guillemot-Legris et al. 2016). Consistently, another study found that C57BL/6J mice submitted to diet-induced obesity presented changes in tissue oxysterols levels in plasma and in the adipose (Wooten et al. 2014).

The ARC in hypothalamus is located close to median eminence, a circumventricular region that has fenestrated capillaries, and is composed by populations of first-order neurons that integrate peripheral signals and posteriorly produce and release neuropeptides and neurotransmitters for control the whole-body energy homeostasis (Roh and Kim 2016). As the silencing of *Cyp46a1* gene in hippocampus results in cholesterol accumulation in neurons and subsequently apoptotic death, we hypothesized that the silencing of *Cyp46a1* mouse gene in the ARC, could lead to a reduction of Cyp46a1 enzymatic activity, a consequent diminution of 24-OHC levels and an increase of cholesterol accumulation in ARC neurons, namely in the orexigenic and anorexigenic neurons. As the ARC is implicated in the control of whole-body

energy metabolism, and oxysterols levels are altered in obesity, we hypothesize that the silencing of *Cyp46a1* gene could lead to an obesity and TIIDM phenotypes.

Dietary fat overconsumption is well known to be a crucial factor in weight gain and obesity (Swinburn et al. 2004). Consistently, our results show that an HFD leads to an increase of food intake and total and cumulative BW gain in C57BL/6J wild-type mice.

Previous studies documented that mice fed with HFD show a significant reduction of *POMC* mRNA expression (-55%) in the ARC, comparatively to mice fed with Chow (Lin, Storlien, and Huang 2000). It was also documented that *NPY* mRNA expression is decrease in the ARC of mice fed with HFD and that this decrease is probably a counter-regulatory mechanism or a consequence of the circulating Lep levels increase (Beck 2006).

According to our hypothesis, in the experimental groups where the *Cyp46a1* gene was silenced, the animals presented significant alterations in whole body metabolism. The Chow AAV5-sh*Cyp46a1* animals, presented an increase in the cumulative BW gain accompanied by an increase in cumulative food and water intake comparatively to the Chow Non-injected animals, suggesting that the silencing of *Cyp46a1* gene mimics the effects of an HFD. In the same line, the HFD AAV5-sh*Cyp46a1* animals, presented an increase in the cumulative BW gain, however, there was a decrease in the total and cumulative food intake comparatively to the HFD Non-injected animals, whereas no alterations were found in water intake. These results suggest that the silencing of *Cyp46a1* mouse gene in the ARC could be compromising the orexigenic and anorexigenic genetic expression, signaling pathways and neuropeptides secretion. Actually, mutations in the POMC anorexigenic neurons result in severe early-onset obesity (Krude et al. 1998; Yaswen et al. 1999). Moreover, the ablation of POMC anorexigenic neurons in mice results in hyperphagia and in body weight gain (Gropp et al. 2005), which is consistent with the phenotype observed in Chow AAV5-sh*Cyp46a1* animals. The central administration or genetic overexpression of AgRP also results in a decrease in the energy expenditure and in obesity (Graham et al. 1997; Small et al. 2003).

Another hypothesis to explain our data is that the silencing of *Cyp46a1* mouse gene results in hypothalamic dysfunctions involving defects in insulin and Lep signaling pathways, which can result in obesity. For example, dysfunctions of IRS-PI3K signaling pathway in the brain or in the pancreas cause obesity and diabetes (Könner and Brüning 2012). Lep acts in the inhibition of AgRP orexigenic neurons, through the LepR, leading to an inhibition of food consumption. In fact, it was reported that mice lacking *LepR* on POMC anorexigenic neurons

presented an increase in BW leading to impaired energy homeostasis (Balthasar et al. 2004). In the AgRP/NPY orexigenic neurons, the loss of *LepR* expression results in an obesity phenotype, including hyperphagia and reduced energy expenditure in mice (Luo et al. 2011). This hypothesis is consistent with the results observed in the AAV5-sh*Cyp46a1* animals, thus suggesting that the silencing of *Cyp46a1* mouse gene leads to defects in insulin and Lep signaling pathways.

Hypothalamic inflammation is correlated with a reduction in POMC and AgRP neurons responsiveness to insulin and Lep, also contributing to dysfunctions in insulin signaling pathway and IR (Valdearcos et al. 2015).

The AgRP/NPY orexigenic neurons have the ability to project their axons into other hypothalamic nuclei, such as PVN, LHA, DMN and VMN, in order to modulate energy homeostasis and the disruption of these intrahypothalamic connections results in obesity phenotypes (Choi and Dallman 1999; Waterson and Horvath 2015). Therefore, another possible hypothesis for explain the phenotypes observed in the AAV5-sh*Cyp46a1* animals, could be that AgRP/NPY neurons have their ability to project their axons into other hypothalamic nuclei compromised.

In the HFD AAV5-sh*Cyp46a1* animals it was observed a decrease in food intake. These animals previously presented a compromised metabolic status, as consequence of an HFD for 4 weeks before the stereotaxic injection. In HFD-induced obesity, beyond the hypothalamic insulin and Lep resistance, the ability of ghrelin to promote food intake in AgRP/NPY neurons is also impaired (Timper and Brüning 2017). This fact could explain why we observed a decrease in the food intake in the HFD AAV5-sh*Cyp46a1* animals. In fact, despite the possible impairment in AgRP/NPY neurons, the ghrelin action on PVN neurons is maintained, resulting in an increase of adiposity that is independent of food intake (Timper and Brüning 2017). Another possible explanation to this decrease in food intake could be related to the WAT secretion of Lep, which is proportional to WAT weight (Friedman 2011). It is well known that obesity and insulin resistance are strongly correlated with alterations in peripheral organs, namely the adipose tissues (Stienstra et al. 2007). The Chow AAV5-sh*Cyp46a1* animals showed a significant increase on WAT weight (Chow AAV5-sh*Cyp46a1*: a mean of 1,7 g of WAT) accompanied with hypertrophy of adipocytes comparatively to the Non-injected animals, suggesting that the silencing of *Cyp46a1* gene mimics the effects of an HFD. In the same way, the HFD AAV5-sh*Cyp46a1* animals presented an increase in WAT weight (HFD AAV5-

sh*Cyp46a1*: a mean of 2,5 g of WAT), accompanied by adipocytes hypertrophy and signals of necrosis. These signals of necrosis in some adipocytes could be driven by hypertrophy and accelerated obesity (Sun et al. 2011). In these animals, the amount of WAT, might result in an increase of Lep secretion, which acts in the hypothalamus leading to an inhibition of AgRP/NPY neurons and the consequent reduction of food intake observed. Beyond the Lep secretion by WAT, a possible dysfunction of adipokines production and secretion, such the TNF-α and IL-6, could result in a chronic low-grade inflammation contributing to the pathogenesis of obesity (Ouchi et al. 2011).

It was shown that obesity induces the whitening of BAT, which is characterized by the accumulation of large lipid droplets, mitochondrial dysfunction and loss of vascularity, approaching the morphology of the unilocular white adipocytes (Shimizu and Walsh 2015). These phenotypic changes could reduce the BAT function and exacerbate the obesity phenotype (Bournat and Brown 2010; Shimizu and Walsh 2015). This is consistent with the results observed in the BAT of the AAV5-sh*Cyp46a1* animals, which presented an increase of lipid droplets in adipocytes, comparatively to the Non-injected animal. In the Chow AAV5-sh*Cyp46a1* animals the impact of the silencing *Cyp46a1* gene in BAT adipocytes appears to mimic an HFD effect, whereas in HFD AAV5-sh*Cyp46a1* animals this silencing appears exacerbate the phenotype of obesity.

We also studied differences between gender, as there are fundamental aspects of whole-body energy homeostasis that are regulated differently in males and females (Mauvais-Jarvis 2015). In fact, the impact of an HFD is more visible in the males mice, which are more vulnerable than females to the BW gain and metabolic alterations (Hwang et al. 2010; Ingvorsen, Karp, and Lelliott 2017). Consistently, our results showed that the male mice are more vulnerable than females to the impact of silencing the *Cyp46a1* gene in the BW gain and to WAT and liver weight gain in both Chow and HFD fed mice.

Silencing *Cyp46a1* gene in the hypothalamus induces hyperglycemia and a diminution of insulin sensitivity in C57BL/6J wild-type mice fed with a Chow and HFD

To understand the mechanisms underlying the obesity phenotype induced by the silencing the *Cyp46a1* mouse gene in ARC, we analyzed the glucose tolerance and insulin sensitivity, as obesity is strongly associated with impaired glucose tolerance and insulin resistance. In fact, dysfunctions in central insulin signaling pathway, especially in the ARC,

results in a disruption of the whole-body energy homeostasis and as consequence a dysfunction in the glucose homeostasis and posteriorly obesity (Zhang, Dodd, and Tiganis 2015). In the C57BL/6J mice, an HFD results in increased BW gain, impaired glucose tolerance and insulin resistance (Winzell and Ahren 2004). Consistently, our results show that an HFD for 4 weeks, results in a decrease of glucose tolerance in C57BL/6J mice.

The AAV5-sh*Cyp46a1* animals showed a decrease in glucose tolerance and in insulin sensitivity comparatively to the Non-injected animals, suggesting that the silencing the *Cyp46a1* mouse gene in ARC may be resulting in dysfunction in hypothalamic insulin signaling. Actually, previous studies observed that the insulin-stimulated activation of PI3K in hypothalamus is decreased in obese rats comparatively to lean rats (Carvalheira et al. 2003). This impairment of insulin signaling in POMC anorexigenic and AgRP orexigenic neurons may contribute to hyperphagia and to the progression into obesity (Könner and Brüning 2012). This fact could explain the results observed in the AAV5-sh*Cyp46a1* animals.

However, the peripheric metabolic organs dysfunctions, such as the adipose tissue, the liver and the pancreas, could be also contributing to the decrease in insulin sensitivity observed in the AAV5-sh*Cyp46a1* animals. Another hypothesis that could explain our results is the suppression of MCR3/4 that could be happen in the hypothalamus, resulting in hyperinsulinemia, impaired glucose tolerance and obesity (Obici et al. 2001).

Altogether, these data point that in the Chow AAV5-sh*Cyp46a1* animals, the impact of the silencing *Cyp46a1* gene appears to mimic an HFD effect, whereas in HFD AAV5-sh*Cyp46a1* mice this silencing exacerbate the phenotype of obesity.

Silencing *Cyp46a1* gene in the hypothalamus induces an increase in organs weight, modifications in lipid content and in the protein levels in adipose tissue

When the storage capacity of the adipose tissue is exceeded, modifications in the endocrine function occurs, through the increase of adipocytokines secretion, and ectopic fat accumulation. This accumulation results in lipotoxicity, which acts in promoting low-grade inflammation and metabolic dysfunctions, such as insulin resistance in several organs (Gross et al. 2017). The obesity is strongly correlated with lipid accumulation in the liver and present a risk factor for the development of fatty liver diseases, such as NAFLD (Stienstra et al. 2007). Nonetheless, impaired oxysterols metabolism was characteristic in the liver affected by NASH (Raselli et al. 2019). Consistently, our results show that the AAV5-sh*Cyp46a1* animals

presented an increase in the liver weight accompanied by lipid accumulation in hepatocytes, characterized by macrovesicular steatosis, microvesicular steatosis and hepatocytes hypertrophy, comparatively to the Non-injected animals. These results suggest that the silencing of *Cyp46a1* mouse gene leads to an increase in liver weight and hepatic steatosis in the C57BL/6J mice fed with both Chow and HFD, contributing to the metabolic dysfunctions found in the AAV5-sh*Cyp46a1* animals.

Adipocytes has been recognized by their role in the regulation of energy homeostasis and body composition (Susan, Castracane, and Christos 2004). The PPAR-γ is a transcription factor that act in the regulation of adipose-specific genes, which play a role in adipogenesis, energy balance and lipid biosynthesis. In fact, PPAR-γ is required for adipocytes differentiation *in vitro* and *in vivo* and it knockout in mice results in a lack of adipose tissue (Barak et al. 1999; Rosen et al. 1999). However, PPAR-γ expression is not strongly modified in obesity (Vidal-Puig et al. 1996; Stienstra et al. 2007). PPAR-γ activation also participates in the regulation of insulin sensitivity and is involved in the inhibition of proinflammatory cytokines (Janani and Kumari 2015). Actually, agonists of PPAR-γ, specifically the thiazolidinediones (TZDs), act in the activation of PPAR-γ, improving the insulin sensitivity and inhibiting inflammatory cytokines (Jiang, Ting, and Seed 1998; Murphy and Holder 2000).

In the WAT, the AAV5-sh*Cyp46a1* animals, both in Chow and HFD groups showed a significant decrease of PPAR-γ protein levels comparatively to the Non-injected animals. Previous studies reported that the lack of PPAR-γ in adipose tissues is correlated with the susceptibility to insulin resistance and lipodystrophy, which is consistent with the decrease of PPAR-γ protein levels and insulin resistance that we observed in the AAV5-sh-*Cyp46a1* animals (He et al. 2003; Corrales, Vidal-Puig, and Medina-Gómez 2018). The PPAR-γ activation inhibits the expression of proinflammatory genes in the macrophages of the adipose tissue (Blaschke et al. 2006). The decrease of PPAR-γ protein levels in the AAV5-sh*Cyp46a1* may suggest the possibility of an inflammatory state in the adipose tissue of these animals.

The PPAR-γ is also implicated as a regulator of brown adipocytes (Lasar et al. 2018). Actually, the activation of PPAR-γ, through TZD, can modulate UCP-1 expression (Kelly et al. 1998). The Chow AAV5-sh*Cyp46a1* did not show any alterations of the PPAR-γ protein levels in the BAT, comparatively to Chow Non-injected animals. On the other hand, the HFD AAV5-sh*Cyp46a1* showed a decrease in PPAR-γ protein levels comparatively to the HFD Non-injected animals.

It was shown that the PPAR-γ ablation in mature white and brown adipocytes result in a decrease in WAT and BAT weight (Imai et al. 2004). Contrarily, in our results we observed a reduction of PPAR-γ protein levels, hypertrophy of white and brown adipocytes, and an increase in WAT weight. These observations could result from a compensatory mechanism, or that some regulators of PPAR-γ are also dysregulated, due to the silencing of *Cyp46a1* gene, which contribute to the reduction of PPAR-γ protein levels. For example, PPAR-γ and CCAAT/enhancer-binding protein α (C/EBP-α), a transcription factor in adipogenesis, promote each other's expression. In fact, fibroblasts lacking C/EBP-α had deficits in PPAR expression and in adipogenesis (Rosen et al. 2002).

The UCP-1, is specifically expressed in the inner membrane of mitochondria in WAT and BAT and has the ability to act in the induction of thermogenesis, thus controlling the energy expenditure (Kozak 2009). The UCP-1 ablation results in obesity in both Chow and HFD fed, promoting an increase of BW, and also in WAT weight (Feldmann et al. 2009). Similarly, the AAV5-sh*Cyp46a1* animals, both in Chow and HFD groups showed a significant decrease of UCP-1 protein levels in WAT comparatively to the Non-injected animals, and an increase of BW gain. In the BAT, UCP-1 ablation results in lipidic accumulation in the adipocytes and a pro-inflammatory state (Bond, Burhans, and Ntambi 2018). Our results show that the Chow AAV5-sh*Cyp46a1* animals did not showed changes in UCP-1 protein levels in BAT comparatively to the Chow Non-injected animals. However, the HFD-AAVsh*Cyp46a1* animals showed a decrease of UCP-1 protein levels in BAT relatively to the HFD Non-injected animals, consistent with the adipocytes hypertrophy observed and possibly suggesting an inflammatory state in these animals.

Overall, these results suggest that the silencing of *Cyp46a1* mouse gene leads to alterations in PPAR-γ and UCP-1 protein levels in WAT and BAT, inducing dysfunctions in the equilibrium between energy consumption and energy expenditure, which is crucial for maintenance of the whole-body energy homeostasis.

Silencing *Cyp46a1* gene in the hypothalamus modify the behavior activity of C57BL/6J mice

The open field behavior test consists in the monitorization of locomotor and anxiety-like behavior in animal models. The animals were placed in the center zone of the floor of the open field test box and their movement activity was recorded. Normally, the rodents spontaneously prefer the periphery zone of the open field box to the middle zone, and this

preference for the periphery is characterized as an anxiety-like behavior (Prut and Belzung 2003). The rearing was scored when mice raised both of front paws from the floor and leaned against a wall, being considered an exploratory behavior (Seibenhener and Wooten 2015). The grooming is an innate behavior that is involved in manutention of hygiene and other processes physiological (Kalueff et al. 2016).

In day-time period, the AAV5-sh*Cyp46a1* animals, show a decrease in the number of entries and time in the middle zone, suggesting an increase of anxiety in these animals, comparatively to the Non-injected animals. The AAV5-sh*Cyp46a1* animals, also show a decrease in the time of rearing, suggesting a decrease in the exploratory behavior and an increase of anxiety.

The HFD AAV5-sh*Cyp46a1* animals presented a decrease in the number of grooming's a comparatively to the Non-injected groups, also suggesting an increase of anxiety.

In the night-time period, rodents are most active; the Chow AAV5-sh*Cyp46a1* animals showed a significant decrease of total distance traveled, in the mean speed, in the number of crossing lines, in the number of entries in the middle zone and an increase in total time immobile, suggesting an anxiety/depressive-like behavior in these animals and a reduction in locomotor activity, may due to the increase of BW weight. In both diet groups, the AAV5-sh*Cyp46a1* animals showed a significant decrease in the time of rearing's comparatively to the Non-injected control animals. The decreases of rearing and grooming behaviors in the AAV5-sh*Cyp46a1* animals, suggests that the silencing of *Cyp46a1* gene could influence a decrease of the exploratory and innate behaviors, resulting in an increase of anxiety.

The phenotype of obesity observed in the Chow AAV5-sh*Cyp46a1* and HFD AAV5-sh*Cyp46a1* animals may contribute to the decrease of total distance traveled, mean speed and to the increase of total time immobile. In fact, previously, it was reported that mice fed with an HFD showed an increase in the time immobile, a decrease in the number the entries and the time spend in the middle zone pointing an anxiety/depressive-like behavior in these animals (Sharma and Fulton 2013). The decrease of total distance traveled and the increase of time spend immobile points a reduction in energy expenditure and possibly BW increase.

In the open field behavior test, the activity of the mouse varies by sex and circadian rhythm (Tatem et al. 2014). In fact, generally in the open field behavior test, the females show an increase in total distance travel and exploratory behavior comparatively to males (Archer 1975; Lipatova et al. 2018). Actually, sex hormones influence behaviors such

anxiety/depression and exploration (Carreira, Cossio, and Britton 2017). Our results show that the impacts of silencing of *Cyp46a1* gene, are more observed in males than females. Consistently to the impacts of silencing of *Cyp46a1* gene in the BW, which are more observable in males than females.

These results suggest that the silencing of *Cyp46a1* mouse gene modify the behavior of C57BL/6J mice, increasing the anxiety-like behavior in Chow and HFD.

Overall, the silencing of *Cyp46a1* gene result in dysfunctions in whole-body homeostasis metabolism in C57BL/6J wild-type mice fed with Chow and HFD, including the increase of BW, dysfunctions of metabolic organs and in exploratory and anxiety-like behavior, indicating the importance of the cholesterol metabolism in the regulation of whole-body homeostasis.

Conclusion and future perspectives

The *Cyp46a1* mouse gene, is crucial gene in the brain cholesterol homeostasis, and in this project, we silenced its expression in the hypothalamus of C57BL/6J wild-type mice, fed with Chow and HFD, in order to investigate its impact on whole-body metabolism.

The silencing of *Cyp46a1* mouse gene in the ARC of mice fed with Chow, led to an increase of BW, food and water intake, a reduction of glucose tolerance, of insulin sensitivity and led to alterations in several metabolic organs. Similarly, the silencing of *Cyp46a1* mouse gene in animals fed with an HFD, led to an increase of BW, a decrease of food intake, of insulin sensitivity and to modifications in different metabolic organs. Moreover, the silencing of *Cyp46a1* mouse gene in the ARC appears to modify the morphology of WAT, BAT and liver in animals fed with both Chow and HFD, as well as to alterations in the levels of important proteins in WAT and BAT. Additionally, the silencing of *Cyp46a1* mouse gene leads to modifications in anxiety-like behavior in the C57BL/6J mice fed with both Chow and HFD.

Altogether, this suggest an important role of the cholesterol metabolism in the brain, specially of the Cyp46a1 enzyme in the control of whole-body homeostasis, as the silencing of *Cyp46a1* gene in ARC led to several metabolic abnormalities.

However, additional studies are needed to continue this project. First, it is essential to confirm the silencing of *Cyp46a1* mouse gene in the hypothalamus, through gene expression analysis by RT-qPCR. Second, it could be interesting to add a new control to the study, with the animals being injected with viral vectors encoding for GFP, in order to discard that the observed effects occurred as a consequence of the stereotaxic injection. Third, it would be interesting to perform the quantification of cholesterol content and oxysterols content in the hypothalamus by mass spectrometry. Fourth, an immunohistochemical analysis of the hypothalamus will be also interesting, namely for neuronal death and neurogenesis markers. Five, gene expression analysis in the hypothalamus and in other metabolic organs, such as the adipose tissue, the liver and the pancreas, for different metabolic mediators, by RT-qPCR, will be also important. For example, we could include the gene expression analysis of POMC/CART, AgRP/NPY, insulin, Lep and ghrelin receptors, GLUT, up-regulators of PPAR-γ, enzymes associated to lipid metabolism, cytokines, adipokines and other molecular targets. Five, it would be interesting to perform histological and protein analysis in other metabolic organs, such as the liver, pancreas, skeletal muscle and spleen, as well as, to continue the protein

analysis in WAT and BAT. Some experiments may also be repeat to confirm the obtained results, as the WB in WAT once the protein extraction techniques were distinct among study groups.

Finally, it would be very interesting to perform the overexpression of *Cyp46a1* in the ARC to investigate if the results are opposite to the ones that we found in this project.

Bibliographic references

Alberti, K. G. M. M., Robert H. Eckel, Scott M. Grundy, Paul Z. Zimmet, James I. Cleeman, Karen A. Donato, Jean-Charles Fruchart, W. Philip T. James, Catherine M. Loria, and Sidney C. Smith. 2009. "Harmonizing the Metabolic Syndrome." *Circulation* 120:1640–45.

Alberti, K. G. M. M., P. Zimmet, and J. Shaw. 2006. "Metabolic Syndrome - a New World-Wide Definition. A Consensus Statement from the International Diabetes Federation." *Diabetic Medicine* 23:469–80.

Alberti, K. G. M. M., Paul Zimmet, and Jonathan Shaw. 2005. "The Metabolic Syndrome - a New Worldwide Definition." *Lancet* 366:1059–62.

Albuquerque, David, Eric Stice, Raquel Rodríguez-López, Licíno Manco, and Clévio Nóbrega. 2015. "Current Review of Genetics of Human Obesity: From Molecular Mechanisms to an Evolutionary Perspective." *Molecular Genetics and Genomics* 290:1191–1221.

Andrews, Zane B. 2011. "Central Mechanisms Involved in the Orexigenic Actions of Ghrelin." *Peptides* 32:2248–55.

Andrikopoulos, Sofianos, Amy R. Blair, Nadia Deluca, Barbara C. Fam, and Joseph Proietto. 2008. "Evaluating the Glucose Tolerance Test in Mice." *American Journal of Physiology - Endocrinology and Metabolism* 295:1323–32.

Archer, John. 1975. "Rodent Sex Differences in Emotional and Related Behavior." *Behavioral Biology* 14:451–79.

Arora, Sarika. 2010. "Surrogate Markers of Insulin Resistance: A Review." *World Journal of Diabetes* 1:36–47.

Aveleira, Célia, Mariana Botelho, Sara Carmo-Silva, Jorge F. Pascoal, Marisa Ferreira-Marques, Clévio Nóbrega, Luísa Cortes, Jorge Valero, Lígia Sousa-Ferreira, Ana R. Álvaro, Magda Santana, Sebastian Kügler, Luís Pereira De Almeida, and Cláudia Cavadas. 2015. "Neuropeptide Y Stimulates Autophagy in Hypothalamic Neurons." *Proceedings of the National Academy of Sciences of the United States of America* 112:E1642–51.

Ayciriex, Sophie, Fathia Djelti, Sandro Alves, Anne Regazzetti, Mathieu Gaudin, Jennifer Varin, Dominique Langui, Ivan Bièche, Eloise Hudry, Delphine Dargère, Patrick Aubourg, Nicolas Auzeil, Olivier Laprévote, and Nathalie Cartier. 2017. "Neuronal Cholesterol Accumulation Induced by Cyp46a1 Down-Regulation in Mouse Hippocampus Disrupts Brain Lipid Homeostasis." *Frontiers in Molecular Neuroscience* 10:1–15.

Balthasar, Nina, Roberto Coppari, Julie McMinn, Shun M. Liu, Charlotte E. Lee, Vinsee Tang, Christopher D. Kenny, Robert A. McGovern, Streamson C. Chua, Joel K. Elmquist, and Bradford B. Lowell. 2004. "Leptin Receptor Signaling in POMC Neurons Is Required for Normal Body Weight Homeostasis." *Neuron* 42:983–91.

Barak, Yaacov, Michael C. Nelson, Estelita S. Ong, Ying Z. Jones, Pilar Ruiz-Lozano, Kenneth R. Chien, Alan Koder, and Ronald M. Evans. 1999. "PPARγ Is Required for Placental, Cardiac, and Adipose Tissue Development." *Molecular Cell* 4:585–95.

Barroso, I., M. Gurnell, V. E. F. Crowley, M. Agostini, J. W. Schwabe, M. A. Soos, G. Li Maslen, T. D. M. Williams, H. Lewis, A. J. Schafer, V. K. K. Chatterjee, and S. O'Rahilly. 1999.

"Dominant Negative Mutations in Human PPARγ Associated with Severe Insulin Resistance, Diabetes Mellitus and Hypertension." *Nature* 402:880–83.

Beck, B. 2006. "Neuropeptide Y in Normal Eating and in Genetic and Dietary-Induced Obesity." *Philosophical Transactions of the Royal Society B: Biological Sciences* 361:1159–85.

Benarroch, Eduardo E. 2008. "Brain Cholesterol Metabolism and Neurologic Disease." *Neurology* 71:1368–73.

Berthoud, Hans-Rudi and Heike Munzberg. 2011. "The Lateral Hypothalamus as Integrator of Metabolic and Environmental Needs: From Electrical Self-Stimulation to Optogenetics." *Physiology and Behavior* 104:29–39.

Biran, Jakob, Maayan Tahor, Einav Wircer, and Gil Levkowitz. 2015. "Role of Developmental Factors in Hypothalamic Function." *Frontiers in Neuroanatomy* 9:1–11.

Björkhem, I. 2006. "Crossing the Barrier: Oxysterols as Cholesterol Transporters and Metabolic Modulators in the Brain." *Journal of Internal Medicine* 260:493–508.

Bjorkhem, Ingemar and Steve Meaney. 2004. "Brain Cholesterol: Long Secret Life behind a Barrier." *Arteriosclerosis, Thrombosis, and Vascular Biology* 24:806–15.

Björkhem, Ingemar, Kalicharan Patra, Adam L. Boxer, and Per Svenningsson. 2018. "24S-Hydroxycholesterol Correlates with Tau and Is Increased in Cerebrospinal Fluid in Parkinson's Disease and Corticobasal Syndrome." *Frontiers in Neurology* 9:1–6.

Blaschke, Florian, Yasunori Takata, Evren Caglayan, Ronald E. Law, and Willa A. Hsueh. 2006. "Obesity, Peroxisome Proliferator-Activated Receptor, and Atherosclerosis in Type 2 Diabetes." *Arteriosclerosis, Thrombosis, and Vascular Biology* 26:28–40.

Bogdanovic, Nenad, Lionel Bretillon, Erik G. Lund, Ulf Diczfalusy, Lars Lannfelt, Bengt Winblad, David W. Russell, and Ingemar Björkhem. 2001. "On the Turnover of Brain Cholesterol in Patients with Alzheimer's Disease. Abnormal Induction of the Cholesterol-Catabolic Enzyme CYP46 in Glial Cells." *Neuroscience Letters* 314:45–48.

Bond, Laura M., Maggie S. Burhans, and James M. Ntambi. 2018. "Uncoupling Protein-1 Deficiency Promotes Brown Adipose Tissue Inflammation and ER Stress." *PLOS ONE* 13:1–11.

Bonora, Enzo, Paolo Moghetti, Carlo Zancanaro, Massimo Cigolini, Marina Querena, Vittorio Cacciatori, Angela Corgnati, and Michele Muggeo. 1989. "Estimates of in Vivo Insulin Action in Man: Comparison of Insulin Tolerance Tests with Euglycemic and Hyperglycemic Glucose Clamp Studies." *Journal of Clinical Endocrinology and Metabolism* 68:374–78.

Bournat, Juan C. and Chester W. Brown. 2010. "Mitochondrial Dysfunction in Obesity." *Current Opinion in Endocrinology, Diabetes and Obesity* 17:446–52.

Boussicault, Lydie, Sandro Alves, Antonin Lamazière, Anabelle Planques, Nicolas Heck, Lara Moumné, Gaëtan Despres, Susanne Bolte, Amélie Hu, Christiane Pagès, Laurie Galvan, Francoise Piguet, Patrick Aubourg, Nathalie Cartier, Jocelyne Caboche, and Sandrine Betuing. 2016. "CYP46A1, the Rate-Limiting Enzyme for Cholesterol Degradation, Is Neuroprotective in Huntington's Disease." *Brain* 139:953–70.

Bretillon, Lionel, Ulf Diczfalusy, Ingemar Björkhem, Marie Annick Maire, Lucy Martine, Corinne Joffre, Niyazi Acar, Alain Bron, and Catherine Creuzot-Garcher. 2007. "Cholesterol-24S-

Hydroxylase (CYP46A1) Is Specifically Expressed in Neurons of the Neural Retina." *Current Eye Research* 32:361–66.

Brown, Audrey E. and Mark Walker. 2016. "Genetics of Insulin Resistance and the Metabolic Syndrome." *Current Cardiology Reports* 18:1–8.

Bruce, K. D. and C. D. Byrne. 2009. "The Metabolic Syndrome: Common Origins of a Multifactorial Disorder." *Postgraduate Medical Journal* 85:614–21.

Burnette, W. Neal. 1981. "'Western Blotting': Electrophoretic Transfer of Proteins from Sodium Dodecyl Sulfate-Polyacrylamide Gels to Unmodified Nitrocellulose and Radiographic Detection with Antibody and Radioiodinated Protein A." *Analytical Biochemistry* 112:195–203.

Calvin, Andrew D., Felipe N. Albuquerque, Francisco Lopez-Jimenez, and Virend K. Somers. 2009. "Obstructive Sleep Apnea, Inflammation, and the Metabolic Syndrome." *Metabolic Syndrome and Related Disorders* 7:271–77.

Carmo-silva, Sara and Cláudia Cavadas. 2017. "Obesity and Brain Function." *Advances in Neurobiology* 19:73–116.

Carreira, María B., Ricardo Cossio, and Gabrielle B. Britton. 2017. "Individual and Sex Differences in High and Low Responder Phenotypes." *Behavioural Processes* 136:20–27.

Carvalheira, J. B. C., E. B. Ribeiro, E. P. Araújo, R. B. Guimarães, M. M. Telles, M. Torsoni, J. A. R. Gontijo, L. A. Velloso, and M. J. A. Saad. 2003. "Selective Impairment of Insulin Signalling in the Hypothalamus of Obese Zucker Rats." *Diabetologia* 46:1629–40.

Cavadas, Cláudia, Célia A. Aveleira, Gabriela F. P. Souza, and Lício A. Velloso. 2016. "The Pathophysiology of Defective Proteostasis in the Hypothalamus - from Obesity to Ageing." *Nature Reviews Endocrinology* 12:723–33.

Chao, Pei Ting, Liang Yang, Susan Aja, Timothy H. Moran, and Sheng Bi. 2011. "Knockdown of NPY Expression in the Dorsomedial Hypothalamus Promotes Development of Brown Adipocytes and Prevents Diet-Induced Obesity." *Cell Metabolism* 13:573–83.

Chen, Jing, Xiaolu Zhang, Handojo Kusumo, Lucio G. Costa, and Marina Guizzetti. 2012. "Cholesterol Efflux Is Differentially Regulated in Neurons and Astrocytes: Implications for Brain Cholesterol Homeostasis." *Biochimica et Biophysica Acta* 1831:263–75.

Choi, Su Jean and Mary F. Dallman. 1999. "Hypothalamic Obesity: Multiple Routes Mediated by Loss of Function in Medial Cell Groups." *Endocrinology* 140:4081–88.

Contreras, Cristina, Rubén Nogueiras, Carlos Diéguez, Kamal Rahmouni, and Miguel López. 2017. "Traveling from the Hypothalamus to the Adipose Tissue: The Thermogenic Pathway." *Redox Biology* 12:854–63.

Cornier, Marc-Andre, Dana Dabele, Teri L. Hernandez, Rachel C. Lindstrom, Amy J. Steig, Nicole R. Stob, Rachael E. Van Pelt, Hong Wang, and Robert H. Eckel. 2008. "Debating the Metabolic Syndrome Debating the Metabolic Syndrome." *Endocrine Reviews* 29:777–822.

Corrales, Patricia, Antonio Vidal-Puig, and Gema Medina-Gómez. 2018. "PPARS and Metabolic Disorders Associated with Challenged Adipose Tissue Plasticity." *International Journal of Molecular Sciences* 19:1–16.

Cowey, Stephanie and Robert W. Hardy. 2006. “The Metabolic Syndrome: A High-Risk State for Cancer?” *The American Journal of Pathology* 169:1505–22.

Cutler, Roy G., Jeremiah Kelly, Kristin Storie, Ward A. Pedersen, Anita Tammara, Kimmo Hatanpaa, Juan C. Troncoso, and Mark P. Mattson. 2004. “Involvement of Oxidative Stress-Induced Abnormalities in Ceramide and Cholesterol Metabolism in Brain Aging and Alzheimer’s Disease.” *Proceedings of the National Academy of Sciences of the United States of America* 101:2070–75.

DeFronzo, Ralph A. and Eleuterio Ferrannini. 1991. “Insulin Resistance.” *Diabetes Care* 14:173–94.

Djelti, Fathia, Jerome Braudeau, Eloise Hudry, Marc Dhenain, Jennifer Varin, Ivan Bièche, Catherine Marquer, Farah Chali, Sophie Ayciriex, Nicolas Auzeil, Sandro Alves, Dominique Langui, Marie Claude Potier, Olivier Laprevote, Michel Vidaud, Charles Duyckaerts, Richard Miles, Patrick Aubourg, and Nathalie Cartier. 2015. “CYP46A1 Inhibition, Brain Cholesterol Accumulation and Neurodegeneration Pave the Way for Alzheimer’s Disease.” *Brain* 138:2383–98.

Eckel, Robert H., Scott M. Grundy, and Paul Z. Zimmet. 2005. “The Metabolic Syndrome.” *Lancet* 365:1415–28.

Elias, Carol F., Charlotte Lee, Joseph Kelly, Carl Aschkenasi, Rexford S. Ahima, Pastor R. Couceyro, Michael J. Kuhar, Clifford B. Saper, and Joel K. Elmquist. 1998. “Leptin Activates Hypothalamic CART Neurons Projecting to the Spinal Cord.” *Neuron* 21:1375–85.

Feldmann, Helena M., Valeria Golozoubova, Barbara Cannon, and Jan Nedergaard. 2009. “UCP1 Ablation Induces Obesity and Abolishes Diet-Induced Thermogenesis in Mice Exempt from Thermal Stress by Living at Thermoneutrality.” *Cell Metabolism* 9:203–9.

Franklin, Keith and George Paxinos. 2019. *Paxinos and Franklin’s the Mouse Brain in Stereotaxic Coordinates*.

Friedman, Jeffrey M. 2011. “Leptin and the Regulation of Body Weight.” *The Keio Journal of Medicine* 60:1–9.

Furukawa, Shigetada, Morihiro Matsuda, Shigetada Furukawa, Takuya Fujita, Michio Shimabukuro, and Masanori Iwaki. 2017. “Increased Oxidative Stress in Obesity and Its Impact on Metabolic Syndrome Find the Latest Version: Increased Oxidative Stress in Obesity and Its Impact on Metabolic Syndrome.” *The Journal of Clinical Investigation* 114:1752–61.

Garcia, Anália Nusya Medeiros, Maria Tereza Cartaxo Muniz, Hugo Rafael Souza E Silva, Helker Albuquerque Da Silva, and Luiz Athayde-Junior. 2009. “Cyp46 Polymorphisms in Alzheimer’s Disease: A Review.” *Journal of Molecular Neuroscience* 39:342–45.

Ginsberg, Henry N. 2000. “Insulin Resistance and Cardiovascular Disease Find the Latest Version: Insulin Resistance and Cardiovascular Disease.” *The Journal of Clinical Investigation* 106:453–58.

Graham, Melissa, John Sutter, Ulla Sarmiento, Ildiko Sarosi, and Kevin Stark. 1997. “Overexpression of AgRP Leads to Obesity in Transgenic Mice.” *Nature Genetics* 15:57–61.

Gropp, Eva, Marya Shanabrough, Erzsebet Borok, Allison W. Xu, Ruth Janoschek, Thorsten Buch, Leona Plum, Nina Balthasar, Brigitte Hampel, Ari Waisman, Gregory S. Barsh, Tamas L. Horvath, and Jens C. Brüning. 2005. "Agouti-Related Peptide-Expressing Neurons Are Mandatory for Feeding." *Nature Neuroscience* 8:1289–91.

Gross, Barbara, Michal Pawlak, Philippe Lefebvre, and Bart Staels. 2017. "PPARs in Obesity-Induced T2DM, Dyslipidaemia and NAFLD." *Nature Reviews Endocrinology* 13:36–49.

Grundy, Scott M. 2004. "Obesity, Metabolic Syndrome, and Cardiovascular Disease." *Journal of Clinical Endocrinology and Metabolism* 89:2595–2600.

Grundy, Scott M. 2016. "Metabolic Syndrome Update." *Trends in Cardiovascular Medicine* 26:364–73.

Guan, Xiao Ming, Hong Yu, Myrna Trumbauer, Easter Frazier, Lex H. T. Van Der Ploeg, and Howard Chen. 1998. "Induction of Neuropeptide Y Expression in Dorsomedial Hypothalamus of Diet-Induced Obese Mice." *NeuroReport* 9:3415–19.

Guillemot-Legris, Owein, Valentin Mutemberezi, Patrice D. Cani, and Giulio G. Muccioli. 2016. "Obesity Is Associated with Changes in Oxysterol Metabolism and Levels in Mice Liver, Hypothalamus, Adipose Tissue and Plasma." *Nature Scientific Reports* 6:1–11.

Hanahan, Douglas and Robert A. Weinberg. 2011. "Hallmarks of Cancer: The next Generation." *Cell* 144:646–74.

He, Weimin, Yaacov Barak, Andrea Hevener, Peter Olson, Debbie Liao, Jamie Le, Michael Nelson, Estelita Ong, Jerrold M. Olefsky, and Ronald M. Evans. 2003. "Adipose-Specific Peroxisome Proliferator-Activated Receptor γ Knockout Causes Insulin Resistance in Fat and Liver but Not in Muscle." *Proceedings of the National Academy of Sciences of the United States of America* 100:15712–17.

Hill, Jennifer W., Carol F. Elias, Makoto Fukuda, Kevin W. Williams, Eric D. Berglund, William L. Holland, You Ree Cho, Jen Chieh Chuang, Yong Xu, Michelle Choi, Danielle Lauzon, Charlotte E. Lee, Roberto Coppari, James A. Richardson, Jeffrey M. Zigman, Streamson Chua, Philipp E. Scherer, Bradford B. Lowell, Jens C. Brüning, and Joel K. Elmquist. 2010. "Direct Insulin and Leptin Action on Pro-Opiomelanocortin Neurons Is Required for Normal Glucose Homeostasis and Fertility." *Cell Metabolism* 11:286–97.

Hundal, Ripudaman S., Martin Krssak, Sylvie Dufour, Didier Laurent, Vincent Lebon, Visvanathan Chandramouli, Silvio E. Inzucchi, William C. Schumann, Kitt F. Petersen, Bernard R. Landau, and Gerald I. Shulman. 2000. "Mechanism by Which Metformin Reduces Glucose Production in Type 2 Diabetes." *Diabetes* 49:2063–69.

Hunter, Steven J. and W. Timothy Garvey. 1998. "Insulin Action and Insulin Resistance: Diseases Involving Defects in Insulin Receptors, Signal Transduction, and the Glucose Transport Effector System." *American Journal of Medicine* 105:331–45.

Hwang, Ling Ling, Chien Hua Wang, Tzu Ling Li, Shih Dar Chang, Li Chun Lin, Ching Ping Chen, Chiung Tong Chen, Keng Chen Liang, Ing Kang Ho, Wei Shiung Yang, and Lih Chu Chiou. 2010. "Sex Differences in High-Fat Diet-Induced Obesity, Metabolic Alterations and Learning, and Synaptic Plasticity Deficits in Mice." *Obesity* 18:463–69.

Imai, Takeshi, Reiko Takakuwa, Sandra Marchand, Emilie Dentz, Jean Marc Bornert, Nadia

Messaddeq, Olivia Wendling, Manuel Mark, Béatrice Desvergne, Walter Wahli, Pierre Chambon, and Daniel Metzger. 2004. “Peroxisome Proliferator-Activated Receptor γ Is Required in Mature White and Brown Adipocytes for Their Survival in the Mouse.” *Proceedings of the National Academy of Sciences of the United States of America* 101:4543–47.

Ingvorsen, C., N. A. Karp, and C. J. Lelliott. 2017. “The Role of Sex and Body Weight on the Metabolic Effects of High-Fat Diet in C57BL/6N Mice.” *Nutrition and Diabetes* 7:261–67.

Janani, C. and Ranjitha Kumari. 2015. “PPAR Gamma Gene - A Review.” *Diabetes and Metabolic Syndrome: Clinical Research and Reviews* 9:46–50.

Jiang, Chengyu, Adrian T. Ting, and Brian Seed. 1998. “PPAR-γ Agonists Inhibit Production of Monocyte Inflammatory Cytokines.” *Nature* 391:82–86.

Kahn, Steven E., Rebecca L. Hull, and Kristina M. Utzschneider. 2006. “Mechanisms Linking Obesity to Insulin Resistance and Type 2 Diabetes.” *Nature* 444:840–46.

Kalueff, Allan V., Adam Michael Stewart, Cai Song, Kent C. Berridge, Ann M. Graybiel, and John C. Fentress. 2016. “Neurobiology of Rodent Self-Grooming and Its Value for Translational Neuroscience.” *Nature Reviews Neuroscience* 17:45–59.

Kaplan, Norman M. 1989. “The Deadly Quartet.” *Archives of Internal Medicine* 149:1514–20.

Kaur, Jaspinder. 2014. “A Comprehensive Review on Metabolic Syndrome.” *Cardiology Research and Practice* 2014:1–21.

Kelly, Linda J., Pasquale P. Vicario, G. Marie Thompson, Mari R. Candelore, Thomas W. Doebber, John Ventre, Margaret S. Wu, Roger Meurer, Michael J. Forrest, Michael W. Conner, Margaret A. Cascieri, and David E. Moller. 1998. “Peroxisome Proliferator-Activated Receptors γ and α Mediate in Vivo Regulation of Uncoupling Protein (UCP-1, UCP-2, UCP-3) Gene Expression.” *Endocrinology* 139:4920–27.

Knowler, William C., Elizabeth Barrett-Connor, Sarah E. Fowler, Richard F. Hamman, John M. Lachin, Elizabeth A. Walker, and David M. Nathan. 2002. “Reduction in the Incidence of Type 2 Diabetes with Lifestyle Intervention or Metformin.” *New England Journal of Medicine* 346:393–403.

Könner, A. Christine and Jens C. Brüning. 2012. “Selective Insulin and Leptin Resistance in Metabolic Disorders.” *Cell Metabolism* 16:144–52.

Kopelman, Peter G. 2000. “Obesity as a Medical Problem.” *Nature* 404:635–43.

Kotronen, Anna, Jukka Westerbacka, Robert Bergholm, Kirsi H. Pietiläinen, and Hannele Yki-Järvinen. 2007. “Liver Fat in the Metabolic Syndrome.” *Journal of Clinical Endocrinology and Metabolism* 92:3490–97.

Kozak, L. P. and R. Anunciado-Koza. 2008. “UCP1: Its Involvement and Utility in Obesity.” *International Journal of Obesity* 32:S32–38.

Kozak, LP. 2009. “UCP1: Its Involvement and Utility in Obesity.” *International Journal of Obesity* 32:32–38.

Krude, Heiko, Heike Biebermann, Werner Luck, Rüdiger Horn, Georg Brabant, and Annette Grüters. 1998. “Severe Early-Onset Obesity, Adrenal Insufficiency and Red Hair Pigmentation Caused by POMC Mutations in Humans.” *Nature Genetics* 19:155–57.

Lasar, David, Matthias Rosenwald, Elke Kiehlmann, Miroslav Balaz, Bettina Tall, Lennart Opitz, Martin E. Lidell, Nicola Zamboni, Petra Krznar, Wenfei Sun, Lukas Varga, Patrik Stefanicka, Jozef Ukropec, Pirjo Nuutila, Kirsi Virtanen, Ez Zoubir Amri, Sven Enerbäck, Walter Wahli, and Christian Wolfrum. 2018. "Peroxisome Proliferator Activated Receptor Gamma Controls Mature Brown Adipocyte Inducibility through Glycerol Kinase." *Cell Reports* 22:760–73.

Lau, Jackie and Herbert Herzog. 2014. "CART in the Regulation of Appetite and Energy Homeostasis." *Frontiers in Neuroscience* 8:1–25.

Lehrke, Michael and Mitchell A. Lazar. 2005. "The Many Faces of PPARγ." *Cell* 123:993–99.

Lin, Shu, Len H. Storlien, and Xu Feng Huang. 2000. "Leptin Receptor, NPY, POMC MRNA Expression in the Diet-Induced Obese Mouse Brain." *Brain Research* 875:89–95.

Lipatova, Olga, Matthew M. Campolattaro, Dawndra C. Dixon, and Ayse Durak. 2018. "Sex Differences and the Role of Acute Stress in the Open-Field Tower Maze." *Physiology and Behavior* 189:16–25.

Lund, Erik G., Joseph M. Guileyardo, and David W. Russell. 1999. "CDNA Cloning of Cholesterol 24-Hydroxylase, a Mediator of Cholesterol Homeostasis in the Brain." *Proceedings of the National Academy of Sciences of the United States of America* 96:7238–43.

Luo, Na, Genevieve Marcelin, Shun Mei Liu, Gary Schwartz, and Streamson Chua. 2011. "Neuropeptide Y and Agouti-Related Peptide Mediate Complementary Functions of Hyperphagia and Reduced Energy Expenditure in Leptin Receptor Deficiency." *Endocrinology* 152:883–89.

Machluf, Yossy, Amos Gutnick, and Gil Levkowitz. 2011. "Development of the Zebrafish Hypothalamus." *Annals of the New York Academy of Sciences* 1220:93–105.

Marchesini, Giulio, Rebecca Marzocchi, Federica Agostini, and Elisabetta Bugianesi. 2005. "Non-Alcoholic Fatty Liver Disease and the Metabolic Syndrome." *Nonalcoholic Fatty Liver Disease: New Insights* 16:421–27.

Martín, Mauricio G., Frank Pfrieger, and Carlos G. Dotti. 2014. "Cholesterol in Brain Disease: Sometimes Determinant and Frequently Implicated." *EMBO Reports* 15:1036–52.

Maruam, Ahmadian, Jae Myoung Suh, Nasun Hah, Christopher Liddle, Annete R. Atkins, Michael Downes, and Ronald M. Evans. 2013. "PPAR Gamma, the Good, the Bad & the Future." *Nature Medicine* 19:557–66.

Mauvais-Jarvis, Franck. 2015. "Sex Differences in Metabolic Homeostasis, Diabetes, and Obesity." *Biology of Sex Differences* 6:1–9.

Mayer, Christopher M., Laura J. Fick, Sarah Gingerich, and Denise D. Belsham. 2009. "Hypothalamic Cell Lines to Investigate Neuroendocrine Control Mechanisms." *Frontiers in Neuroendocrinology* 30:405–23.

McCracken, Emma, Monica Monaghan, and Shiva Sreenivasan. 2017. *Pathophysiology of the Metabolic Syndrome*.

Micucci, Carla, Debora Valli, Giulia Matacchione, and Alfonso Catalano. 2016. "Current Perspectives between Metabolic Syndrome and Cancer." *Oncotarget* 7:38959–72.

Miller, W. C., A. K. Lindeman, J. Wallace, and M. Niederpruem. 1990. "Diet Composition,

Energy Intake, and Exercise in Relation to Body Fat in Men and Women." *American Journal of Clinical Nutrition* 52:426–30.

Moutinho, Miguel, Maria João Nunes, and Elsa Rodrigues. 2016. "Cholesterol 24-Hydroxylase: Brain Cholesterol Metabolism and Beyond." *Biochimica et Biophysica Acta - Molecular and Cell Biology of Lipids* 1861:1911–20.

Murphy, Gregory J. and Julie C. Holder. 2000. "PPAR-γ Agonists: Therapeutic Role in Diabetes, Inflammation and Cancer." *Trends in Pharmacological Sciences* 21:469–74.

Najjar, Sonia. 2003. "Insulin Action: Molecular Basis of Diabetes." *Encyclopedia of Life Sciences* 1–10.

Nóbrega, Clévio and Luís Pereira Almeida. 2018. *Polyglutamine Disorders*.

Nóbrega, Clévio, Liliana Mendonça, Adriana Marcelo, Antonin Lamazière, Sandra Tomé, Gaetan Despres, Carlos A. Matos, Fatich Mechmet, Dominique Langui, Wilfred den Dunnen, Luis Pereira de Almeida, Nathalie Cartier, and Sandro Alves. 2019. "Restoring Brain Cholesterol Turnover Improves Autophagy and Has Therapeutic Potential in Mouse Models of Spinocerebellar Ataxia." *Acta Neuropathologica* 1–22.

Obici, Silvana, Zhaohui Feng, Jianzhen Tan, Li Sen Liu, George Karkanias, and Luciano Rossetti. 2001. "Central Melanocortin Receptors Regulate Insulin Action." *Journal of Clinical Investigation* 108:1079–85.

Olefsky, Jerrold M. and Christopher K. Glass. 2010. "Macrophages, Inflammation, and Insulin Resistance." *Annual Review of Physiology* 72:219–46.

Ouchi, Noriyuki, Jennifer L. Parker, Jesse J. Lugus, and Kenneth Walsh. 2011. "Adipokines in Inflammation and Metabolic Disease." *Nature Reviews Immunology* 11:85–97.

Pessin, Jeffrey E. and Alan R. Saltiel. 2000. "Signaling Pathways in Insulin Action: Molecular Targets of Insulin Resistance." *Journal of Clinical Investigation* 106:165–69.

Petersen, Max C. and Gerald I. Shulman. 2018. "Mechanisms of Insulin Action and Insulin Resistance." *Physiology Reviews* 98:2133–2223.

Petrov, A. M., M. R. Kasimov, and A. L. Zefirov. 2016. "Brain Cholesterol Metabolism and Its Defects: Linkage to Neurodegenerative Diseases and Synaptic Dysfunction." *Acta Naturae* 8:58–73.

Pfrieger, Frank W. and Nicole Ungerer. 2011. "Cholesterol Metabolism in Neurons and Astrocytes." *Progress in Lipid Research* 50:357–71.

Poher, Anne Laure, Christelle Veyrat-Durebex, Jordi Altirriba, Xavier Montet, Didier J. Colin, Aurélie Caillon, Jacqueline Lyautey, and Françoise Rohner-Jeanrenaud. 2015. "Ectopic UCP1 Overexpression in White Adipose Tissue Improves Insulin Sensitivity in Lou/C Rats, a Model of Obesity Resistance." *Diabetes* 64:3700–3712.

Porte, Daniel, Denis G. Baskin, and Michael W. Schwartz. 2005. "Insulin Signaling in the Central Nervous System." *Diabetes* 54:1264–76.

Prut, Laetitia and Catherine Belzung. 2003. "The Open Field as a Paradigm to Measure the Effects of Drugs on Anxiety-like Behaviors: A Review." *European Journal of Pharmacology* 463:3–33.

Qin, Cheng, Jiaheng Li, and Ke Tang. 2018. "The Paraventricular Nucleus of the Hypothalamus:

Development, Function, and Human Diseases." *Endocrinology* 159:3458–72.

Ramirez, Denise M. O., Stefan Andersson, and David W. Russell. 2008. "Neuronal Expression and Subcellular Localization of Cholesterol 24-Hydroxylase in the Mouse Brain." *The Journal of Comparative Neurology* 507:1676–93.

Raselli, Tina, Tom Hearn, Annika Wyss, Kirstin Atrott, Alain Peter, Isabelle Frey-Wagner, Marianne R. Spalinger, Ewerton M. Maggio, Andreas W. Sailer, Johannes Schmitt, Philipp Schreiner, Anja Moncsek, Joachim Mertens, Michael Scharl, William J. Griffiths, Marco Bueter, Andreas Geier, Gerhard Rogler, Yuqin Wang, and Benjamin Misselwitz. 2019. "Elevated Oxysterol Levels in Human and Mouse Livers Reflect Nonalcoholic Steatohepatitis." *Journal of Lipid Research* 60:1270–83.

Reaven, G. M. 1988. "Role of Insulin Resistance in Human Disease." *Diabetes* 37:1595–1607.

Richard, Denis and Frederic Picard. 2011. "Brown Far Biology and Thermogenesis." *Frontiers in Bioscience* 16:1233–60.

Roh, Eun and Min Seon Kim. 2016. "Brain Regulation of Energy Metabolism." *Endocrinology and Metabolism* 31:519–24.

Rosen, Evan D., Chung-hsin Hsu, Xinzhong Wang, Shuichi Sakai, Mason W. Freeman, Frank J. Gonzalez, and Bruce M. Spiegelman. 2002. "C/EBP Induces Adipogenesis through PPARγ: A Unified Pathway." *Genes and Development* 16:22–26.

Rosen, Evan D., Pasha Sarraf, Amy E. Troy, Gary Bradwin, Kathryn Moore, David S. Milstone, Bruce M. Spiegelman, and Richard M. Mortensen. 1999. "PPARγ Is Required for the Differentiation of Adipose Tissue in Vivo and in Vitro." *Molecular Cell* 4:611–17.

Russell, David W., Rebekkah W. Halford, Denise M. O. Ramirez, Rahul Shah, and Tiina Kotti. 2009. "Cholesterol 24-Hydroxylase: An Enzyme of Cholesterol Turnover in the Brain." *Annual Review of Biochemistry* 78:1017–40.

Saklayen, Mohammad G. 2018. "The Global Epidemic of the Metabolic Syndrome." *Current Hypertension Reports* 20:1–8.

Saper, Clifford B. and Bradford B. Lowell. 2014. "The Hypothalamus." *Current Biology* 24:1111–16.

Sarafidis, Panteleimon A. and Peter M. Nilsson. 2006. "The Metabolic Syndrome: A Glance at Its History." *Journal of Hypertension* 24:621–26.

Schmeltz, L. and B. Metzger. 2007. *Diabetes/Syndrome X*.

Schmitz, Gerd and Thomas Langmann. 2001. "Structure, Function and Regulation of the ABC1 Gene Product." *Current Opinion in Lipidology* 12:129–40.

Seibenhener, Michael L. and Michael C. Wooten. 2015. "Use of the Open Field Maze to Measure Locomotor and Anxiety-like Behavior in Mice." *Journal of Visualized Experiments* e52434:1–6.

Seoane-Collazo, Patricia, Johan Fernø, Francisco Gonzalez, Carlos Diéguez, Rosaura Leis, Rubén Nogueiras, and Miguel López. 2015. "Hypothalamic-Autonomic Control of Energy Homeostasis." *Endocrine* 50:276–91.

Sevin, Caroline, Abdellatif Benraiss, Debby Van Dam, Delphine Bonnin, Guy Nagels, Lucie Verot, Ingrid Laurendeau, Michel Vidaud, Volkmar Gieselmann, Marie Vanier, Peter Paul

De Deyn, Patrick Aubourg, and Nathalie Cartier. 2006. “Intracerebral Adeno-Associated Virus-Mediated Gene Transfer in Rapidly Progressive Forms of Metachromatic Leukodystrophy.” *Human Molecular Genetics* 15:53–64.

Shabalina, Irina G., Natasa Petrovic, Jasper M. A. DeJong, Anastasia V. Kalinovich, Barbara Cannon, and Jan Nedergaard. 2013. “UCP1 in Brite/Beige Adipose Tissue Mitochondria Is Functionally Thermogenic.” *Cell Reports* 5:1196–1203.

Sharma, S. and S. Fulton. 2013. “Diet-Induced Obesity Promotes Depressive-like Behaviour That Is Associated with Neural Adaptations in Brain Reward Circuitry.” *International Journal of Obesity* 37:382–89.

Shimizu, Ippei and Kenneth Walsh. 2015. “The Whitening of Brown Fat and Its Implications for Weight Management in Obesity.” *Current Obesity Reports* 4:224–29.

Small, C. J., Y. L. Liu, S. A. Stanley, I. P. Connoley, A. Kennedy, M. J. Stock, and S. R. Bloom. 2003. “Chronic CNS Administration of Agouti-Related Protein (Agrp) Reduces Energy Expenditure.” *International Journal of Obesity* 27:530–33.

Stienstra, Rinke, Caroline Duval, M. Michael, and Sander Kersten. 2007. “PPARs, Obesity, and Inflammation.” *PPAR Research* 2007:1–10.

Sun, Kai, Christine M. Kusminski, Philipp E. Scherer, Kai Sun, Christine M. Kusminski, and Philipp E. Scherer. 2011. “Adipose Tissue Remodeling and Obesity Find the Latest Version: Review Series Adipose Tissue Remodeling and Obesity.” *The Journal of Clinical Investigation* 121:2094–2101.

Sun, Kan, Jianmin Liu, and Guang Ning. 2012. “Active Smoking and Risk of Metabolic Syndrome: A Meta-Analysis of Prospective Studies.” *PLOS ONE* 7:1–9.

Surwit, R. S., C. M. Kuhn, C. Cochrane, J. A. McCubbin, and M. N. Feinglos. 1988. “Diet-Induced Type II Diabetes in C57BL/6J Mice.” *Diabetes* 37:1163–67.

Susan, Gale, Daniel Castracane, and Mantzoros Christos. 2004. “Energy Homeostasis, Obesity and Eating Disorders: Recent Advances in Endocrinology.” *Obesity and Metabolism* 1:39.

Suzuki, Ryo, Kevin Lee, Enxuan Jing, Sudha B. Biddinger, Jeffrey G. McDonald, Thomas J. Montine, Suzanne Craft, and C. Ronald Kahn. 2010. “Diabetes and Insulin in Regulation of Brain Cholesterol Metabolism.” *Cell Metabolism* 12:567–79.

Swanson, L. .. and P. E. Sawchenko. 1980. “Paraventricular Nucleus: A Site for the Integration of Neuroendocrine and Autonomic Mechanisms.” *Neuroendocrinology* 31:410–17.

Swinburn, B. A., I. Caterson, J. C. Seidell, and W. P. T. James. 2004. “Diet, Nutrition and the Prevention of Excess Weight Gain and Obesity.” *Public Health Nutrition* 7:123–46.

Tasali, Esra and Mary S. M. Ip. 2008. “Obstructive Sleep Apnea and Metabolic Syndrome: Alterations in Glucose Metabolism and Inflammation.” *Proceedings of the American Thoracic Society* 5:207–17.

Tatem, Kathleen S., James L. Quinn, Aditi Phadke, Qing Yu, Heather Gordish-Dressman, and Kanneboyina Nagaraju. 2014. “Behavioral and Locomotor Measurements Using an Open Field Activity Monitoring System for Skeletal Muscle Diseases.” *Journal of Visualized Experiments* e51785:1–7.

Timper, Katharina and Jens C. Brüning. 2017. “Hypothalamic Circuits Regulating Appetite and

Energy Homeostasis: Pathways to Obesity." *Disease Models and Mechanisms* 10:679–89.

Tokarz, Victoria L., Patrick E. MacDonald, and Amira Klip. 2018. "The Cell Biology of Systemic Insulin Function." *Journal of Cell Biology* 217:1–17.

Ulven, Stine Marie, Knut Tomas Dalen, Jan Åke Gustafsson, and Hilde Irene Nebb. 2005. "LXR Is Crucial in Lipid Metabolism." *Prostaglandins Leukotrienes and Essential Fatty Acids* 73:59–63.

Valdearcos, Martin, Allison W. Xu, and Suneil K. Koliwad. 2015. "Hypothalamic Inflammation in the Control of Metabolic Function." *Annual Review of Physiology* 77:131–60.

Vance, Jean E. 2012. "Dysregulation of Cholesterol Balance in the Brain: Contribution to Neurodegenerative Diseases." *Disease Models and Mechanisms* 5:746–55.

Vázquez-Vela, Maria Eugenia Frigolet, Nimbe Torres, and Armando R. Tovar. 2008. "White Adipose Tissue as Endocrine Organ and Its Role in Obesity." *Archives of Medical Research* 39:715–28.

Vidal-Puig, Antonio, Mercedes Jimenez-Liñan, Bradford B. Lowell, Andreas Hamann, Erding Hu, Bruce Spiegelman, Jeffrey S. Flier, and David E. Moller. 1996. "Regulation of PPAR γ Gene Expression by Nutrition and Obesity in Rodents." *Journal of Clinical Investigation* 97:2553–61.

Waterson, Michael J. and Tamas L. Horvath. 2015. "Neuronal Regulation of Energy Homeostasis: Beyond the Hypothalamus and Feeding." *Cell Metabolism* 22:962–70.

West, D. B., C. N. Boozer, D. L. Moody, and R. L. Atkinson. 1992. "Dietary Obesity in Nine Inbred Mouse Strains." *American Journal of Physiology - Regulatory Integrative and Comparative Physiology* 262:R1025–32.

Wilcox, Gisela. 2005. "Insulin and Insulin Resistance." *The Clinal Biochemist Reviews* 26:19–39.

Winzell, Maria Sörhede and Bo Ahren. 2004. "A Model for Studying Mechanisms and Treatment of Impaired Glucose Tolerance and Type 2 Diabetes." *Diabetes* 237:215–19.

Wisse, Brent E. 2004. "The Inflammatory Syndrome: The Role of Adipose Tissue Cytokines in Metabolic Disorders Linked to Obesity." *Journal of the American Society of Nephrology* 15:2792–2800.

Wood, W. Gibson, Friedhelm Schroeder, Nicolai A. Avdulov, Svetlana V. Chochina, and Urule Igbavboa. 1999. "Recent Advances in Brain Cholesterol Dynamics: Transport, Domains, and Alzheimer's Disease." *Lipids* 34:225–34.

Wooten, Joshua S., Huaizhu Wu, Joe Raya, Xiaoyuan Dai Perrard, John Gaubatz, and Ron C. Hoogeveen. 2014. "The Influence of an Obesogenic Diet on Oxysterol Metabolism in C57BL/6J Mice." *Cholesterol* 2014:1–11.

Wronska, A. and Z. Kmiec. 2012. "Structural and Biochemical Characteristics of Various White Adipose Tissue Depots." *Acta Physiologica* 205:194–208.

Wu, Ju, Paul Cohen, and Bruce M. Spiegelman. 2013. "Adaptive Thermogenesis in Adipocytes: Is Beige the New Brown?" *Genes and Development* 27:234–50.

Yang, Ling, Ping Li, Suneng Fu, Ediz S. Calay, and Gökhan S. Hotamisligil. 2010. "Defective Hepatic Autophagy in Obesity Promotes ER Stress and Causes Insulin Resistance." *Cell*

Metabolism 11:467–78.

Yaswen, Linda, Nicole Diehl, Miles B. Brennan, and Ute Hochgeschwender. 1999. “Obesity in the Mouse Model of Pro-Opiomelanocortin Deficiency Responds to Peripheral Melanocortin.” *Nature Medicine* 5:1066–70.

Yorimitsu, T. and D. J. Klionsky. 2005. “Autophagy: Molecular Machinery for Self-Eating.” *Cell Death and Differentiation* 12:1542–52.

Zagmutt, Sebastián, Paula Mera, M. Carmen Soler-Vázquez, Laura Herrero, and Dolors Serra. 2018. “Targeting AgRP Neurons to Maintain Energy Balance: Lessons from Animal Models.” *Biochemical Pharmacology* 155:224–32.

Zhang, Juan and Qiang Liu. 2015. “Cholesterol Metabolism and Homeostasis in the Brain.” *Protein and Cell* 6:254–64.

Zhang, Zhong Yin, Garron T. Dodd, and Tony Tiganis. 2015. “Protein Tyrosine Phosphatases in Hypothalamic Insulin and Leptin Signaling.” *Trends in Pharmacological Sciences* 36:661–74.

Annexes

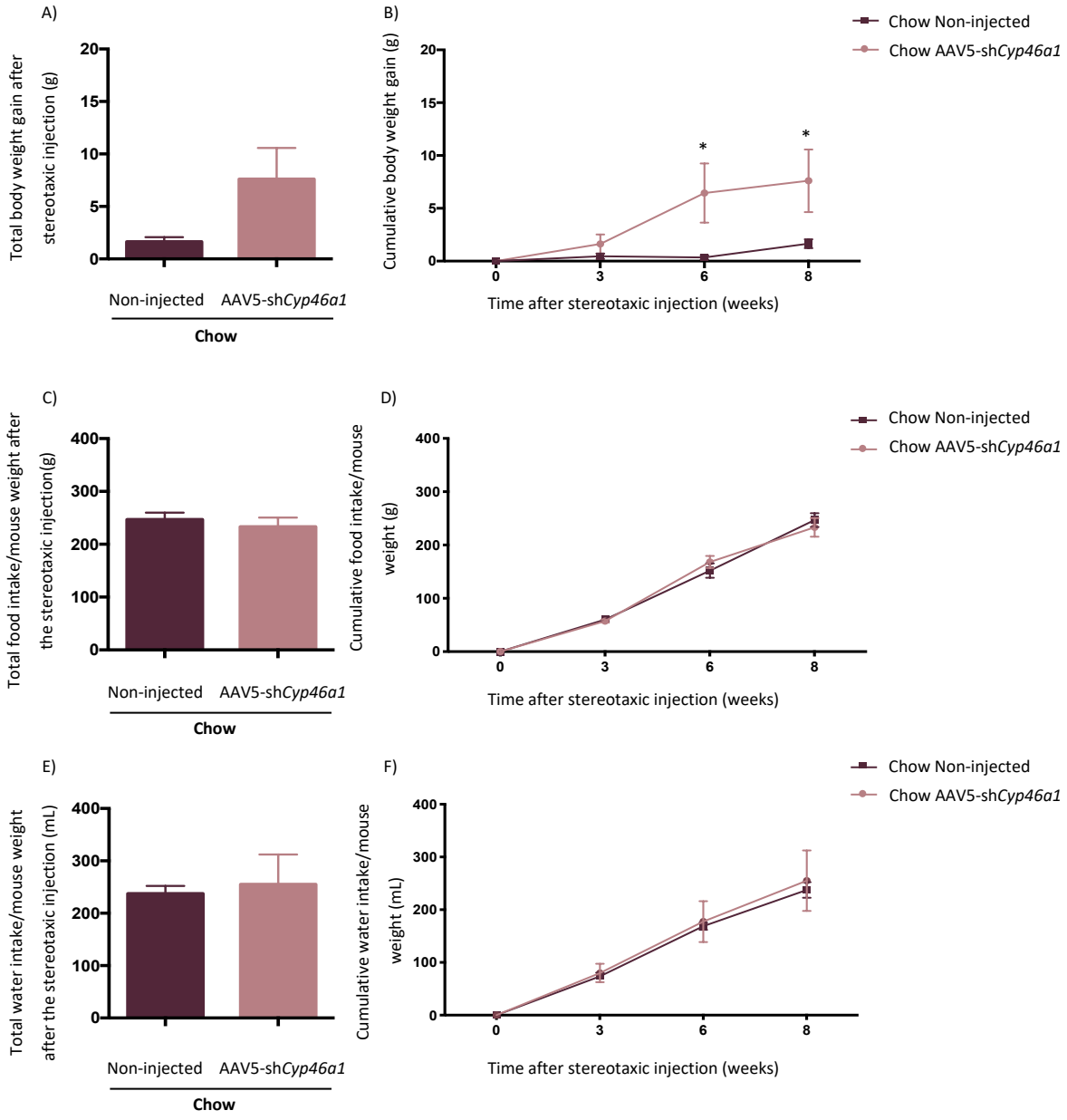

Annex 1| Silencing *Cyp46a1* gene in the hypothalamus induces an increase in body weight of C57BL/6J females mice fed with a Chow

In the 4th week of the study the stereotaxic injections were performed in C57BL/6J wild-type mice fed with Chow. The stereotaxic injection was performed in each side of the ARC to deliver the AAV5-sh*Cyp46a1*. An analysis of the total and cumulative BW gain, food and water intake from the 4th until the twelfth week of the study was performed between females [Females: Chow Non-injected – (*n*=4); Chow AAV5-sh*Cyp46a1* – (*n=4)*]. **A)** The Chow AAV5-sh*Cyp46a1* animals presented an increase in the total BW gain comparatively to Chow Non-injected animals [Chow Non-injected (1,650 ± 0,4245); *n=4* versus Chow AAV5-sh*Cyp46a1* (7,610 ± 2,965); *n=4* – *P*-value =0,0937]. **B)** The Chow AAV5-sh*Cyp46a1* animals exhibited a significant increase of body weight gain relatively to Chow Non-injected animals in the 6th and 8th week, after the stereotaxic injection [Chow Non-injected: *n=4* versus Chow AAV5-

sh*Cyp46a1*: *n=4* – 0: *P*-value > 0,9999; 3: *P*-value > 0,9999; 6: *P*-value =0,0315; 8: *P*-value =0,0368]. **C)** The Chow AAV5-sh*Cyp46a1* animals did not showed alterations in the total food intake comparatively to Chow Non-injected animals [Chow Non-injected (246,8 ± 12,96); *n=4* versus Chow AAV5-sh*Cyp46a1* (233,1 ± 17,37); *n=4* – *P*-value =0,5505]. **D)** The Chow AAV5-sh*Cyp46a1* animals did not presented alterations in cumulative food intake comparatively to the Chow Non-injected animals [Chow Non-injected: *n=4* versus Chow AAV5-sh*Cyp46a1*: *n=4* – 0: *P*-value >0,9999; 3: *P*-value >0,9999; 6: *P*-value >0,9999; 8: *P*-value >0,9999]. **E)** The Chow AAV5-sh*Cyp46a1* animals did not showed alterations in the total water intake comparatively to the Chow Non-injected animals [Chow Non-injected (237,5 ± 14,81); *n=4* versus Chow AAV5-sh*Cyp46a1* (255,0 ± 57,32); *n=4* – *P*-value =0,7775]. **F)** The Chow AAV5-sh*Cyp46a1* animals did not exhibited alterations in cumulative water intake comparatively to the Non-injected animals [Chow Non-injected: *n=4* versus Chow AAV5-sh*Cyp46a1*: *n=4* – 0: *P*-value >0,9999; 3: *P*-value >0,9999; 6: *P*-value >0,9999; 8: *P*-value >0,9999]. Data were represented as mean ± SEM. [*P*-value < 0,05 (*), *P*-value < 0,01 (**), *P*-value < 0,001 (***), *P*-value < 0,0001 (****)] - unpaired Student's t-test: A-E-G; Two-way ANOVA with Bonferroni's multiple comparisons test: B-F-H. **Abbreviations: AAV5:** adeno-associated vectors of the serotype 5; **BW:** body weight; **Chow:** low fat control diet; **sh:** short hairpin.

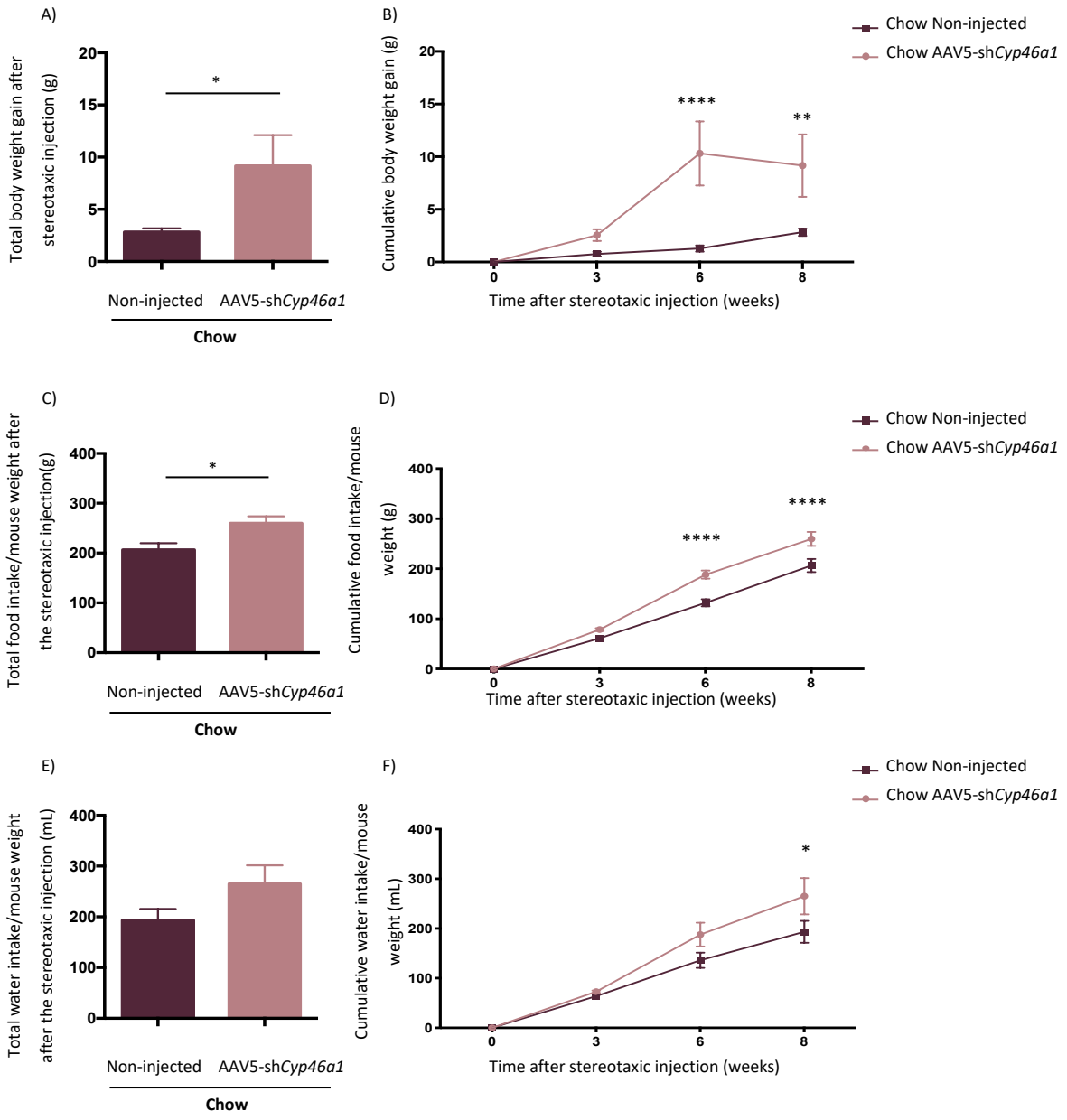

Annex 2| Silencing *Cyp46a1* gene in the hypothalamus induces an increase in body weight of C57BL/6J males mice fed with a Chow

An analysis of the total and cumulative BW gain, food and water intake from the 4th until the twelfth week of the study was performed between males [Males: Chow Non-injected – (*n*=9); Chow AAV5-sh*Cyp46a1* – (*n=7)*]. **A)** The Chow AAV5-sh*Cyp46a1* animals presented a significant increase in the total BW gain comparatively to Chow Non-injected animals [Chow Non-injected (2,829 ± 0,3534); *n=9* versus Chow AAV5-sh*Cyp46a1* (9,154 ± 2,614); *n=7* – *P*-value =0,0297]. **B)** The Chow AAV5-sh*Cyp46a1* animals exhibited a significant increase of body weight gain relatively to Chow Non-injected animals in the 6th and 8th week, after the stereotaxic injection [Chow Non-injected: *n=9* versus Chow AAV5-sh*Cyp46a1*: *n=7* – 0: *P*-value > 0,9999; 3: *P*-value =0,8459; 6: *P*-value <0,0001; 8: *P*-value =0,0064]. **C)** The Chow AAV5-sh*Cyp46a1* animals presented a significant increase in the total food intake comparatively to Chow Non-injected animals [Chow Non-injected (206,5 ± 13,16); *n=9* versus Chow AAV5-sh*Cyp46a1* (259,7 ± 13,94); *n=7* – *P*-value =0,0156]. **D)** The Chow AAV5-sh*Cyp46a1* animals showed a significant

increase of food intake, in the 6th and 8th week, comparatively to the Chow Non-injected animals [Chow Non-injected: *n=9* versus Chow AAV5-sh*Cyp46a1*: *n=7* – 0: *P*-value >0,9999; 3: *P*-value =0,5206; 6: *P*-value <0,0001; 8: *P*-value <0,0001]. **E)** The Chow AAV5-sh*Cyp46a1* animals showed an increase in total water intake, comparatively to the Chow Non-injected animals [Chow Non-injected (193,3 ± 22,03); *n=9* versus Chow AAV5-sh*Cyp46a1* (265,0 ± 36,43); *n=7* – *P*-value =0,0991]. **F)** The Chow AAV5-sh*Cyp46a1* animals showed a significant increase in water intake, in the 8th week, comparatively to the Chow Non-injected animals [Chow Non-injected: *n=9* versus Chow AAV5-sh*Cyp46a1*: *n=7* – 0: *P*-value >0,9999; 3: *P*-value >0,9999; 6: *P*-value =0,1617; 8: *P*-value =0,0209]. Data were represented as mean ± SEM. [*P*-value < 0,05 (*), *P*-value < 0,01 (**), *P*-value < 0,001 (***), *P*-value < 0,0001 (****)] - unpaired Student's t-test: A-E-G; Two-way ANOVA with Bonferroni's multiple comparisons test: B-F-H. **Abbreviations: AAV5:** adeno-associated vectors of the serotype 5; **BW:** body eight; **Chow:** low fat control diet; **sh:** short hairpin.

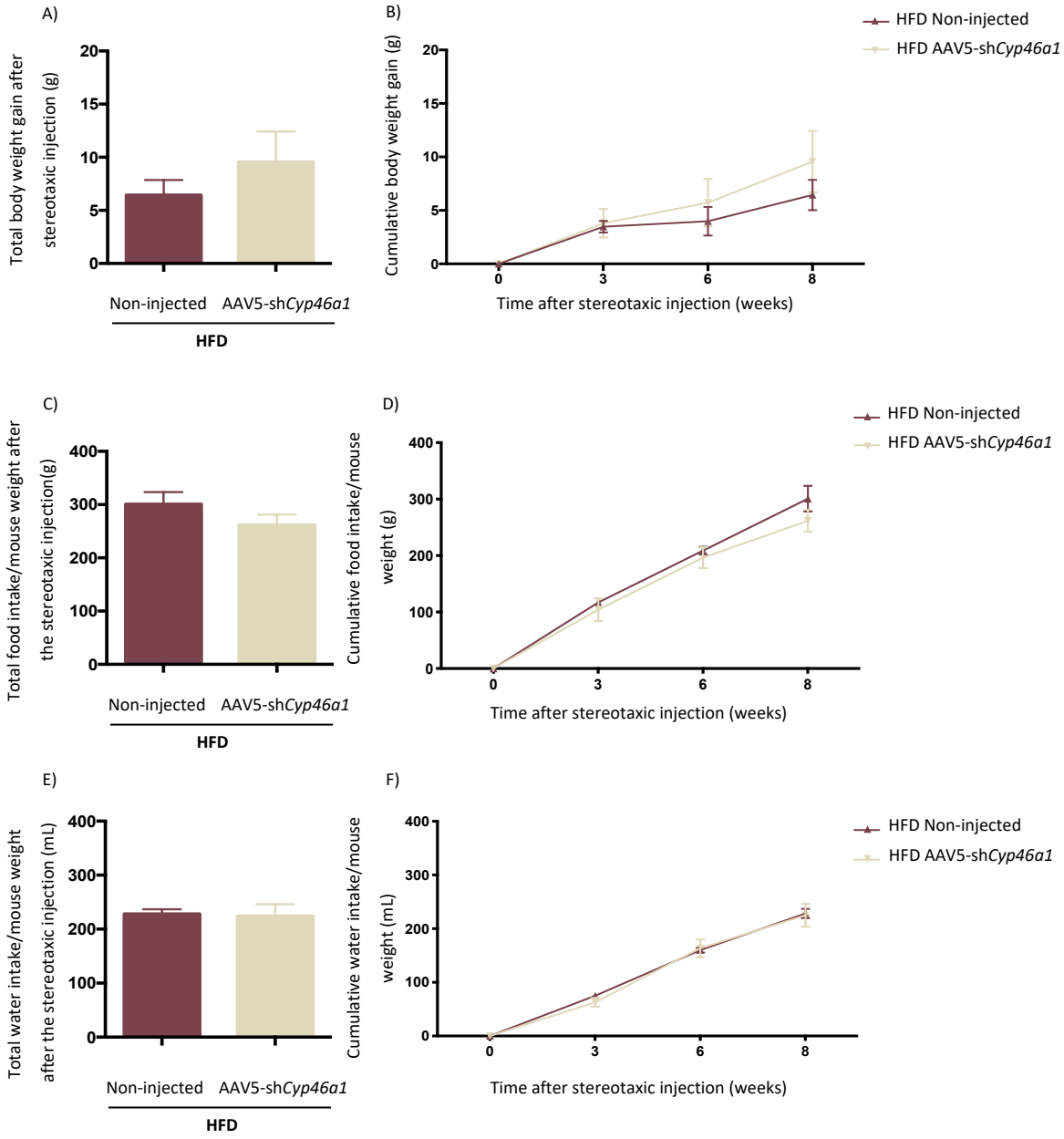

Annex 3| Silencing *Cyp46a1* gene in the hypothalamus induces an increase in body weight of C57BL/6J females mice fed with an HFD

An analysis of the total and cumulative BW gain, food and water intake from the 4th until the twelfth week of the study was performed between females [Females: HFD Non-injected – (*n*=6); HFD AAV5-sh*Cyp46a1* – (*n=7)*]. **A)** The HFD AAV5-sh*Cyp46a1* animals did not presented alterations in the total BW gain comparatively to HFD Non-injected animals [HFD Non-injected (6,440 ± 1,413); *n=6* versus HFD AAV5-sh*Cyp46a1* (9,561 ± 2,865); *n=7* – *P*-value =0,3748]. **B)** The HFD AAV5-sh*Cyp46a1* animals did not showed alterations in cumulative BW gain comparatively to the HFD Non-injected animals [HFD Non-injected: *n=6* versus HFD AAV5-sh*Cyp46a1*: *n=7* – 0: *P*-value > 0,9999; 3: *P*-value =0,9998; 6: *P*-value =0,9110; 8: *P*-value =0,5489]. **C)** The HFD AAV5-sh*Cyp46a1* animals did not presented alterations in the total food intake comparatively to HFD Non-injected animals [HFD Non-injected (300,9 ± 22,72); *n=6* versus HFD AAV5-sh*Cyp46a1* (261,7 ± 19,50); *n=6* – *P*-value =0,2198]. **D)** The HFD AAV5-sh*Cyp46a1* animals did not presented alterations in cumulative food intake comparatively to the HFD Non-injected animals [HFD Non-injected: *n=6* versus HFD AAV5-sh*Cyp46a1*: *n=7* – 0: *P*-value >0,9999; 3: *P*-value >0,9999; 6: *P*-value >0,9999; 8: *P*-value =0,2771]. **E)** The Chow AAV5-sh*Cyp46a1* did not showed alterations in the total water intake comparatively to the HFD Non-injected animals [HFD Non-injected (228,3 ± 8,653); *n=6* versus HFD AAV5-sh*Cyp46a1* (224,3 ± 21,84); *n=6* – *P*-value =0,8745]. **F)** The HFD AAV5-sh*Cyp46a1* animals did not exhibited alterations in cumulative water intake comparatively to the HFD Non-injected animals [HFD Non-injected: *n=6* versus HFD AAV5-sh*Cyp46a1*: *n=7* – 0: *P*-value >0,9999; 3: *P*-value >0,9999; 6: *P*-value >0,9999; 8: *P*-value >0,9999]. Data were represented as mean ± SEM. [*P*-value < 0,05 (*), *P*-value < 0,01 (**), *P*-value < 0,001 (***), *P*-value < 0,0001 (****)] - unpaired Student's t-test: A-E-G; Two-way ANOVA with Bonferroni's multiple comparisons test: B-F-H. **Abbreviations: AAV5:** adeno-associated vectors of the serotype 5; **BW:** body weight; **HFD:** high fat diet; **sh:** short hairpin.

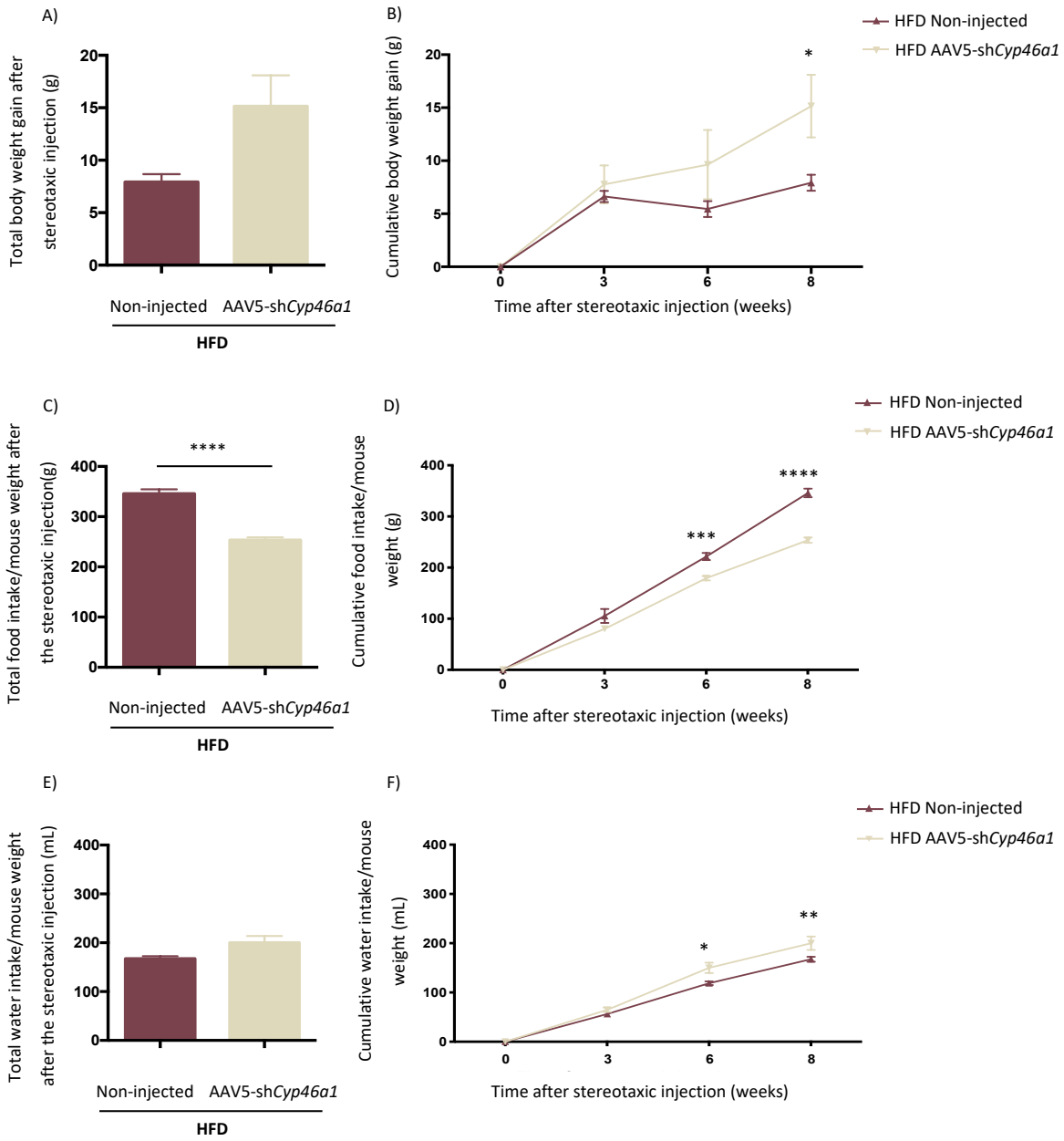

Annex 4| Silencing *Cyp46a1* gene in the hypothalamus induces an increase in body weight of C57BL/6J males mice fed with an HFD

An analysis of the total and cumulative BW gain, food and water intake from the 4th until the twelfth week of the study was performed between males [Males: HFD Non-injected – (*n*=4); HFD AAV5-sh*Cyp46a1* – (*n=4)*]. **A)** The HFD AAV5-sh*Cyp46a1* animals presented an increase in the total BW gain comparatively to HFD Non-injected animals [HFD Non-injected (7,925 ± 0,7522); *n=4* versus HFD AAV5-sh*Cyp46a1* (15,15 ± 2,950); *n=4* – *P*-value =0,0503]. **B)** The HFD AAV5-sh*Cyp46a1* animals presented a significant increase of BW gain comparatively to the HFD Non-injected animals in the 8th week after the stereotaxic injection [HFD Non-injected: *n=4* versus HFD AAV5-sh*Cyp46a1*: *n=4* – 0: *P*-value > 0,9999; 3: *P*-value >0,9999; 6: *P*-value =0,3988; 8: *P*-value =0,0276]. **C)** The HFD AAV5-sh*Cyp46a1* animals showed a statistically significant reduction in the total food intake comparatively to HFD Non-injected animals [HFD Non-injected (253,6 ± 5,169); *n=4* versus HFD AAV5-sh*Cyp46a1* (346,0 ± 8,349);

n=4 – *P*-value <0,0001. **D)** The HFD AAV5-sh*Cyp46a1* animals showed a significant reduction of food intake in the 6th and 8th week comparatively to the HFD Non-injected animals [HFD Non-injected: *n=4* versus HFD AAV5-sh*Cyp46a1*: *n=4* – 0: *P*-value > 0,9999; 3: *P*-value =0,0525; 6: *P*-value =0,0006; 8: *P*-value <0,0001]. **E)** The HFD AAV5-sh*Cyp46a1* animals did not showed significant changes in total water intake relatively to the HFD Non-injected animals [HFD Non-injected (167,5 ± 4,922); *n=4* versus HFD AAV5-sh*Cyp46a1* (200,0 ± 13,71); *n=4* – *P*-value =0,0671]. **F)** The HFD AAV5-sh*Cyp46a1* animals showed a significant increase in water intake, in the 6th and 8th week, comparatively to the HFD Non-injected animals [HFD Non-injected: *n=4* versus HFD AAV5-sh*Cyp46a1*: *n=4* – 0: *P*-value >0,9999; 3: *P*-value >0,9999; 6: *P*-value =0,0127; 8: *P*-value =0,0092]. Data were represented as mean ± SEM. [*P*-value < 0,05 (*), *P*-value < 0,01 (**), *P*-value < 0,001 (***), *P*-value < 0,0001 (****)] - unpaired Student's t-test: A-E-G; Two-way ANOVA with Bonferroni's multiple comparisons test: B-F-H. **Abbreviations: AAV5:** adeno-associated vectors of the serotype 5; **BW:** body weight; **HFD:** high fat diet; **sh:** short hairpin.

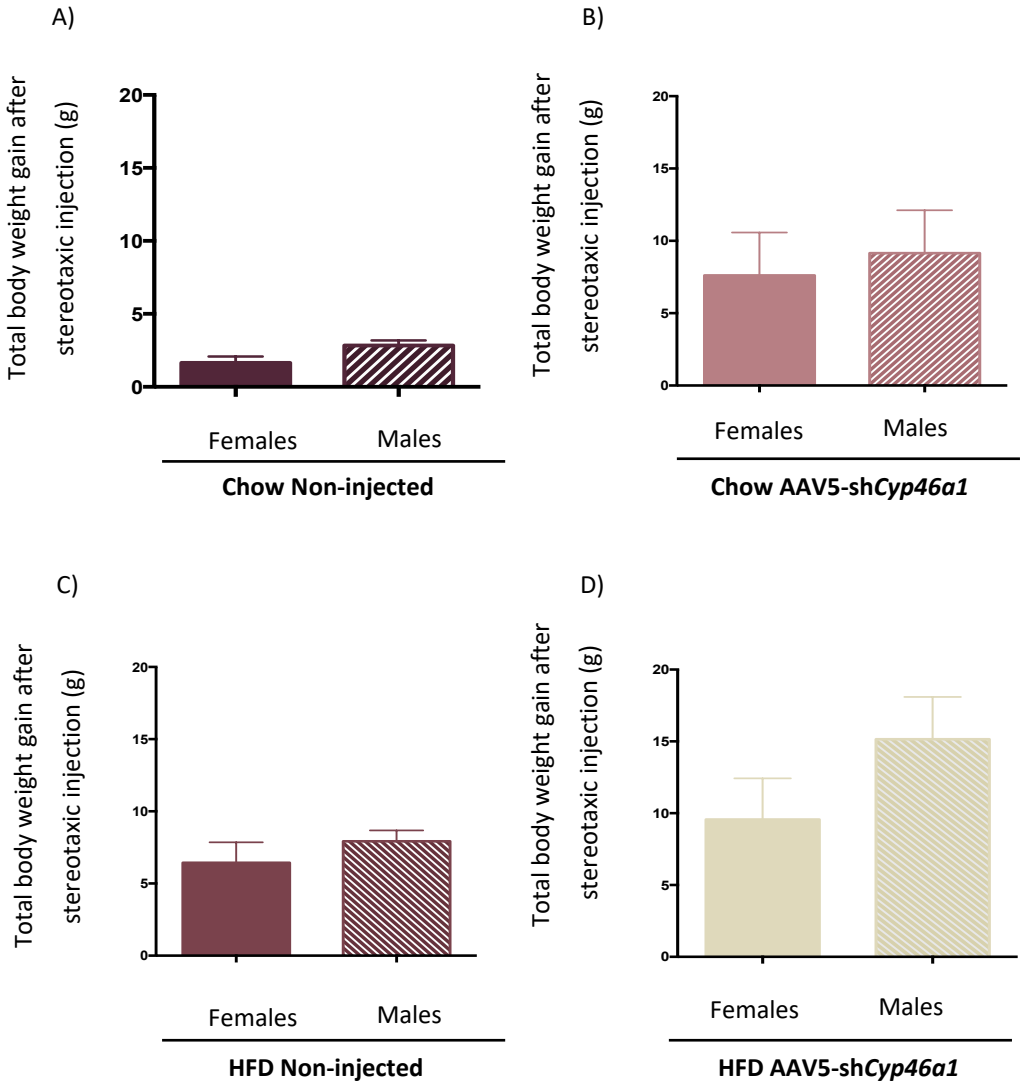

Annex 5| Body weight comparison between C57BL/6J wild-type females and males for each study group

The analysis of the total BW gain was also performed comparing females and males of the same study group. **A)** The Chow Non-injected males did not show significant modifications in the total BW gain

comparatively to the Chow Non-injected females [Females: Chow Non-injected (1,650 ± 0,4245); *n=4* versus Males: Chow Non-injected (2,829 ± 0,3534); *n=9* – *P*-value =0,0774]. **B)** The Chow AAV5-sh*Cyp46a1* males did not showed significant modifications in the total BW gain comparatively to the Chow AAV5-sh*Cyp46a1* females [Females: Chow AAV5-sh*Cyp46a1* (7,610 ± 2,965); *n=4* versus Males: Chow AAV5-sh*Cyp46a1* (9,154 ± 2,614); *n=7* – *P*-value =0,0297]. **C)** The HFD Non-injected males did not show significant modifications in the total BW gain comparatively to the HFD Non-injected females [Females: HFD Non-injected (6,440 ± 1,413); *n=6* versus Males: HFD Non-injected (7,925 ± 0,7522); *n=4* – *P*-value =0,0297]. **D)** The HFD AAV5-sh*Cyp46a1* males show an increase in the total BW gain comparatively to the HFD AAV5-sh*Cyp46a1* females [Females: HFD AAV5-sh*Cyp46a1* (9,561 ± 2,865); *n=7* versus Males: HFD AAV5-sh*Cyp46a1* (15,15 ± 2,950); *n=4* – *P*-value =0,2387]. Data were represented as mean ± SEM. [*P*-value < 0,05 (*), *P*-value < 0,01 (**), *P*-value < 0,001 (***), *P*-value < 0,0001 (****)] - unpaired Student's t-test: A-B-C-D; **Abbreviations: AAV5:** adeno-associated vectors of the serotype 5; **BW:** body weight; **Chow:** low fat control diet; **HFD:** high fat diet; **sh:** short hairpin.

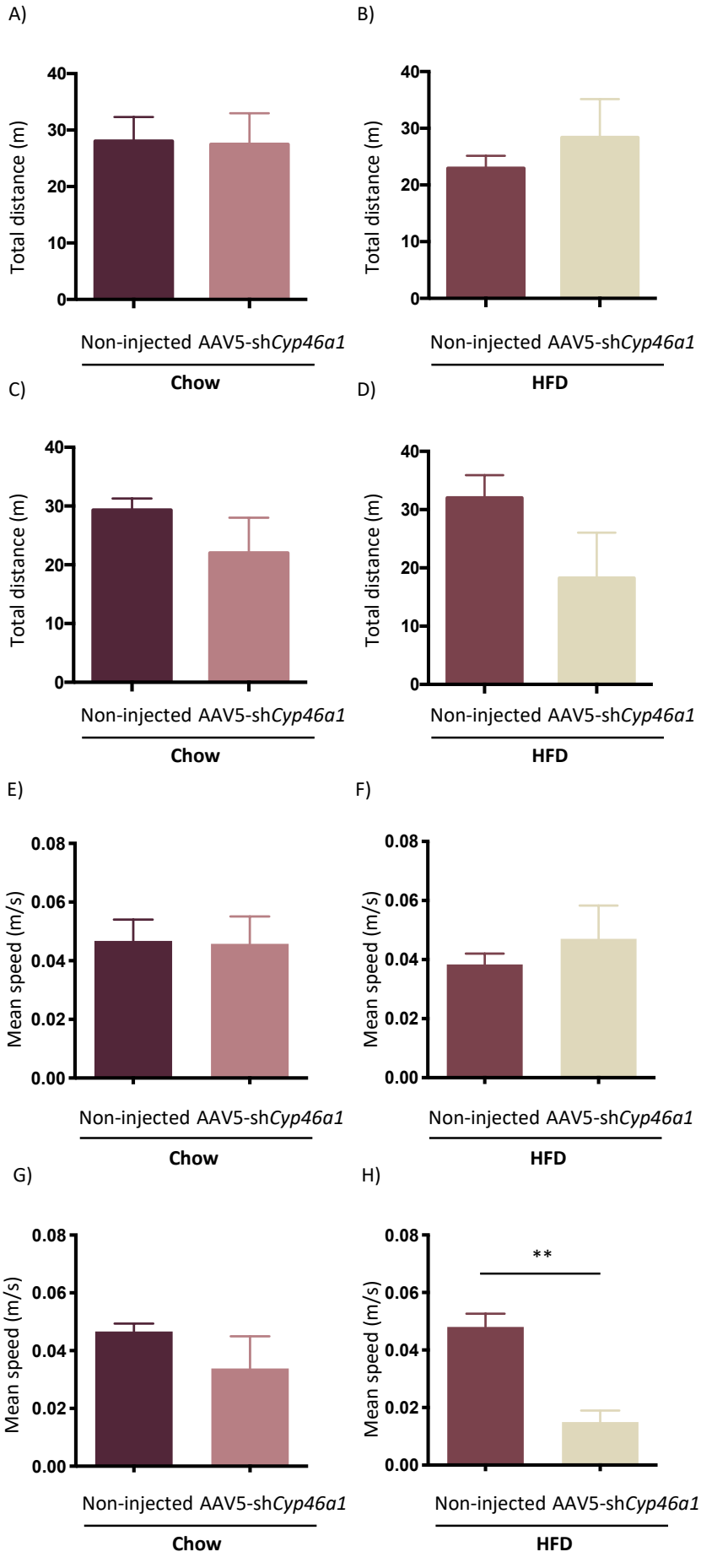
A)
B)
Total distance (m)
40
30
20
10
0
Non-injected
AAV5-shCyp46a1
Chow
HFD
C)
D)
E)
F)
Mean speed (m/s)
0.08
0.06
0.04
0.02
0.00
G)
H)
**

Annex 6| Silencing *Cyp46a1* gene in the hypothalamus, of C57BL/6J wild-type females and males fed with Chow and HFD, did not modified the total distance traveled, in the day-time period

The animals were subjected to an open field behavior test in the twelfth week which consisted in placing the mouse in a wall-closed box and the motor activity was recorded for 10 min in day-time period. **A)** Between females, the Chow AAV5-sh*Cyp46a1* animals did not showed significant alterations in the total distance traveled comparatively to the Chow Non-injected animals. **B)** Between females, the HFD AAV5-sh*Cyp46a1* did not showed significant modifications in the total distance traveled comparatively to the HFD Non-injected animals. **C)** Between males, the Chow AAV5-sh*Cyp46a1* did not showed significant alterations in the total distance traveled comparatively to the Chow Non-injected animals. **D)** Between males, the HFD AAV5-sh*Cyp46a1* animals presented a decrease in the total distance traveled comparatively to the HFD Non-injected animals. **E)** Between females, the Chow AAV5-sh*Cyp46a1* animals did not showed significant modifications in the mean speed episodes comparatively to the Chow Non-injected animals. **F)** Between females, the HFD AAV5-sh*Cyp46a1* animals did not presented significant modifications in the mean speed comparatively to the HFD Non-injected animals. **G)** Between males, the Chow AAV5-sh*Cyp46a1* animals did not presented significant alterations in the mean speed comparatively to the Chow Non-injected animals. **H)** Between males, the HFD AAV5-sh*Cyp46a1* animals show a significant decrease in the mean speed comparatively to the HFD Non-injected animals. Data were represented as mean ± SEM. [Chow Non-injected: *n=13*, female: *n=4* and male: *n=9*; Chow AAV5-sh*Cyp46a1: n=11*, female: *n=4* and male: *n=7*; HFD Non-injected: *n=10*, female: *n=6* and male: *n=4*; HFD AAV5-sh*Cyp46a1*: *n=11*, female: *n=7* and male: *n=4*]. [*P*-value < 0,05 (*), *P*-value < 0,01 (**), *P*-value < 0,001 (***), *P*-value < 0,0001 (****)] – unpaired Student's t-test: A-B-C-D-E-F-G-H; **Abbreviations: Chow:** low fat control diet; **HFD:** high fat diet; **AAV5:** adeno-associated vectors of the serotype 5; **sh:** short hairpin.

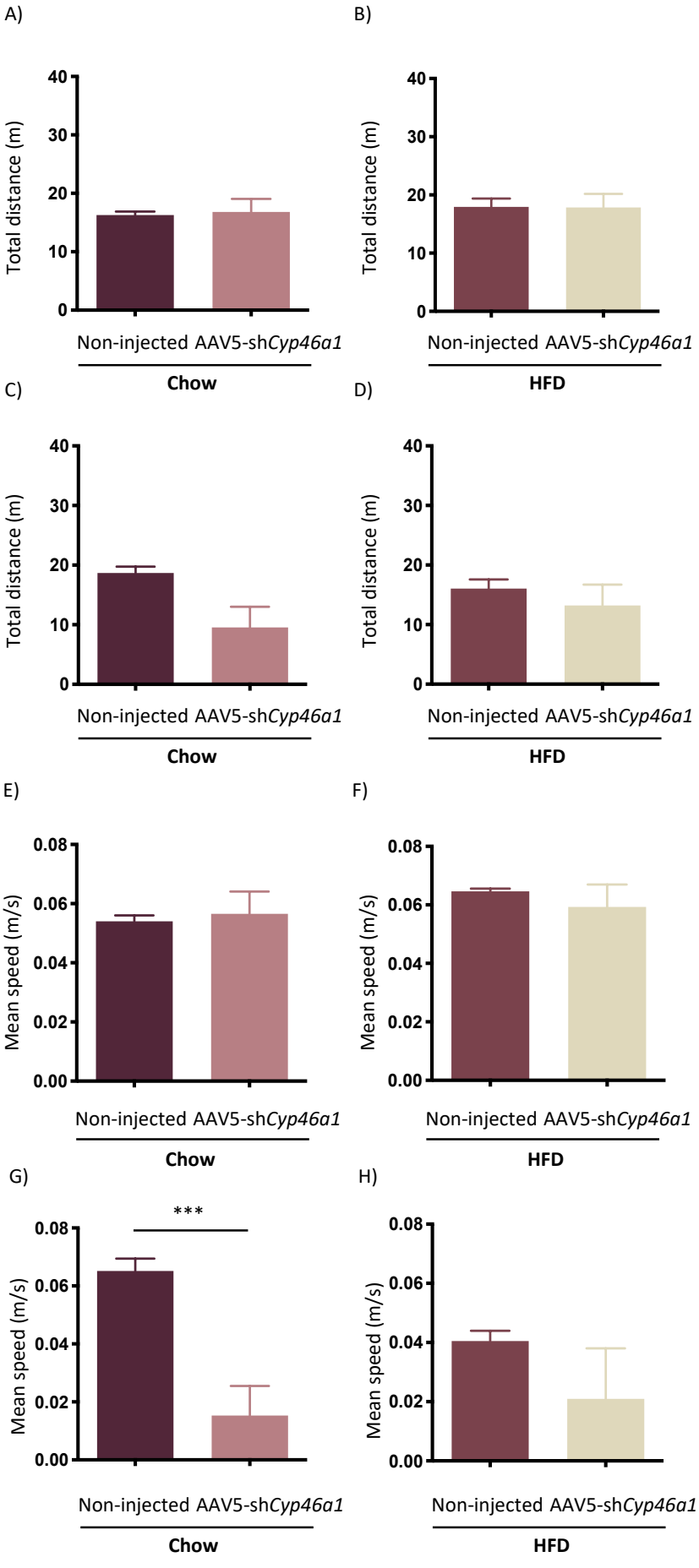
A)
B)
Total distance (m)
40
30
20
10
0
Non-injected
AAV5-sh*Cyp46a1*
Chow
HFD
C)
D)
E)
F)
Mean speed (m/s)
0.08
0.06
0.04
0.02
0.00
G)
H)
***

Annex 7| Silencing *Cyp46a1* gene in the hypothalamus, of C57BL/6J wild-type females and males fed with Chow and HFD, did not altered the total distance traveled, in the night-time period

The animals were subjected to an open field behavior test in the twelfth week which consisted in placing the mouse in a wall-closed box and the motor activity was recorded for 5 min in night-time period. **A)** Between females, the Chow AAV5-sh*Cyp46a1* animals did not exhibited significant modifications in the total distance traveled comparatively to the Chow Non-injected animals. **B)** Between females, the HFD AAV5-sh*Cyp46a1* did not showed significant changes in the total distance traveled comparatively to the HFD Non-injected animals. **C)** Between males, the Chow AAV5-sh*Cyp46a1* did not showed significant alterations in the total distance traveled comparatively to the Chow Non-injected animals. **D)** Between males, the HFD AAV5-sh*Cyp46a1* animals did not showed modifications in the total distance traveled comparatively to the HFD Non-injected animals. **E)** Between females, the Chow AAV5-sh*Cyp46a1* animals did not showed significant changes in the mean speed episodes comparatively to the Chow Non-injected animals. **F)** Between females, the HFD AAV5-sh*Cyp46a1* animals did not showed significant modifications in the mean speed comparatively to the HFD Non-injected animals. **G)** Between males, the Chow AAV5-sh*Cyp46a1* animals presented a significant decrease in the mean speed comparatively to the Chow Non-injected animals. **H)** Between males, the HFD AAV5-sh*Cyp46a1* animals did not presented changes in the mean speed comparatively to the HFD Non-injected animals. Data were represented as mean ± SEM. [Chow Non-injected: *n=8*, female: *n=2* and male: *n=6*; Chow AAV5-sh*Cyp46a1: n=5*, female: *n=2* and male: *n=3*; HFD Non-injected: *n=6*, female: *n=4* and male: *n=2*; HFD AAV5-sh*Cyp46a1*: *n=5*, female: *n=3* and male: *n=2*]. [*P*-value < 0,05 (*), *P*-value < 0,01 (**), *P*-value < 0,001 (***), *P*-value < 0,0001 (****)] – unpaired Student's t-test: A-B-C-D-E-F-G-H; **Abbreviations: Chow:** low fat control diet; **HFD:** high fat diet; **AAV5:** adeno-associated vectors of the serotype 5; **sh:** short hairpin.

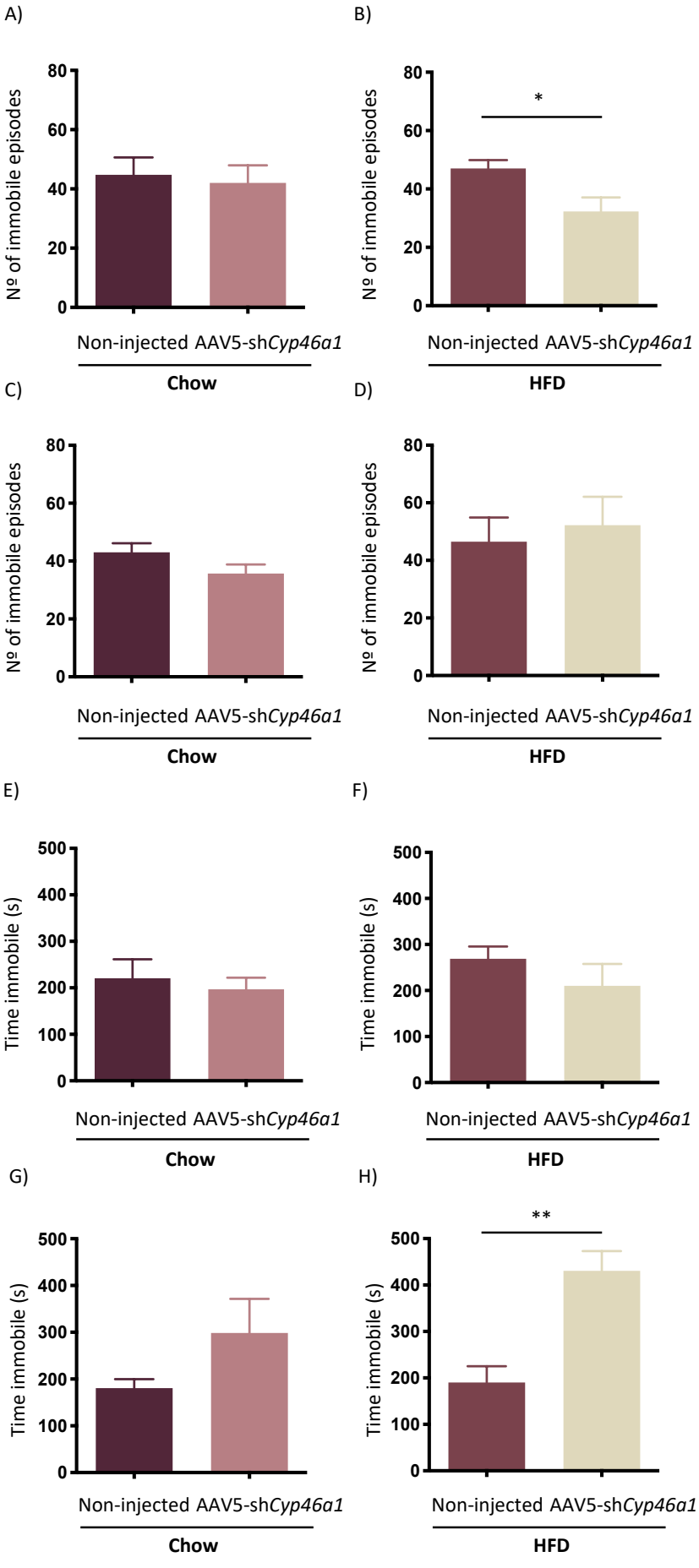
A)
B)
Nº of immobile episodes
80
60
40
20
0
*
Non-injected
AAV5-shCyp46a1
Chow
HFD
C)
D)
E)
F)
Time immobile (s)
500
400
300
200
100
G)
H)
**

Annex 8| Silencing *Cyp46a1* gene in the hypothalamus of C57BL/6J wild-type males fed with HFD modify the number of immobile episodes and the time spend immobile, in the day-time period

A) Between females, the Chow AAV5-sh*Cyp46a1* animals did not showed significant alterations in the number of immobile episodes comparatively to the Chow Non-injected animals. **B)** Between females, the HFD AAV5-sh*Cyp46a1* showed a significant decrease in the number of immobile episodes comparatively to the HFD Non-injected animals. **C)** Between males, the Chow AAV5-sh*Cyp46a1* showed a decrease in the number of immobile episodes comparatively to the Chow Non-injected animals. **D)** Between males, the HFD AAV5-sh*Cyp46a1* animals did not presented modifications in the number of immobile episodes comparatively to the HFD Non-injected animals. **E)** Between females, the Chow AAV5-sh*Cyp46a1* animals did not showed significant modifications in the time spend immobile comparatively to the Chow Non-injected animals. **F)** Between females, the HFD AAV5-sh*Cyp46a1* animals did not presented significant changes in the time spend immobile comparatively to the HFD Non-injected animals. **G)** Between males, the Chow AAV5-sh*Cyp46a1* animals presented an increase in the time spend immobile comparatively to the Chow Non-injected animals. **H)** Between males, the HFD AAV5-sh*Cyp46a1* animals show a significant increase in the time spend immobile comparatively to the HFD Non-injected animals. Data were represented as mean ± SEM [Chow Non-injected: *n=13*, female: *n=4* and male: *n=9*; Chow AAV5-sh*Cyp46a1: n=11*, female: *n=4* and male: *n=7*; HFD Non-injected: *n=10*, female: *n=6* and male: *n=4*; HFD AAV5-sh*Cyp46a1*: *n=11*, female: *n=7* and male: *n=4*]. [*P*-value < 0,05 (*), *P*-value < 0,01 (**), *P*-value < 0,001 (***), *P*-value < 0,0001 (****)] – unpaired Student's t-test: A-B-C-D-E-F-G-H; **Abbreviations: Chow:** low fat control diet; **HFD:** high fat diet; **AAV5:** adeno-associated vectors of the serotype 5; **sh:** short hairpin.

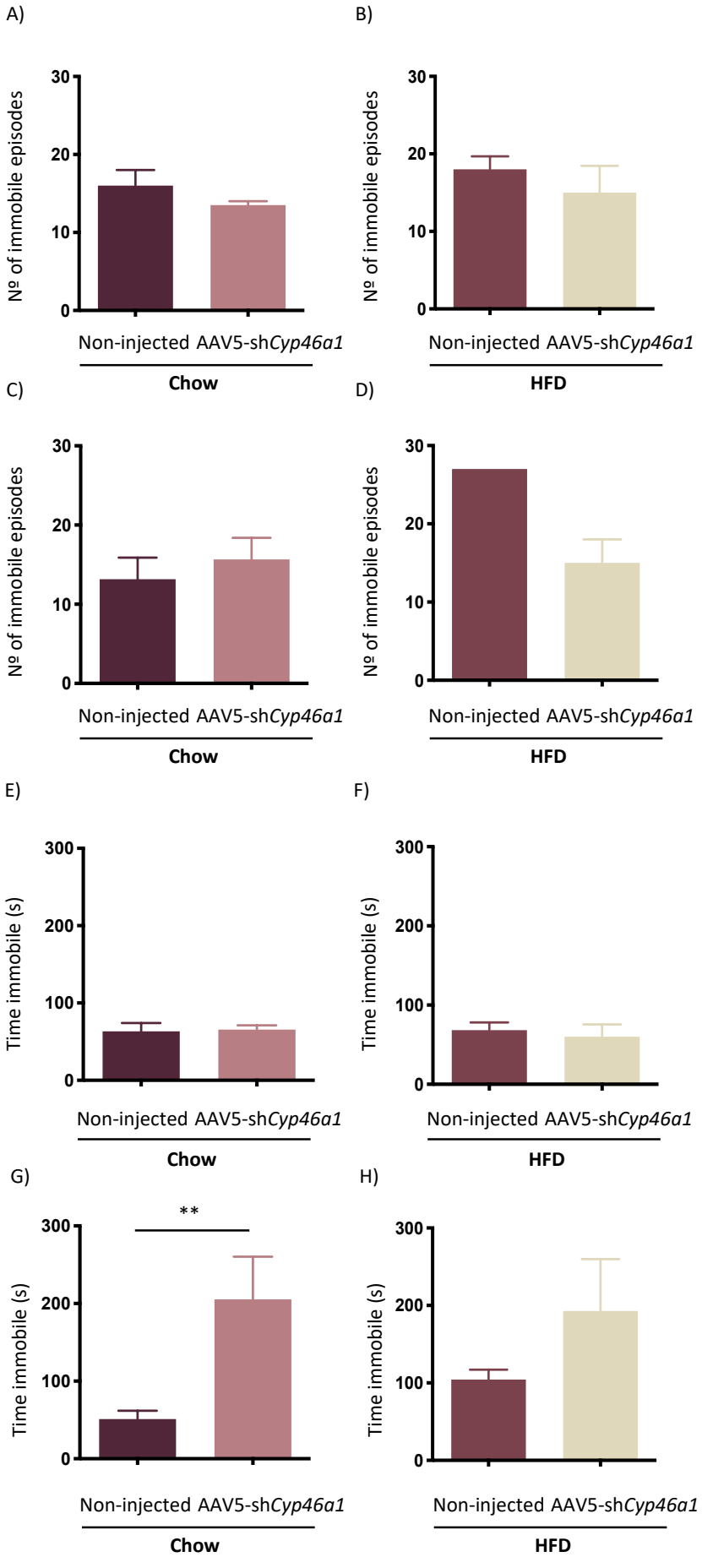
A)
B)
Nº of immobile episodes
30
20
10
0
Non-injected
AAV5-shCyp46a1
Chow
HFD
C)
D)
E)
F)
Time immobile (s)
300
200
100
0
G)
H)
**

Annex 9| Silencing *Cyp46a1* gene in the hypothalamus, of C57BL/6J wild-type males fed with Chow, decreases the time spend immobile in the night-time period

A) Between females, the Chow AAV5-sh*Cyp46a1* animals did not showed significant alterations in the number of immobile episodes comparatively to the Chow Non-injected animals. **B)** Between females, the HFD AAV5-sh*Cyp46a1* did not showed significant changes in the number of immobile episodes comparatively to the HFD Non-injected animals. **C)** Between males, the Chow AAV5-sh*Cyp46a1* did not presented alterations in the number of immobile episodes comparatively to the Chow Non-injected animals. **D)** Between males, the HFD AAV5-sh*Cyp46a1* animals presented a decrease in the number of immobile episodes comparatively to the HFD Non-injected animals. **E)** Between females, the Chow AAV5-sh*Cyp46a1* animals did not showed significant modifications in the time spend immobile comparatively to the Chow Non-injected animals. **F)** Between females, the HFD AAV5-sh*Cyp46a1* animals did not presented significant changes in the time spend immobile comparatively to the HFD Non-injected animals. **G)** Between males, the Chow AAV5-sh*Cyp46a1* animals presented a significant increase in the time spend immobile comparatively to the Chow Non-injected animals. **H)** Between males, the HFD AAV5-sh*Cyp46a1* animals did not showed modifications in the time spend immobile comparatively to the HFD Non-injected animals. Data were represented as mean ± SEM. [Chow Non-injected: *n=8*, female: *n=2* and male: *n=6*; Chow AAV5-sh*Cyp46a1: n=5*, female: *n=2* and male: *n=3*; HFD Non-injected: *n=6*, female: *n=4* and male: *n=2*; HFD AAV5-sh*Cyp46a1*: *n=5*, female: *n=3* and male: *n=2*]. [*P*-value < 0,05 (*), *P*-value < 0,01 (**), *P*-value < 0,001 (***), *P*-value < 0,0001 (****)] – unpaired Student's t-test: A-B-C-D-E-F-G-H; **Abbreviations: Chow:** low fat control diet; **HFD:** high fat diet; **AAV5:** adeno-associated vectors of the serotype 5; **sh:** short hairpin.

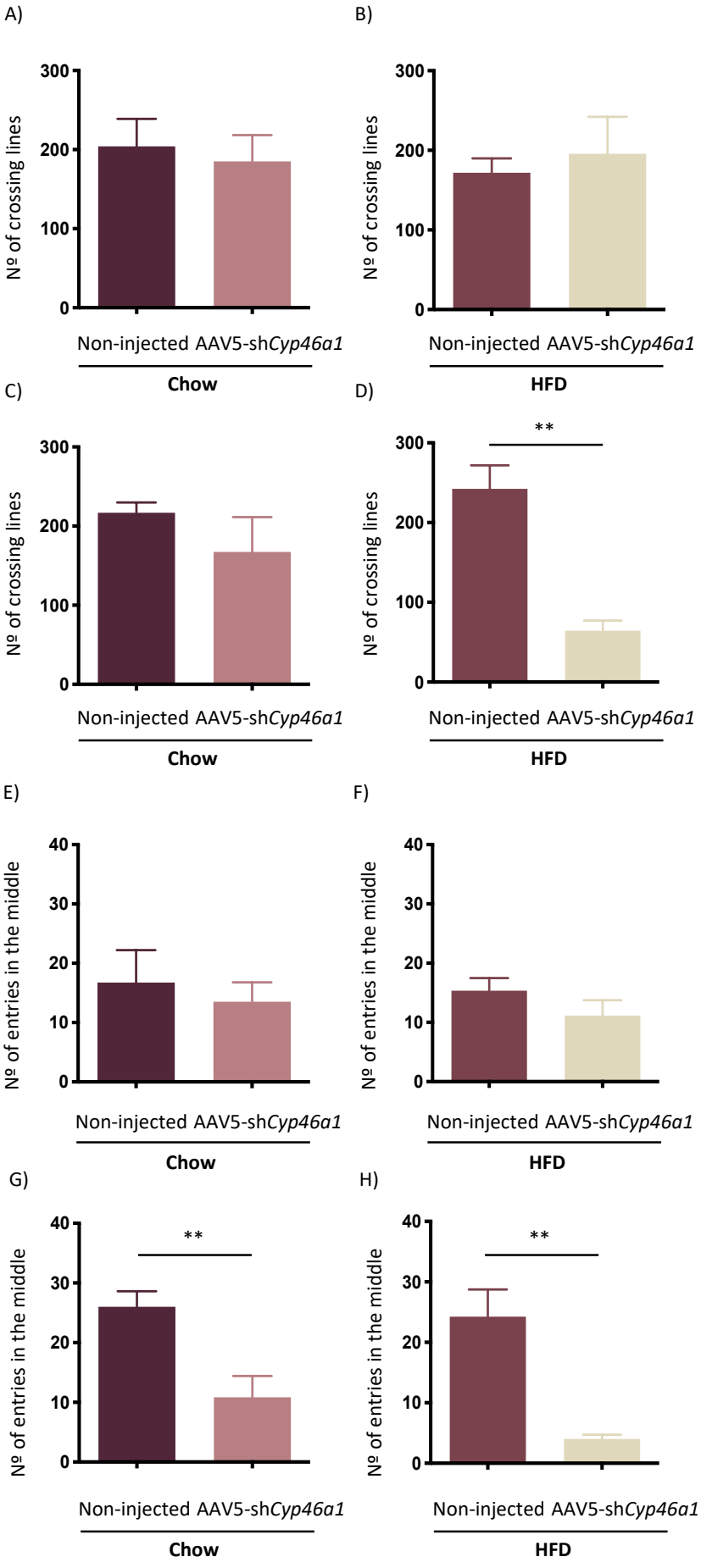
A)
B)
300
200
100
0
Nº of crossing lines
Non-injected
AAV5-sh*Cyp46a1*
Chow
HFD
C)
D)
**
E)
F)
40
30
20
10
Nº of entries in the middle
G)
H)

Annex 10| Silencing *Cyp46a1* gene in the hypothalamus, of C57BL/6J wild-type females and males fed with Chow and HFD, modify the number of crossing lines and the number of entries in the middle, in the day-time period

A) Between females, the Chow AAV5-sh*Cyp46a1* animals did not showed significant alterations in the number of crossing lines comparatively to the Chow Non-injected animals. **B)** Between females, the HFD AAV5-sh*Cyp46a1* did not showed significant modifications in the number of crossing lines comparatively to the HFD Non-injected animals. **C)** Between males, the Chow AAV5-sh*Cyp46a1* did not showed alterations in the number of crossing lines comparatively to the Chow Non-injected animals. **D)** Between males, the HFD AAV5-sh*Cyp46a1* animals presented a significant decrease in the number of crossing lines comparatively to the HFD Non-injected animals. **E)** Between females, the Chow AAV5-sh*Cyp46a1* animals did not showed significant modifications in the number of entries in the middle comparatively to the Chow Non-injected animals. **F)** Between females, the HFD AAV5-sh*Cyp46a1* animals did not presented changes in the number of entries in the middle comparatively to the HFD Non-injected animals. **G)** Between males, the Chow AAV5-sh*Cyp46a1* animals presented a significant decrease in the number of entries in the middle comparatively to the Chow Non-injected animals. **H)** Between males, the HFD AAV5-sh*Cyp46a1* animals show a significant decrease in the number of entries in the middle comparatively to the HFD Non-injected animals. Data were represented as mean ± SEM [Chow Non-injected: *n=13*, female: *n=4* and male: *n=9*; Chow AAV5-sh*Cyp46a1: n=11*, female: *n=4* and male: *n=7*; HFD Non-injected: *n=10*, female: *n=6* and male: *n=4*; HFD AAV5-sh*Cyp46a1*: *n=11*, female: *n=7* and male: *n=4*]. [*P*-value < 0,05 (*), *P*-value < 0,01 (**), *P*-value < 0,001 (***), *P*-value < 0,0001 (****)] – unpaired Student's t-test: A-B-C-D-E-F-G-H; **Abbreviations: Chow:** low fat control diet; **HFD:** high fat diet; **AAV5:** adeno-associated vectors of the serotype 5; **sh:** short hairpin.

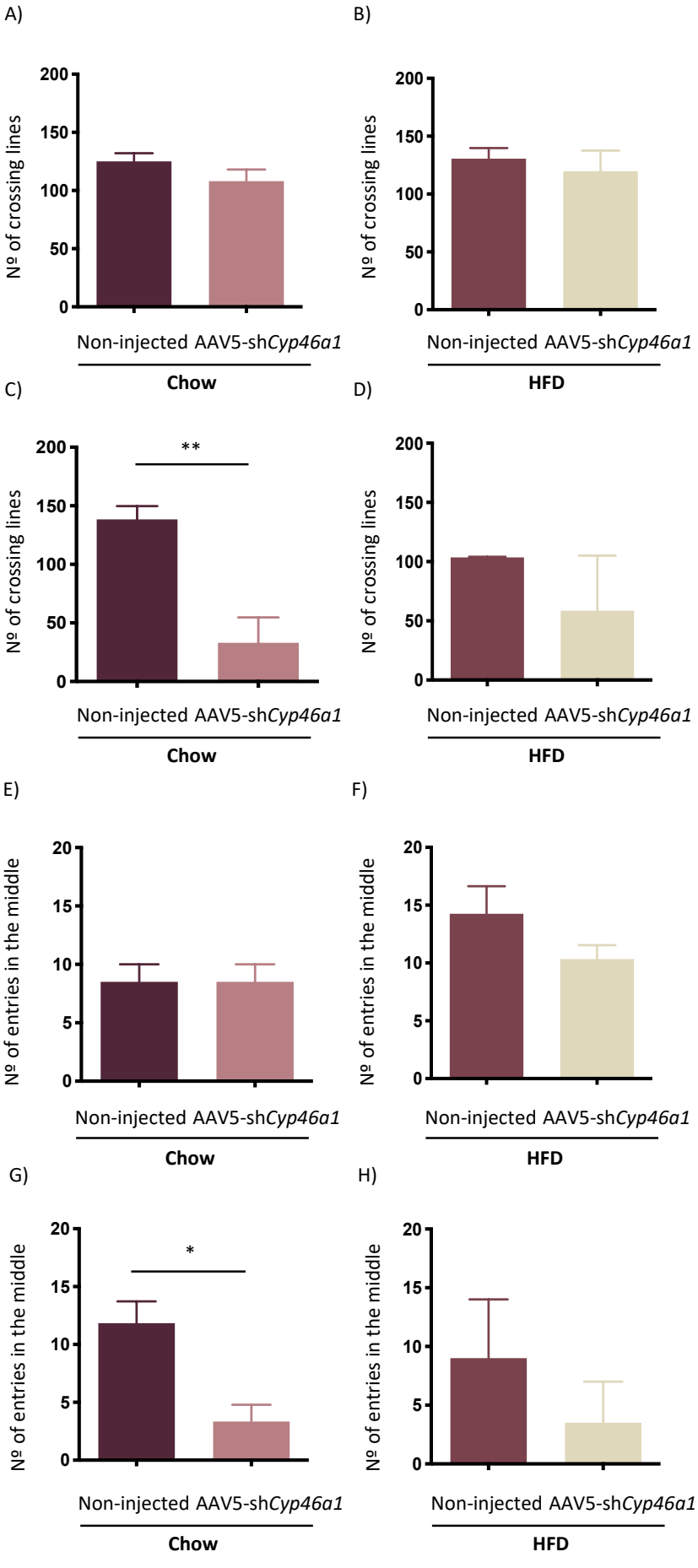
A)
B)
Nº of crossing lines
200
150
100
50
0
Non-injected
AAV5-shCyp46a1
Chow
HFD
C)
D)
**
E)
F)
Nº of entries in the middle
20
15
10
5
G)
H)
*

Annex 11| Silencing *Cyp46a1* gene in the hypothalamus, of C57BL/6J wild-type males fed with Chow, modify the number of crossing lines and the number of entries in the middle, in the night-time period

A) Between females, the Chow AAV5-sh*Cyp46a1* animals did not showed significant alterations in the number of crossing lines comparatively to the Chow Non-injected animals. **B)** Between females, the HFD AAV5-sh*Cyp46a1* did not showed significant modifications in the number of crossing lines comparatively to the HFD Non-injected animals. **C)** Between males, the Chow AAV5-sh*Cyp46a1* showed a significant decrease in the number of crossing lines comparatively to the Chow Non-injected animals. **D)** Between males, the HFD AAV5-sh*Cyp46a1* animals did not showed alterations in the number of crossing lines comparatively to the HFD Non-injected animals. **E)** Between females, the Chow AAV5-sh*Cyp46a1* animals did not showed significant modifications in the number of entries in the middle comparatively to the Chow Non-injected animals. **F)** Between females, the HFD AAV5-sh*Cyp46a1* animals did not presented alterations in the number of entries in the middle comparatively to the HFD Non-injected animals. **G)** Between males, the Chow AAV5-sh*Cyp46a1* animals presented a significant decrease in the number of entries in the middle comparatively to the Chow Non-injected animals. **H)** Between males, the HFD AAV5-sh*Cyp46a1* animals did not show modifications in the number of entries in the middle comparatively to the HFD Non-injected animals. Data were represented as mean ± SEM. [Chow Non-injected: *n=8*, female: *n=2* and male: *n=6*; Chow AAV5-sh*Cyp46a1: n=5*, female: *n=2* and male: *n=3*; HFD Non-injected: *n=6*, female: *n=4* and male: *n=2*; HFD AAV5-sh*Cyp46a1*: *n=5*, female: *n=3* and male: *n=2*]. *P*-value < 0,05 (*), *P*-value < 0,01 (**), *P*-value < 0,001 (***), *P*-value < 0,0001 (****)] – unpaired Student's t-test: A-B-C-D-E-F-G-H; **Abbreviations: Chow:** low fat control diet; **HFD:** high fat diet; **AAV5:** adeno-associated vectors of the serotype 5; **sh:** short hairpin.

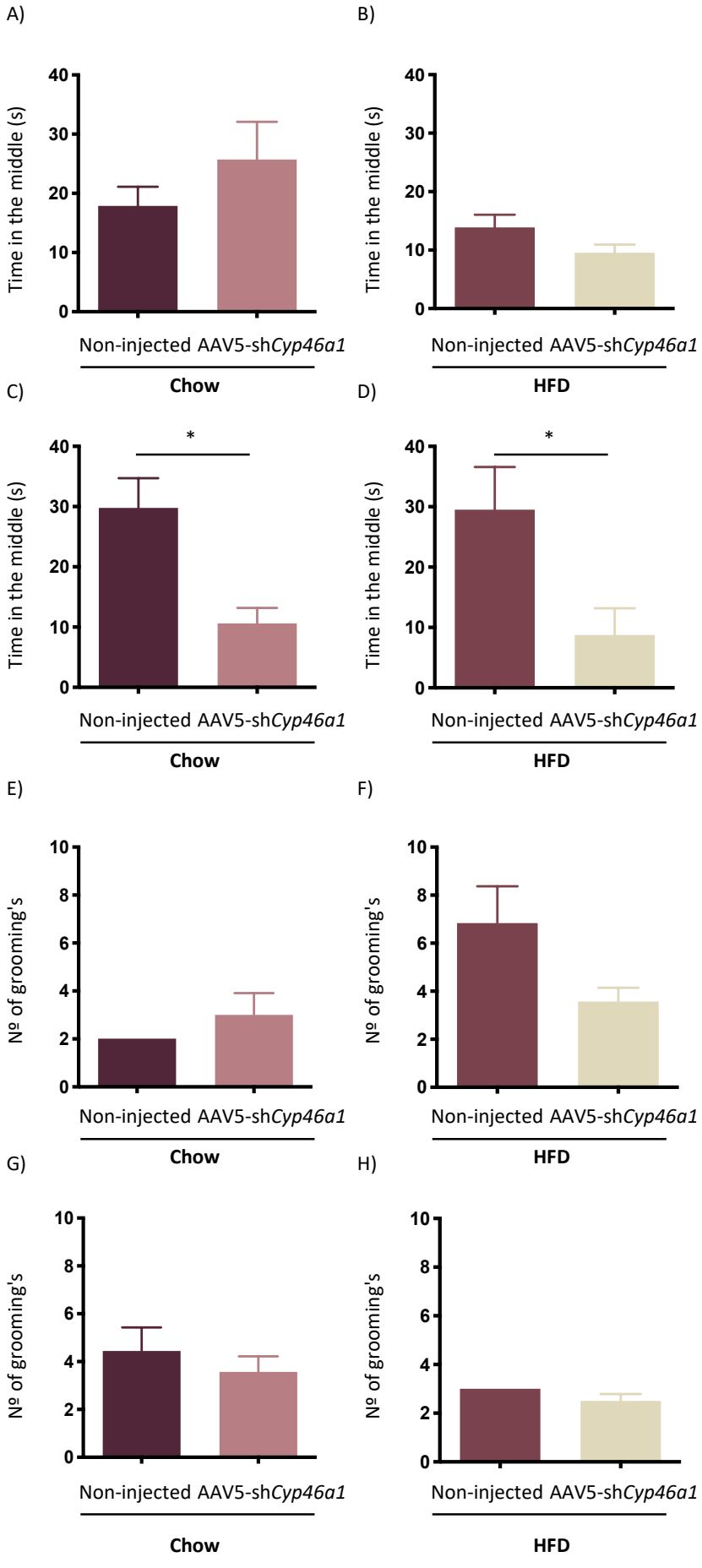
A)
B)
Time in the middle (s)
40
30
20
10
0
Non-injected
AAV5-sh*Cyp46a1*
Chow
HFD
C)
D)
*
E)
F)
Nº of grooming's
10
8
6
4
2
0
G)
H)

Annex 12| Silencing *Cyp46a1* gene in the hypothalamus of C57BL/6J wild-type males fed with Chow and HFD decreases the time spend in the middle, in the day-time period

A) Between females, the Chow AAV5-sh*Cyp46a1* animals did not showed significant alterations in the time spend in the middle comparatively to the Chow Non-injected animals. **B)** Between females, the HFD AAV5-sh*Cyp46a1* did not showed significant changes in the time spend in the middle comparatively to the HFD Non-injected animals. **C)** Between males, the Chow AAV5-sh*Cyp46a1* showed a significant decrease in the time spend in the middle comparatively to the Chow Non-injected animals. **D)** Between males, the HFD AAV5-sh*Cyp46a1* animals presented a significant decrease in the time spend in the middle comparatively to the HFD Non-injected animals. **E)** Between females, the Chow AAV5-sh*Cyp46a1* animals did not showed significant modifications in the number of grooming's comparatively to the Chow Non-injected animals. **F)** Between females, the HFD AAV5-sh*Cyp46a1* animals presented a decrease in the number of grooming's comparatively to the HFD Non-injected animals. **G)** Between males, the Chow AAV5-sh*Cyp46a1* animals did not presented alterations in the number of grooming's comparatively to the Chow Non-injected animals. **H)** Between males, the HFD AAV5-sh*Cyp46a1* animals did not showed changes in the number of grooming's comparatively to the HFD Non-injected animals. Data were represented as mean ± SEM [Chow Non-injected: *n=13*, female: *n=4* and male: *n=9*; Chow AAV5-sh*Cyp46a1: n=11*, female: *n=4* and male: *n=7*; HFD Non-injected: *n=10*, female: *n=6* and male: *n=4*; HFD AAV5-sh*Cyp46a1*: *n=11*, female: *n=7* and male: *n=4*]. [*P*-value < 0,05 (*), *P*-value < 0,01 (**), *P*-value < 0,001 (***), *P*-value < 0,0001 (****)] – unpaired Student's t-test: A-B-C-D-E-F-G-H; **Abbreviations: Chow:** low fat control diet; **HFD:** high fat diet; **AAV5:** adeno-associated vectors of the serotype 5; **sh:** short hairpin.

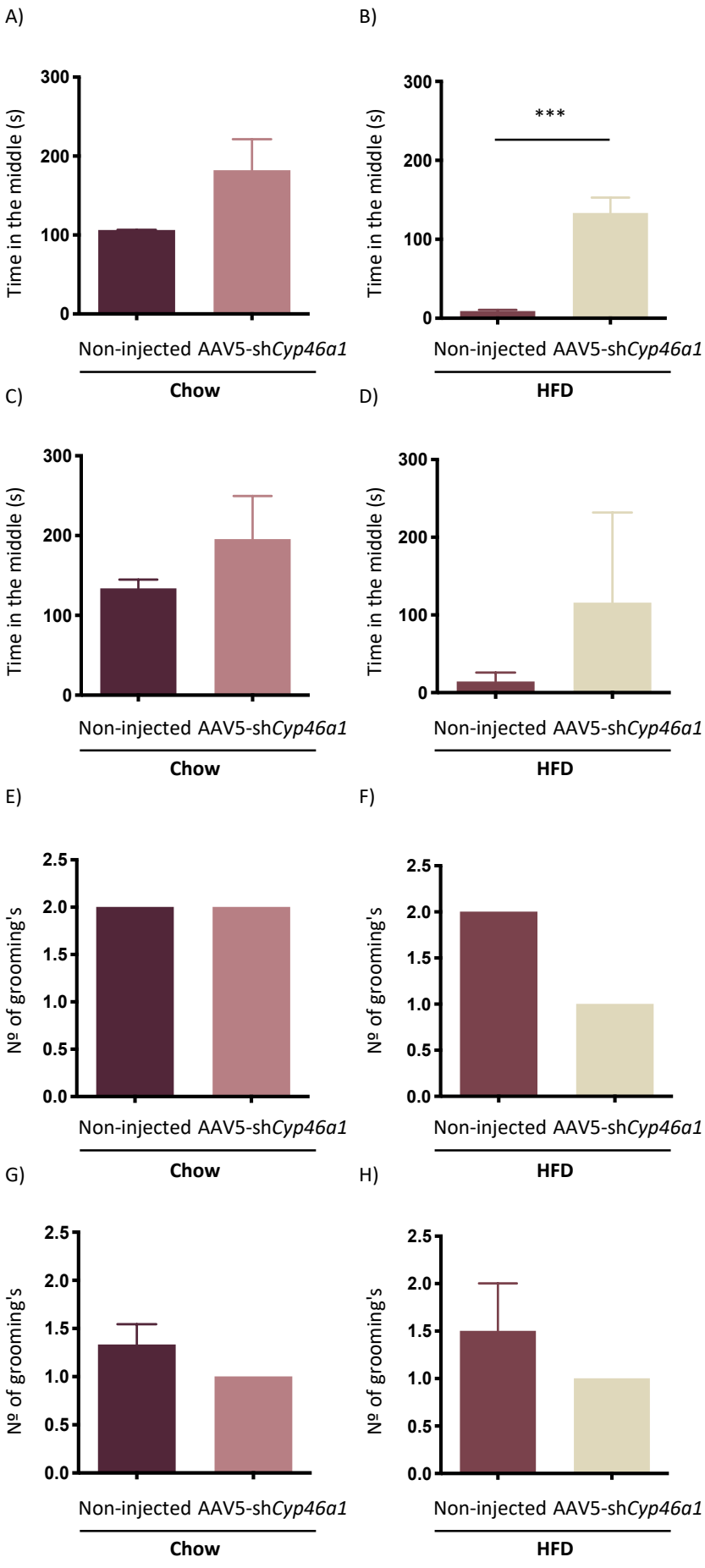
A)
B)
Time in the middle (s)
300
200
100
0
***
Non-injected
AAV5-sh*Cyp46a1*
Chow
HFD
C)
D)
E)
F)
Nº of grooming's
2.5
2.0
1.5
1.0
0.5
0.0
G)
H)

Annex 13| Silencing *Cyp46a1* gene in the hypothalamus, of C57BL/6J wild-type males and females fed with Chow and HFD, increases the time spend in the middle in the night-time period

A) Between females, the Chow AAV5-sh*Cyp46a1* animals showed an increase in the time spend in the middle comparatively to the Chow Non-injected animals. **B)** Between females, the HFD AAV5-sh*Cyp46a1* presented a significant increase in the time spend in the middle comparatively to the HFD Non-injected animals. **C)** Between males, the Chow AAV5-sh*Cyp46a1* showed a significant decrease in the time spend in the middle comparatively to the Chow Non-injected animals. **D)** Between males, the HFD AAV5-sh*Cyp46a1* animals presented an increase in the time spend in the middle comparatively to the HFD Non-injected animals. **E)** Between females, the Chow AAV5-sh*Cyp46a1* animals did not showed significant modifications in the number of grooming's comparatively to the Chow Non-injected animals. **F)** Between females, the HFD AAV5-sh*Cyp46a1* animals did not presented modifications in the number of grooming's comparatively to the HFD Non-injected animals. **G)** Between males, the Chow AAV5-sh*Cyp46a1* animals did not presented alterations in the number of grooming's comparatively to the Chow Non-injected animals. **H)** Between males, the HFD AAV5-sh*Cyp46a1* animals did not showed changes in the number of grooming's comparatively to the HFD Non-injected animals. Data were represented as mean ± SEM. [Chow Non-injected: *n=8*, female: *n=2* and male: *n=6*; Chow AAV5-sh*Cyp46a1: n=5*, female: *n=2* and male: *n=3*; HFD Non-injected: *n=6*, female: *n=4* and male: *n=2*; HFD AAV5-sh*Cyp46a1*: *n=5*, female: *n=3* and male: *n=2*]. [*P*-value < 0,05 (*), *P*-value < 0,01 (**), *P*-value < 0,001 (***), *P*-value < 0,0001 (****)] – unpaired Student's t-test: A-B-C-D-E-F-G-H; **Abbreviations: Chow:** low fat control diet; **HFD:** high fat diet; **AAV5:** adeno-associated vectors of the serotype 5; **sh:** short hairpin.

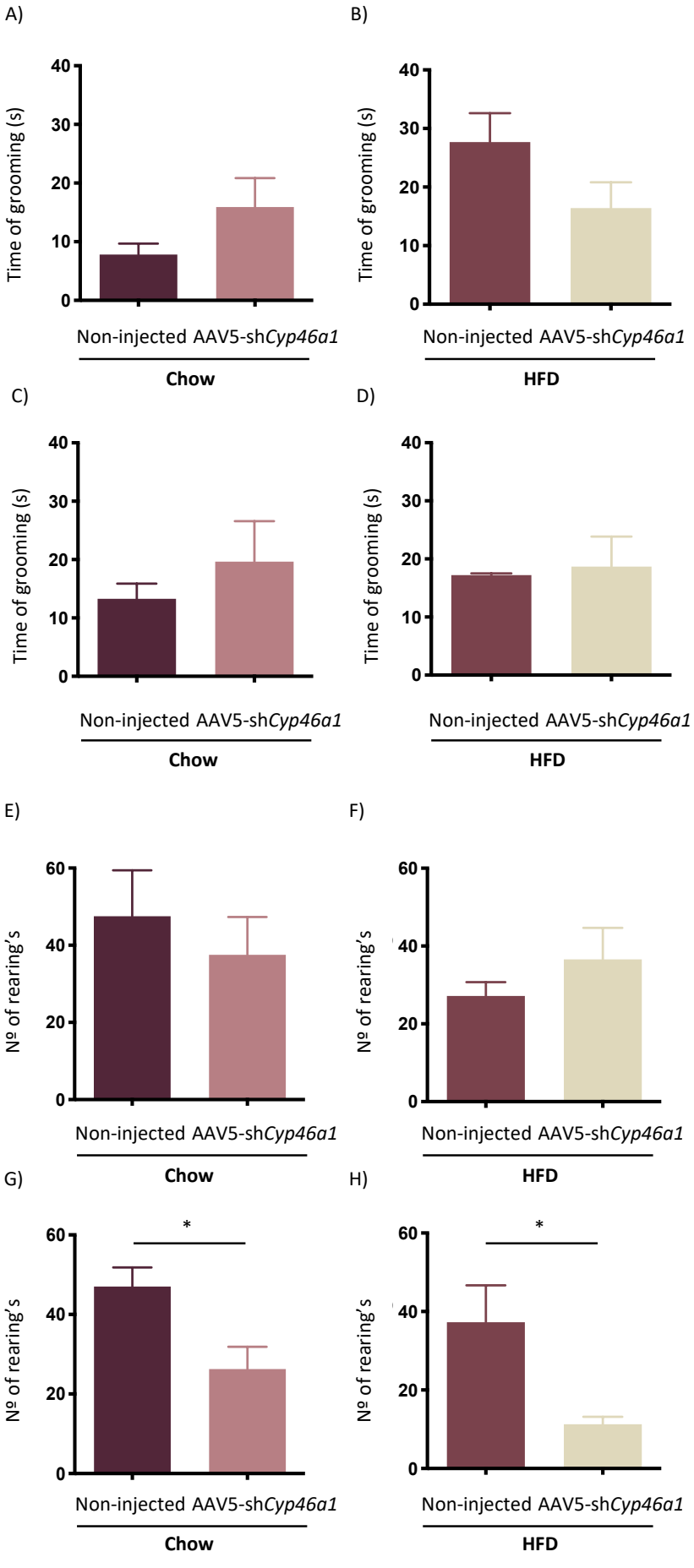
A)
B)
Time of grooming (s)
40
30
20
10
0
Non-injected
AAV5-sh*Cyp46a1*
Chow
HFD
C)
D)
E)
F)
Nº of rearing's
60
40
20
G)
H)
*

Annex 14| Silencing *Cyp46a1* gene in the hypothalamus, of C57BL/6J wild-type males fed with Chow and HFD, decreases the number of rearing's in the day-time period

A) Between females, the Chow AAV5-sh*Cyp46a1* animals show an increase in the time of grooming comparatively to the Chow Non-injected animals. **B)** Between females, the HFD AAV5-sh*Cyp46a1* presented a decrease in the time of grooming comparatively to the HFD Non-injected animals. **C)** Between males, the Chow AAV5-sh*Cyp46a1* did not showed alterations in the time of grooming comparatively to the Chow Non-injected animals. **D)** Between males, the HFD AAV5-sh*Cyp46a1* animals did not presented alterations in the time of grooming comparatively to the HFD Non-injected animals. **E)** Between females, the Chow AAV5-sh*Cyp46a1* animals did not showed significant modifications in the number of rearing's comparatively to the Chow Non-injected animals. **F)** Between females, the HFD AAV5-sh*Cyp46a1* animals did not presented changes in the number of rearing's comparatively to the HFD Non-injected animals. **G)** Between males, the Chow AAV5-sh*Cyp46a1* animals presented a significant decrease in the number of rearing's comparatively to the Chow Non-injected animals. **H)** Between males, the HFD AAV5-sh*Cyp46a1* animals show a significant decrease in the number of rearing's comparatively to the HFD Non-injected animals. Data were represented as mean ± SEM [Chow Non-injected: *n=13*, female: *n=4* and male: *n=9*; Chow AAV5-sh*Cyp46a1: n=11*, female: *n=4* and male: *n=7*; HFD Non-injected: *n=10*, female: *n=6* and male: *n=4*; HFD AAV5-sh*Cyp46a1*: *n=11*, female: *n=7* and male: *n=4*]. [*P*-value < 0,05 (*), *P*-value < 0,01 (**), *P*-value < 0,001 (***), *P*-value < 0,0001 (****)] – unpaired Student's t-test: A-B-C-D-E-F-G-H; **Abbreviations: Chow:** low fat control diet; **HFD:** high fat diet; **AAV5:** adeno-associated vectors of the serotype 5; **sh:** short hairpin.

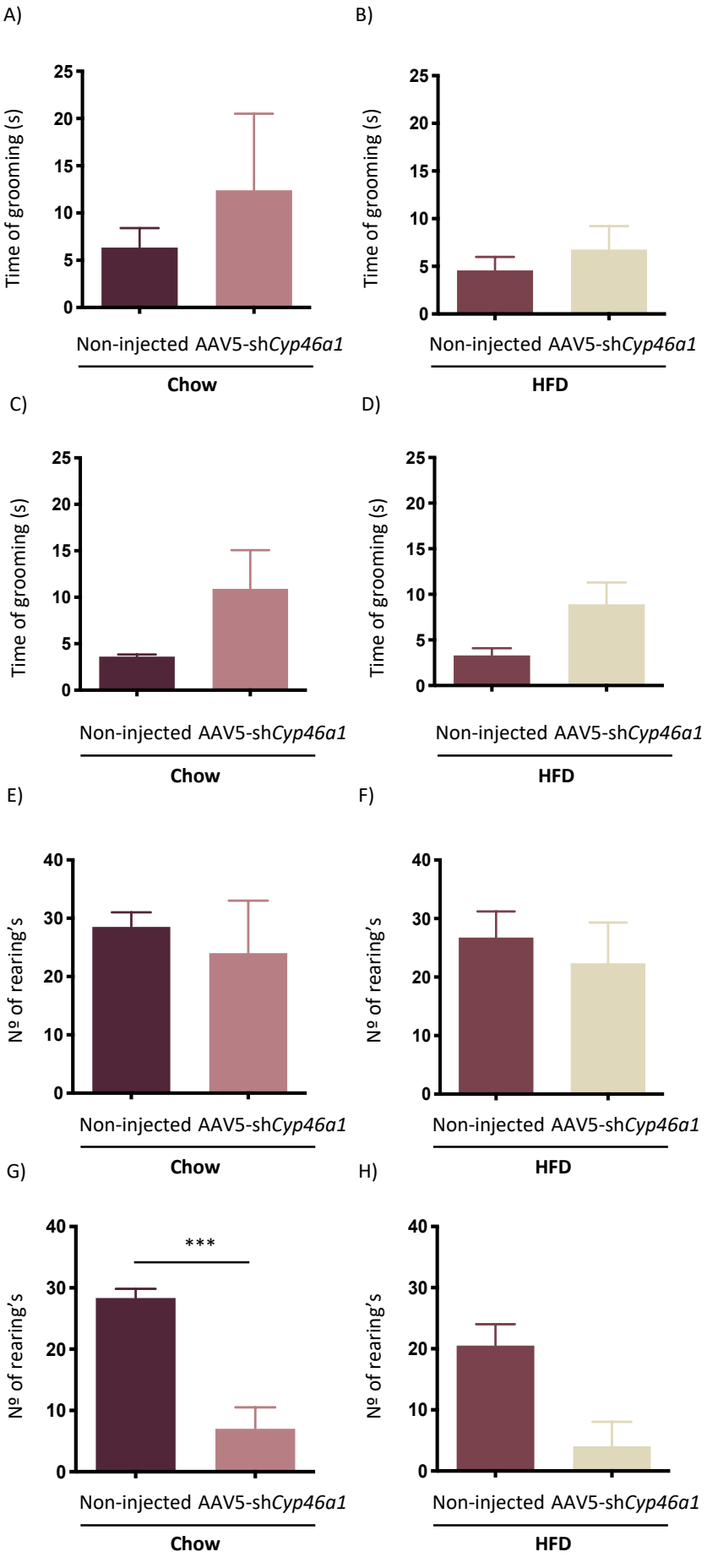
A)
B)
Time of grooming (s)
25
20
15
10
5
0
Non-injected
AAV5-sh*Cyp46a1*
Chow
HFD
C)
D)
E)
F)
Nº of rearing's
40
30
20
10
G)
H)
***

Annex 15| Silencing *Cyp46a1* gene in the hypothalamus, of C57BL/6J wild-type males fed with Chow and HFD, alters time of grooming and the number of rearing's in the night-time period

A) Between females, the Chow AAV5-sh*Cyp46a1* animals did not showed alterations in the time of grooming comparatively to the Chow Non-injected animals. **B)** Between females, the HFD AAV5-sh*Cyp46a1* did not presented alterations in the time of grooming comparatively to the HFD Non-injected animals. **C)** Between males, the Chow AAV5-sh*Cyp46a1* showed an increase in the time of grooming comparatively to the Chow Non-injected animals. **D)** Between males, the HFD AAV5-sh*Cyp46a1* animals presented an increase in the time of grooming comparatively to the HFD Non-injected animals. **E)** Between females, the Chow AAV5-sh*Cyp46a1* animals did not showed significant modifications in the number of rearing's comparatively to the Chow Non-injected animals. **F)** Between females, the HFD AAV5-sh*Cyp46a1* animals did not presented alterations in the number of rearing's comparatively to the HFD Non-injected animals. **G)** Between males, the Chow AAV5-sh*Cyp46a1* animals presented a significant decrease in the number of rearing's comparatively to the Chow Non-injected animals. **H)** Between males, the HFD AAV5-sh*Cyp46a1* animals showed a decrease in the number of rearing's comparatively to the HFD Non-injected animals. Data were represented as mean ± SEM. [Chow Non-injected: *n=8*, female: *n=2* and male: *n=6*; Chow AAV5-sh*Cyp46a1: n=5*, female: *n=2* and male: *n=3*; HFD Non-injected: *n=6*, female: *n=4* and male: *n=2*; HFD AAV5-sh*Cyp46a1*: *n=5*, female: *n=3* and male: *n=2*]. [*P*-value < 0,05 (*), *P*-value < 0,01 (**), *P*-value < 0,001 (***), *P*-value < 0,0001 (****)] – unpaired Student's t-test: A-B-C-D-E-F-G-H; **Abbreviations: Chow:** low fat control diet; **HFD:** high fat diet; **AAV5:** adeno-associated vectors of the serotype 5; **sh:** short hairpin.

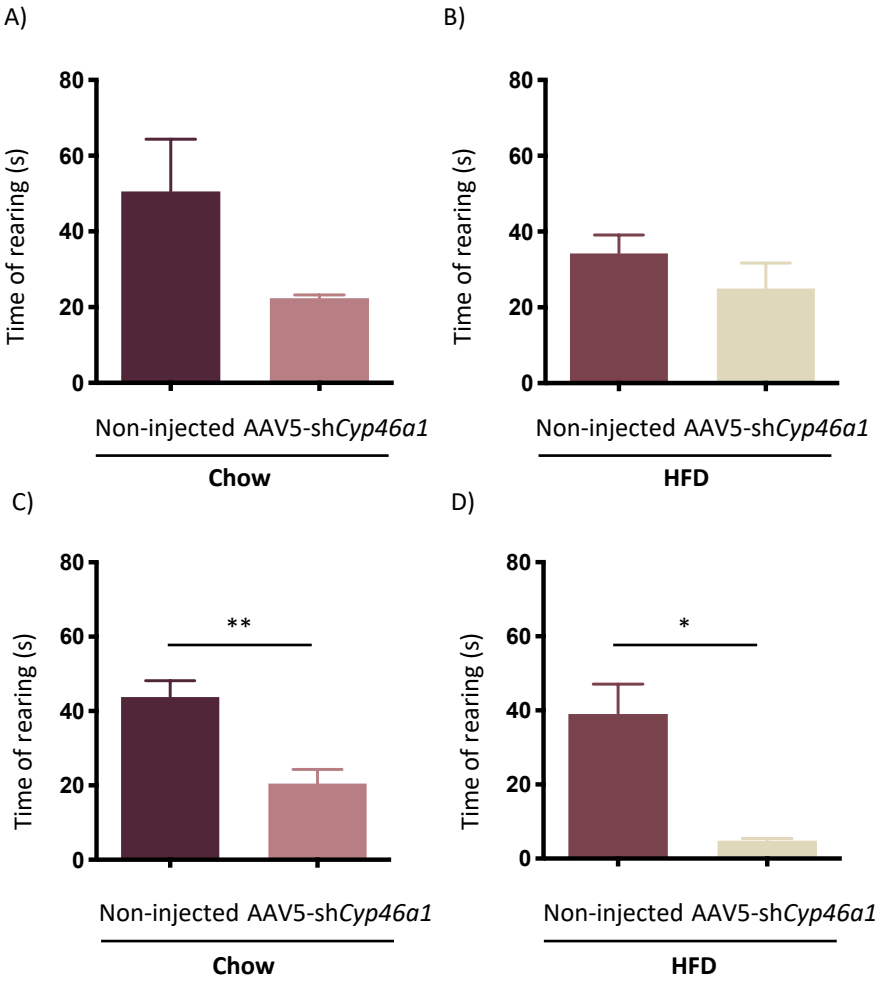

Annex 16| Silencing *Cyp46a1* gene in the hypothalamus, of C57BL/6J wild-type males fed with Chow and HFD, decreases the time of rearing in the day-time period

A) Between females, the Chow AAV5-sh*Cyp46a1* animals showed a decrease in the time of rearing comparatively to the Chow Non-injected animals. **B)** Between females, the HFD AAV5-sh*Cyp46a1* animals did not presented modifications in the time of rearing comparatively to the HFD Non-injected animals. **C)** Between males, the Chow AAV5-sh*Cyp46a1* animals presented a significant decrease in the time of rearing comparatively to the Chow Non-injected animals. **D)** Between males, the HFD AAV5-sh*Cyp46a1* animals showed a significant decrease in the time of rearing comparatively to the HFD Non-injected animals. Data were represented as mean ± SEM [Chow Non-injected: *n=13*, female: *n=4* and male: *n=9*; Chow AAV5-sh*Cyp46a1: n=11*, female: *n=4* and male: *n=7*; HFD Non-injected: *n=10*, female: *n=6* and male: *n=4*; HFD AAV5-sh*Cyp46a1*: *n=11*, female: *n=7* and male: *n=4*]. [*P*-value < 0,05 (*), *P*-value < 0,01 (**), *P*-value < 0,001 (***), *P*-value < 0,0001 (****)] – unpaired Student's t-test: A-B-C-D; **Abbreviations: Chow:** low fat control diet; **HFD:** high fat diet; **AAV5:** adeno-associated vectors of the serotype 5; **sh:** short hairpin.

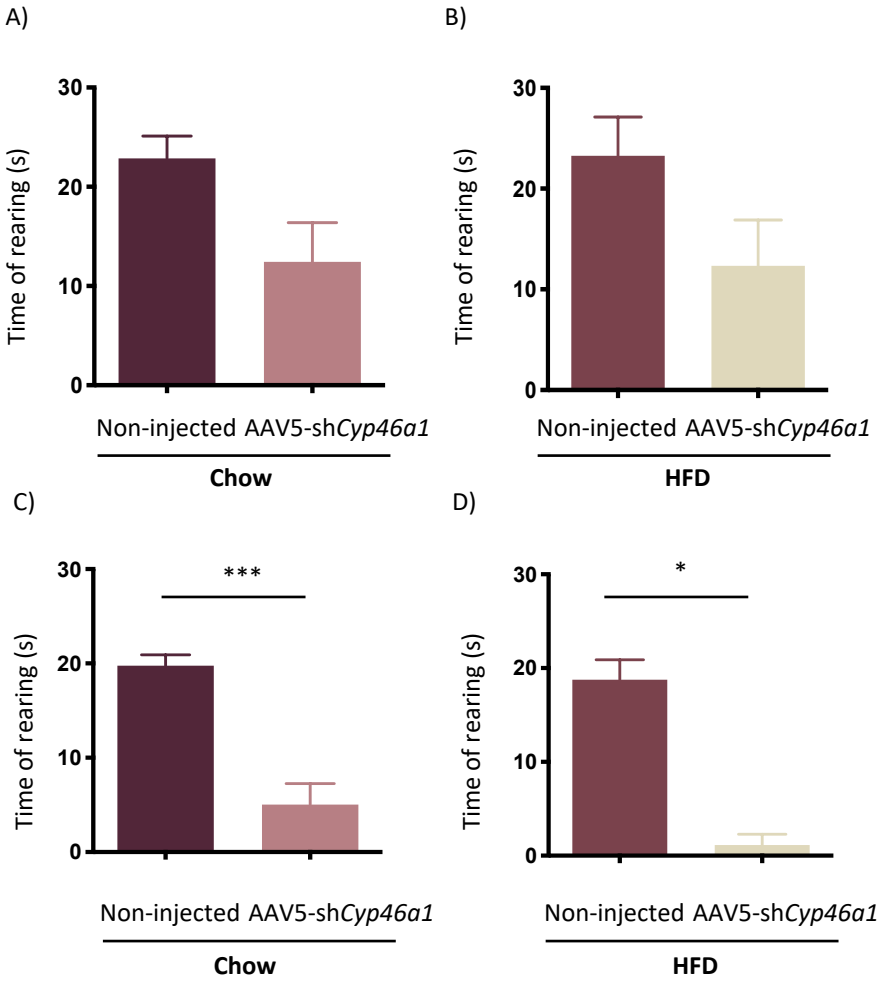

Annex 17| Silencing *Cyp46a1* gene in the hypothalamus, of C57BL/6J wild-type males fed with Chow and HFD, decreases the time of rearing in the night-time period

A) Between females, the Chow AAV5-sh*Cyp46a1* animals showed a decrease in the time of rearing comparatively to the Chow Non-injected animals. **B)** Between females, the HFD AAV5-sh*Cyp46a1* animals presented a decrease in the time of rearing comparatively to the HFD Non-injected animals. **C)** Between males, the Chow AAV5-sh*Cyp46a1* animals presented a significant decrease in the time of rearing comparatively to the Chow Non-injected animals. **D)** Between males, the HFD AAV5-sh*Cyp46a1* animals showed a significant decrease in the time of rearing comparatively to the HFD Non-injected animals. Data were represented as mean ± SEM. [Chow Non-injected: *n=8*, female: *n=2* and male: *n=6*; Chow AAV5-sh*Cyp46a1: n=5*, female: *n=2* and male: *n=3*; HFD Non-injected: *n=6*, female: *n=4* and male: *n=2*; HFD AAV5-sh*Cyp46a1*: *n=5*, female: *n=3* and male: *n=2*]. [*P*-value < 0,05 (*), *P*-value < 0,01 (**), *P*-value < 0,001 (***), *P*-value < 0,0001 (****)] – unpaired Student's t-test: A-B-C-D; **Abbreviations: Chow:** low fat control diet; **HFD:** high fat diet; **AAV5:** adeno-associated vectors of the serotype 5; **sh:** short hairpin.

Annex 18| Silencing *Cyp46a1* gene in the hypothalamus modifies behavior activity of C57BL/6J mice females fed with a Chow and HFD in the day-time period

Day – Females						
	Chow (*n=8*)			**HFD** (*n=13*)		
	Non-injected	AAV5-sh*Cyp46a1*	*P*-value	Non-injected	AAV5-sh*Cyp46a1*	*P*-value
Total distance (m)	28,06 ± 4,273	27,50 ± 5,488	0,9383	22,96 ± 2,179	28,38 ± 6,781	0,4925
Mean speed (m/s)	0,0467 ± 0,007	0,0457 ± 0,0093	0,9353	0,03833 ± 0,003	0,047 ± 0,0113	0,5114
Nº of immobile episodes	44,75 ± 5,893	42,00 ± 5,972	0,7542	47,00 ± 2,887	32,29 ± 4,839	0,0296 (↓)
Time immobile (s)	220,8 ± 40,81	197,0 ± 24,97	0,6362	266,8 ± 27,06	210,1 ± 47,57	0,3285
Nº of crossing lines	204,0 ± 34,77	185,0 ± 33,26	0,7066	171,8 ± 17,94	195 ± 46,51	0,6621
Nº of entries in the middle	16,75 ± 5,452	13,50 ± 3,279	0,6277	15,33 ± 2,140	11,14 ± 2,604	0,2495
Time in the middle (s)	17,88 ± 3,249	25,70 ± 6,384	0,3166	13,87 ± 2,189	9,543 ± 1,392	0,1138
Nº of grooming' s	2,00 ± 0,0	3,00 ± 0,9129	0,3970	6,833 ± 1,537	3,571 ± 0,5714	0,0581 (↓)
Time of grooming (s)	7,825 ± 1,863	15,93 ± 4,924	0,1748 (↑)	27,68 ± 4,950	16,40 ± 4,412	0,1158 (↓)
Nº of rearing' s	47,50 ± 11,93	37,50 ± 9,845	0,5418	27,17 ± 3,572	36,57 ± 8,091	0,3380
Time of rearing (s)	50,58 ± 13,79	22,37 ± 0,8667	0,1447 (↓)	34,22 ± 4,889	24,94 ± 6,766	0,3050

Annex 18: Shows the parameters analyzed in the day-time period for females of each study group with respective mean ± SEM and *P*-value [Chow Non-injected: *n=13*, female: *n=4* and male: *n=9*; Chow AAV5-sh*Cyp46a1: n=11*, female: *n=4* and male: *n=7*; HFD Non-injected: *n=10*, female: *n=6* and male:

n=4; HFD AAV5-sh*Cyp46a1*: *n=11*, female: *n=7* and male: *n=4*]. [*P*-value < 0,05 (*), *P*-value < 0,01 (**), *P*-value < 0,001 (***), *P*-value < 0,0001 (****)] – unpaired Student's t-test; **Abbreviations: Chow:** low fat control diet; **HFD:** high fat diet; **AAV5:** adeno-associated vectors of the serotype 5; **sh:** short hairpin**;** **SEM:** standard error of mean; ↓ **:** statistically significant decrease; ↓ **:** non-significant decrease; ↑ : statistically significant increase; ↑ : non-significant decrease.

Annex 19| Silencing *Cyp46a1* gene in the hypothalamus modifies behavior activity of C57BL/6J mice males fed with a Chow and HFD in the day-time period

Day - Males						
	Chow (*n=16*)			**HFD** (*n=8*)		
	Non-injected	AAV5-sh*Cyp46a1*	*P*-value	Non-injected	AAV5-sh*Cyp46a1*	*P*-value
Total distance (m)	29,30 ± 1,979	21,99 ± 6,003	0,2236	32,03 ± 3,875	18,25 ± 7,801	0,1343 (↓)
Mean speed (m/s)	0,0467 ± 0,002	0,03386 ± 0,011	0,2283	0,0480 ± 0,00465	0,015 ± 0,0039	0,0017 (↓)
Nº of immobile episodes	43,00 ± 3,158	35,71 ± 3,092	0,1282 (↓)	46,50 ± 8,411	52,25 ± 9,852	0,6727
Time immobile (s)	180,8 ± 19,08	298,6 ± 72,73	0,1010 (↑)	190,1 ± 34,95	430,8 ± 42,52	0,0047 (↑)
Nº of crossing lines	216 ± 12,91	167,4 ± 43,94	0,2487	242,3 ± 29,55	64,25 ± 12,93	0,0015 (↓)
Nº of entries in the middle	26,00 ± 2,625	10,86 ± 3,562	0,0035 (↓)	24,25 ± 4,526	4,00 ± 0,7071	0,0044 (↓)
Time in the middle (s)	29,79 ± 4,922	10,60 ± 2,600	0,0107 (↓)	29,50 ± 7,098	8,750 ± 4,422	0,0477 (↓)
Nº of grooming' s	4,444 ± 0,9876	3,571 ± 0,649	0,5007	3,00 ± 0,0	2,50 ± 0,2887	0,2031
Time of grooming (s)	13,27 ± 2,607	19,65 ± 6,932	0,3385	17,20 ± 0,3055	18,68 ± 5,161	0,8189
Nº of rearing' s	47,00 ± 4,813	26,29 ± 5,567	0,0136 (↓)	37,25 ± 9,437	11,25 ± 1,931	0,0356 (↓)
Time of rearing (s)	43,78 ± 4,397	20,50 ± 3,808	0,0017 (↓)	39,00 ± 8,103	4,833 ± 0,6173	0,0162 (↓)

Annex 19: Shows the parameters analyzed in the day-time period for males of each study group with respective mean ± SEM and *P*-value [Chow Non-injected: *n=13*, female: *n=4* and male: *n=9*; Chow AAV5-sh*Cyp46a1: n=11*, female: *n=4* and male: *n=7*; HFD Non-injected: *n=10,* female: *n=6* and male:

n=4; HFD AAV5-sh*Cyp46a1*: *n=11*, female: *n=7* and male: *n=4*]. [*P*-value < 0,05 (*), *P*-value < 0,01 (**), *P*-value < 0,001 (***), *P*-value < 0,0001 (****)] – unpaired Student's t-test; **Abbreviations: Chow:** low fat control diet; **HFD:** high fat diet; **AAV5:** adeno-associated vectors of the serotype 5; **sh:** short hairpin**;** **SEM:** standard error of mean; ↓ **:** statistically significant decrease; ↓ **:** non-significant decrease; ↑ : statistically significant increase; ↑ : non-significant decrease.

Annex 20| Silencing *Cyp46a1* gene in the hypothalamus modifies behavior activity of C57BL/6J mice females fed with a Chow and HFD in the night-time period

Night - Females						
	Chow (*n=4*)			**HFD** (*n=7*)		
	Non-injected	AAV5-sh*Cyp46a1*	*P*-value	Non-injected	AAV5-sh*Cyp46a1*	*P*-value
Total distance (m)	16,24 ± 0,6155	16,83 ± 2,234	0,8210	17,95 ± 1,434	17,87 ± 2,330	0,9760
Mean speed (m/s)	0,0540 ± 0,0020	0,0565 ± 0,007	0,7779	0,065 ± 0,0009	0,0593 ± 0,008	0,5253
Nº of immobile episodes	16,00 ± 2,00	13,50 ± 0,500	0,3491	18,00 ± 1,683	15,00 ± 3,464	0,4326
Time immobile (s)	63,45 ± 10,65	65,65 ± 5,350	0,8706	68,35 ± 9,897	60,00 ± 15,59	0,6539
Nº of crossing lines	125,0 ± 7,00	108,0 ± 10,00	0,2983	130,5 ± 9,260	119,7 ± 17,89	0,5846
Nº of entries in the middle	8,500 ± 1,500	8,500 ± 1500	>0,999	14,25 ± 2,394	10,33 ± 1,202	0,2493
Time in the middle (s)	106,4 ± 0,200	182,0 ± 39,30	0,1943 (↑)	9,075 ± 1,499	133,3 ± 19,65	0,0007 (↑)
Nº of grooming' s	-	-	-	-	-	-
Time of grooming (s)	6,350 ± 2,050	12,40 ± 8,100	0,5443	4,575 ± 1,417	6,733 ± 2,458	0,4530
Nº of rearing' s	28,50 ± 2,500	24,00 ± 9,00	0,6775	26,75 ± 4,479	22,33 ± 6,984	0,5997
Time of rearing (s)	22,85 ± 2,250	12,45 ± 3,950	0,1494 (↓)	23,28 ± 3,849	12,33 ± 4,551	0,1246 (↓)

Annex 20: Shows the parameters analyzed in the night-time period for females of each study group with respective mean ± SEM and *P*-value [Chow Non-injected: *n=8*, female: *n=2* and male: *n=6*; Chow AAV5-sh*Cyp46a1: n=5*, female: *n=2* and male: *n=3*; HFD Non-injected: *n=6*, female: *n=4* and male: *n=2*; HFD AAV5-sh*Cyp46a1*: *n=5*, female: *n=3* and male: *n=2*]. [*P*-value < 0,05 (*), *P*-value < 0,01 (**), *P*-value < 0,001 (***), *P*-value < 0,0001 (****)] – unpaired Student's t-test; **Abbreviations: Chow:** low fat control diet; **HFD:** high fat diet; **AAV5:** adeno-associated vectors of the serotype 5; **sh:** short hairpin**; SEM:** standard error of mean; ↓ **:** statistically significant decrease; ↓ **:** non-significant decrease; ↑ : statistically significant increase; ↑ : non-significant decrease.

Annex 21| Silencing *Cyp46a1* gene in the hypothalamus modifies behavior activity of C57BL/6J mice males fed with a Chow and HFD in the night-time period

Night - Males						
	Chow (*n=9*)			**HFD** (*n=4*)		
	Non-injected	AAV5-sh*Cyp46a1*	*P*-value	Non-injected	AAV5-sh*Cyp46a1*	*P*-value
Total distance (m)	19,49 ± 1,280	11,93 ± 7,569	0,2568	23,13 ± 10,93	17,84 ± 11,98	0,7606
Mean speed (m/s)	0,06517 ± 0,0043	0,0153 ± 0,0101	0,0010 (↓)	0,0405 ± 0,004	0,0210 ± 0,0170	0,3780
Nº of immobile episodes	13,17 ± 2,713	15,67 ± 2,728	0,5839	27,00 ± 0,0	15,00 ± 3,00	0,0572 (↓)
Time immobile (s)	51,17 ± 10,60	205 ± 54,92	0,0056 (↑)	104,3 ± 12,70	192,8 ± 67,00	0,3239
Nº of crossing lines	138,3 ± 11,40	33,00 ± 21,78	0,0020 (↓)	103,5 ± 0,500	58,50 ± 46,50	0,4353
Nº of entries in the middle	11,83 ± 1,887	3,333 ± 1,453	0,0227 (↓)	9,00 ± 5,00	3,500 ± 3,500	0,4626
Time in the middle (s)	133,8 ± 11,17	195,7 ± 54,03	0,1565 (↑)	14,35 ± 11,45	115,9 ± 115,9	0,4752
Nº of grooming' s	1,333 ± 0,2108	1,00 ± 0,0	0,4198	1,500 ± 0,500	1,00 ± 0,0	0,4226
Time of grooming (s)	3,620 ± 0,2154	10,90 ± 4,173	0,0549 (↑)	3,300 ± 0,800	8,900 ± 2,400	0,1573 (↑)
Nº of rearing' s	28,33 ± 1,520	7,00 ± 3,512	0,0003 (↓)	20,50 ± 3,500	4,00 ± 4,00	0,0900 (↓)
Time of rearing (s)	19,75 ± 1,168	5,033 ± 2,234	0,0003 (↓)	18,75 ± 2,150	1,150 ± 1,50	0,0187 (↓)

Annex 21: Shows the parameters analyzed in the night-time period for males of each study group with respective mean ± SEM and *P*-value [Chow Non-injected: *n=8*, female: *n=2* and male: *n=6*; Chow AAV5-

sh*Cyp46a1: n=5*, female: *n=2* and male: *n=3*; HFD Non-injected: *n=6*, female: *n=4* and male: *n=2*; HFD AAV5-sh*Cyp46a1*: *n=5*, female: *n=3* and male: *n=2*]. [*P*-value < 0,05 (*), *P*-value < 0,01 (**), *P*-value < 0,001 (***), *P*-value < 0,0001 (****)] – unpaired Student's t-test; **Abbreviations: Chow:** low fat control diet; **HFD:** high fat diet; **AAV5:** adeno-associated vectors of the serotype 5; **sh:** short hairpin**; SEM:** standard error of mean; ↓ **:** statistically significant decrease; ↓ **:** non-significant decrease; ↑ : statistically significant increase; ↑ : non-significant decrease.

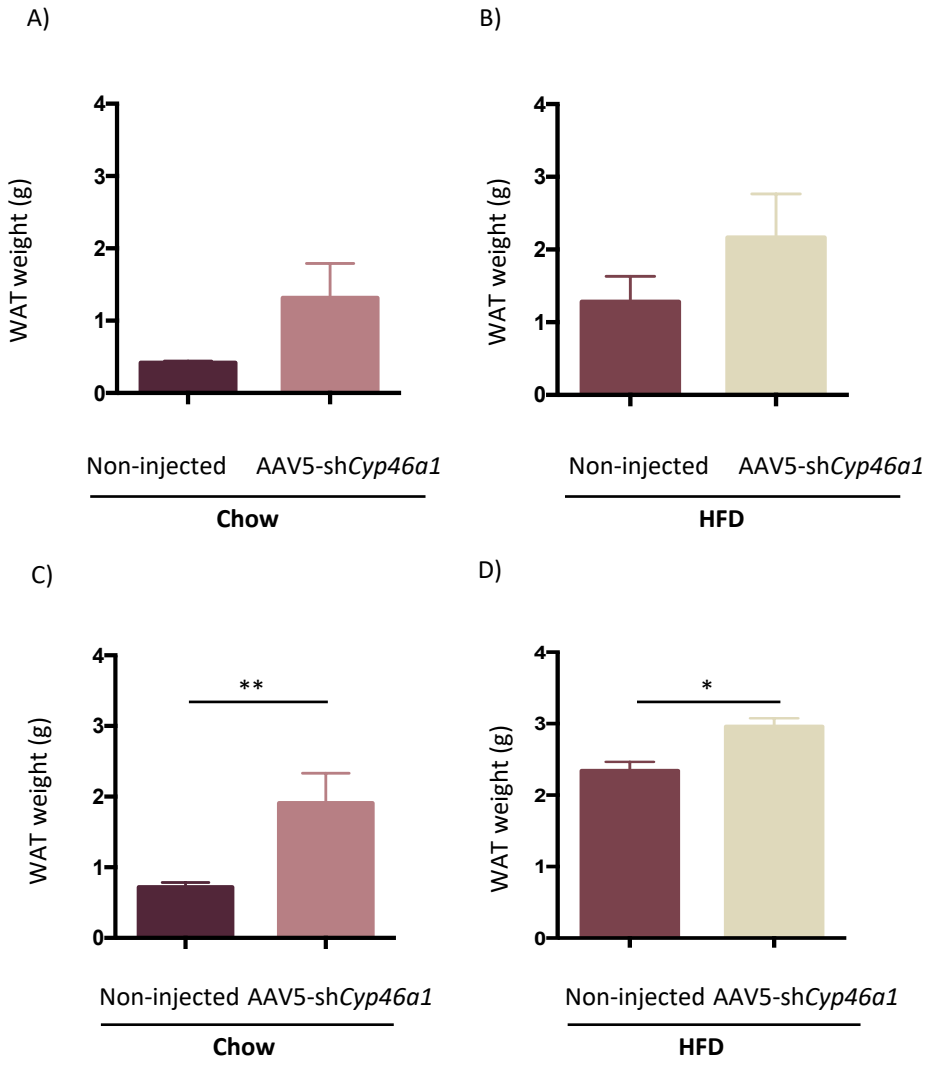

Annex 22 | Silencing *Cyp46a1* gene in the hypothalamus induces an increased in WAT weight of C57BL/6J females and males fed with a Chow and HFD

A) Between females, the Chow AAV5-sh*Cyp46a1* animals presented an increase in WAT weight, comparatively to the Chow Non-injected animals [Chow Non-injected (0,4169 ± 0,02456); *n=4* versus Chow AAV5-sh*Cyp46a1* (1,317 ± 0,4754); *n=4* – *P*-value =0,1077]. **B)** Between females, the HFD AAV5-sh*Cyp46a1* animals presented an increase in WAT weight, relatively to the HFD Non-injected groups [HFD Non-injected (1,281 ± 0,3504); *n=6* versus HFD AAV5-sh*Cyp46a1* (2,166 ± 0,5995); *n=7* – *P*-value =0,2489]. **C)** Between males, the Chow AAV5-sh*Cyp46a1* animals presented a significant increase in WAT weight, comparatively to the Chow Non-injected animals [Chow Non-injected (0,7183 ± 0,657); *n=9* versus Chow AAV5-sh*Cyp46a1* (1,907 ± 0,422); *n=7* – *P*-value =0,0070]. **D)** Between males, the HFD

AAV5-sh*Cyp46a1* animals presented a significant increase in WAT weight, relatively to the HFD Non-injected animals [HFD Non-injected (2,342 ± 0,1250); *n=4* versus HFD AAV5-sh*Cyp46a1* (2,962 ± 0,1147); *n=4* – *P*-value =0,0106]. Data were represented as mean ± SEM. [*P*-value < 0,05 (*), *P*-value < 0,01 (**), *P*-value < 0,001 (***), *P*-value < 0,0001 (****)] – unpaired Student's t-test: A-B-C-D; **Abbreviations: WAT:** white adipose tissue; **Chow:** low fat control diet; **HFD:** high fat diet; **AAV5:** adeno-associated vectors of the serotype 5; **sh:** short hairpin.

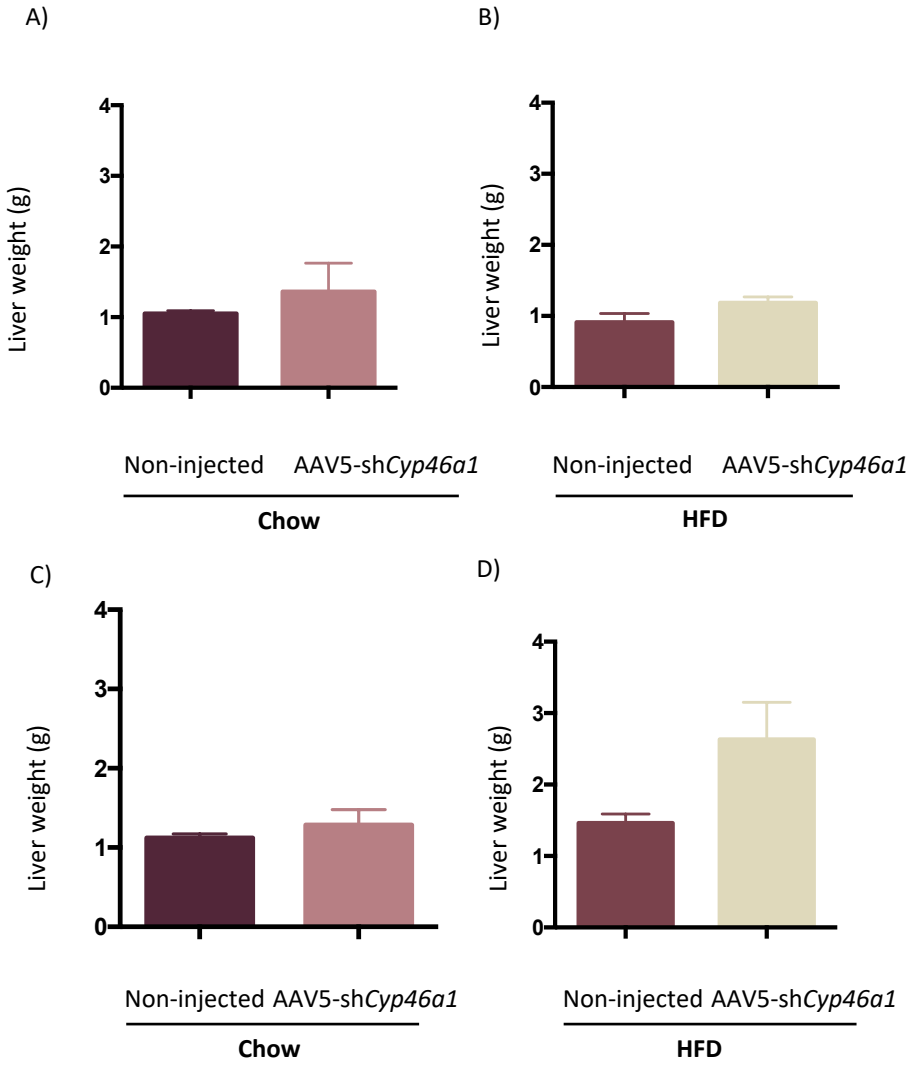

Annex 23| Silencing *Cyp46a1* gene in the hypothalamus induces an increased in WAT weight of C57BL/6J females and males fed with a Chow and HFD

A) Between females, the Chow AAV5-sh*Cyp46a1* animals presented an increase in liver weight, comparatively to the Chow Non-injected animals [Chow Non-injected (1,050 ± 0,04024); *n=4* versus Chow AAV5-sh*Cyp46a1* (1,362 ± 0,4042); *n=4* – *P*-value =0,4721]. **B)** Between females, the HFD AAV5-sh*Cyp46a1* animals presented an increase in liver weight, relatively to the HFD Non-injected groups [HFD Non-injected (0,9113 ± 0,1253); *n=6* versus HFD AAV5-sh*Cyp46a1* (1,186 ± 0,08125); *n=7* – *P*-value =0,0961]. **C)** Between males, the Chow AAV5-sh*Cyp46a1* animals showed an increase in liver weight, comparatively to the Chow Non-injected animals [Chow Non-injected (1,120 ± 0,05008); *n=9* versus Chow AAV5-sh*Cyp46a1* (1,286 ± 0,1913); *n=7* – *P*-value =0,331]. **D)** Between males, the HFD

AAV5-sh*Cyp46a1* animals presented an increase in liver weight, comparatively to the HFD Non-injected animals [HFD Non-injected (1,461 ± 0,1280); *n=4* versus HFD AAV5-sh*Cyp46a1* (2,631 ± 0,5209); *n=4* – *P*-value =0,0718]. Data were represented as mean ± SEM. [*P*-value < 0,05 (*), *P*-value < 0,01 (**), *P*-value < 0,001 (***), *P*-value < 0,0001 (****)] – unpaired Student's t-test: A-B-C-D; **Abbreviations: Chow:** low fat control diet; **HFD:** high fat diet; **AAV5:** adeno-associated vectors of the serotype 5; **sh:** short hairpin.